The Thermodynamic Properties of the f-Elements and their Compounds. Part 2. The Lanthanide and Actinide Oxides

Rudy J. M. Konings, Ondrej Beneš, Attila Kovács, Dario Manara, David Sedmidubský, Lev Gorokhov, Vladimir S. Iorish, Vladimir Yungman, E. Shenyavskaya, and E. Osina

Citation: Journal of Physical and Chemical Reference Data **43**, 013101 (2014); doi: 10.1063/1.4825256
View online: http://dx.doi.org/10.1063/1.4825256
View Table of Contents: http://scitation.aip.org/content/aip/journal/jpcrd/43/1?ver=pdfcov
Published by the AIP Publishing

The Thermodynamic Properties of the *f*-Elements and their Compounds. Part 2. The Lanthanide and Actinide Oxides

Rudy J. M. Konings,[a] **Ondrej Beneš, Attila Kovács, Dario Manara, and David Sedmidubský**[b]
European Commission, Joint Research Centre, Institute for Transuranium Elements, P.O. Box 2340, 76125 Karlsruhe, Germany

Lev Gorokhov, Vladimir S. Iorish,[c] **Vladimir Yungman, E. Shenyavskaya, and E. Osina**
Joint Institute for High Temperatures, Russian Academy of Sciences, 13-2 Izhorskaya Street, Moscow 125412, Russia

(Received 24 August 2012; accepted 4 March 2013; published online 10 January 2014)

A comprehensive review of the thermodynamic properties of the oxide compounds of the lanthanide and actinide elements is presented. The available literature data for the solid, liquid, and gaseous state have been analysed and recommended values are presented. In case experimental data are missing, estimates have been made based on the trends in the two series, which are extensively discussed. © *2014 Euratom.* [http://dx.doi.org/10.1063/1.4825256]

CONTENTS

[a]Electronic mail: rudy.konings@ec.europa.eu.
[b]Permanent address: Institute of Chemical Technology, Technická 5, 16626 Praha 6, Czech Republic.
[c]Deceased on May 2012.

List of Tables

List of Figures

1. Introduction

The thermodynamic properties of the 4*f* (lanthanides) and 5*f* (actinides) elements and their compounds have been subject of many studies since the Second World War, strongly stimulated by the demands of the nuclear technology. The development of nuclear reactor fuels based on uranium, thorium or plutonium and the understanding of the effects of fission product accumulation in the fuel, a significant fraction of which belongs to the lanthanide group, required such fundamental data. At the same time, many studies of the (thermodynamic) properties of the *f*-elements were stimulated by the scientific interest in the role of the *f*-elements in the chemical bonding, and particularly the differences between the 4*f* and 5*f* series.

Pioneering work on the major actinides has been performed during the Manhattan Project in the USA. The researchers in this project started many systematic studies of uranium and plutonium and its compounds, the results of which became available in literature in the 1950s. At the meetings organised in the frame of the *Peaceful Uses of Atomic Energy* initiative and also at the early *Symposia on Thermodynamics of Nuclear Materials* organised by the *International Atomic Energy Agency* a rapid expansion of the knowledge of the thermodynamic properties of the actinide elements and their compounds was presented. During the same period, the separation methods for the lanthanides, which are difficult due to their chemical similarity, improved significantly to yield these elements in sufficient pure form that was needed for accurate thermochemical and thermophysical measurements.[1,2]

In the 1960s and 1970s a wealth of scientific information on the *f*-elements has been published, the lanthanides as well as uranium and thorium being available in pure form to many researchers, and the other actinides being produced in significant quantities for studies at nuclear research laboratories. As a result, the understanding of the trends and systematics of their properties has improved considerably, revealing the differences between the localised 4*f* electrons in the lanthanides and the heavy actinides (Am-Lr) and the itinerant 5*f* electrons of the light actinides (Th-Np).

In this work, we will present a comprehensive review of the thermodynamic properties of the oxides of the lanthanides and actinides, based on critical review of the available literature according to procedures described in Secs. 2.1–2.5.

2. Approach

2.1. Thermal functions of condensed phases

The approach adopted in this review is based on a critical evaluation of the thermal functions (heat capacity, entropy, enthalpy increment) and enthalpies of formation of the lanthanide and actinide oxides using, when possible, the primary experimental data as reported in literature. To describe these as a function of temperature it is necessary to include the data on the structural transformations (including melting point).

The reported transition and melting temperatures have been corrected to the International Temperature Scale ITS-90. Though generally no detailed information is given about the standards used and it is not specifically stated to which earlier temperature scales the data refer, it is assumed that the results between 1948 and 1968 refer to IPTS-48 and between 1969 and 1990 to IPTS-68. Especially in the transition years this may not always be correct. The differences between ITS-90 and IPTS-68 and IPTS-68 and IPTS-48 are shown in Fig. 1.

The low-temperature heat capacity data and the resulting entropies have not been corrected nor refitted. First, the changes in the temperature scales in the range T = (0 to 300) K are small, and, second, refitting would only marginally change the results. In case of more than one set of experimental data covering the temperature range from close to 0 K to room temperature, often a motivated choice for one of them is made, based on sample purity and/or calorimetric accuracy. In other cases a joint treatment has been made using overlapping polynomial equations.

The high-temperature heat capacity of the solid phases has been obtained by refitting of the experimental data reported. The following polynomial equation for the enthalpy increment $\{H^\circ(T) - H^\circ(298.15\ K)\}$ has been adopted

$$\{H^\circ(T) - H^\circ(298.15\ K)\} = \sum A_n (T/K)^n \qquad (1)$$

with $n = -1$ to 2, but in case of anomalous behavior of the heat capacity with n up to 4. This corresponds to a heat capacity equation of the type

$$C_p(T) = a_{-2}(T/K)^{-2} + \sum a_n (T/K)^n. \qquad (2)$$

A difficult question to be answered is that of the temperature correction of high-temperature heat capacity and enthalpy data. As can be seen in Fig. 1 the temperature corrections become significant (>2 K) above 2000 K. For heat capacity data, which are rare above this temperature, the correction is straightforward, and has been made. However, for enthalpy increment data the corrections are not trivial as they depend on the type of device used and the condition of the sample. In case of the device was calibrated with a known standard (for example, sapphire) the temperature correction should also be made for the standard, and hence not only the temperature but also the enthalpy conversion factor is affected. Also in case of encapsulated samples the temperature correction should lead to an enthalpy correction, as the contribution of the encapsulation material would change. Since the required details are generally lacking to make the corrections properly, the experimental enthalpy data have not been corrected.

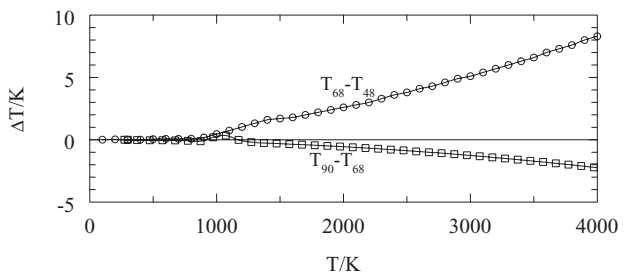

FIG. 1. The temperature corrections according to various temperature scales.

All literature data starting from 1945 have been collected systematically. When no experimental data were given in the papers, they have been extracted from digitalized graphs.

2.2. Enthalpies of formation of condensed phases

The derivation of the enthalpies of formation from calorimetric data was done by recalculation of the thermochemical reaction schemes (Hess cycles) using a consistent set of auxiliary data, and has been partially reported in earlier work[3] that was updated where necessary. For the solution calorimetric studies the partial molar enthalpy of formation of an acid solution (sln) at the concentration given, has been calculated from the enthalpy of formation of the infinitely dilute acid,[4] the enthalpy of formation of the HX solutions[5] and the densities of the HX solutions at 298.15 K,[6] neglecting the influence of the dissolved ions. Uncertainty limits of the measurements, as listed in the tables or text, are always the values given in the original paper, because in many cases they could not be recalculated due to lack of information. As a consequence they might refer to one standard deviation of the mean, twice the standard deviation of the mean, or the 95% confidence interval, which is not always clear. When combining data from different sources to a selected value, a weighted mean is therefore considered not justified and the uncertainty limit of the selected (mean) value has been estimated. Auxiliary data recommended by CODATA or values consistent with the CODATA selection[4] have been employed.

2.3. Thermal functions of gases

Thermal functions of the diatomic molecules were calculated in the present work using the approach developed by Gurvich *et al.*[7] The vibrational-rotational partition functions were calculated by direct summation over vibrational levels and by integration with respect to rotational levels. The upper limit of integration was assumed linearly decreasing with vibrational quantum number.

The electronic partition functions were calculated taking into account all experimentally known and estimated data on excited states. The value of Q_{int} and its derivatives were evaluated assuming that $Q^{(i)}_{vib,rot} = (p_i/p_X)^{(X)}_{vib,rot}$. This approach is well justified in the case of the molecules under consideration though the most of these molecules have numerous low-lying states, which contribute considerably to the thermal functions. The point is that these states as a rule belong to the same electron configuration as the ground state. It is well known that the states of the same configuration have close values of vibrational and rotational constants. Therefore, the tables of molecular constants present the vibrational and rotational constants only for the ground state. The only exception is the YbO molecule for which the ground state configuration gives only one state, namely, the $X^1\Sigma$ state, while the low-lying states belong to the other configurations with quite different molecular constants. The excited states are presented

in the tables in two blocks for experimentally known and estimated states with corresponding statistical weights. The uncertainties in the energies of experimental states are usually small, but for estimated states they can amount to 10%–20% of the listed values.

For simplification of introducing a huge number of high-energy excited electronic states for molecules under consideration, containing *f* and *d* open shells, in the present work the approach of the density of states estimation was applied. In this approach, a group of high-energy states with close energies are united in one state with fixed (mostly rounded) energy and average statistical weight. This division into groups of states is being done in a way that does not interfere with the accuracy of the thermal functions calculation. Errors of the calculated thermal functions depend mostly on the accuracy of the data on molecular constants. At room temperature, the uncertainties in heat capacity as a rule do not exceed 0.3–0.5 J K^{-1} mol^{-1}. At higher temperatures, the uncertainties become larger because of the increasing contribution of excited states and errors of these estimations. In heat capacity the uncertainties can reach 3–5 J K^{-1} mol^{-1} at 4000 K, or even larger for molecules that entirely lack experimental data, such as PaO, NpO, AmO, CmO, or PuO.

The thermal function of the polyatomic molecules were calculated using the rigid-rotor harmonic oscillator approach,[7,8] that includes general approximations for the translational, rotation and vibrational contributions, and a direct summation of the electronic partition function.

The heat capacity values were approximated by two conjugated equations of the form:

$$C_p^\circ(T) = a_{-2}(T/\mathrm{K})^{-2} + \sum a_n (T/\mathrm{K})^n. \quad (3)$$

The accuracy of the approximation is around 0.1 J K^{-1} mol^{-1} over full temperature range from 298.15 to 4000 K.

The nomenclature used in the tables of molecular properties of the gaseous species is summarized in Table 1. The fundamental constants as recommended by CODATA are used in this work.

2.4. Enthalpies of formation of gases

The aim of this review is to select the most reliable enthalpies of formation for MO, MO_2, and MO_3 molecules based on calculations with new thermal functions of these molecules, and to take into consideration new experimental data and quantum chemical calculations not included in previous assessments.

The recommended enthalpies of formation at the standard temperature T = 298.15 K have been selected in this review after critical analysis of all accessible published experimental data on high-temperature equilibriums for reactions in the gas phase or in condensed and gas phases. The enthalpies of reactions were calculated from the equilibrium constants by the "second-law" and the "third-law" methods.[7,9] By the former, the enthalpy of reaction at the mean temperature of experiments T_{mean} is obtained from the temperature dependence of equilibrium constant, K_p, measured in some temperature interval:

$$\frac{\Delta_r H^\circ(T_{mean})}{R} = -\frac{d(\ln K_p)}{d(1/T)}. \quad (4)$$

The value T_{mean} is calculated using equation $T_{mean} = (n^{-1}\sum T_i^{-1})^{-1}$, where n is the number of experimental points. The $\Delta_r H^\circ(T_{mean})$ value so obtained is reduced to the reference temperature 298.15 K:

$$\Delta_r H^\circ(298.15\ \mathrm{K}) = \Delta_r H^\circ(T_{mean}) - \Delta_r\{\Delta_{298.15}^{T_{mean}} H^\circ\}. \quad (5)$$

In the "third-law" method, $\Delta_r H^\circ(298.15\ \mathrm{K})$ is obtained from every experimental K_p value

$$\Delta_r H^\circ(298.15\,K) = T\Delta_r\phi - RT\ln K_p, \quad (6)$$

using the free energy functions (or reduced Gibbs energies) ϕ, which is defined as

$$\phi = -\{G^\circ(T) - H^\circ(298.15\ \mathrm{K})\}/\mathrm{T}, \quad (7)$$

$$= S^\circ(T) - \frac{\Delta_{298.15}^T H^\circ}{T}, \quad (8)$$

for each reactant. The enthalpy of formation for the molecule under study, $\Delta_f H^\circ(298.15\ \mathrm{K})$ is calculated from the enthalpy of a reaction using known enthalpies of formation for all other reactants.

The uncertainties ascribed to selected $\Delta_f H^\circ(298.15\ \mathrm{K})$ values reflect statistical errors, uncertainties in the thermal functions, and uncertainties in enthalpies of formation for all other reaction participants. Most experimental measurements for equilibriums involving the considered molecules were carried out by Knudsen effusion (KE) and mass spectrometric methods (MS), or by combination of both. In the case of MS measurements, the term RT ln(1.5) was added to reflect uncertainties of equilibrium constants calculated from ion currents, due to uncertainties in ionization cross sections. Agreement of the second- and third-law values was regarded as an indication of reliability of experimental data.

TABLE 1. Nomenclature of the molecular properties for the di- and polyatomic species

Symbol	Name	Symbol	Name
T_e	Electronic energy level	σ	Symmetry number
p	Degeneracy (of T_e)	$I_A I_B I_C$	Product of moments of inertia
ω_e	Fundamental harmonic vibrational frequency	ν_i	Fundamental vibrational frequency
$\omega_e x_e$	Anharmonicity correction		
β_e	Rotational constant		
α_e	Rotational-vibration interaction constant		
D_e	Centrifugal distortion constant		

2.5. Consistency and completeness

We have tried to maintain the internal consistency of the recommended data as much as possible, but in view of the complex interrelationships in some of the analysed systems (e.g., Ce-O, U-O or Pu-O) and the fact that data from other sources have been used this cannot be fully guaranteed. The review has been performed progressively during a period of several years. New information that became available during and just after this period has been incorporated as far as possible, but in some cases the implications of adopting new (more accurate) values were too far-reaching to be implemented. These cases are clearly identified in the text.

3. The Lanthanide Oxides in Solid and Liquid State

3.1. La_2O_3(cr,l)

3.1.1. Polymorphism and melting point

Lanthanum(III) oxide has a A-type hexagonal sesquioxide structure (space group $P\bar{3}m1$) at room temperature. It transforms to a H-type hexagonal structure upon heating. Foex and Traverse[10] suggest that this transformation is a simple displacement rearrangement of the lattice,[10] as in $\alpha \rightarrow \beta$ quartz. Foex and Traverse,[10] Lopato *et al.*[11] and Wehner *et al.*[12] all reported the A → H transition at T = 2313 K, Shevthenko and Lopato[13] at T = 2303 K, and[14] at (2319 ± 5) K. The H phase subsequently transforms into a cubic X-type structure (space group $Im\bar{3}m$) and the transformation temperatures were reported as T = 2383, 2413, 2363, and 2373 K, (2383 ± 5) K, respectively. Except for the recent work by Ushakov and Navrotsky,[14] all other measurements must be converted to ITS-90. The measurements of Foex and Traverse[10] must be corrected by +14 K, following the procedure outlined by Coutures and Rand.[15] Lopato *et al.*,[11] Wehner *et al.*,[12] and Shevthenko and Lopato[13] reported no (detailed) information on the calibration of their measurements, but assuming the data refer to IPTS-68, a correction of −1 K needs to be applied. We select T_{trs} = (2313 ± 30) K for the A → H transformation, T_{trs} = (2383 ± 30) K for the H → X transformation.

Various measurements of the melting temperature of solid La_2O_3 have been reported as summarized in Table 2, which is based on the IUPAC review by Coutures and Rand;[15] the results being corrected to ITS-90. The recent value for the melting by temperature by Ushakov and Navrotsky[14] is in excellent agreement with the selected values by Coutures and Rand,[15] and the latter is retained, T_{fus} = (2577 ± 15) K.

TABLE 2. Temperature of melting of lanthanum sesquioxide (after Coutures and Rand[15])

	T_{fus}/K	
Authors	Reported	ITS-90
Wartenberg and Reusch[16]	2588	2581
Lambertson and Gunzel[17]	2483 ± 20	2489 ± 20
Sata and Kiyoura[18]	2577 ± 2	2583 ± 2
Foex[19]	2573	2587
Mordovin *et al.*[20]	2493 ± 30	2496 ± 30
Noguchi and Mizuno[21]	2530 ± 20	2532 ± 20
Treswjatskii *et al.*[22a]	2583 ± 20	2582 ± 20
Coutures *et al.*[23]	2593 ± 10	2592 ± 10
Wehner *et al.*[12]	2563 ± 30	
Mizuno *et al.*[24]	2569 ± 20	2555 ± 20
Yoshimura *et al.*[25]	2573 ± 5	2576 ± 5
Shevthenko and Lopato[13]	2583	2582
Ushakov and Navrotsky[14]		2574 ± 10
Selected value:		2577 ± 15

[a]Also reported by Lopato *et al.*[11]

3.1.2. Heat capacity and entropy

Low-temperature heat capacity measurements for La_2O_3 have been reported by three different research groups: Goldstein *et al.*[26] from 16 to 300 K, King *et al.*[27] from 50 to 300 K, and Justice and Westrum, Jr.[28] from 5 to 350 K. The measurements reasonably agree to about T = 200 K; above this temperature the differences significantly increase. The selected standard entropy of La_2O_3 has been derived from the measurement by Justice and Westrum, Jr.,[28] which is considered to be the most accurate

$$S^\circ(298.15\ \mathrm{K}) = (127.32 \pm 0.84)\ \mathrm{J\,K^{-1}\,mol^{-1}}.$$

The high-temperature enthalpy increment of La_2O_3(cr) has been measured by Blomeke and Ziegler[29] from 380 to 1170 K, King *et al.*[27] from 399 K to 1797 K, Yashvili *et al.*[30] from 380 to 1650 K and Sedmidubský *et al.*[31] from 689 to 1291 K, which are in perfect agreement, as shown in Fig. 2. The measurements smoothly join the low-temperature heat capacity measurements by Justice and Westrum, Jr.[28] Basili *et al.*[32] measured the heat capacity of La_2O_3 from 400 to 850 K. Their results, only presented in graphical form, reasonably agree with the enthalpy measurements to about 550 K. The heat capacity above 298.15 K for A-type La_2O_3 can be represented by the equation (298.15 to 1800 K):

$$C_p^\circ(T)/\mathrm{J\,K^{-1}\,mol^{-1}} = 120.6805 + 13.42414 \times 10^{-3}(T/\mathrm{K}) - 14.13668 \times 10^{5}(T/\mathrm{K})^{-2}$$

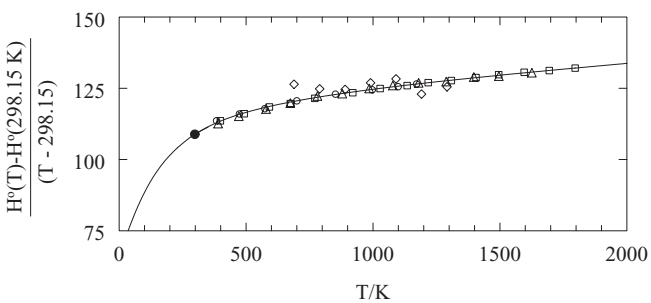

FIG. 2. The reduced enthalpy increment (in J K^{-1} mol^{-1}) of La_2O_3; ○, Blomeke and Ziegler[29]; □, Yashvili *et al.*[30]; △, King *et al.*[27]; ◇, Sedmidubský *et al.*[31]; •, value derived from the low-temperature measurements by Justice and Westrum, Jr.;[28] the curve shows the recommended equation.

derived from a fit of the combined enthalpy results of Blomeke and Ziegler,[29] King *et al.*[27] and Yashvili *et al.*,[30] which are considered the most accurate. The boundary condition $C_p^\circ(298.15) = 108.78\ J\ K^{-1}\ mol^{-1}$ was applied, as derived from the low-temperature heat capacity measurements.[28]

Heat-capacity or enthalpy measurements have not been reported for the H, X, and liquid phases of La_2O_3 and we estimate

$$C_p^\circ(H, T) = C_p^\circ(X, T) = 150\ J\,K^{-1}\,mol^{-1},$$
$$C_p^\circ(liq, T) = 162\ J\,K^{-1}\,mol^{-1}.$$

The transition enthalpies of La_2O_3 have been measured by Ushakov and Navrotsky[14] recently, using high temperature thermal analysis

$$\Delta_{trs}H^\circ(A \rightarrow H) = (23 \pm 5)\ kJ\,mol^{-1},$$
$$\Delta_{trs}H^\circ(H \rightarrow X) = (17 \pm 5)\ kJ\,mol^{-1},$$
$$\Delta_{fus}H^\circ = (78 \pm 10)\ kJ\,mol^{-1}.$$

These values have been selected here. They are only partially corresponding to the observation by Foex and Traverse[10] who noted a moderate thermal effect for the A → H transformation by DTA (differential thermal analysis), and a significant one for the H → X. Wu and Pelton[33] concluded from the fact that the liquidus at the La_2O_3 side of the phase La_2O_3–Al_2O_3 phase diagram does not show clear discontinuities, that the entropy changes of the A → H and H → X transformations are very small. They also concluded that the limiting slope of the liquid line in this phase diagram suggests an entropy of fusion of 25.1 $J\ K^{-1}\ mol^{-1}$, in fair agreement with the value found by Ushakov and Navrotsky,[14] 30.3 $J\ K^{-1}\ mol^{-1}$.

3.1.3. Enthalpy of formation

The enthalpy of formation of La_2O_3 has been assessed by Cordfunke and Konings[34] recently, and we accept the selected value from that work, since no new information has been published since

$$\Delta_fH^\circ(La_2O_3, cr, 298.15\ K) = -(1791.6 \pm 2.0)\ kJ\,mol^{-1}.$$

All values relevant to the derivation of the standard enthalpy of formation of lanthanum sesquioxide are summarized in Table 3. Huber, Jr. and Holley, Jr.[35] determined the enthalpy of formation by combustion of a very pure sample of metal. This value has been confirmed by several authors using solution calorimetry.[36–38] However, the values for the enthalpy of solution of La(cr) differ significantly.[37–39] As discussed by Cordfunke and Konings,[34] the results of Merli *et al.*[39] can be considered as the most accurate since they made their measurements on a well-defined sample. Therefore, the results of the other studies were recalculated using the values from this study, some obtained by inter- or extrapolation. The resulting enthalpies of formation are in excellent agreement with the combustion value and the selected value is the mean of the combustion value by Huber, Jr. and Holley, Jr.,[35] and the recalculated values obtained from and the enthalpy of solution measurements Montgomery and Hubert,[36] Fitzgibbon *et al.*,[37] and Gvelesiani and Yashvili.[38]

TABLE 3. The enthalpy of formation of La_2O_3(cr) at 298.15 K; ΔH_1° is the enthalpy of solution of La(cr), ΔH_2° of La_2O_3(cr) in HCl(aq), respectively (after Cordfunke and Konings[34])

Authors	Method[a]	ΔH_1°/kJ mol^{-1}	ΔH_2°/kJ mol^{-1}	Δ_fH°/kJ mol^{-1}
Muthmann and Weis[40]	C			−1857.7
Matignon[41]	S			−1789.0
Kremers and Stevens[42]	C			−1912.1
Moose and Parr[43]	C			−1907.1
Beck[44]	S		−439.3	
Roth *et al.*[45]	C			−2255 ± 17
Huber, Jr. and Holley, Jr.[35]	C			−1793.1 ± 0.8
von Wartenberg[46]	S (0.1)		−468.6 ± 6.3	
Montgomery and Hubert[36]	S (0.51)	[−704.1 ± 1.2][b]	−474.4 ± 1.6	−1791.3 ± 2.5
Fitzgibbon *et al.*[37]	S (1.0)	−705.5 ± 1.3	−474.4 ± 0.4	−1794.2 ± 2.7
		[−704.4 ± 1.2][c]		−1792.0 ± 2.7
	S(1.0)	−705.6 ± 1.3	−473.8 ± 0.4	−1794.8 ± 2.7
		[−704.4 ± 1.2][c]		−1792.5 ± 2.7
Gvelesiani and Yashvili[38]	S (1.0)	−708.0 ± 2.0	−475.3 ± 3.3	−1798.2 ± 5.2
		[−704.4 ± 1.2][c]		−1791.0 ± 4.1
	S (1.5)	−708.8 ± 2.9	−475.3 ± 1.8	−1799.9 ± 6.1
		[−704.7 ± 1.2][b]		−1791.7 ± 3.0
Oppermann *et al.*[47]	S (4.0)	[−706.2 ± 1.1][b]	−472.6 ± 0.3	−1798.2 ± 2.4
Selected value:				−1791.6 ± 2.0

[a]C: combustion calorimetry; S: solution calorimetry; values in parentheses give the concentration of the solvent in mol dm^{-3}.
[b]Estimated/interpolated from the results of Merli *et al.*[39]
[c]Merli *et al.*[39]

3.2. CeO_2(cr,l)

3.2.1. Melting point

Cerium dioxide has a cubic fluorite structure (space group $Fm\bar{3}m$) up to the melting point. The reported values for the temperature of melting are very dissimilar (Table 4), which is due to the fact that this compound starts to lose oxygen at elevated temperatures to form a substiochiometric CeO_{2-x} phase. The melting point for CeO_2 strongly depends on the atmosphere under which the liquid phase is produced.[48] For example, Mordovin *et al.*[20] detected the liquid phase already at 2670 K, when heating ceria in an argon atmosphere. On the other hand many other authors[10,49–51] observed higher values of the melting point while heating CeO_2 under a strongly oxidising atmosphere (pure pressurised O_2, air, or a mixture of oxygen and an inert gas at high pressure): between 2753 and 3073 K. Also Manara *et al.*,[52] in a recent unpublished investigation of the melting behavior of CeO_2, performed measurements both under oxidising and reducing atmospheres, obtaining 2743 and 2675 K, respectively. In this last study, however, heating under high oxygen pressures could not be realised. Since the highest values are the most likely to correspond to quasistoichiometric CeO_2, we select $T_{fus} = (3083 \pm 50)$ K as the best melting point for stoichiometric cerium dioxide, the uncertainty being assigned by us. This is in line with the the suggestion of Du *et al.*[53] that the melting point of CeO_2 must be between those of the group IVB dioxides and the actinide dioxides.

3.2.2. Heat capacity and entropy

The low-temperature heat capacity of CeO_2 has been measured by Westrum, Jr. and Beale, Jr.[56] from 5 to 300 K. The entropy, as derived from these measurements, is adopted here as

$$S^\circ(298.15\ \mathrm{K}) = (62.29 \pm 0.07)\ \mathrm{J\,K^{-1}\,mol^{-1}}.$$

High-temperature enthalpy increments have been reported by Kuznetsov *et al.*[57] in the temperature range from 608 to 1172 K, King *et al.*[27] from 400 to 1800 K (only smoothed values are given in the paper), Pears *et al.*[58] from 640 to 2044 K, Mezaki *et al.*[59] from 490 to 1140 K, and Yashvili *et al.*[60] from 391 to 1624 K. These data are in reasonable agreement, as shown in Fig. 3.

TABLE 4. Temperature of melting of cerium dioxide

	T_{fus}/K	
Authors	Reported	ITS-90
Ruff[54]	2246	
von Wartenberg and Gurr[55]	2873	
Trombe[50a]	3073	3077
Tshieryepanov and Trjesvyatsky[49b]	3083	3087
Foex and Traverse[10]	2753	2768
Mordovin *et al.*[20]	2670 ± 30	2673 ± 30
Watson[51]	2873	2872
Selected value:		3083 ± 50

[a]Paper not available to us, cited from Noguchi and Mizuno.[21]
[b]Paper not available to us, cited from Du *et al.*[53]

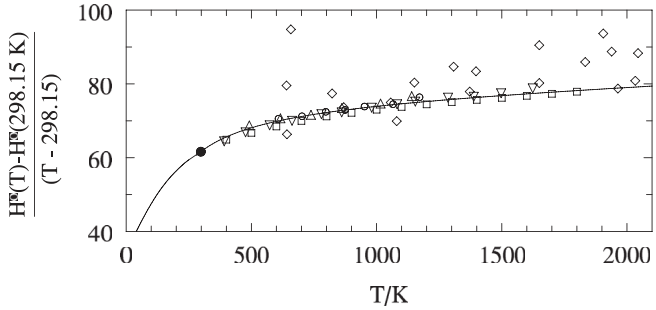

FIG. 3. The reduced enthalpy increment (in J K^{-1} mol^{-1}) of CeO_2; ○, Kuznetsov *et al.*[57]; □, King *et al.*[27]; △, Mezaki *et al.*[59]; ▽, Yashvili *et al.*[60]; ◊, Pears *et al.*[58]; •, value derived from the low-temperature measurements by Westrum, Jr. and Beale, Jr.;[56] the curve shows the recommended equation.

High-temperature heat capacities have been measured by Riess *et al.*[61] by adiabatic scanning calorimetry (350–900 K). The results, presented as an equation only, are in excellent agreement with the values derived from the enthalpy increment measurements. Gallagher and Dworzak[62] determined the heat capacity between 418 and 758 K by DSC (differential scanning calorimetry). These data are, however, much too low to join the low-temperature data by Westrum, Jr. and Beale, Jr.[56]

The enthalpy data have been combined, and constrained $C_p^\circ(298.15\ \mathrm{K}) = 61.63\ \mathrm{J\,K^{-1}\,mol^{-1}}$ from the low temperature data,[56] resulting in the following heat capacity equation:

$$C_p^\circ/(\mathrm{J\,K^{-1}\,mol^{-1}}) = 74.4814 + 5.83682 \times 10^{-3}(\mathrm{T/K}) - 1.29710 \times 10^{6}(\mathrm{T/K})^{-2}.$$

This equation is extrapolated to the melting point, which might neglect possible anomalous increase in the heat capacity as observed in other fcc dioxides of *f*-elements such as ThO_2 and UO_2. The heat capacity of the liquid has been estimated as

$$C_p^\circ(CeO_2, \mathrm{liq}, \mathrm{T}) = 120\ \mathrm{J\,K^{-1}\,mol^{-1}}.$$

The entropy of fusion is assumed to be the same as that of the isostructural UO_2 phase ($22.4\ \mathrm{J\,K^{-1}\,mol^{-1}}$), which is the only fcc dioxide for which this quantity is well defined. We thus obtain for the enthalpy of fusion

$$\Delta_{fus}H^\circ(CeO_2) = (69 \pm 5)\ \mathrm{kJ\,mol^{-1}}.$$

3.2.3. Enthalpy of formation

The standard molar enthalpy of formation of CeO_2(cr) has been determined by Huber, Jr. and Holley, Jr.[35] by oxygen-bomb combustion calorimetry using a well-analyzed sample of cerium metal, giving $\Delta_f H°(298.15\ \mathrm{K}) = -(1088.6 \pm 1.4)\ \mathrm{kJ\,mol^{-1}}$. This value, which was carefully corrected for impurities, is in excellent agreement with the result by Baker *et al.*[63] of a later oxygen-bomb combustion calorimetric investigation carried out in the same laboratory,

$\Delta_f H°(298.15\ K) = -(1090.4 \pm 0.8)\ kJ\ mol^{-1}$. We have selected the latter value because it is based on a cerium metal sample of significantly higher purity

$$\Delta_f H°(CeO_2, cr, 298.15K) = -(1090.4 \pm 1.0)\ kJ\,mol^{-1}.$$

The results of early investigations[40,43,64] are mainly of historical interest due to a poor quality of materials and experimental techniques available at that time.

3.3. Ce_2O_3(cr,l)

3.3.1. Polymorphism and melting point

At room temperature, cerium sesquioxide has a hexagonal A-type structure (space group $P\bar{3}m1$). Pankratz and Kelly[65] observed a transition at 1050 K from the A-type sesquioxide to a high-temperature modification but it should be noted that their sample had the hyperstoichiometric composition ($Ce_2O_{3.33}$). This transition has not been reported by other investigators, and does not fit into the general structure diagram on the lanthanide sesquioxides (Fig. 4). We therefore attribute it to this specific composition and not to the sesquioxide phase, and according to the phase diagram of the Ce-O system it could represent the phase boundary of the $\{Ce_2O_3+Ce_6O_{10}\}$ two-phase field.

Lopato *et al.*[11] and Shevthenko and Lopato[13] reported that A-type Ce_2O_3 transforms to a hexagonal H-type structure at 2393 K. They also found that the H-type phase transforms to a cubic X-type structure at 2407 K. No information on the calibration of these measurements has been found, but assuming the data refer to IPTS-68, a correction of −1 K needs to be applied for ITS-90. We select $T_{trs} = (2392 \pm 30)$ K for the A → H transformation, $T_{trs} = (2406 \pm 30)$ K for the H → X transformation.

The various data for the melting temperature have been summarized in Table 5, which is based on the IUPAC review by Coutures and Rand;[15] the results being corrected to ITS-90. The selected melting point is (2512 ± 50) K.

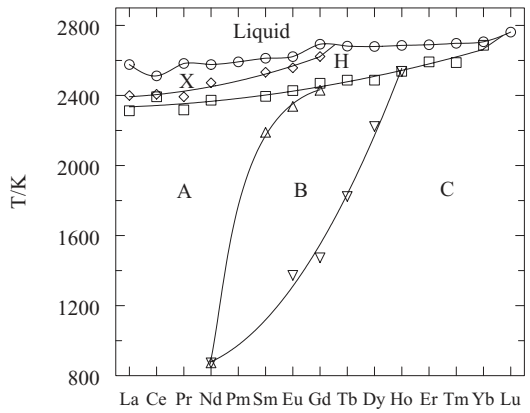

FIG. 4. The polymorphism in the Ln_2O_3 series as a function of temperature.

TABLE 5. Temperature of melting of cerium sesquioxide (after Coutures and Rand[15])

	T_{fus}/K	
Authors	Reported	ITS-90
Sata and Kiyoura[18]	2483 ± 10	2489 ± 2
Mordovin *et al.*[20]	2415 ± 30	2429 ± 30
Treswjatskii *et al.*[22]	2513 ± 20	2512 ± 20
Shevthenko and Lopato[13]	2513	2512
Selected value:		2512 ± 15

3.3.2. Heat capacity and entropy

Low-temperature heat capacity measurements on cerium sesquioxide have been reported by Weller and King[66] in the range from 53 to –296 K, Justice and Westrum, Jr.[67] in the range from 5 to 345 K, and Huntelaar *et al.*[68] from 5 to 400 K. The data by Weller and King cover a smaller temperature range and, moreover, were obtained using a sample with composition $Ce_2O_{3.33}$. The sample of Justice and Westrum, Jr.[67] was reported to refer to the composition ($Ce_2O_{3.02}$) but this was later doubted by the authors[69] who suggested that the true composition was likely $Ce_2O_{3.33}$ also. For that reason the data by Huntelaar *et al.*[68] are preferred. Hence, the standard entropy, as derived by the latter authors, has been adopted here as

$$S°(298.15\ K) = (148.1 \pm 0.4)\ J\,K^{-1}\,mol^{-1}.$$

High-temperature enthalpy increment measurements have been reported by Pankratz and Kelly[65] from 398 to 1501 K, Kuznetsov *et al.*[70] from 578 to 1116 K and Huntelaar *et al.*[68] from 473 to 883 K. The data of Pankratz and Kelly[65] refer to the nonstoichiometric composition ($Ce_2O_{3.33}$). The authors corrected them for the presence of CeO_2, but in view of the unexplained phase transition observed in the results (see above), the correctness of this approach may be doubted. The results of Kuznetsov *et al.*[70] and Huntelaar *et al.*[68] are in reasonable agreement and fit the low-temperature data. However, the former results also indicate an anomalous increase near 1000 K, which might indicate that their sample had not the stoichiometric composition and that the agreement is fortuitous. For that reason our selected heat capacity equation is based on the results of Huntelaar *et al.*[68] only, which was constrained to $C_p°(298.15) = 115.0$, as derived from the low-temperature heat capacity measurements by the same authors,

$$C_p°/(J\,K^{-1}\,mol^{-1}) = 113.736 + 28.4344 \times 10^{-3}(T/K) - 0.641205 \times 10^{6}(T/K)^{-2}.$$

Basili *et al.*[32] determined the heat capacity of Ce_2O_3 between 440 and 1100 K by means of a plane temperature waves method. Venkata Krishnan and Nagarajan[71] measured the heat capacity from 280 to 820 K by DSC. Their data, read from a graph, are in reasonable agreement with the heat capacity derived from the enthalpy increments.

The enthalpies of transition between the high-temperature modifications have been estimated, in absence of experimental

data. For the (A → H) we have assumed that the entropy of transition varies regularly between the known values for La_2O_3 and Gd_2O_3. For the (H → X) and (X → liquid) transitions we have assumed the entropies to be the same as for La_2O_3:

$$\Delta_{trs}H^\circ(A \rightarrow H) = (28 \pm 8)\ \text{kJ mol}^{-1},$$
$$\Delta_{trs}H^\circ(H \rightarrow X) = (19 \pm 5)\ \text{kJ mol}^{-1},$$
$$\Delta_{fus}H^\circ = (85 \pm 10)\ \text{kJ mol}^{-1}.$$

For the heat capacity of the high temperature phases we estimate

$$C_p^\circ(H, T) = C_p^\circ(X, T) = 145\ \text{J K}^{-1}\ \text{mol}^{-1},$$
$$C_p^\circ(\text{liq}, T) = 157\ \text{J K}^{-1}\ \text{mol}^{-1}.$$

3.3.3. Enthalpy of formation

Several combustion calorimetric studies have been reported for the reaction

$$Ce_2O_3(\text{cr}) + \frac{1}{2}O_2(\text{g}) = 2CeO_2(\text{cr}).$$

The results for the enthalpy of reaction are discordant, as summarized in Table 6. As suggested by Cordfunke and Konings,[34] this variation may be due to (i) differences in the O/M ratio of the starting material Ce_2O_3(cr), (ii) impurities in Ce_2O_3(cr) resulting from the fabrication by reduction of the dioxide (e.g., residual carbon has a big impact on the combustion values), and (iii) differences in the final state of the reaction product CeO_2 that is known to have a large range of substoichiometric compositions.

Huntelaar *et al.*[68] measured the enthalpy of solution of a well-defined sample of Ce_2O_3(cr) in 0.25 mol dm^{-3} HCl(aq) from which the enthalpy of formation is derived as Δ_fH° (298.15 K) = −(1813.1 ± 0.8) kJ mol^{-1}. Putnam *et al.*[74] measured the enthalpy of formation by high-temperature oxide-melt solution calorimetry. Recalculating their measurements with the selected value for the enthalpy of formation of CeO_2, gives Δ_fH°(298.15 K) = −(1809.2 ± 5.2) kJ mol^{-1}. As noted by Morss and Konings[76] these results give an anomalous value for the hypothetical solution enthalpy of the reaction,

$$LnO_{1.5} + 3H^+(\text{aq}) = Ln^{3+}(\text{aq}) + \frac{3}{2}H_2O(\text{l}),$$

compared to the other lanthanide sesquioxides. For that reason we select the enthalpy of formation from the combustion study by Baker and Holley, Jr.[73] that was performed with $CeO_{1.5+x}$ samples that were carefully analysed and were extrapolated to $CeO_{1.500}$:

$$\Delta_fH^\circ(Ce_2O_3, \text{cr}, 298.15\ \text{K}) = -(1799.8 \pm 1.8)\ \text{kJ mol}^{-1}.$$

This value is different from the one selected by Cordfunke and Konings.[34]

3.4. PrO_2(cr,l)

3.4.1. Structure

PrO_2 has a face-centered cubic structure (space group $Fm\bar{3}m$). Hyde *et al.*[77] showed that PrO_2 is stable up to 587 K and Ushakov and Navtrosky[78] up to 663 K in oxygen gas. Above this temperature it decomposes to Pr_6O_{11}.

3.4.2. Heat capacity and entropy

The heat capacity of PrO_2 has been measured by Gardiner *et al.*[79] from 2.4 to 23 K, showing a lambda anomaly due to the antiferromagnetic ordering at ~13.5 K. No measurements of the heat capacity of PrO_2 in a wider temperature range have been made from which the standard entropy could be derived. For that reason the standard entropy has been estimated from the systematics in the lanthanide and actinide oxides as

$$S^\circ(298.15\ \text{K}) = (80.8 \pm 2.0)\ \text{J K}^{-1}\ \text{mol}^{-1}.$$

TABLE 6. The enthalpy of formation of Ce_2O_3(cr) at 298.15 K; ΔH_1° and ΔH_2° are the enthalpies of solution of Ce(cr) and Ce_2O_3(cr) in HCl(aq), respectively (after Cordfunke and Konings[34])

Authors	Method[a]	ΔH_1°/kJ mol^{-1}	ΔH_2°/kJ mol^{-1}	Δ_fH°/kJ mol^{-1}
Kuznetsov *et al.*[57]	C			−1823.4 ± 1.8[b]
Mah[72]	C			−1790.2 ± 1.5[c]
Baker and Holley, Jr.[73]	C			−1799.8 ± 1.8[d]
Huntelaar *et al.*[68]	S (0.25)	[−699.2 ± 0.2][e]	−442.7 ± 0.6	−1813.1 ± 0.8
				−1813.2 ± 3.2[f]
Putnam *et al.*[74]	H			−1809.2 ± 5.2
Selected value:				−1813.0 ± 2.0

[a]C: combustion calorimetry; S: solution calorimetry; values in parentheses give the concentration of the solvent in mol dm^{-3}; H = high temperature oxide melt solution calorimetry.
[b]For the enthalpy of the reaction $Ce_2O_3(\text{cr}) + \frac{1}{2}O_2(\text{g}) = 2CeO_2(\text{cr})$ the following value was used: −357.4 ± 1.1 kJ mol^{-1}.
[c]*idem*, −390.6 ± 0.4 kJ mol^{-1}.
[d]*idem*, −381.0 ± 0.7 kJ mol^{-1}.
[e]Spedding and Miller.[75]
[f]Cycle based on $CeCl_3$.

In a similar manner the high temperature heat capacity for the temperature range from 298.15 to 600 K was estimated as

$$C_p^\circ/(\mathrm{J\,K^{-1}\,mol^{-1}}) = 72.981 + 16.628 \times 10^{-3}(\mathrm{T/K}) - 0.9990 \times 10^{6}(\mathrm{T/K})^{-2}.$$

3.4.3. Enthalpy of formation

The enthalpy of formation of PrO_2 was determined by Eyring *et al.*[80] and Gramsch and Morss[81] using solution calorimetry in nitric acid. Recalculation of the results yields $-(949.3 \pm 4.3)$ kJ mol^{-1} and $-(959.1 \pm 2.3)$ kJ mol^{-1}, respectively, being significantly different, entirely due to differences in the solution enthalpies. The selected enthalpy of formation is derived from the work by Gramsch and Morss,[81] as it is based on an excellently characterised sample

$$\Delta_f H^\circ(PrO_2,\ \mathrm{cr},\ 298.15\ \mathrm{K}) = -(959.1 \pm 2.3)\ \mathrm{kJ\,mol^{-1}}.$$

Ushakov and Navtrosky[78] measured the enthalpy of the reaction

$$PrO_2 = \frac{1}{6}Pr_6O_{11}(\mathrm{cr}) + \frac{1}{12}O_2(\mathrm{g})$$

by DSC obtaining $\Delta_r H^\circ(298.15\ \mathrm{K}) = (10 \pm 2)$ kJ mol^{-1} at 663 K. Using the enthalpies of formation of PrO_2 and $PrO_{1.833}$ selected in this work, we calculate $\Delta_r H^\circ(298.15\ \mathrm{K}) = (9.6 \pm 5.8)$ kJ mol^{-1}, in excellent agreement.

3.5. $PrO_{1.833}$(cr,l)

3.5.1. Melting point

$PrO_{1.833}$ (also designated as Pr_6O_{11}) has a triclinic crystal structure (space group $P\bar{1}$). Pankratz[82] found a phase transition around 760 K. However, it can be concluded from the $PrO_{1.5}$–PrO_2 phase diagram proposed by Turcotte *et al.*[83] that the upper limit of stability of $PrO_{1.833}$ is about 750 K; above this temperature the PrO_{2-x} phase is stable in equilibrium with O_2(g).

Mordovin *et al.*[20] reported the melting point of $PrO_{1.833}$ as $T = (2315 \pm 30)$ K in Ar atmosphere, but mentioned that substantial dissociation of the sample occurred. The relevance of this measurement must thus be doubted.

3.5.2. Heat capacity and entropy

The low-temperature heat capacity of $PrO_{1.833}$ has not been measured. The selected standard entropy is interpolated between PrO_2(cr) and $PrO_{1.5}$:

$$S^\circ(298.15\ \mathrm{K}) = (79.2 \pm 2.0)\ \mathrm{J\,K^{-1}\,mol^{-1}}$$

The high-temperature enthalpy increment of $PrO_{1.833}$ was measured by Pankratz[82] from 398 to 1052 K and by Blomeke and Ziegler[29] from 383 to 1172 K. The data are in good agreement at low temperatures, but the difference increases steadily up to 1033 K where Pankratz[82] observed a phase transformation, whereas Blomeke and Ziegler[29] did not. As discussed above this phase transformation is very likely the peritectic decomposition. Since the sample of Blomeke and Ziegler[29] was heated in a capsule above this temperature before the measurement, (partial) decomposition probably has occurred, and their results might refer to the PrO_{2-x} phase. For that reason the data of Pankratz[82] below 760 K have been fitted to a polynomial equation, yielding for the heat capacity:

$$C_p^\circ/(\mathrm{J\,K^{-1}\,mol^{-1}}) = 68.4932 + 15.9207 \times 10^{-3}(\mathrm{T/K}) - 0.80968 \times 10^{6}(\mathrm{T/K})^{-2}.$$

3.5.3. Enthalpy of formation

The enthalpy of formation of $PrO_{1.833}$ was measured by Stubblefield *et al.*[84] by solution calorimetry and by Fitzgibbon *et al.*[85] using both solution and combustion calorimetry. The recalculated values are summarized in Table 7, based on a Hess cycle with Pr_2O_3. The results are in reasonable agreement and we select

$$\Delta_f H^\circ(PrO_{1.833},\ \mathrm{cr},\ 298.15\ \mathrm{K}) = -(944.6 \pm 2.5)\ \mathrm{kJ\,mol^{-1}}.$$

TABLE 7. The enthalpy of formation of $PrO_{1.833}$ and Pr_2O_3(cr) at 298.15 K; ΔH_1° and ΔH_2° are the enthalpies of solution of Pr(cr) and $PrO_{1.833}$(cr) in HNO_3(aq), Pr(cr) and Pr_2O_3(cr) in HCl(aq) or HNO_3(aq), respectively (after Cordfunke and Konings[34])

Authors	Method[a]	ΔH_1°/kJ mol^{-1}	ΔH_2°/kJ mol^{-1}	$\Delta_f H^\circ$/kJ mol^{-1}
$PrO_{1.833}$				
Stubblefield *et al.*[84]	S (6.0)		-183.3 ± 0.4	-943.5 ± 2.1
Fitzgibbon *et al.*[85]	S (6.0)		-179.6 ± 2.0	-947.0 ± 2.3
	S (6.0)		-179.9 ± 2.0	-947.0 ± 3.2
	C			-943.2 ± 0.8
Selected value:				-944.6 ± 2.5
Pr_2O_3				
Stubblefield *et al.*[84]	S (6.0)[b]	$[-1020.9 \pm 3.4]$[c]	-447.7 ± 0.8	-1831.6 ± 3.5
Fitzgibbon *et al.*[85]	S (2.0)	-692.2 ± 1.3	-432.0 ± 1.4	-1809.9 ± 3.0
Selected value:				-1809.9 ± 3.0

[a]C: combustion calorimetry; S: solution calorimetry; values in parentheses give the concentration of the solvent in mol dm^{-3}
[b]The enthalpy of solution in HNO_3(aq).
[c]The enthalpy of solution of Pr in 6.0 mol dm^{-3} HNO_3(aq) is from Ref. 86.

TABLE 8. The enthalpy of formation of phases in the PrO_2-$PrO_{1.5}$ system

Compound	$\Delta_f H°(298.15\ K)/kJ\ mol^{-1}$	Authors
$PrO_{1.703}$	$-(926.3 \pm 2.2)$	Stubblefield *et al.*[84]
$PrO_{1.717}$	$-(928.4 \pm 2.6)$	Fitzgibbon *et al.*[85]
$PrO_{1.804}$	$-(938.9 \pm 2.0)$	Fitzgibbon *et al.*[85]

The enthalpies of formation of several other PrO_{2-x} compositions were measured by Stubblefield *et al.*[84] and Fitzgibbon *et al.*[85] by solution calorimetry, the recalculated results are given in Table 8. These values show a regular trend between $PrO_{1.5}$ and PrO_2, as shown in Fig. 5.

3.6. Pr_2O_3(cr,l)

3.6.1. Polymorphism and melting point

At room temperature praseodymium sesquioxide has the rare earth hexagonal A-type structure (space group $P\bar{3}m1$).

Lopato *et al.*[11] reported that A-type Pr_2O_3 transforms to a hexagonal H-type structure at T = 2318 K, and Shevthenko and Lopato[13] at T = 2303 K. They also found that the H-type phase transforms to a cubic X-type structure at T = 2393 K[11] and T = 2403 K.[13] No information on the calibration of these measurements has been found, but assuming the data refer to IPTS-68, a correction of −1 K needs to be applied for ITS-90. The results by Kravchonskaya *et al.*[87] are in agreement, but these authors only presented them in graphical form (A → H at about 2314 K and H → X at about 2417 K, as extracted from digitized graphs). We select $T_{trs} = (2310 \pm 30)$ K for the A → H transformation, $T_{trs} = (2397 \pm 30)$ K for the H → X transformation.

The measurements of the melting temperature of Pr_2O_3 have been summarized in Table 9, which is based on the IUPAC review by Coutures and Rand;[15] the results being corrected to ITS-90. The selected melting point is (2583 ± 25) K.

3.6.2. Heat capacity and entropy

The low-temperature heat capacity of A-Pr_2O_3 has been measured by Lyutsareva *et al.*, unpublished results as cited by Gruber *et al.*[69] Their results are somewhat high near room temperature, and were smoothed together with the high-temperature data by Gruber *et al.*[69] giving no weight to the results above 185 K. The derived standard entropy at T = 298.15 K is selected here

$$S°(298.15\ K) = (152.7 \pm 0.3)\ J\,K^{-1}\,mol^{-1}.$$

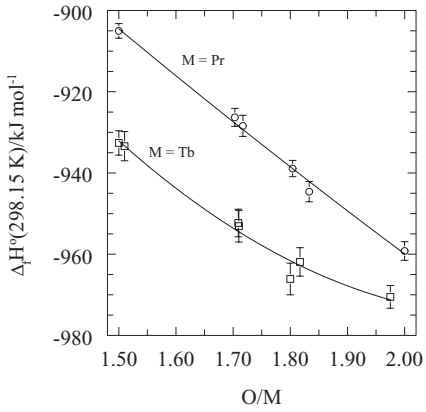

FIG. 5. The enthalpy of formation of compositions in the PrO_2-$PrO_{1.5}$ (□) and TbO_2-$TbO_{1.5}$ (□) systems.

TABLE 9. Temperature of melting of praseodymium sesquioxide

	T_{fus}/K	
Authors	Reported	ITS-90
Foex[19]	2668	2582
Mordovin *et al.*[20]	2390 ± 30	2493 ± 30
Treswjatskii *et al.*[22]	2533 ± 20	2532 ± 20
Coutures *et al.*[23]	2585 ± 10	2584 ± 10
Kravchonskaya *et al.*[87]	2573[a]	
Mizuno *et al.*[24]	2549 ± 20	2535 ± 20
Shevthenko and Lopato[13]	2553	2552
Selected value:		2583 ± 25

[a]Derived digitally from the graph for the HfO_2-Pr_2O_3 diagram.

The high-temperature enthalpy increment of A-Pr_2O_3 has been measured by Pankratz[82] and Kuznetsov and Rezukhina.[88] The former study covers the temperature range from 298.15 to 1800 K. The latter the temperature range from 293 to 1200 K and have only been reported in the form of an equation. Our recommended heat capacity equation is solely based on the results of Pankratz,[82] constrained to $C_p°(298.15\ K) = 118.15\ J\,K^{-1}\,mol^{-1}$ from the low-temperature measurements:

$$C_p°/(J\,K^{-1}\,mol^{-1}) = 121.6594 + 25.5611 \times 10^{-3}(T/K) - 0.98942 \times 10^{6}(T/K)^{-2}.$$

This equation is extrapolated to the transition temperature. No heat-capacity or enthalpy measurements have been reported for the H, X, and liquid phases of Pr_2O_3. The properties of these modifications have been estimated in a similar way as for La_2O_3 and Ce_2O_3. We thus obtain for the transition enthalpies

$$\Delta_{trs}H°(A \rightarrow H) = (28 \pm 8)\ kJ\,mol^{-1},$$
$$\Delta_{trs}H°(H \rightarrow X) = (19 \pm 5)\ kJ\,mol^{-1},$$
$$\Delta_{fus}H° = (88 \pm 10)\ kJ\,mol^{-1}.$$

For the heat capacity of the high temperature modifications of Pr_2O_3 we estimate

$$C_p°(H, T) = C_p°(X, T) = 145\ J\,K^{-1}\,mol^{-1},$$
$$C_p°(liq, T) = 157\ J\,K^{-1}\,mol^{-1}.$$

3.6.3. Enthalpy of formation

The enthalpy of formation of Pr_2O_3 has been assessed by Cordfunke and Konings[34] recently, and we accept the selected value from that work, since no new information has been published since

$$\Delta_f H°(Pr_2O_3,\ cr,\ 298.15\ K) = -(1809.9 \pm 3.0)\ kJ\,mol^{-1}.$$

This value is based on the solution calorimetric study by Fitzgibbon *et al.*,[85] who measured the enthalpy of solution of both Pr(cr) and Pr_2O_3(cr) in 2.0 mol dm^{-3} HCl(aq) (see Table 7). Stubblefield *et al.*[84] determined the enthalpy of reaction of Pr_2O_3(cr) with 6.0 mol dm^{-3} HNO_3(aq), but this approach is considered less reliable since some of the hydrogen that is produced during dissolution of the metal, might reduce the nitric acid.

3.7. Nd_2O_3(cr,l)

3.7.1. Polymorphism and melting point

Nd_2O_3 has a peculiar place in the lanthanide sequioxide series. It commonly has a A-type hexagonal sesquioxide structure (space group $P\bar{3}m1$) at room temperature, but also the C-type structure occurs at room temperature. Systematic studies[89] suggest that the C-form is the thermodynamically stable modification from room temperature to about T = 873–923 K. Impurities may affect this phase stability, but it is now generally accepted that the boundary between the A and C rare earth structures occurs near or at Nd_2O_3 (see Fig. 4). However, as most of the thermodynamic measurements reported in literature have been made for the A-type phase, our recommended values refer to this phase.

Pankratz *et al.*[90] found a small thermal anomaly at ~1345 K by drop calorimetry whose origin is unknown (see below).

At high temperatures Nd_2O_3 exhibits the common complex polymorphism of the light rare earth oxides. The phase transition to a H-type hexagonal structure (space group $P6_3/mmc$) is observed at T = 2375 K (Refs. 10,11 and 91) and T = 2333 K.[13] This phase subsequently transforms to a cubic structure (space group $Im\bar{3}m$) at T = 2473 K.[10,11,91] These measurements must all be converted to ITS-90. The measurements of Foex and Traverse[10] must be corrected by +14 K, following the procedure outlined by Coutures and Rand.[15] Lopato *et al.*,[11] Wehner *et al.*,[12] and Shevthenko and Lopato[13] reported no (detailed) information on the calibration of their measurements, but assuming the data refer to IPTS-68, a correction of −1 K needs to be applied. We select T_{trs} = (2379 ± 30) K for the A → H transformation, T_{trs} = (2477 ± 30) K for the H → X transformation.

The measurements of the melting temperature of Nd_2O_3 have been summarized in Table 10, which is based on the IUPAC review by Coutures and Rand.[15] The selected melting point is (2577 ± 15) K.

TABLE 10. Temperature of melting of neodymium sesquioxide (after Coutures and Rand[15])

	T_{fus}/K	
Authors	Reported	ITS-90
Lambertson and Gunzel[17]	2545 ± 20	2551 ± 20
Foex[19]	2583	2598
Mordovin *et al.*[20]	2486 ± 30	2489 ± 30
Noguchi and Mizuno[21]	2506 ± 20	2510 ± 20
Gibby *et al.*[92]	2573 ± 25	2572 ± 25
Treswjatskii *et al.*[22]	2593 ± 20	2592 ± 20
Coutures *et al.*[23]	2598 ± 10	2597 ± 10
Bober *et al.*[93]	2540 ± 40	2539 ± 40
Mizuno *et al.*[24]	2563 ± 20	2550 ± 20
Shevthenko and Lopato[13]	2573	2572
Coutures[94]	2613 ± 10	2612 ± 10
Salikhov and Kan[95]		2564 ± 10
Selected value:		2577 ± 15

3.7.2. Heat capacity and entropy

The low-temperature heat capacity of A-type Nd_2O_3 has been measured by Goldstein *et al.*[26] from 16 to 300 K, and by Justice and Westrum Jr.[28] from 5 to 350 K. Above 100 K both data sets agree within 0.5%, below 100 K the deviations significantly increase. The recommended standard entropy of Nd_2O_3 is derived from the low-temperature heat capacity data of Justice and Westrum Jr.[28] who obtained $S°(298.15\ K) - S°(5\ K) = 146.65\ J\ K^{-1}\ mol^{-1}$. Justice and Westrum estimated $S°(5\ K) - S°(0\ K) = 11.80\ J\ K^{-1}\ mol^{-1}$, accounting for the 2*R* ln (2) contribution of the ground state doublet of the $^4I_{9/2}$ multiplet, resulting in

$$S°(298.15\ K) = (158.7 \pm 1.0)\ J\ K^{-1}\ mol^{-1}.$$

The high-temperature enthalpy increment has been measured by Blomeke and Ziegler[29] from 384 to 1172 K and Pankratz *et al.*[90] from 400 to 1795 K. The data of the two studies are in excellent agreement and smoothly join the low-temperature data (Fig. 6). Pankratz *et al.*[90] observed a minor thermal anomaly near 1395 K. We think this is an experimental artefact, as high temperature X-ray diffraction studies[10,96] do not reveal any evidence for such a transformation. Our recommended heat capacity equation is based on a polynomial fit of the results of both studies. The equation is constrained to $C_p^\circ = 111.34\ J\ K^{-1}\ mol^{-1}$ from the low-temperature measurements.[28] We thus obtain

$$C_p^\circ/(J\,K^{-1}\,mol^{-1}) = 117.1079 + 28.13655 \times 10^{-3}(T/K) - 1.25845 \times 10^{6}(T/K)^{-2}.$$

This equation is extrapolated to the transition temperature. No heat-capacity or enthalpy measurements have been reported for the H, X, and liquid phases of Nd_2O_3. The properties of these modifications have been estimated in a similar way as for La_2O_3 and La_2O_3. We thus obtain for the transition enthalpies

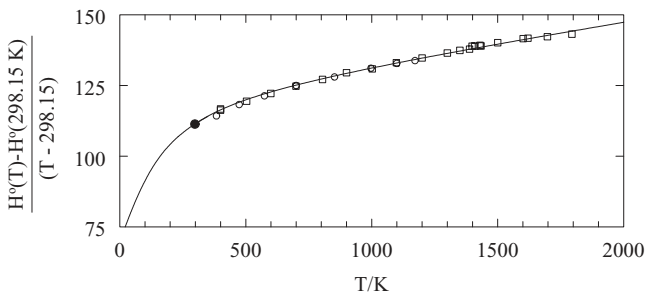

FIG. 6. The reduced enthalpy increment (in J $K^{-1}\,mol^{-1}$) of Nd_2O_3; ○, Blomeke and Ziegler[29]; □, King *et al.*[27]; •, value derived from the low-temperature measurements by Justice and Westrum, Jr.;[28] the curve shows the recommended equation.

$$\Delta_{trs}H^\circ(A \rightarrow H) = (29 \pm 8)\ \text{kJ mol}^{-1},$$
$$\Delta_{trs}H^\circ(H \rightarrow X) = (20 \pm 5)\ \text{kJ mol}^{-1},$$
$$\Delta_{fus}H^\circ = (88 \pm 10)\ \text{kJ mol}^{-1}.$$

For the heat capacity of the high temperature modifications of Nd_2O_3 we estimate

$$C_p^\circ(H, T) = C_p^\circ(X, T) = 145\ \text{J K}^{-1}\ \text{mol}^{-1},$$
$$C_p^\circ(\text{liq}, T) = 160\ \text{J K}^{-1}\ \text{mol}^{-1}.$$

3.7.3. Enthalpy of formation

The enthalpy of formation of hexagonal Nd_2O_3 has been assessed by Cordfunke and Konings[34] recently, and we accept the selected value from that work, because no new information has been published since

$$\Delta_f H^\circ(Nd_2O_3,\ \text{cr},\ 298.15\ \text{K}) = -(1806.9 \pm 3.0)\ \text{kJ mol}^{-1}.$$

This value has been derived from the studies listed in Table 11 (corrected for some errors), that have been employing solution as well as combustion calorimetry. The three combustion calorimetric measurements[40,98,99] are in reasonable agreement, but the value by Huber Jr. and Holley Jr.,[98] $\Delta_f H^\circ(298.15\ \text{K}) = -(1808.1 \pm 1.0)\ \text{kJ mol}^{-1}$, was considered to be far more accurate since the starting materials were of rather high purity and the combustion was complete. The solution calorimetric studies heavily rely on the value for the enthalpy of solution of Nd metal used in the Hess cycle to derive the enthalpy of formation of Nd_2O_3. Cordfunke and Konings[34] therefore used the enthalpy of solution of Nd(cr) in HCl(aq) by Merli *et al.*,[39] Tiflova,[106] and Stuve,[105] which are consistent with each other and measured on high-purity Nd(cr) samples, to recalculate the reported measurements in a systematic manner. The selected enthalpy of formation is the mean of the results of Huber Jr. and Holley Jr.[98] and the values derived from the results of Fitzgibbon *et al.*[100] and Popova and Monaenkova.[103]

3.8. Pm_2O_3(cr,l)

3.8.1. Polymorphism and melting point

The monoclinic B-type (space group C2/m) and the cubic C-type (space group $Fm\overline{3}m$) rare earth sesquioxides structure of Pm_2O_3 have been found at room temperature, like is the case for its neighboring sesquioxides. According to the generally accepted stability diagram of the lanthanide sesquioxides, the C-type structure is probably the thermodynamic stable modification at room temperature. Chikalla *et al.*[107] found that the B-type form is stable above about T = 1073 K, which is in reasonable agreement with the trend in the lanthanide sesquioxides as shown in Fig. 4, but claimed that this transition is irreversible. They determined the transition temperatures and the melting point, which we select here after a correction of −1 K, assuming the data refer to IPTS-68: T = (2013 ± 20) K for the B → A transformation, T = (2407 ± 20) K for the A → H transformation, and T = (2497 ± 20) K for the H → X transformation.

The melting point of Pm_2O_3 was measured by Gibby *et al.*[108] as T = (2408 ± 30) K, and by Chikalla *et al.*[107] as T = (2593 ± 30) K. The former value is significantly lower than those of the neighboring Nd_2O_3 and Sm_2O_3, and must be in error. We therefore select the value of Chikalla *et al.*[107] which becomes T = (2592 ± 30) K on ITS-90.

3.8.2. Heat capacity and entropy

Konings[109] estimated the standard entropy of Pm_2O_3 from a systematic analysis of the trend in the lanthanide sesquioxides, describing the entropy as the sum of the lattice and excess components. The lattice component was obtained by interpolation of the values for La_2O_3, Gd_2O_3, and Lu_2O_3, the excess component from the ground state degeneracy of the $^2F_{7/2}$ multiplet. This value is selected here

$$S^\circ(298.15\ \text{K}) = (158.0 \pm 5.0)\ \text{J K}^{-1}\ \text{mol}^{-1}.$$

TABLE 11. The enthalpy of formation of Nd_2O_3(cr) at 298.15 K; ΔH_1° and ΔH_2° are the enthalpies of solution of Nd(cr) and Nd_2O_3(cr) in HCl(aq), respectively (after Cordfunke and Konings[34])

Authors	Method[a]	ΔH_1°/kJ mol^{-1}	ΔH_2°/kJ mol^{-1}	$\Delta_f H^\circ$/kJ mol^{-1}
Muthmann and Weis[40]	C			−1820
Matignon[97]	S (0.5)		−441.4	
Huber, Jr. and Holley, Jr.[98]	C			−1808.1 ± 1.0
Spedding *et al.*[99]	C			−1798.2
				−1789.2
Fitzgibbon *et al.*[100]	S (2.0)	[−691.7 ± 1.5][b]	−434.0 ± 0.6	−1807.1 ± 3.1
	S (4.0)	[−693.6 ± 1.5][c]	−438.3 ± 1.3	−1807.3 ± 2.2
Yashvili and Gvelesiani[101]	S (1.0)	[−689.6 ± 2.0][d]	−434.7 ± 2.1	−1799.6 ± 4.5
Morss *et al.*[102]	S (6.0)	[−695.7 ± 1.8][c]	−419.6 ± 6.0	−1831.7 ± 7.0
Popova and Monaenkova[103]	S (2.19)	−686.8 ± 1.0	−434.2 ± 0.7	−1797.1 ± 2.1
		[−690.8 ± 1.6][e]		−1805.1 ± 3.3
		[−691.9 ± 2.0][d]		−1807.3 ± 4.1
Hennig and Oppermann[104]	S (4.0)	[−691.7 ± 1.5][b]	−419.5 ± 0.4	−1816.1 ± 1.9
Selected value:				−1806.9 ± 3.0

[a]C: combustion calorimetry; S: solution calorimetry; values in parentheses give the concentration of the solvent in mol dm^{-3};
[b]Estimated from the data of Merli *et al.*[39]
[c]Stuve[105]
[d]Merli *et al.*[39]
[e]Tiflova.[106]

The high temperature heat capacity equations for C-Pm_2O_3 (298–1073 K) and B-Pm_2O_3 (1073–2013 K) have been estimated from the values for the other lanthanide sesquioxides as

$$C_p^\circ(C,T)/(J\,K^{-1}\,mol^{-1}) = 122.9493 + 30.0141 \times 10^{-3}(T/K) - 1.85217 \times 10^{6}(T/K)^{-2}$$

$$C_p^\circ(B,T)/(J\,K^{-1}\,mol^{-1}) = 129.454 + 19.960 \times 10^{-3}(T/K).$$

For the heat capacity high temperature modifications we have assumed the same values as estimated for Sm_2O_3 (see below)

$$C_p^\circ(H,T) = C_p^\circ(X,T) = 165\ J\,K^{-1}\,mol^{-1},$$
$$C_p^\circ(liq,T) = 179\ J\cdot K^{-1}\,mol^{-1}.$$

The transition enthalpies have been estimated as outlined for Ce_2O_3:

$$\Delta_{trs}H^\circ(C \rightarrow B) = (7 \pm 3)\ kJ\,mol^{-1},$$
$$\Delta_{trs}H^\circ(B \rightarrow A) = (6 \pm 3)\ kJ\,mol^{-1},$$
$$\Delta_{trs}H^\circ(A \rightarrow H) = (31 \pm 8)\ kJ\,mol^{-1},$$
$$\Delta_{trs}H^\circ(H \rightarrow X) = (20 \pm 5)\ kJ\,mol^{-1},$$
$$\Delta_{fus}H^\circ = (88 \pm 10)\ mol^{-1}.$$

3.8.3. Enthalpy of formation

Experimental values for the standard molar enthalpy of formation of promethium sesquioxide are not available in the literature. The selected $\Delta_fH^\circ(298.15\ K)$ value has been estimated by Cordfunke and Konings[34] using the dependence of $\Delta_fH^\circ(Ln_2O_3, cr) - 2\Delta_fH^\circ(Ln^{3+}, aq)$ on the atomic radii of the trivalent lanthanides and the enthalpy of formation of $Pm^{3+}(aq)$. $Pm_2O_3(cr)$ is a boundary compound of the domains of existence of the hexagonal and monoclinic rare earth sesquioxides, both crystal structures are acceptable for promethium sesquioxide with equal degree of probability.[110] Assuming the hexagonal crystal structure of $Pm_2O_3(cr)$ to be the stable form, the enthalpy of formation was calculated as

$$\Delta_fH^\circ(Pm_2O_3,\ cr) = -(1811 \pm 21)\ kJ\,mol^{-1}.$$

3.9. Sm_2O_3(cr,l)

3.9.1. Polymorphism and melting point

The monoclinic B-type (space group C2/m) as well as the cubic C-type (space group $Fm\bar{3}m$) structures of samarium sesquioxide have been reported to be stable at room temperature. According to the generally accepted stability diagram of the lanthanide sesquioxides (see Fig. 4), the C-type structure is probably the thermodynamic stable modification from room temperature to about 900 K. However, the energetics of the two modifications are probably very close and the transformation kinetics very sluggish. Since most of the thermodynamic measurements have been made for the B modification, our recommended values refer to this phase only.

TABLE 12. Temperature of melting of samarium sesquioxide (after Coutures and Rand[15])

	T_{fus}/K	
Authors	Reported	ITS-90
Wisnyi and Pijanowski[111]	2573 ± 50	2590 ± 50
Curtis and Johnson[112]	2623 ± 50	2626 ± 50
Foex[19]	2593	2607
Mordovin *et al.*[20]	2536 ± 30	2539 ± 30
Noguchi and Mizuno[21]	2506 ± 20	2509 ± 20
Gibby *et al.*[92]	2623 ± 25	2622 ± 25
Treswjatskii *et al.*[22]	2613 ± 20	2612 ± 20
Coutures *et al.*[23]	2598 ± 10	2598 ± 10
Mizuno *et al.*[24]	2583	2570
Shevthenko and Lopato[13]	2583	2582
Selected value:		2613 ± 15

Foex and Traverse[10] reported that B-type Sm_2O_3 transforms to the A-type Ln_2O_3 structure at ~2173 K. They also found that the A → H and H → X transformation occurs at ~2373 and 2473–2523 K, respectively. These values must be converted to ITS-90 using the procedure outlined by Coutures and Rand,[15] leading to a correction of +14 K. Lopato *et al.*[11] reported the B → A transformation at T = 2193 K and the A → H and H → X transformations at T = 2403 K and T = 2553 K, respectively. Shevthenko and Lopato[13] reported the B → A transformation at T = 2143 K, the A → H at T = 2343 K, and the H → X transformations at T = 2498 K. No information on the calibration of these measurements has been found, but assuming the data refer to IPTS-68, a correction of −1 K needs to be applied to convert to ITS-90. We select T_{trs} = (2190 ± 20) K for the B → A transformation, T_{trs} = (2395 ± 20) K for the A → H transformation and T_{trs} = (2533 ± 30) K for the H → X transformation.

The measurements of the melting temperature of Sm_2O_3 have been summarized in Table 12, which is based on the IUPAC review by Coutures and Rand.[15] The selected melting point is (2613 ± 15) K.

3.9.2. Heat capacity and entropy

The low-temperature heat capacity of B-type Sm_2O_3 has been measured by Justice and Westrum Jr.[113] from 10 to 350 K. They obtained $S^\circ(298.15\ K) - S^\circ(10\ K) = 138.99\ J\,K^{-1}\,mol^{-1}$. Extrapolation of these results to T = 0 K, and accounting for the 2Rln (2) contribution of the ground state doublet of the split $^6H_{7/2}$ multiplet, gives for the entropy at T = 298.15 K:

$$S^\circ(298.15\ K) = (150.6 \pm 0.3)\ J\,K^{-1}\,mol^{-1}.$$

The high-temperature enthalpy increment of Sm_2O_3 has been measured by Curtis and Johnson,[112] Pankratz *et al.*,[114] and Gvelesiani *et al.*[115]. The latter two groups measured the B-type hexagonal and the C-type cubic modifications, the results being in good agreement (Fig. 7). Curtis and Johnson[112] reported data on a sample consisting of a mixture of B and C, their results being in poor agreement with the other results. Pankratz *et al.*[114] reported a transition (at about 1195 K) with a small enthalpy effect (1.045 kJ mol^{-1}) for B-type Sm_2O_3 that was not observed by Gvelesiani *et al.*[115]. Also DTA analysis by Curtis and Johnson[112] did not reveal phase transformations up

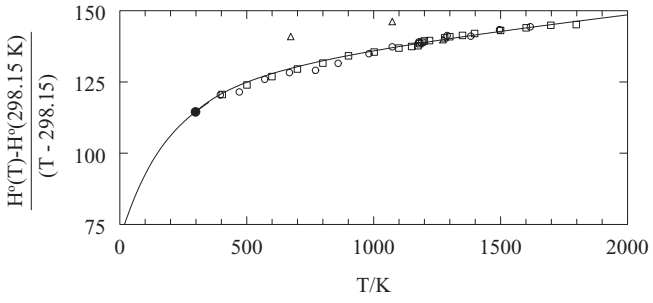

FIG. 7. The reduced enthalpy increment (in J K^{-1} mol^{-1}) of B-Sm_2O_3; ○, Gvelesiani *et al.*[115]; □, Pankratz *et al.*[114]; △, Curtis and Johnson[112]; •, value derived from the low-temperature measurements by Justice and Westrum Jr.[113]; the curve shows the recommended equation.

to 1403 K. Since there is no additional confirmation of this effect, we have neglected it in our analysis. Our recommended heat capacity equation for B-Sm_2O_3 is based on the combined results of Pankratz *et al.*[114] and Gvelesiani *et al.*[115]:

$$C_p^\circ/(\mathrm{J\,K^{-1}\,mol^{-1}}) = 129.7953 + 19.03114 \times 10^{-3}(\mathrm{T/K}) - 1.86227 \times 10^{6}(\mathrm{T/K})^{-2}.$$

This equation is constrained to $C_p^\circ(298.15\ \mathrm{K}) = 114.52\ \mathrm{J\,K^{-1}\,mol^{-1}}$, as derived from the low-temperature measurements Justice and Westrum Jr.[113] For C-Sm_2O_3 we obtain (without constraint)

$$C_p^\circ/(\mathrm{J\cdot K^{-1}\,mol^{-1}}) = 132.4358 + 18.7799 \times 10^{-3}(\mathrm{T/K}) - 2.40860 \times 10^{6}(\mathrm{T/K})^{-2}.$$

The entropy change of the C → B transformation in the lanthanide sesquioxides was estimated from high pressure studies by Hoekstra[116] as 6.3 J K^{-1} mol^{-1} using the Clausius-Clapeyron equation, which is selected here. This quantity can also be estimated from the differences of the enthalpy equations at the transition temperature (−0.3 kJ mol^{-1} at 900 K), plus the difference in the enthalpies of formation at 298.15 K (3.8 ± 6.2 kJ mol^{-1}), giving $\Delta_{trs}H^\circ = (3.5 \pm 6.2)$ kJ mol^{-1} corresponding to $\Delta_{trs}S^\circ = 3.9$ J K^{-1} mol^{-1}, in fair agreement with Hoekstra's estimate.[116]

No heat-capacity or enthalpy measurements have been reported for the H, X, and liquid phases of Sm_2O_3. The properties of these modifications have been estimated in a similar way as for La_2O_3 and Ce_2O_3. We thus obtain for the transition enthalpies

$$\Delta_{trs}H^\circ(\mathrm{C \rightarrow B}) = (6 \pm 3)\ \mathrm{kJ\,mol^{-1}}$$
$$\Delta_{trs}H^\circ(\mathrm{B \rightarrow A}) = (7 \pm 3)\ \mathrm{kJ\,mol^{-1}}$$
$$\Delta_{trs}H^\circ(\mathrm{A \rightarrow H}) = (32 \pm 8)\ \mathrm{kJ\,mol^{-1}}$$
$$\Delta_{trs}H^\circ(\mathrm{H \rightarrow X}) = (20 \pm 5)\ \mathrm{kJ\,mol^{-1}}$$
$$\Delta_{fus}H^\circ = (89 \pm 10)\ \mathrm{kJ\,mol^{-1}}$$

For the heat capacity of the high temperature modifications of Sm_2O_3 we estimate

$$C_p^\circ(\mathrm{A,T}) = 140\ \mathrm{J\,K^{-1}\,mol^{-1}}$$
$$C_p^\circ(\mathrm{H,T}) = C_p^\circ(\mathrm{X,T}) = 165\ \mathrm{J\,K^{-1}\,mol^{-1}}$$
$$C_p^\circ(\mathrm{liq,T}) = 179\ J\ \mathrm{K^{-1}\,mol^{-1}}.$$

3.9.3. Enthalpy of formation

The enthalpy of formation of monoclinic and cubic Sm_2O_3 have been assessed by Cordfunke and Konings[34] recently, and we accept the selected value from that work, since no new information has been published since

$$\Delta_fH^\circ(\mathrm{Sm_2O_3, monoclinic, 298.15\,K}) = -(1823.0 \pm 4.0)\ \mathrm{kJ\,mol^{-1}}$$
$$\Delta_fH^\circ(\mathrm{Sm_2O_3, cubic, 298.15\ K}) = -(1826.8 \pm 4.8)\ \mathrm{kJ\,mol^{-1}}.$$

The values for the enthalpy of formation of monoclinic Sm_2O_3 obtained by Huber Jr. *et al.*[117] and Baker *et al.*[118] by oxygen-bomb combustion calorimetry and by Baker *et al.*[118] using solution calorimetry are in reasonable agreement (see Table 13), and are the basis for the selected value. Later results by Gvelesiani and Yashvili[38] significantly deviate from this value, but the nonmetallic impurities in their samples are not reported, which could be an explanation for the difference. The measurements by Hennig and Oppermann[119] of the enthalpy of solution of Sm_2O_3 in HCl(aq) is in good agreement with the

TABLE 13. The enthalpy of formation of Sm_2O_3(cr) at 298.15 K; ΔH_1° and ΔH_2° are the enthalpies of solution of Sm(cr) and Sm_2O_3(cr) in HCl(aq), respectively (after Cordfunke and Konings[34])

Authors	Method[a]	ΔH_1°/kJ mol^{-1}	ΔH_2°/kJ mol^{-1}	Δ_fH°/kJ mol^{-1}
Huber Jr. *et al.*[117]	C			−1815.4 ± 2.0
Montgomery and Hubert[36]	S (0.48)		−408.8 ± 1.4	
Spedding *et al.*[99]	C			−1777.3
Gvelesiani and Yashvili[38]	S (0.7)	−683.7 ± 5.4	−389.5 ± 0.4	−1835.4 ± 10.8
	S (1.0)	−682.6 ± 2.2	−391.2 ± 3.6	−1831.5 ± 5.7
Baker *et al.*[118]	C			−1824.2 ± 2.6
	S (2.0)	−690.1 ± 1.3	−417.1 ± 1.2	−1820.8 ± 2.9
	S (3.99)	−689.5 ± 3.8	−406.7 ± 4.6	−1830.7 ± 8.9
Hennig and Oppermann[119]	S (4.0)		−412.8 ± 0.5	−1824.6 ± 7.6[b]
Selected value:				−1823.0 ± 4.0

[a]C: combustion calorimetry; S: solution calorimetry; values in parentheses give the concentration of the solvent in mol dm^{-3}

[b]Using ΔH_1° from Baker *et al.*[118]

results by Baker *et al.*[118] However, because of the poor characterisation of the Sm_2O_3 sample and the fact that the measurements by Hennig and Opperman deviate significantly for most of the lanthanide sesquioxides (see La_2O_3, Nd_2O_3, and Eu_2O_3) this value was not taken into account by Cordfunke and Konings.[34]

The enthalpy of formation of cubic Sm_2O_3 was also derived from the work of Baker *et al.*[118] and Gvelesiani and Yashvili,[38] who both determined the value for $\Delta_{trs}H°$(monoclinic/cubic) by solution calorimetric measurements of the two crystallographic modifications. As discussed by Cordfunke and Konings[34] the results are in reasonable agreement, $-(3.7 \pm 2.6)$ kJ mol^{-1} and $= -(5.5 \pm 4.0)$ kJ mol^{-1}, respectively, but the value of Baker *et al.*[118] is preferred for reasons given in the preceding paragraph.

3.10. Eu_2O_3(cr,l)

3.10.1. Polymorphism and melting point

Europium sesquioxide has a complex polymorphism: both the monoclinic (B-structure) and the cubic (C-structure) are found to coexist at room temperature. At standard pressure conditions the C form is the most stable form, the B form thus being metastable. The C-Eu_2O_3 phase has a fluorite-type cubic structure (space group $Fm\bar{3}m$). The B-Eu_2O_3 form is the monoclinic modification of europium sesquioxide (space group $C2/m$).

The C → B transformation has been studied extensively. Stecura[120] reported that this transition is irreversible, but most other studies have found that the transformation kinetics are sluggish but reversible. The temperature was found at 1348 K (Ref. 121) and 1373 K.[89] Ainscough *et al.*[122] observed significant differences in the transformation temperature and rate for air and hydrogen atmospheres, the transformation taking place faster and at lower temperature (75 K) in air. This was confirmed by Suzuki *et al.*[123] for air and vacuum. More recently Sukhushina *et al.*[124] measured the oxygen potential of stoichiometric B-Eu_2O_3 and C–Eu_2O_3 between 1150 and 1450 K. From the results they derive $T_{trs} = 1350.6$ K from the intersection of the curves. The phase transformations at high temperatures have been studied by Foex and Traverse.[10] They reported the B → A transformation at T = 2313 K, the A → H transformation at T = 2413 K, and the H → X transformation at T = 2543 K. These results must be converted to ITS-90 by +14 K, following the procedure outlined by Coutures and Rand.[15]

We select $T_{trs} = (1350 \pm 15)$ K for the C → B transformation, $T_{trs} = (2327 \pm 30)$ K for the B → A transformation, $T_{trs} = (2427 \pm 30)$ K for the A → H transformation, and $T_{trs} = (2557 \pm 30)$ K for the H → X transformation.

The measurements of the melting temperature of Eu_2O_3 have been summarized in Table 14, which is based on the IUPAC review by Coutures and Rand[15]; the results being corrected to ITS-90. The selected melting point is (2622 ± 20) K.

TABLE 14. Temperature of melting of europium sesquioxide (after Coutures and Rand[15])

	T_{fus}/K	
Authors	Reported	ITS-90
Wisnyi and Pijanowski[111]	2323 ± 30	2339 ± 30
Schneider[125]	2513 ± 10	2519 ± 10
Foex[19]	2603	2617
Mordovin *et al.*[20]	2276 ± 30	2278 ± 30
Noguchi and Mizuno[21]	2564 ± 20	2567 ± 20
Coutures *et al.*[23]	2633 ± 10	2632 ± 10
Mizuno *et al.*[24]	2618 ± 20	2605 ± 20
Selected value:		2622 ± 20

3.10.2. Heat capacity and entropy

The low-temperature heat capacity of C-Eu_2O_3 has been measured by Lyutsareva *et al.*[126] from 7 to 319 K and these authors also measured the low-temperature heat capacity of B-Eu_2O_3 from 8 to 311 K. The heat capacity and standard entropy values for B-Eu_2O_3 are consistent with the results for the other A- and B-type Ln_2O_3 compounds considering the lattice and excess electronic components.[127] For that reason we recommend the entropy value for B-Eu_2O_3 from this work, with an increased uncertainty:

$$S°(298.15\ \text{K}) = (143.5 \pm 0.5)\ \text{J K}^{-1}\ \text{mol}^{-1}.$$

The heat capacity and entropy values for C-Eu_2O_3, on the other hand, only poorly agree with the results for the C-type Ln_2O_3 compounds, giving a too high lattice component above 200 K after subtraction of the excess heat capacity using crystal field data for Eu^{3+} in a cubic (C) environment. A similar observation was made for Pr_2O_3 measured by the same authors (see above). We therefore reject the standard entropy $S°(298.15\ \text{K}) = (142.24 \pm 0.14)\ \text{J K}^{-1}\ \text{mol}^{-1}$ derived from that work, and estimate for C-Eu_2O_3:

$$S°(298.15\ \text{K}) = (136.4 \pm 2.0)\ \text{J K}^{-1}\ \text{mol}^{-1}.$$

The high-temperature enthalpy increment of C-Eu_2O_3 has been reported by Pankratz and King,[128] and Tsagareishvili and Gvelesiani.[129] The two data sets are in reasonable agreement. These results also show a slight misfit with the low-temperature data (see Fig. 8), confirming these are probably too high. The combined results have been fitted to the polynomial equation, to yield for the heat capacity

$$C_p°/(\text{J K}^{-1}\ \text{mol}^{-1}) = 136.2978 + 14.9877 \times 10^{-3}(\text{T/K}) - 1.4993 \times 10^{6}(\text{T/K})^{-2}.$$

This equation is constrained to $C_p°(298.15\ \text{K}) = 123.9\ \text{J K}^{-1}\ \text{mol}^{-1}$ as estimated by us, and not to $C_p°(298.15\ \text{K}) = 127.09\ \text{J K}^{-1}\ \text{mol}^{-1}$ as derived from the low-temperature heat capacity measurements.

The high-temperature enthalpy increment of B-Eu_2O_3 has also been determined by Curtis and Tharp,[130] Pankratz and King,[128] and Gvelesiani *et al.*[115]; the latter article also includes some numerical results from previously reported measurements by Tsagareishvili and Gvelesiani.[129] The results of Pankratz and King[128] and Gvelesiani *et al.*[115] are in poorer agreement, the former being up to 2.5% lower, in contrast to the results for C-Eu_2O_3. An unexplained transition at ~900 K

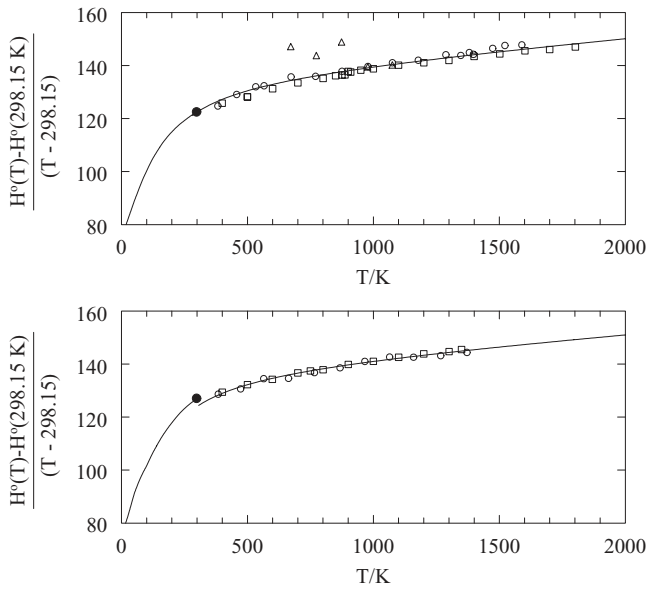

FIG. 8. The reduced enthalpy increment (in J K^{-1} mol^{-1}) of B-Eu_2O_3 (top) and C-Eu_2O_3 (bottom); ○, Gvelesiani *et al.*[115]; □, Pankratz and King[128]; △;[130] •, value derived from the low-temperature measurements by Lyutsareva *et al.*[126]; the curves show the recommended equations.

was observed by Pankratz and King[128] which was not present in the results of Gvelesiani *et al.*,[115] nor found in high temperature dilatometry studies.[130,131] The recommended value is derived from the polynomial fit of the data by Pankratz and King[128] and Gvelesiani *et al.*,[115] constrained to $C_p^\circ(298.15\ K) = 122.33\ J\ K^{-1}\ mol^{-1}$,[126] yielding for the heat capacity:

$$C_p^\circ/(J\,K^{-1}\,mol^{-1}) = 133.3906 + 16.6443 \times 10^{-3}(T/K) - 1.42435 \times 10^{6}(T/K)^{-2}.$$

The enthalpy of the C → B transition can be approximated from the differences of the enthalpy equations at the transition temperature (−1.2 kJ mol^{-1} at 1300 K), plus the difference in the enthalpies of formation at 298.15 K (+12.1 kJ mol^{-1}), yielding $\Delta_{trs}S^\circ = 8.1\ J\ K^{-1}\,mol^{-1}$, in fair agreement with Hoekstra's estimate, $\Delta_{trs}S^\circ = 6.3\ J\ K^{-1}\ mol^{-1}$ from high pressure studies.[116] We select the latter value, giving

$$\Delta_{trs}H^\circ(C \rightarrow B) = (9 \pm 3)\ kJ\,mol^{-1}$$

Heat-capacity or enthalpy measurements have not been reported for the H, X, and liquid phases of Eu_2O_3. Foex and Traverse[10] found that the thermal effects of the B → A transformation are average compared to the other transformations. The properties of these modifications have been estimated in a similar way as for Ce_2O_3. We thus obtain for the transition enthalpies

$$\Delta_{trs}H^\circ(B \rightarrow A) = (7 \pm 2)\ kJ\,mol^{-1},$$
$$\Delta_{trs}H^\circ(A \rightarrow H) = (33 \pm 8)\ kJ\,mol^{-1},$$
$$\Delta_{trs}H^\circ(H \rightarrow X) = (21 \pm 5)\ kJ\,mol^{-1},$$
$$\Delta_{fus}H^\circ = (89 \pm 10)\ kJ\,mol^{-1}.$$

For the heat capacity of the high temperature modifications of Eu_2O_3 we estimate

$$C_p^\circ(A, T) = 141\ J\,K^{-1}\,mol^{-1}$$
$$C_p^\circ(H, T) = C_p^\circ(X, T) = 144\ J\,K^{-1}\,mol^{-1}$$
$$C_p^\circ(liq, T) = 156\ J\,K^{-1}\,mol^{-1}$$

3.10.3. Enthalpy of formation

The enthalpy of formation of monoclinic as well as cubic Eu_2O_3 has been assessed by Cordfunke and Konings[34] recently, and we accept the selected values from that work, since no new information has been published since

$$\Delta_fH^\circ(Eu_2O_3, monoclinic, 298.15\ K) = -(1650.4 \pm 4.0)\ kJ\,mol^{-1},$$
$$\Delta_fH^\circ(Eu_2O_3,\ cubic,\ 298.15\ K) = -(1662.5 \pm 6.0)\ kJ \cdot mol^{-1}.$$

The value for monoclinic europium sesquioxide is based on an analysis of combustion as well as solution calorimetry studies, as shown in Table 15. The selected value is the mean of the results by Holley and coworkers.[132,133] Their results

TABLE 15. The enthalpy of formation of monoclinic Eu_2O_3(cr) at 298.15 K; ΔH_1° and ΔH_2° are the enthalpies of solution of Eu(cr) and Eu_2O_3(cr) in HCl(aq), respectively

Authors	Method[a]	ΔH_1°/kJ mol^{-1}	ΔH_2°/kJ mol^{-1}	Δ_fH°/kJ mol^{-1}
Huber Jr. *et al.*[132]	C			−1648.1 ± 3.8
Yashvili and Gvelesiani[101]	S (1.0)	−632.6 ± 3.8	−397.5 ± 3.8	−1725.5 ± 8.5
		[−607 ± 4][b]		−1674.0 ± 8.9
Fitzgibbon *et al.*[133]	C			−1651.0 ± 3.8
	S (4.0)	−605.2 ± 2.9	−416.8 ± 1.5	−1652.0 ± 6.0
	S (6.0)	[−589.9 ± 2.9][c]	−415.2 ± 2.7	−1624.5 ± 6.4
		[−603 ± 4][b]		−1650.7 ± 8.0
Hennig *et al.*[134]	S (4.0)	[−583.0 ± 2.5][c]	−338.3 ± 0.3	−1686.2 ± 5.0
				−1730.6 ± 5.8[d]
selected value:				−1650.4 ± 4.0

[a]C: combustion calorimetry; S: solution calorimetry; values in parentheses give the concentration of the solvent in mol dm^{-3};
[b]Estimated by Cordfunke and Konings[34] from studies for various lanthanide metals at 1.0, 3.0 and 6.0 mol dm^{-3} HCl (aq) by Merli *et al.*[39];
[c]Stuve[135]
[d]Using ΔH_1° from Fitzgibbon *et al.*[133]

obtained by combustion calorimetry are in excellent agreement. The value derived from solution calorimetric measurements of Eu(cr) and Eu_2O_3(cr) in 4.0 mol dm^{-3} HCl(aq) excellently agrees with these. Further support is obtained from the measurements of the enthalpy of solution of Eu_2O_3(cr) in 6.0 mol dm^{-3} HCl(aq) by Fitzgibbon *et al.*,[133] combined with an estimated value of the enthalpy of solution of Eu(cr) in the same solvent. The value derived from the work by Yashvili and Gvelesiani,[101] who measured the enthalpies of solution of Eu(cr) and Eu_2O_3(cr) in 1.0 mol dm^{-3} HCl(aq), deviates considerably, even when recalculated with an estimated enthalpy of solution of Eu(cr) in 1.0 HCl(aq). Also the value derived from the measurements by Hennig *et al.*,[134] who measured the enthalpy of solution of Eu_2O_3 in 4.0 mol dm^{-3} HCl(aq), disagrees, already evident from the much lower enthalpy of solution compared to Fitzgibbon *et al.*[133]

The enthalpy of formation of cubic Eu_2O_3 was derived by Cordfunke and Konings[34] from two different sources. Fitzgibbon *et al.*[133] determined $\Delta_{trs}H°$(monoclinic/cubic) $= -(11.13 \pm 1.17)$ kJ mol^{-1} by solution calorimetry in four different solvents, resulting in $\Delta_f H°(298.15\ K) = -(1661.1 \pm 6.3)$ kJ mol^{-1}. An almost identical value, $\Delta_f H°(298.15\ K) = -(1663.3 \pm 5.9)$ kJ mol^{-1}, was derived from the enthalpy of solution of cubic Eu_2O_3 in 4.0 mol dm^{-3} HCl(aq) by Stuve[135] and the enthalpy of solution of Eu(cr) by Fitzgibbon *et al.*.[133] This latter value was preferred over Stube's value.

3.11. Eu_3O_4(cr)

3.11.1. Polymorphism and melting point

Trieuropium tetraoxide has an orthorhombic crystal structure (space group Pnam). Bedford and Catalano[136] suggest that Eu_3O_4 melts congruently at 2273 K.

3.11.2. Heat capacity and entropy

The low-temperature heat capacity of Eu_3O_4 has not been measured. The standard entropy can be derived from the second-law reaction entropy derived from vaporisation measurements of the reaction:

$$3Eu_3O_4(cr) = 4Eu_2O_3(monoclinic) + Eu(g)$$

for which $\Delta S° = (118 \pm 3.4)$ J K^{-1} mol^{-1} at 1810 K was found by Haschke and Eick,[137] yielding $S°(298.15\ K) = (314.6 \pm 3.1)$ J K^{-1} mol^{-1}. This entropy value at 298.15 K is very close the sum of the oxides B-Eu_2O_3 and EuO, (307.9 ± 2.2) J K^{-1} mol^{-1}. We select

$$S°(298.15\ K) = (315 \pm 4)\ J\,K^{-1}\,mol^{-1}$$

The high-temperature enthalpy increment of Eu_3O_4 has been estimated by Haschke and Eick[137] as

$$C_p^\circ/(J\,K^{-1}\,mol^{-1}) = 182.464 + 26.108 \times 10^{-3}(T/K).$$

It should be noted that in the range 300–900 K, this equation is substantially higher than the sum of the oxides B-Eu_2O_3 and EuO.

3.11.3. Enthalpy of formation

The enthalpy of formation of Eu_3O_4 has been derived from the enthalpy of reaction derived by Haschke and Eick[137] of the vaporisation reaction (see Sec. 3.11.2) , $\Delta_r H = (360.7 \pm 5.9)$ kJ mol^{-1}, resulting in:

$$\Delta_f H(Eu_3O_4,\ cr,\ 298.15\ K) = (2276 \pm 10)\ kJ\,mol^{-1}$$

3.12. EuO(cr)

3.12.1. Polymorphism and melting point

Europium monoxide has a face-centered cubic structure (space group $Fm\bar{3}m$).[138] McMasters *et al.*[139] observed no phase transitions up to 1724 K. According to the phase diagram of the Eu-O system proposed by McCarthy and White[140] EuO decomposes peritectically at about 1793 K. Shafer *et al.*[141] suggest that EuO exhibits hypo- as well as hyperstiochiometry composition ranges, and that the liquidus of the oxygen rich compositions increases to (2238 ± 10) K, in agreement with the values reported by Reed and Fahey,[142] (2253 ± 20) K, and Bedford and Catalano,[136] (2263 ± 30) K.

3.12.2. Heat capacity and entropy

The low-temperature heat capacity of EuO has been measured by Teany and Moruzzi[143] from 16 to 300 K. They observed a sharp anomaly with Curie temperature $T_c = 69.3$ K, also found by Shafer *et al.*[141] by electrical conductivity measurements. The total entropy of the transition was found to be corresponding to the theoretical value $R\ln(8)$. The standard entropy of EuO has been derived from these measurements:

$$S°(298.15\ K) = (83.6 \pm 0.8)\,J\,K^{-1}\,mol^{-1}.$$

The high-temperature enthalpy increment has been measured by McMasters *et al.*[139] The two data sets are in good agreement and the high-temperature data can be represented by the polynomial equation (419 to 1724 K):

$$C_p^\circ/(J\,K^{-1}\,mol^{-1}) = 46.5453 + 7.360 \times 10^{-3}(T/K)^2$$

which is a refit of the experimental data, omitting several extreme outliers.

3.12.3. Enthalpy of formation

The enthalpy of formation of $EuO_{1.02}$ was determined by Burnett[144] by solution calorimetry yielding $\Delta_f H°(298.15\ K) = -(607.0 \pm 4.1)$ kJ mol^{-1}, and Huber and Holley Jr.,[145,146] by oxygen combustion calorimetry yielding $\Delta_f H°(298.15\ K) = -(599.6 \pm 2.1)$ kJ mol^{-1}, in good agreement. Assuming that $EuO_{1.02}$ is a ideal solid solution $(0.96EuO + 0.04EuO_{1.5})$ these values have been recalculated and the mean value has been selected,

$$\Delta_f H°(EuO,\ cr,\ 298.15\ K) = -(593.2 \pm 5.0)\ kJ\,mol^{-1}.$$

3.13. Gd_2O_3(cr,l)

3.13.1. Polymorphism and melting point

At room temperature, gadolinium sesquioxide has the rare earth cubic C-type structure (space group $Ia\bar{3}$), though the monoclinic B-type structure can also be maintained to room temperature. The C → B transformation, which is sluggish but reversible, was found at 1298 K by Shafer and Roy,[147] 1523 K by Roth and Schneider[121] and 1473 K by Warshaw and Roy,[89] the latter being selected here because of the careful analysis made in that work. In view of the approximate nature, no attempt has been made to correct these values to ITS-90.

Foex and Traverse[10] determined the temperatures of the B → A, A → H and H → X transformations by thermal analysis, without giving numerical results. From the thermogram we deduce the values ~2403, ~2423, and ~2623 K. They also determined the transformation of H-type Gd_2O_3 to the X-type Ln_2O_3 structure at ~2623 K using XRD. These values must be converted to ITS-90 using the procedure outlined by Coutures and Rand,[15] leading to a correction of +15 K. Lopato *et al.*[11] reported that the transformations B → A and A → H occur in the temperature range 2443-2473 K and that H → X transformation occurs close to the melting point (2633–2653 K). Barkhatov *et al.*[148] reported the transformation temperature for B → A and A → H as (2443 ± 10) K and (2481 ± 10) K from drop calorimetric measurements and (2436 ± 10) K and (2470 ± 15) K from electrical conductivity measurements, respectively. No information on the calibration of these measurements has been found, but assuming the data refer to IPTS-68, a correction of −1 K needs to be applied to convert to ITS-90. We select T_{trs} = (2430 ± 30) K for the B → A transformation, T_{trs} = (2470 ± 30) K for the A → H transformation and T_{trs} = (2538 ± 20) K for the H → X transformation. The measurements of the melting temperature of Gd_2O_3 have been summarized in Table 16, which is based on the IUPAC review by Coutures and Rand.[15] The selected melting point is (2693 ± 15) K.

TABLE 16. Temperature of melting of gadolinium sesquioxide (after Coutures and Rand[15])

	T_{fus}/K	
Authors	Reported	ITS-90
Wisnyi and Pijanowski[111]	2603 ± 20	2620 ± 20
Curtis and Johnson[112]	2623 ± 50	2626 ± 50
Foex[19]	2668	2683
Mordovin *et al.*[20]	2597 ± 30	2599 ± 30
Noguchi and Mizuno[21]	2603 ± 20	2606 ± 20
Spiridonov *et al.*[149]	2573	2576
Treswjatskii *et al.*[22]	2653 ± 20	2652 ± 20
Coutures *et al.*[23]	2713 ± 10	2712 ± 10
Mizuno *et al.*[24]	2667	2655
Yoshimura *et al.*[25]	2666	2672 ± 15
Mizuno *et al.*[150]		2686 ± 25
Shevthenko and Lopato[13]	2683	2682
Salikhov and Kan[95]		2666 ± 10
Kang *et al.*[151]		2701 ± 20
Selected value:		2693 ± 15

3.13.2. Heat capacity and entropy

The low-temperature heat capacity of C-Gd_2O_3 has been measured by Justice and Westrum Jr.[113] from T = (7 to 346) K and Stewart *et al.*[152] from T = (1.4 to 18) K, the results being in acceptable agreement in the overlapping temperature range. The results show a thermal anomaly, which is related to the removal of the ground state degeneracy. Stewart *et al.*[152] concluded from the relatively large crystal field splitting needed to reproduce the peak and from EPR measurements that the anomaly in the cubic form is not a Schottky-type transition, as suggested by Miller *et al.*,[153] but is related to a magnetic ordering. The entropy of the transition is, however, close to $2R\ln(2J+1) = 2R\ln(8)$ expected for the contribution of the ground state $^8F_{7/2}$ multiplet. The results give for the entropy of C-Gd_2O_3 at T = 298.15 K:

$$S^\circ(Gd_2O_3,\ \text{cubic},\ 298.15\ \text{K}) = (150.6 \pm 0.2)\ \text{J K}^{-1}\ \text{mol}^{-1}.$$

The low-temperature heat capacity of B-Gd_2O_3 was measured by Konings *et al.*[127] from 5 to 400 K and by Rosenblum *et al.*[154] from 1.6 to 12.5 K. The latter authors found a lambda-type transition with a maximum at T = 3.80 K. The transition entropy is almost identical to the theoretical value $2R\ln(8) = 4.16R$. The absolute entropy at T = 298.15 K is

$$S^\circ(Gd_2O_3,\ \text{monoclinic},\ 298.15\ \text{K}) = (157.1 \pm 0.2)\ \text{J K}^{-1}\ \text{mol}^{-1}.$$

The high-temperature enthalpy increment of C-Gd_2O_3 has been determined by Curtis and Johnson,[112] Pankratz and King,[128] and Tsagareishvili *et al.*[155] The results are in good agreement, as shown in Fig. 9. Our recommended heat capacity equation for C-Gd_2O_3 is based on the combined results of

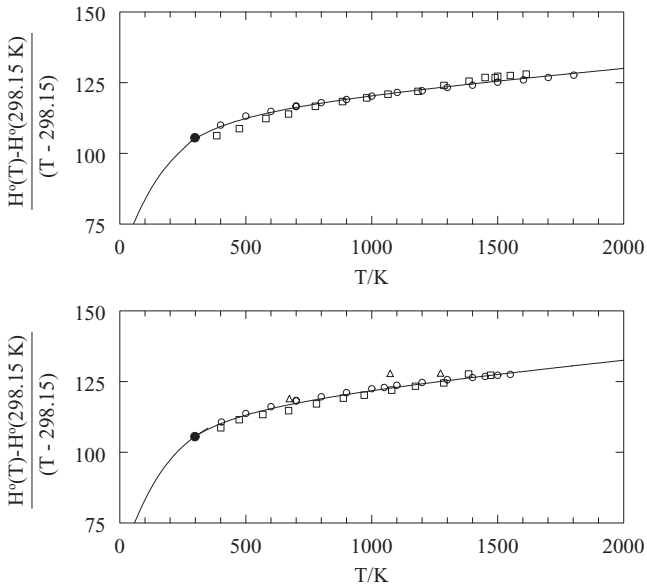

FIG. 9. The reduced enthalpy increment (in J K^{-1} mol^{-1}) of B-Gd_2O_3 (top) and C-Gd_2O_3 (bottom); ○, Pankratz and King[128]; □, Tsagareishvili *et al.*[155]; △ Curtis and Johnson[112]; •, value derived from the low-temperature measurements by Justice and Westrum Jr.[113] for C-Gd_2O_3 and Konings *et al.*[127] for B-Gd_2O_3; the curves show the recommended equations.

the latter two studies, constrained to $C_p^\circ = 105.52\ J\ K^{-1}\ mol^{-1}$ from the low-temperature measurements:[113]

$$C_p^\circ/(J\,K^{-1}\,mol^{-1}) = 114.8086 + 17.2911 \times 10^{-3}(T/K) - 1.28397 \times 10^{6}(T/K)^{-2}.$$

The results of Pankratz and King[128] and Tsagareishvili *et al.*[155] for B-Gd_2O_3 differ significantly at the lowest temperatures. We have fitted the combined results into a polynomial fit, constrained to $C_p^\circ = 105.1\ J\ K^{-1}\ mol^{-1}$ from the low-temperature measurements[113] to give for the heat capacity of B-Gd_2O_3:

$$C_p^\circ/(J\,K^{-1}\,mol^{-1}) = 114.6104 + 15.2344 \times 10^{-3}(T/K) - 1.24917 \times 10^{6}(T/K)^{-2}.$$

The entropy of the C → B transition was estimated from high-pressure studies by Hoekstra[116] as $6.3\ J\,K^{-1}\,mol^{-1}$ using the Clausius-Clapeyron equation. This value is confirmed by the difference in the entropies of the B- and C-modifications of Gd_2O_3 at 298.15 K (see above), $6.5\ J\ K^{-1}\,mol^{-1}$. Unlike Sm_2O_3 and Eu_2O_3 the transition enthalpy cannot be derived from experimental enthalpy data, as the difference in the enthalpies of formation at 298.15 K is not known. Barkhatov *et al.*[148] reported enthalpy increment measurements for Gd_2O_3 from which the enthalpies of the B → A and A → H transformations were derived as $(6.3 \pm 3.3)\ kJ\ mol^{-1}$ and $(34.7 \pm 3.3)\ kJ\ mol^{-1}$. Heat-capacity or enthalpy measurements have not been reported for the X and liquid phases of Gd_2O_3. The properties of these modifications have been estimated in a similar way as for La_2O_3 and Ce_2O_3. We thus obtain for the transition enthalpies

$$\Delta_{trs}H^\circ(C \rightarrow B) = (9 \pm 2)\ kJ\,mol^{-1},$$
$$\Delta_{trs}H^\circ(B \rightarrow A) = (6.3 \pm 3.3)\ kJ\,mol^{-1},$$
$$\Delta_{trs}H^\circ(A \rightarrow H) = (34.7 \pm 3.3)\ kJ\,mol^{-1},$$
$$\Delta_{trs}H^\circ(H \rightarrow X) = (20 \pm 5)\ kJ\,mol^{-1},$$
$$\Delta_{fus}H^\circ = (92 \pm 10)\ kJ\,mol^{-1}.$$

For the heat capacity of the high temperature A, H, and X modifications and liquid Gd_2O_3 we estimate

$$C_p^\circ(A,T) = 142\ J\,K^{-1}\,mol^{-1},$$
$$C_p^\circ(H,T) = C_p^\circ(X,T) = 130; J\,K^{-1}\,mol^{-1},$$
$$C_p^\circ(liq,T) = 140; J\,K^{-1}\,mol^{-1},$$

3.13.3. Enthalpy of formation

The enthalpy of formation of monoclinic Gd_2O_3 has been assessed by Cordfunke and Konings[34] recently, and we accept the selected values from that work, since no new information has been published since

$$\Delta_fH^\circ(Gd_2O_3,\ cr,\ 298.15\ K) = -(1819.7 \pm 3.6)\ kJ\,mol^{-1}.$$

This value is solely based on the combustion calorimetric study by Huber, Jr. and Holley, Jr.,[156] who used 97.05 mass % pure gadolinium metal (Table 17). The combustion value by Spedding *et al.*[99] is much less accurate due to incomplete combustion and lack of analytical characterization of the sample of Gd(cr). The values derived from the solution calorimetric study by Yashvili and Gvelesiani,[101] who determined the enthalpies of solution of Gd(cr) and Gd_2O_3(cr) in 6.0 mol dm^{-3} HCl(aq), are in reasonable agreement, but as discussed by Cordfunke and Konings,[34] they are considered significantly less accurate, especially in view of the difficulties of the slow dissolution of Gd_2O_3(cr) in HCl(aq).

TABLE 17. The enthalpy of formation of Gd_2O_3(cr) at 298.15 K; ΔH_1° and ΔH_2° are the enthalpies of solution of Gd(cr) and Gd_2O_3(cr) in HCl(aq), respectively (after Cordfunke and Konings[34])

Authors	Method[a]	ΔH_1°/kJ mol^{-1}	ΔH_2°/kJ mol^{-1}	Δ_fH°/kJ mol^{-1}
Huber Jr. and Holley Jr.[156]	C			−1819.7 ± 3.6
Spedding *et al.*[99]	C			−1786.2
Yashvili and Gvelesiani[101]	S (6.0)	−694.5 ± 1.7	−422.6 ± 1.3	−1826.3 ± 3.7
		[−694.9 ± 1.0][b]		−1829.5 ± 2.6
				−1828.2 ± 3.6[c]
Selected value:				−1819.7 ± 3.6

[a]C: combustion calorimetry; S: solution calorimetry; values in parentheses give the concentration of the solvent in mol dm^{-3}.
[b]Merli *et al.*[39]
[c]Cycle based on $GdCl_3$.[39]

3.14. TbO_2(cr)

3.14.1. Structure

TbO_2 has a face-centered cubic structure (space group $Fm\bar{3}m$) at room temperature. The upper stability of this phase has not been studied in detail. The phase diagram suggested by Lowe and Eyring[157] indicates that the TbO_{2-x} is stable up to about 1400 K.

3.14.2. Heat capacity and entropy

No measurements of the heat capacity of TbO_2 have been made. The standard entropy has been estimated as

$$S^\circ(298.15\ K) = (86.9 \pm 3.0)\ J\,K^{-1}\,mol^{-1}$$

from the systematics in the lanthanide and actinide oxides. In a similar manner the high temperature heat capacity was estimated as

$$C_p^\circ/(J\,K^{-1}\,mol^{-1}) = 73.259 + 13.2023 \times 10^{-3}(T/K) - 1.0424 \times 10^{6}(T/K)^{-2}.$$

3.14.3. Enthalpy of formation

The enthalpy of formation of TbO_2 was determined by Stubblefield *et al.*[84] and Fitzgibbon and Holley Jr.[158] using solution calorimetry. Both research groups reported results for samples with varying O/Tb ratios. After recalculation and extrapolation to O/Tb = 2.0, as shown in Fig. 5, we obtain for the selected enthalpy of formation:

$$\Delta_fH^\circ(TbO_2,\ cr,\ 298.15\ K) = -(972.2 \pm 5.0)\ kJ\,mol^{-1}.$$

TABLE 18. The enthalpy of formation of phases in the TbO_2-$TbO_{1.5}$ system

Composition	$\Delta_f H°(298.15\ K)$	Authors
	kJ mol^{-1}	
$TbO_{1.510}$	−(933.4 ± 3.6)	Fitzgibbon and Holley, Jr.[158]
$TbO_{1.709}$	−(952.3 ± 3.4)	Fitzgibbon and Holley, Jr.[158]
$TbO_{1.710}$	−(953.1 ± 3.9)	Stubblefield *et al.*[84]
$TbO_{1.800}$	−(966.1 ± 3.3)	Stubblefield *et al.*[84]
$TbO_{1.817}$	−(961.9 ± 3.5)	Fitzgibbon and Holley, Jr.[158]
$TbO_{1.975}$	−(970.5 ± 2.8)	Fitzgibbon and Holley, Jr.[158]

The enthalpies of formation (recalculated) of the compositions with various O/Tb ratios used for this calculation are given in Table 18.

3.15. Tb_6O_{11}(cr),$Tb_{11}O_{20}$(cr),Tb_4O_7(cr), Tb_7O_{12}(cr)

3.15.1. Structure

In addition to the TbO_{2-x} phase, a number of defined stoichiometric Tb_nO_m phases were reported to exist: $TbO_{1.833}$ (Tb_6O_{11}) as well as $TbO_{1.818}$ ($Tb_{11}O_{20}$) have a triclinic crystal structure ($P\bar{1}$), $TbO_{1.75}$ (Tb_4O_7) has a cubic crystal structure ($Fm\bar{3}m$), and $TbO_{1.714}$ (Tb_7O_{12}) has a trigonal crystal structure ($R\bar{3}$).

3.15.2. Heat capacity and entropy

Heat capacity data for the stoichiometric Tb_nO_m phases are limited to the measurement for Tb_4O_7 by Hill[159] from 0.5 to 22 K, revealing an antiferromagnetic transition at and 7.85 K. For that reason we recommend that the standard entropies and the high temperature heat capacity are interpolated between TbO_2 and Tb_2O_3.

3.15.3. Enthalpy of formation

The enthalpies of formation of a number of phases with varying O/Tb ratios have been measured by Stubblefield *et al.*[84] and Fitzgibbon and Holley Jr.[158] and the recalculated values are listed in Table 18. As shown in Fig. 5, the experimental enthalpies of formation of the Tb_nO_m phases are in good agreement and fit to a regular trend, slightly more nonlinear compared to the Pr-O system. We have interpolated the enthalpies of formation of the Tb_nO_m phases from this trend as

$$\Delta_f H°(TbO_{1.833},\ cr,\ 298.15\ K) = -(945.8 \pm 5.0)\ kJ\,mol^{-1},$$
$$\Delta_f H°(TbO_{1.818},\ cr,\ 298.15\ K) = -(957.8 \pm 5.0)\ kJ\,mol^{-1},$$
$$\Delta_f H°(TbO_{1.750},\ cr,\ 298.15\ K) = -(962.9 \pm 5.0)\ kJ\,mol^{-1},$$
$$\Delta_f H°(TbO_{1.714},\ cr,\ 298.15\ K) = -(963.8 \pm 5.0)\ kJ\,mol^{-1}.$$

3.16. Tb_2O_3(cr,l)

3.16.1. Polymorphism and melting point

At room temperature, terbium sesquioxide has the rare earth cubic C-type structure (space group $Ia\bar{3}$). Warshaw and Roy[89] found the C → B transformation at 2148 K. Foex and Traverse[10] determined this transformation temperature as 1823 K.

TABLE 19. Temperature of melting of terbium sesquioxide (after Coutures and Rand[15])

	T_{fus} K	
Authors	Reported	ITS-90
Foex[19]	2663	2678
Mordovin *et al.*[20]	2566 ± 30	2569 ± 30
Noguchi and Mizuno[21]	2577 ± 20	2580 ± 20
Treswjatskii *et al.*[22]	2643 ± 20	2642 ± 20
Coutures *et al.*[23]	2683 ± 10	2682 ± 10
Shevthenko and Lopato[13]	2673	2672
Selected value:		2682 ± 15

The B → H transformation was also determined by Foex and Traverse[10] using thermal analysis at 2473 K. These values must be converted to ITS-90 using the procedure outlined by Coutures and Rand,[15] leading to a correction of +15 K. Lopato *et al.*[11] reported that the B → H transformation occurs at 2448 K and the H → X transformation close to the melting point (2613–2643 K). No information on the calibration of these measurements has been found, but assuming the data refer to IPTS-68, a correction of −1 K needs to be applied to convert to ITS-90. We select $T_{trs} = (1823 \pm 30)$ K for the C → B transformation and $T_{trs} = (2488 \pm 30)$ K for the B → H transformation, solely based on the work of Foex and Traverse.[10]

The measurements of the melting temperature of Tb_2O_3 have been summarized in Table 19, which is based on the IUPAC review by Coutures and Rand.[15] The selected melting point is (2682 ± 15) K.

3.16.2. Heat capacity and entropy

The low-temperature heat capacity of Tb_2O_3 has been measured by Hill[159] from 0.5 to 22 K, revealing an antiferromagnetic transition at 2.42 K. These results are too limited to derive the standard entropy and the selected value for this quantity is the value estimated by Konings[109] from the trend in the lattice component in the lanthanide sesquioxides and the calculated excess contribution calculated from the crystal field energies:

$$S°(298.15\ K) = (159.2 \pm 3.0)\ J\,K^{-1}\,mol^{-1}.$$

The high-temperature enthalpy increment of C-Tb_2O_3 has been determined by Pankratz *et al.*[114] from 414 to 1599 K. The results have been fitted to a polynomial equation constrained to $C_p°(298.15\ K) = 116.0\ J\,K^{-1}\,mol^{-1}$, estimated in a similar way as the entropy value. We thus derive for the heat capacity,

$$C_p°/(J\,K^{-1}\,mol^{-1}) = 120.6682 + 22.17194 \times 10^{-3}(T/K) - 1.00261 \times 10^{6}(T/K)^{-2}.$$

For the estimation of the enthalpy change of the C → B phase transformation we accept the Hoekstra's estimate for the entropy of transition (6.3 J K^{-1} mol^{-1}),[116] to give

$$\Delta_{trs}H°(C \rightarrow B) = (12 \pm 4)\ kJ\,mol^{-1}.$$

For the heat capacity of B-Tb_2O_3 we estimate

$$C_p^\circ(B, T) = 152\ J\,K^{-1}\,mol^{-1}.$$

Foex and Traverse[10] found that the B → H transformation corresponds to a strong peak in the DTA analysis. Wu and Pelton[33] argued that the B → H transformation has the same entropy change as the C → H (see under Er_2O_3) for which they suggested $\Delta_{trs}S^\circ(B \rightarrow H) = 7.2\ J\,K^{-1}\,mol^{-1}$ from analysis of Ln_2O_3-Al_2O_3 phase diagrams. For the entropy of fusion in these systems they derived $\Delta_{trs}S^\circ(H \rightarrow \text{liquid}) = 17.9\ J\,K^{-1}\,mol^{-1}$ in a similar manner. These numbers would suggest an appreciably lower sum for the entropies of the transformation from C to liquid compared to Gd_2O_3, whereas an almost constant value could be expected, based on the known data for the lanthanide trifluorides.[160] The selected values are consistent with the latter assumption:

$$\Delta_{trs}H^\circ(B \rightarrow H) = (55 \pm 8)\ kJ\,mol^{-1},$$
$$\Delta_{fus}H^\circ = (83 \pm 8)\ kJ\,mol^{-1}.$$

For the heat capacity of the high temperature modification H and the liquid phase of Tb_2O_3 we estimate

$$C_p^\circ(H, T) = 170\ J\,K^{-1}\,mol^{-1},$$
$$C_p^\circ(liq, T) = 182\ J\,K^{-1}\,mol^{-1}.$$

3.16.3. Enthalpy of formation

The enthalpy of formation of monoclinic cubic Tb_2O_3 has been assessed by Cordfunke and Konings[34] recently, and we accept the selected values from that work, since no new information has been published since

$$\Delta_f H^\circ(Tb_2O_3,\ cr,\ 298.15\ K) = -(1865.2 \pm 6.0)\ kJ\,mol^{-1}.$$

This value is based on an analysis of two solution calorimetry studies, as shown in Table 20. Stubblefield *et al.*[84] measured the enthalpy of solution of Tb_2O_3(cr) in 6.0 mol dm^{-3} HNO_3(aq). However, the thermochemical reaction cycle was considered to be not highly reliable, since not all the auxiliary thermodynamic data important for that calculation are known with sufficient accuracy. Fitzgibbon and Holley, Jr.[158] measured the enthalpy of formation of $TbO_{1.510}$(cr) using a thermochemical cycle which involves the solution of terbium metal and the oxide in 1.0 mol dm^{-3} HCl(aq) and 6.0 mol dm^{-3} HNO_3(aq), respectively. Different solvents were used to avoid reduction of HNO_3(aq) by terbium metal and oxidation of some of the HCl by the oxide. In order to combine the results in the two solvents, the enthalpy of solution of terbium carbonate was measured in both solvents. The enthalpy of formation of $TbO_{1.50}$ was obtained by extrapolation (Fig. 5), being in excellent agreement with the value by Stubblefield *et al.*[84]

3.17. Dy_2O_3(cr,l)

3.17.1. Polymorphism and melting point

At room temperature, dysprosium sesquioxide has the rare earth cubic C-type structure (space group $Ia\bar{3}$). Warshaw and Roy[89] found the C → B transformation at 2423 K. Foex and Traverse[10] and Lopato *et al.*[11] determined this transformation temperature as 2223 K. In view of the approximate nature, no attempt has been made to correct these values to ITS-90. The B → H transformation was determined by Foex and Traverse[10] using thermal analysis at T = 2473 K. This values must be converted to ITS-90 using the procedure outlined by Coutures and Rand,[15] leading to a correction of +15 K. Lopato *et al.*[11] reported that the B → H transformation occurs at 2463 K. No information on the calibration of these measurements has been found, but assuming the data refer to IPTS-68, a correction of −1 K needs to be applied to convert to ITS-90. We select T_{trs} = (2223 ± 30) K for the C → B transformation and T_{trs} = (2488 ± 30) K for the B → H transformation, solely based on the work of Foex and Traverse.[10]

The measurements of the melting temperature of Dy_2O_3 have been summarized in Table 21, which is based on the IUPAC review by Coutures and Rand[15]; the results being corrected to ITS-90. The selected melting point is (2680 ± 15) K.

3.17.2. Heat capacity and entropy

The low-temperature heat capacity of Dy_2O_3 has been measured by Justice and Westrum, Jr.[161] from 10 to 350 K. At the lower temperature range, the tail of a thermal anomaly was observed, which is related to the removal of the ground state degeneracy. Extrapolation of these results to T = 0 K, and accounting for the 2Rln (2) contribution of the lowest level of the $^6H_{15/2}$ ground state multiplet, gives for the entropy at

TABLE 20. The enthalpy of formation of Tb_2O_3(cr) at 298.15 K; ΔH_1° and ΔH_2° are the enthalpies of solution of Tb(cr) and Tb_2O_3(cr) in HCl(aq), respectively (after Cordfunke and Konings[34])

Authors	Method[a]	ΔH_1°/kJ mol^{-1}	ΔH_2°/kJ mol^{-1}	$\Delta_f H^\circ$/kJ mol^{-1}
Stubblefield *et al.*[84]	S (1.0)[b]		−395.0 ± 2.5	−1864.5 ± 8.4
Fitzgibbon and Holley, Jr.[158]	S (1.0)[b]		−392.5 ± 5.0	−1865.2 ± 6.0
Selected value:				−1865.2 ± 6.0

[a]C: combustion calorimetry; S: solution calorimetry; values in parentheses give the concentration of the solvent in mol dm^{-3}.
[b]Solvent was HNO_3(aq).

TABLE 21. Temperature of melting of dysprosium sesquioxide (after Coutures and Rand[15])

	T_{fus}/K	
Authors	Reported	ITS-90
Wisnyi and Pijanowski[111]	2613 ± 20	2629 ± 20
Foex[19]	2663	2678
Mordovin *et al.*[20]	2566 ± 30	2569 ± 30
Noguchi and Mizuno[21]	2501 ± 20	2504 ± 20
Treswjatskii *et al.*[22]	2633 ± 20	2632 ± 20
Coutures *et al.*[23]	2683 ± 10	2682 ± 10
Mizuno *et al.*[24]	2628 ± 20	2615 ± 20
Shevthenko and Lopato[13]	2673	2672
Selected value:		2680 ± 15

T = 298.15 K:

$$S^\circ(298.15\ \mathrm{K}) = (149.8 \pm 0.15)\ \mathrm{J\,K^{-1}\,mol^{-1}}.$$

The high-temperature enthalpy increment of Dy_2O_3 has been measured by Pankratz and Kelly[65] from 417 to 1801 K. The results are in good agreement with the low temperature heat capacity data. Pankratz and Kelly[65] observed a minor thermal anomaly between 1823 and 1863 K, whose origin is not clear. Since the enthalpy effect is very small (<1 kJ mol^{-1}) and has not yet been confirmed by other techniques, and similar unconfirmed transitions have been reported by this group of researchers for other rare-earth sesquioxides, we have neglected it. The data have been fitted to a polynomial equation, constrained to $C_p^\circ = 116.27$ J K^{-1} mol^{-1} from the low-temperature measurements,[161] yielding for the heat capacity:

$$C_p^\circ/(\mathrm{J\,K^{-1}\,mol^{-1}}) = 121.2302 + 15.27609 \times 10^{-3}(\mathrm{T/K}) - 0.84580 \times 10^{6}(\mathrm{T/K})^{-2}.$$

For the heat capacity of B-Dy_2O_3 we estimate

$$C_p^\circ(\mathrm{B,T}) = 155\ \mathrm{J\,K^{-1}\,mol^{-1}}.$$

For transition and fusion entropies we assume the same values as for the iso-structural changes in Tb_2O_3, yielding

$$\Delta_{trs}H^\circ(\mathrm{C \rightarrow B}) = (14 \pm 5)\ \mathrm{kJ\,mol^{-1}},$$
$$\Delta_{trs}H^\circ(\mathrm{B \rightarrow H}) = (55 \pm 8)\ \mathrm{kJ\,mol^{-1}},$$
$$\Delta_{fus}H^\circ = (83 \pm 8)\ \mathrm{kJ\,mol^{-1}}.$$

For the heat capacity of the high temperature H modification and liquid phase of Dy_2O_3 we estimate

$$C_p^\circ(\mathrm{H,T}) = 173\ \mathrm{J\,K^{-1}\,mol^{-1}}$$
$$C_p^\circ(\mathrm{liq,T}) = 188\ \mathrm{J\,K^{-1}\,mol^{-1}}.$$

3.17.3. Enthalpy of formation

The enthalpy of formation of cubic Dy_2O_3 has been assessed by Cordfunke and Konings[34] recently, and we accept the selected values from that work, since no new information has been published since

$$\Delta_f H^\circ(Dy_2O_3,\ \mathrm{cr},\ 298.15\mathrm{K}) = -(1863.4 \pm 5.0)\ \mathrm{kJ\,mol^{-1}}.$$

The selected value is based on the study by Huber, Jr. *et al.*[162] who used both solution calorimetry and oxygen bomb combustion calorimetry (Table 22). The results from the earlier publication by the same group[163] based on the combustion calorimetric measurements, seems to be less accurate, since the sample of dysprosium metal was less pure than that used in the later investigation.

3.18. Ho_2O_3(cr,l)

3.18.1. Polymorphism and melting point

At room temperature, holmium sesquioxide has the rare earth cubic C-type structure (space group $Ia\bar{3}$). Foex and Traverse[10] found the C → B transformation at 2523 K and Lopato *et al.*[11] between 2463 K and 2493 K. The B → H transformation was only determined by Foex and Traverse[10] using thermal analysis near 2573 K. The values of Foex and Traverse[10] values must be converted to ITS-90 using the procedure outlined by Coutures and Rand,[15] leading to a correction of +15 K. We select T_{trs} = (2538 ± 30) K for the C → B transformation and T_{trs} = (2588 ± 30) K for the B → H transformation.

The measurements of the melting temperature of Ho_2O_3 have been summarized in Table 23, which is based on the IUPAC review by Coutures and Rand[15]; the results being corrected to ITS-90. The selected melting point is (2686 ± 15) K.

3.18.2. Heat capacity and entropy

The low-temperature heat capacity of Ho_2O_3 has been measured by Justice and Westrum Jr.[161] from 10 to 350 K.

TABLE 22. The enthalpy of formation of Dy_2O_3(cr) at 298.15 K; ΔH_1° and ΔH_2° are the enthalpies of solution of Dy(cr) and Dy_2O_3(cr) in HCl(aq), respectively (after Cordfunke and Konings[34])

Authors	Method[a]	ΔH_1°/kJ mol^{-1}	ΔH_2°/kJ mol^{-1}	$\Delta_f H^\circ$/kJ mol^{-1}
Huber, Jr. *et al.*[163]	C			−1865.2 ± 3.8
Huber, Jr. *et al.*[162]	C			−1862.9 ± 4.2
	S (4.0)[b]	−695.3 ± 2.9	−385.1 ± 3.4	−1863.9 ± 6.7
Selected value:				−1863.4 ± 5.0

[a] C: combustion calorimetry; S: solution calorimetry; values in parentheses give the concentration of the solvent in mol dm^{-3}.
[b] solvent was HNO_3(aq).

TABLE 23. Temperature of melting of holmium sesquioxide (after Coutures and Rand[15])

	T_{fus}/K	
Authors	Reported	ITS-90
Foex[19]	2668	2683
Mordovin *et al.*[20]	2626 ± 30	2629 ± 30
Noguchi and Mizuno[21]	2603 ± 20	2606 ± 20
Treswjatskii *et al.*[22]	2643 ± 20	2642 ± 20
Coutures *et al.*[23]	2693 ± 10	2692 ± 10
Mizuno *et al.*[24]	2638 ± 20	2625 ± 20
Shevthenko and Lopato[13]	2673	2672
Salikhov and Kan[95]		2664 ± 10
Selected value:		2686 ± 15

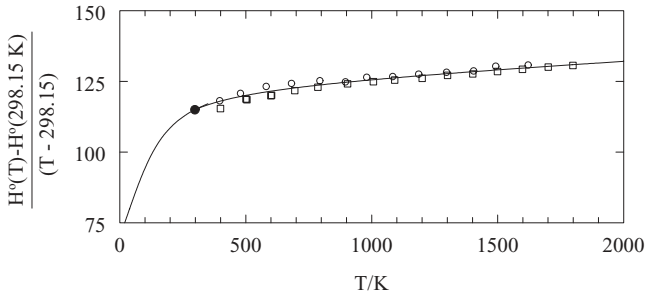

FIG. 10. The reduced enthalpy increment (in J K^{-1} mol^{-1}) of Ho_2O_3; ○, Tsagareishvili and Gvelesiani[164]; □, Pankratz *et al.*[90]; •, value derived from the low-temperature measurements by Justice and Westrum Jr.[113]; the curve shows the recommended equation.

Extrapolation of these results to T = 0 K, and accounting for the contribution of the lowest level of the $^5I_{15/2}$ ground state multiplet, gives for the entropy at T = 298.15 K:

$$S^\circ(298.15\ \mathrm{K}) = (156.38 \pm 0.15)\ \mathrm{J\,K^{-1}\,mol^{-1}}$$

The high-temperature enthalpy increment of Ho_2O_3 has been measured by Pankratz *et al.*[90] from 400 to 1799 K and by Tsagareishvili and Gvelesiani[164] from 397 to 1621 K. The results of Pankratz *et al.*[90] tend to be somewhat lower at the lowest temperatures and moreover, do not agree particularly well with the low-temperature heat capacity data (Fig. 10). Our recommended heat-capacity equation is based on a polynomial fit of the results of both studies. The equation is constrained to $C_p^\circ = 114.98\ \mathrm{J\,K^{-1}\,mol^{-1}}$ from the low-temperature measurements,[113] thus agreeing better with the results of Tsagareishvili and Gvelesiani[164] in the low temperature range. We thus obtain

$$C_p^\circ/(\mathrm{J\,K^{-1}\,mol^{-1}}) = 121.9340 + 10.11623 \times 10^{-3}(\mathrm{T/K}) - 0.886280 \times 10^{6}(\mathrm{T/K})^{-2}.$$

For transition and fusion entropies we assume the same values as for the isostructural changes in Tb_2O_3, yielding

$$\Delta_{trs}H^\circ(\mathrm{C} \rightarrow \mathrm{B}) = (16 \pm 5)\ \mathrm{kJ\,mol^{-1}},$$
$$\Delta_{trs}H^\circ(\mathrm{B} \rightarrow \mathrm{H}) = (57 \pm 8)\ \mathrm{kJ\,mol^{-1}},$$
$$\Delta_{fus}H^\circ = (83 \pm 8)\ \mathrm{kJ\,mol^{-1}}.$$

For the heat capacity of the high temperature B and H modifications and of liquid Ho_2O_3 we estimate

$$C_p^\circ(Ho_2O_3, \mathrm{B}, \mathrm{T}) = 135\ \mathrm{J\,K^{-1}\,mol^{-1}},$$
$$C_p^\circ(Ho_2O_3, \mathrm{H}, \mathrm{T}) = 149\ \mathrm{J\,K^{-1}\,mol^{-1}},$$
$$C_p^\circ(Ho_2O_3, \mathrm{liq}, \mathrm{T}) = 162\ \mathrm{J\,K^{-1}\,mol^{-1}}.$$

3.18.3. Enthalpy of formation

The enthalpy of formation of cubic Ho_2O_3 has been assessed by Cordfunke and Konings[34] recently, and we accept the selected values from that work, since no new information has been published since

$$\Delta_fH^\circ(Ho_2O_3,\ \mathrm{cr},\ 298.15\ \mathrm{K}) = -(1883.3 \pm 8.2)\ \mathrm{kJ\,mol^{-1}}.$$

This value is based on the oxygen-bomb combustion calorimetric measurements by Huber Jr. *et al.*[165] and the solution calorimetric measurements of Ho_2O_3(cr) in 4.0 mol dm^{-3} HCl (aq) by Morss *et al.*[166] For the analysis of the latter study, Morss *et al.*[166] used an estimated enthalpy of solution of Ho(cr) in the same medium, as the measurement of the latter quantity by Stuve[167] was considered not reliable. Cordfunke and Konings[34] combined the enthalpy of solution of Ho_2O_3(cr) in 4.0 mol dm^{-3} HCl(aq) with the enthalpy of solution of $HoCl_3$(cr) in the same medium by Stuve,[167] obtaining a value in good agreement with the combustion value (see Table 24).

TABLE 24. The enthalpy of formation of Ho_2O_3(cr) at 298.15 K; ΔH_1° and ΔH_2° are the enthalpies of solution of Ho(cr) and Ho_2O_3(cr) in HCl(aq), respectively (after Cordfunke and Konings[34])

Authors	Method[a]	ΔH_1°/kJ mol^{-1}	ΔH_2°/kJ mol^{-1}	Δ_fH°/kJ mol^{-1}
Huber Jr. *et al.*[165]	C			−1881.0 ± 5.0
Morss *et al.*[166]	S (4.0)		−379.1 ± 5.2[b]	−1887.3 ± 9.5[c]
		[−710.5 ± 7.1][c]		−1900.3 ± 15.1
				−1885.7 ± 7.3[d]
Selected value:				−1883.3 ± 8.2

[a]C: combustion calorimetry; S: solution calorimetry; values in parentheses give the concentration of the solvent in mol dm^{-3};
[b]uncertainty recalculated.
[c]using $\Delta H_1^\circ = -704 \pm 4$ as suggested by Morss *et al.*[166]
[d]cycle based on $HoCl_3$ as explained in the text.

TABLE 25. Temperature of melting of erbium sesquioxide (after Coutures and Rand[15])

Authors	T_{fus}/K Reported	T_{fus}/K ITS-90
Foex[19]	2673	2688
Mordovin *et al.*[20]	2661 ± 30	2664 ± 30
Noguchi and Mizuno[21]	2618 ± 20	2621 ± 20
Treswjatskii *et al.*[22]	2663 ± 20	2662 ± 20
Coutures *et al.*[23]	2693 ± 10	2692 ± 10
Mizuno *et al.*[24]	2648 ± 20	2636 ± 20
Shevthenko and Lopato[13]	2693	2692
Salikhov and Kan[95]		2686 ± 10
Selected value:		2690 ± 15

3.19. Er_2O_3(cr,l)

3.19.1. Polymorphism and melting point

At room temperature, erbium sesquioxide has the rare earth cubic C-type structure (space group $Ia\bar{3}$). Foex and Traverse[10] found the C → H transformation near T = 2523 K using thermal analysis. This value must be converted to ITS-90 using the procedure outlined by Coutures and Rand,[15] leading to a correction of +15 K. Lopato *et al.*[11] found the transformation at 2593 K. No information on the calibration of these measurements has been found, but assuming the data refer to IPTS-68, a correction of −1 K needs to be applied to convert to ITS-90. We select T_{trs} = (2538 ± 30) K, solely based on the results of Foex and Traverse.[10]

The measurements of the melting temperature of Er_2O_3 have been summarized in Table 25, which is based on the IUPAC review by Coutures and Rand[15]; the results being corrected to ITS-90. The selected melting point is (2690 ± 15) K.

3.19.2. Heat capacity and entropy

The low-temperature heat capacity of Er_2O_3 has been measured by Justice and Westrum Jr.[161] from 10 to 350 K. Extrapolation of these results to T = 0 K, and accounting for the 2Rln(2) contribution of the lowest level of the $^5I_{15/2}$ ground state multiplet. Tang *et al.*[168] found by calorimetric measurements in the temperature range 1.5 to 15 K that Er_2O_3 orders antiferromagnetically with Néel temperature of 3.3 K. The entropy associated with the measured peak is close to 3/4 of 2Rln(2). Since there are two nonequivalent Er^{3+} sites in Er_2O_3, occurring in the ratio 3:1, the observed anomaly corresponds to the ordering of one of the sites, the ordering of the other occurring at lower temperature. The total entropy at T = 298.15 K derived from these results is

$$S^\circ(298.15\ \mathrm{K}) = (153.13 \pm 0.15)\ \mathrm{J\,K^{-1}\,mol^{-1}}.$$

The high-temperature enthalpy increment of Er_2O_3 has been measured by Pankratz *et al.*[90] from 399 to 1797 K and by Tsagareishvili and Gvelesiani[169] from 387 to 1625 K. The results of Pankratz *et al.*[90] tend to be somewhat lower at the lowest temperatures (Fig. 11). Our recommended heat-capacity equation is based on a polynomial fit of the results of both studies. The equation is constrained to C_p° = 108.49 J K^{-1} mol^{-1} from the low-temperature measurements.[161] We thus obtain

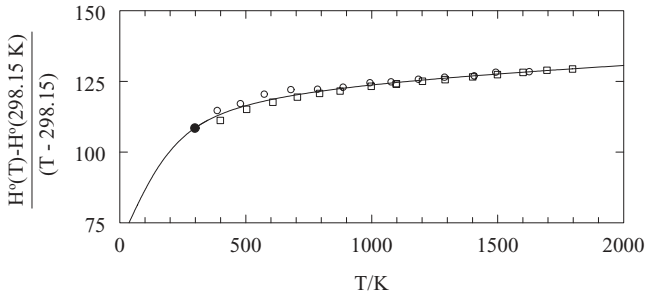

FIG. 11. The reduced enthalpy increment (in J K^{-1} mol^{-1}) of Er_2O_3; ○, Tsagareishvili and Gvelesiani[169]; □, Pankratz *et al.*[90]; •, value derived from the low-temperature measurements by Justice and Westrum Jr.[161]; the curve shows the recommended equation.

$$C_p^\circ/(\mathrm{J\,K^{-1}\,mol^{-1}}) = 123.2921 + 8.62245 \times 10^{-3}(T/K) - 1.54433 \times 10^{6}(T/K)^{-2}.$$

Wu and Pelton[33] argued that the C → H transformation has a significant entropy effect, as changes in the liquidus slopes can be observed in the Er_2O_3–Al_2O_3 and Ho_2O_3–Al_2O_3 phase diagrams. From the limiting slope at the Ln_2O_3 side and the change in slope at the transformation temperatures they derived $\Delta_{trs}S^\circ$(C → H) = 7.2 J K^{-1} mol^{-1}, and $\Delta_{trs}S^\circ$(H → liquid) = 17.9 J K^{-1} mol^{-1}. These numbers would suggest an appreciable lower sum for the entropies of the transformation from the C form to the liquid phase compared to the other cubic lanthanides, whereas an almost constant value could be expected, based on the known data for the lanthanide trifluorides.[160] Our selected values are based on the assumption that the entropy changes for the C → H transformation and fusion are identical to those of Y_2O_3 as measured by Shpil'rain *et al.*[170] using drop calorimetry:

$$\Delta_{trs}H^\circ(\mathrm{C} \rightarrow \mathrm{H}) = (25 \pm 5)\ \mathrm{kJ\,mol^{-1}}$$
$$\Delta_{fus}H^\circ = (83 \pm 5)\ \mathrm{kJ\,mol^{-1}}$$

For the heat capacity of the high temperature modification H and liquid Er_2O_3 we estimate

$$C_p^\circ(Er_2O_3, \mathrm{H}, T) = 162\ \mathrm{J\,K^{-1}\,mol^{-1}},$$
$$C_p^\circ(Er_2O_3, \mathrm{liq}, T) = 176\ \mathrm{J\,K^{-1}\,mol^{-1}}.$$

3.19.3. Enthalpy of formation

The enthalpy of formation of cubic Er_2O_3 has been assessed by Cordfunke and Konings[34] recently, and we accept the selected values from that work, since no new information has been published since

$$\Delta_f H^\circ(Er_2O_3,\ \mathrm{cr}, 298.15\ \mathrm{K}) = -(1900.1 \pm 6.5)\ \mathrm{kJ\,mol^{-1}}.$$

This value is based on an analysis of the calorimetric studies listed in Table 26. Huber Jr. *et al.*[171] and Spedding *et al.*[99] determined the enthalpy of formation of Er_2O_3(cr) by oxygen bomb calorimery. The derived values differ considerable, but

TABLE 26. The enthalpy of formation of Er_2O_3(cr) at 298.15 K; ΔH_1° and ΔH_2° are the enthalpies of solution of Er(cr) and Er_2O_3(cr) in HCl(aq), respectively (after Cordfunke and Konings[34])

Authors	Method[a]	ΔH_1°/kJ mol^{-1}	ΔH_2°/kJ mol^{-1}	$\Delta_f H^\circ$/kJ mol^{-1}
Huber Jr. *et al.*[171]	C			-1897.8 ± 3.8
Spedding *et al.*[99]	C			-1762.8
Montgomery and Stuve[172]	S (1.40)	$[-705.6 \pm 1.4]$[b]	-370.6 ± 3.7	-1898.2 ± 4.6
Morss *et al.*[166]	S (1.40)		-364.6 ± 1.9[c]	-1904.2 ± 3.4
Selected value:				-1900.1 ± 6.5

[a]C: combustion calorimetry; S: solution calorimetry; values in parentheses give the concentration of the solvent in mol dm^{-3}.
[b]Fuger and Morrs.[173]
[c]Uncertainty recalculated.

the work of the former authors is considered to be much more reliable due to the fact that the erbium metal used was well characterised. This is supported by the good agreement with the enthalpy of formation values derived from solution calorimetry ~1.4 mol dm^{-3} HCl(aq) by Montgomery and Stuve[172] and Morss *et al.*[166] These values were combined with the enathlpy of solution of Er(cr) by Fuger *et al.*[173]

3.20. Tm_2O_3(cr,l)

3.20.1. Polymorphism and melting point

At room temperature, thulium sesquioxide has the rare earth cubic C-type structure (space group $Ia\bar{3}$). Foex and Traverse[10] found the B → H transformation near T = 2573 K using thermal analysis. This value must be converted to ITS-90 using the procedure outlined by Coutures and Rand,[15] leading to a correction of +15 K. We thus select $T_{trs} = (2588 \pm 30)$ K.

The melting temperature of Tm_2O_3 has been measured by Treswjatskii *et al.*[22] to be (2653 ± 20) K. However, the melting temperature determinations of the lanthanide sesquioxides by these authors are systematically low by 30–50 K compared to our selected values. Shevthenko and Lopato[13] measured the melting point to be T = 2683 K, which would be T = 2682 K on ITS-90. Coutures *et al.*[23] estimated the melting temperature as (2698 ± 20) K from the trend in the lanthanide sesquioxides. We select $T_{fus} = (2682 \pm 30)$ K.

3.20.2. Heat capacity and entropy

The low-temperature heat capacity of Tm_2O_3 has been measured by Justice *et al.*[174] from 6 to 350 K. They obtained $S^\circ(298.15\ K) - S^\circ(10\ K) = 138.70\ J\ K^{-1}\ mol^{-1}$, and extrapolated the results to T = 0 K using lattice and electronic contributions. This gives

$$S^\circ(298.15\ K) = (139.7 \pm 0.4)\ J\,K^{-1}\,mol^{-1}.$$

The high-temperature enthalpy increment of Tm_2O_3 has been measured by Pankratz *et al.*[90] from 397 to 1801 K and Tsagareishvili and Gvelesiani[129] from 397 to 1607 K. These data are in fair agreement, but both are somewhat low at the lowest temperatures compared to the low-temperature data (Fig. 12). At high temperatures the results tend to diverge, the results of Tsagareishvili and Gvelesiani[129] being significantly higher. Moreover, the results of Pankratz *et al.*[90] indicate a minor thermal anomaly near 1680 K, whose origin is not clear. Since the enthalpy effect is very small (~ 1.3 kJ mol^{-1}), and similar unconfirmed transitions have been reported by this group for other rare-earth sesquioxides, we have neglected it. Our recommended heat-capacity equation is based on a polynomial fit of the results of both studies, but since the results of Pankratz *et al.*[90] cover a wider temperature range, they dominate the high temperature part of the curve. The equation is constrained to $C_p^\circ = 116.73\ J\ K^{-1}\ mol^{-1}$ from the low-temperature measurements.[161] We thus obtain

$$C_p^\circ/(J\,K^{-1}\,mol^{-1}) = 128.4322 + 5.23209 \times 10^{-3}(T/K) - 1.17891 \times 10^{6}(T/K)^{-2}.$$

The entropies of the C → H transformation and melting are assumed to be the same as for Er_2O_3. This yields

$$\Delta_{trs}H^\circ(C \rightarrow H) = (26 \pm 5)\ kJ\,mol^{-1},$$
$$\Delta_{fus}H^\circ = (83 \pm 8)\ kJ\,mol^{-1}.$$

For the heat capacity of the high temperature modification H and liquid Tm_2O_3 we estimate

$$C_p^\circ(Tm_2O_3, H, T) = 155\ J\,K^{-1}\,mol^{-1},$$
$$C_p^\circ(Tm_2O_3, liq, T) = 168\ J\,K^{-1}\,mol^{-1}.$$

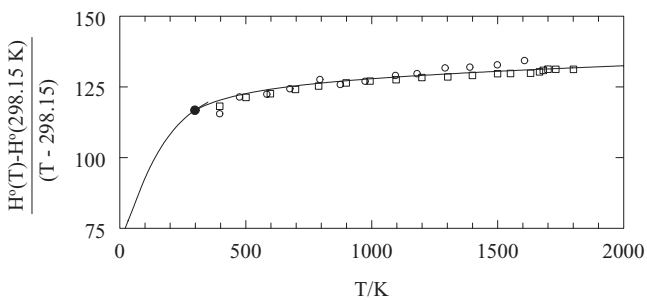

FIG. 12. The reduced enthalpy increment (in J K^{-1} mol^{-1}) of Tm_2O_3; ○, Tsagareishvili and Gvelesiani[129]; □, Pankratz *et al.*[90]; •, value derived from the low-temperature measurements by Justice *et al.*[174]; the curve shows the recommended equation.

3.20.3. Enthalpy of formation

There is only one determination of the standard molar enthalpy of formation of cubic thulium sesquioxide, which was performed by Huber Jr. *et al.*[175] using oxygen-bomb combustion calorimetry, and this value was selected by Cordfunke and Konings[34]:

$$\Delta_f H^\circ(Tm_2O_3,\ cr,\ 298.15\ K) = -(1889.3 \pm 5.7)\ kJ\ mol^{-1}.$$

It is the weighted mean of the results for two samples of Tm(cr) containing significantly different amounts of impurities. Also the extent of combustion varied significantly (88.67% to 99.67% of completion). After correction, Huber Jr. *et al.*[175] obtained the values $\Delta_f H^\circ(298.15\ K) = -(1894.8 \pm 8.3)$ kJ mol^{-1} and $\Delta_f H^\circ(298.15\ K) = -(1884.3 \pm 7.9)$ kJ mol^{-1}, respectively.

3.21. Yb_2O_3(cr,l)

3.21.1. Polymorphism and melting point

At room temperature, ytterbium sesquioxide has the rare earth cubic C-type structure (space group $Ia\bar{3}$). Foex and Traverse[10] found the B → H transformation very close to the melting point. Lopato *et al.*[11] reported this transformation 20 K below the melting point. We thus select $T_{trs} = (2687 \pm 20)$ K.

The measurements of the melting temperature of Yb_2O_3 have been summarized in Table 27, which is based on the IUPAC review by Coutures and Rand[15]; the results being corrected to ITS-90. The selected melting point is (2707 ± 15) K.

3.21.2. Heat capacity and entropy

The low-temperature heat capacity of Yb_2O_3 has been measured by Justice and Westrum Jr.[113] from 10 to 350 K. They obtained $S^\circ(298.15\ K) - S^\circ(10\ K) = 121.42$ J K^{-1} mol^{-1}. They extrapolated the results to T = 0 K, and added $2R \ln(2)$ for the contribution of the ground state doublet of the split $^2F_{7/2}$ multiplet. Li *et al.*[176] confirmed this by calorimetric measurements in the temperature range 1.5–15 K. These measurements reveal that Yb_2O_3 orders antiferromagnetically with Néel temperature of 2.3 K, with an entropy close to

TABLE 27. Temperature of melting of ytterbium sesquioxide (after Coutures and Rand[15])

	T_{fus}/K	
Authors	Reported	ITS-90
Foex[19]	2693	2708
Mordovin *et al.*[20]	2646 ± 30	2649 ± 30
Noguchi and Mizuno[21]	2628 ± 20	2631 ± 20
Treswjatskii *et al.*[22]	2673 ± 20	2672 ± 20
Coutures *et al.*[23]	2708 ± 10	2707 ± 10
Mizuno *et al.*[24]	2660 ± 20	2648 ± 20
Shevthenko and Lopato[13]	2723	2722
Selected value:		2707 ± 15

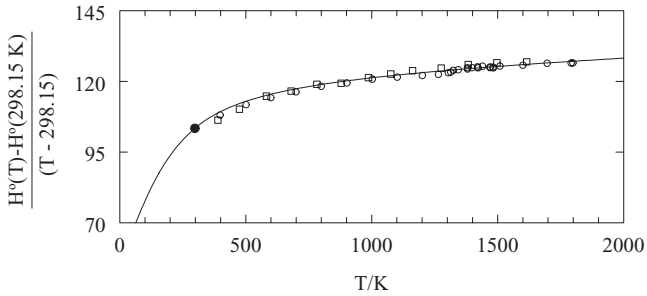

FIG. 13. The reduced enthalpy increment (in J K^{-1} mol^{-1}) of Yb_2O_3; ○, Tsagareishvili and Gvelesiani[129]; □, Pankratz *et al.*[90]; •, value derived from the low-temperature measurements by Justice *et al.*[174]; the curve shows the recommended equation.

$2R \ln(2)$. Thus, we obtain for the entropy at T = 298.15 K:

$$S^\circ(298.15\ K) = (133.1 \pm 0.3)\ J\ K^{-1}\ mol^{-1}.$$

The high-temperature enthalpy increment of Yb_2O_3 has been measured by Pankratz *et al.*[90] from 400 to 1798 K and Tsagareishvili and Gvelesiani[129] from 384 to 1588 K. These data are in good agreement, and fit the low-temperature heat capacity data very well (Fig. 13). Our recommended heat-capacity equation is based on a polynomial fit of the results of both studies, which is constrained to $C_p^\circ = 115.35$ J K^{-1} mol^{-1} from the low-temperature measurements.[113] We thus obtain

$$C_p^\circ/(J\ K^{-1}\ mol^{-1}) = 130.6438 + 3.34628 \times 10^{-3}(T/K) - 1.44820 \times 10^{6}(T/K)^{-2}.$$

The entropies of the C → H transformation and melting are assumed to be the same as for Er_2O_3. This yields

$$\Delta_{trs}H^\circ(C \rightarrow H) = (27 \pm 5)\ kJ\ mol^{-1},$$
$$\Delta_{fus}H^\circ = (84 \pm 8)\ kJ\ mol^{-1}.$$

For the heat capacity of the high temperature modification H and liquid Yb_2O_3 we estimate

$$C_p^\circ(Yb_2O_3, H, T) = 134\ J\ K^{-1}\ mol^{-1},$$
$$C_p^\circ(Yb_2O_3, liq, T) = 146\ J\ K^{-1}\ mol^{-1}.$$

3.21.3. Enthalpy of formation

The only experimental value has been reported by Huber Jr. *et al.*,[163] based on the results of oxygen-bomb combustion calorimetric measurements of 97.2 mass % pure Yb(cr) sample. This value, which includes a careful correction for impurities, was adopted by Cordfunke and Konings[34] with an increased uncertainty, and is also selected here

$$\Delta_f H^\circ(Yb_2O_3,\ cr,\ 298.15\ K) = -(1814.5 \pm 6.0)\ kJ\ mol^{-1}.$$

3.22. Lu_2O_3(cr,l)

3.22.1. Melting point

At room temperature, lutetium sesquioxide has the rare earth cubic C-type structure (space group $Ia\bar{3}$), which is stable

TABLE 28. Temperature of melting of lutetium sesquioxide (after Coutures and Rand[15])

	T_{fus}/K	
Authors	Reported	ITS-90
Mordovin *et al.*[20]	2741 ± 30	2744 ± 30
Noguchi and Mizuno[21]	2700 ± 10	2704 ± 10
Coutures *et al.*[23]	2763 ± 10	2762 ± 10
Shirvinskaya and Popova[177]	2643	2642
Mizuno *et al.*[24]	2733 ± 20	2722 ± 20
Shevthenko and Lopato[13]	2783	2782
Selected value:		2762 ± 15

up to the melting point. The measurements of the melting temperature of Lu_2O_3 have been summarized in Table 28, which is based on the review by Coutures and Rand[15]; the results being corrected to ITS-90. The selected melting point is (2762 ± 15) K.

3.22.2. Heat capacity and entropy

The low-temperature heat capacity of Lu_2O_3 has been measured by Justice *et al.*[174] from 6 to 350 K. The standard entropy derived from these data is

$$S^\circ(298.15\ \mathrm{K}) = (109.96 \pm 0.13)\ \mathrm{J\,K^{-1}\,mol^{-1}}.$$

The high-temperature heat capacity is derived from the enthalpy drop calorimetric measurements by Pankratz and Kelly[65] and Yashvili *et al.*,[30] which are in excellent agreement (Fig. 14). The experimental data have been fitted to a polynomial equation, with boundary condition $C_p^\circ(298.15) = 101.75\ \mathrm{J\ K^{-1}\,mol^{-1}}$ from the low-temperature measurements:[174]

$$C_p^\circ/(\mathrm{J\,K^{-1}\,mol^{-1}}) = 122.4593 + 7.29001 \times 10^{-3}(\mathrm{T/K}) - 2.03414 \times 10^{6}(\mathrm{T/K})^{-2}.$$

This equation is extrapolated to the melting point. Neither the heat capacity of the liquid phase nor the enthalpy of fusion are known. Our estimates for these quantities are approximate values obtained from the trend in the lanthanide sesquioxide series and comparison to the lanthanide trifluorides:

$$C_p^\circ(Lu_2O_3, \mathrm{liq}, \mathrm{T}) = 152\ \mathrm{J\,K^{-1}\,mol^{-1}}.$$

$$\Delta_{fus}H^\circ(Lu_2O_3) = (113 \pm 10)\ \mathrm{kJ\,mol^{-1}}.$$

3.22.3. Enthalpy of formation

The standard enthalpy of formation of cubic Lu_2O_3(cr) is based on the oxygen-bomb combustion calorimetric study by Huber Jr. *et al.*[178] These authors used two well-analysed samples of lutetium metal, and obtained for the enthalpy of formation the values $\Delta_fH^\circ(298.15\ \mathrm{K}) = -(1891.8 \pm 14.2)$ kJ mol^{-1} and $\Delta_fH^\circ(298.15\ \mathrm{K}) = -(1870.9 \pm 9.1)$ kJ mol^{-1}, after correction for impurities. As suggested by Cordfunke and Konings[34] the weighted mean of the two results is selected

$$\Delta_fH^\circ(Lu_2O_3,\ \mathrm{cr},\ 298.15\ \mathrm{K}) = -(1877.0 \pm 7.7)\ \mathrm{kJ\,mol^{-1}}.$$

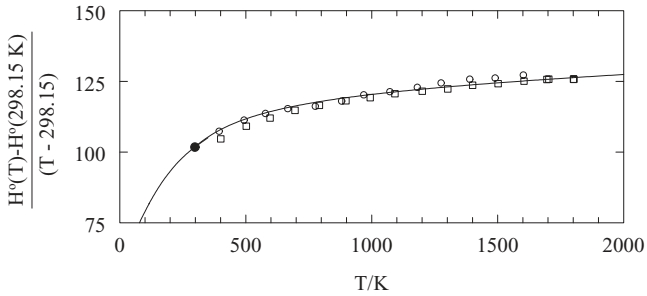

FIG. 14. The reduced enthalpy increment (in J K^{-1} mol^{-1}) of Lu_2O_3; ○, Yashvili *et al.*[30]; □, Pankratz and Kelly[65]; •, value derived from the low-temperature measurements by Justice *et al.*[174]; the curve shows the recommended equation.

4. The Gaseous Lanthanide Oxides

4.1. LaO(g)

4.1.1. Heat capacity and entropy

Thermal functions of LaO(g) in the standard state have been calculated using the molecular constants given in Table 29.

The molecule of LaO is well investigated. Seven electronic states $X^2\Sigma^+$, $A'^2\Delta$, $A^2\Pi$, $B^2\Sigma^+$, $C^2\Pi$, $D^2\Sigma^+$, and $F^2\Sigma^+$ were observed and analyzed in emission and absorption spectra. The comprehensive reviews of spectral data published before 1975 were given by Huber and Herzberg[179] and up to 1980 by Gurvich *et al.*[180] Later numerous works were done to improve the molecular constants of LaO by Bernard and Sibai,[181] Suarez,[182] Carette,[183] Bernard and Vergès,[184] and Steimle and Virgo[185] using traditional methods of investigation; by Bernard *et al.*[186] and Childs *et al.*[187] applying the laser induced fluorescence method; by Suenram *et al.*[188] and Törring *et al.*,[189] who studied the microwave rotational spectrum of LaO. The fundamental frequencies for $La^{16}O$ and $La^{18}O$ were observed in Ar-matrix by Andrews *et al.*[190] (796.7 and 756.1 cm^{-1} for, respectively), and by Zhang *et al.*[191] (796.7 and 756.8 cm^{-1} , respectively) Taking into account the matrix shift the fundamental frequencies obtained in matrices are in agreement with the gas phase data.

Ab initio results for the ground state of LaO by Hong *et al.*,[192] Dolg and Stoll,[193] Dolg *et al.*,[194] and Cao *et al.*[195] show remarkable agreement with the experimental data. *Ab initio* calculations for excited states predicted also the existence of the unobserved doublet states $^2\Phi$, $^2\Delta$, $^2\Pi$, $^2\Sigma$ by Marquez *et al.*[196] and Kotzian *et al.*[197] and quartet states $1^4\Pi$, $1^4\Phi$, $1^4\Delta$ and $2^4\Pi$ by Schampsand *et al.*[198] The Ligand field calculations by Kaledin *et al.*[199] and Schampsand *et al.*[198] resulted in the configuration assignment of the experimentally known states. The existence of the quartet state at the energy 17200 ± 800 cm^{-1} was confirmed by Klingeler *et al.*[200] when studying the photoelectron spectra of LaO^-. All the theoretical

TABLE 29. Molecular constants of LaO(g)

No.	State	T_e	ω_e	$\omega_e x_e$	B_e	$\alpha_e 10^3$	$D_e 10^7$	r_e	p_i
		cm^{-1}						pm	
0[a]	$X^2\Sigma^+$	0	817.026	2.1292[b]	0.3525201	1.424[c]	2.63	182.5	2
1[a]	$A'\,^2\Delta_{3/2}$	7493.4							2
2[a]	$A'\,^2\Delta_{5/2}$	8191.2							2
3[a]	$A^2\Pi$	13094.53							4
4[a]	$B^2\Sigma$	17878.73							2
5[a]	$C^2\Pi$	22740.38							4
6[a]	$D^2\Sigma$	26958.96							2
7[a]	$F^2\Sigma$	28 015							4
8[d]		17 200							8
9[d]		18 500							8
10[d]		21 200							8
11[d]		24 000							20
12[d]		25 900							8
13[d]		30 200							12
14[d]		35 000							30
15[d]		40 000							36

[a]Experimental state.
[b]$\omega_e y_e = -3.15 \times 10^{-3}$ cm^{-1}.
[c]$\alpha_2 10^6 = -2.97$ cm^{-1}.
[d]Estimated state.

data with some corrections were used in the present work to estimate unobserved electronic states (see Table 29).

The accepted constants for the $^2\Sigma^+$ state (see Table 29) were obtained from the analysis of the high-resolution laser excited fluorescence $B^2\Sigma^+$ - $X^2\Sigma^+$ transition ($v' \leq 4, v'' \leq 5$) by Bernard *et al.*[186] In their treatment the authors fixed rotational constants at the very precise values derived by Törring *et al.*[189] from the microwave spectrum for the levels $v = 0$-2. The selected vibrational constants quite well describe the extensive but less accurate data given by Schoonveld and Sundaram[201] for $v'' \leq 11$.

The derived standard entropy at room temperature is

$$S^\circ(298.15\ \mathrm{K}) = (239.594 \pm 0.03)\ \mathrm{J\,K^{-1}\,mol^{-1}}.$$

and the coefficients of the equations for the heat capacity are

$$C_p^\circ/(\mathrm{J\,K^{-1}\,mol^{-1}}) = 28.0550 + 21.9688 \times 10^{-3}(\mathrm{T/K}) - 19.25691 \times 10^{-6}(\mathrm{T/K})^2 + 6.083418 \times 10^{-9}(\mathrm{T/K})^3 - 1.145313 \times 10^{5}(\mathrm{T/K})^{-2}$$

for the 298.15 –1200 K range, and

$$C_p^\circ/(\mathrm{J\,K^{-1}\,mol^{-1}}) = 41.7593 - 6.82858 \times 10^{-3}(\mathrm{T/K}) + 3.529957 \times 10^{-6}(\mathrm{T/K})^2 - 0.281197 \times 10^{-9}(\mathrm{T/K})^3 - 1.500459 \times 10^{6}(\mathrm{T/K})^{-2}$$

for the 1200–4000 K range.

4.1.2. Enthalpy of formation

Results of determination of LaO(g) enthalpy of formation are presented in Table 30. The experimental data considered in the calculations consist mainly of Knudsen effusion, mass spectrometric, and combined measurements. In an early investigation of lanthanum sesquioxide vaporization behavior[202] using Knudsen effusion method, the principal mode of vaporization from tungsten cell was found to be

$$La_2O_3(cr) = 2LaO(g) + O(g),$$

with the steady-state condition corresponding to slightly substoichiometric composition $La_2O_{2.96}$, and thermochemical assessment of the mass-loss data was made according to this equation. In a later detailed study by Ackermann and Rauh[203] it was found, however, that evaporation from tungsten results in LaO partial pressures higher than in the case of evaporation from rhenium cell, due to significant decrease of oxygen pressure for substoichiometric lanthanum sesquioxide. In the case of a rhenium cell, a substantially lower reducing effect of the cell material was found. From the data obtained by Ackermann and Rauh[203] it follows that Knudsen effusion data assessed under assumption of congruent lanthanum sesquioxide vaporization will lead to overestimated LnO stability. The only exception is the set of experimental data for lanthanum sesquioxide vaporization[203] from the rhenium effusion cell, corrected for slight deviation of the sample composition from exact stoichiometry.

The first mass spectrometric determination of the enthalpy of formation of LaO(g) has been carried out by Chupka *et al.*[204] who investigated the La_2O_3(cr) + La(l) system. Later, Ackermann and Rauh[203] investigated the same system in more detail using a combination of Knudsen effusion and mass spectrometry. It was shown that the vapor pressure of La in the system is slightly lower than over pure lanthanum but tends to that at decreasing temperatures. In general, the measurements performed in both investigations can be used in selecting of recommended value for the enthalpy of formation of LaO(g), with more weight to more precise and reliable data of Ackermann and Rauh.[203]

TABLE 30. The enthalpy of formation of LaO(g), in kJ mol^{-1}

Authors	T/K	Method[a]	Reaction	$\Delta_r H°(298.15\ K)$	$\Delta_f H°(298.15\ K)$
Chupka *et al.*[204]	M	1775–1865	$\frac{1}{3}La(g) + \frac{1}{3}La_2O_3(cr) = LaO(g)$	348.8 ± 19	−105.1 ± 20
Goldstein *et al.*[202]	K	2234–2441	$La_2O_3(cr) = 2LaO(g) + O(g)$	1774.2 ± 8.3	−133.3 ± 10
Smoes *et al.*[205]	M	1810–2220	$ScO(g) + La(g) = Sc(g) + LaO(g)$	−119.3 ± 6.8	−122.7 ± 8
	M	1890–2270	$YO(g) + La(g) = Y(g) + LaO(g)$	−81.0 ± 7.2	−120.6 ± 8
Ames *et al.*[206]	M	1890–2220	$Y(g) + LaO(g) = YO(g) + La(g)$	77.0 ± 7.1	−116.6 ± 8
	M	1870–2080	$Sc(g) + LaO(g) = ScO(g) + La(g)$	111.8 ± 6.7	−115.2 ± 8
Coppens *et al.*[207]	M	1877–2088	$SiO(g) + La(g) = Si(g) + LaO(g)$	−2.0 ± 7.8	−120.8 ± 9
Coppens *et al.*[208]	M	2146–2270	$B(g) + LaO(g) = BO(g) + La(g)$	−11.5 ± 13	−113.7 ± 15
Ackermann and Rauh[203]	K (W cell)	2258–2427	$La_2O_3(cr) = 2LaO(g) + O(g)$	1785.6 ± 6.8	−127.6 ± 8
	M/K (Re cell)	1800–2300	$La_2O_3(cr) = 2LaO(g) + O(g)$	1801.9 ± 12	−119.4 ± 8
	M/K	1516–1904	$La_2O_3(cr) + La(l) = 3LaO(g)$	1435.7 ± 5.8	−118.6 ± 4
	M	1783–2184	$La(g) + YO(g) = LaO(g) + Y(g)$	−82.4 ± 6.7	−122.0 ± 8
Parr[210]	M/P		$D_0(LaO) = 793.7 \pm 3.0$		−118.7 ± 4
Gole and Chalek[209]	C		$D_0(LaO) \geq 790.1 \pm 4.2$		≤−115.1 ± 5
Selected value:			$D_0(LaO) = 796.1 \pm 8$		−119.0 ± 8

[a]K = Knudsen effusion; M = mass spectrometry; P = photoionization; C = beam-gas chemiluminescence.

Several mass spectrometric works deal with the LaO(g) + M(g) oxygen exchange reactions.[203,205–208] Only reactions without other lanthanides were taken into consideration. All MO molecules involved are characterized by reliable values of enthalpy of formation, taken from the reference book "*Thermodynamic Properties of Individual Substances.*"[7,180]

The selected value

$$\Delta_f H°(LaO,\ g,\ 298.15\,K) = -(119\ \pm 8)\ kJ\,mol^{-1}$$

is taken as rounded average of the third-law values calculated from all mentioned works except data of Goldstein *et al.*[202] and Ackermann and Rauh[203] on evaporation of lanthanum sesquioxide from tungsten cells. The data on chemiluminescence[209] and photoionization of LaO molecules[210] confirm the selected value. The selected enthalpy of formation corresponds to a dissociation energy of LaO molecule $D_0(LaO) = (796 \pm 8)$ kJ mol^{-1}.

4.2. CeO_2(g)

4.2.1. Heat capacity and entropy

The infrared spectrum of the CeO_2 molecule isolated in inert gas matrices has been determined by DeKock and Weltner Jr.,[211] Gabelnick *et al.*[212] and Willson and Andrews.[213] The results indicate that the molecule has a bent structure (C_{2v}), an approximate bond distance of 188 pm was derived.[212] This geometry was confirmed by quantum chemical calculations by Heinemaan *et al.*,[214] Hülsen *et al.*,[215] and Todorova *et al.*[216] We have selected the bond distance (182 pm) and bond angle (126°) from the CASPT2 computations by Todorova *et al.*[216] The experimental values for the stretching frequencies, $\nu_1 = 757$ cm^{-1} and $\nu_3 = 737$ cm^{-1} have been adopted here. The experimental bending frequency, $\nu_2 = 262$ cm^{-1} that is selected for the calculations of the thermal functions, is significantly higher than the value derived from the CASPT2 calculations, $\nu_2 = 102$ cm^{-1}.[216] DeKock and Weltner, Jr.[211] studied the electronic spectrum of CeO_2 and found no electronic levels below 15 000 cm^{-1}. In our calculations we have included some estimated higher energy levels (Table 31). The derived entropy at room temperature is

$$S°(298.15\ K) = (274.417 \pm 3.0)\ J\,K^{-1}\,mol^{-1}$$

and the coefficients of the equations for the heat capacity are

$$C_p°/(J\,K^{-1}\,mol^{-1}) = 37.7646 + 55.1209 \times 10^{-3}(T/K) - 57.1816 \times 10^{-6}(T/K)^2 + 21.2692 \times 10^{-9}(T/K)^3 - 2.6077 \times 10^{5}(T/K)^{-2}$$

for the 298.15–900 K range, and

$$C_p°/(J\,K^{-1}\,mol^{-1}) = 55.9864 + 2.90431 \times 10^{-3}(T/K) - 1.4361 \times 10^{-6}(T/K)^2 + 0.25254 \times 10^{-9}(T/K)^3 - 1.11908 \times 10^{6}(T/K)^{-2}$$

for the 900–4000 K range.

4.2.2. Enthalpy of formation

Vapor pressure measurements of CeO_2 have been reported by Shukarev and Semenov,[217] Benezech and Foex,[218] Piacente *et al.*,[219] and Ackermann and Rauh.[220] The results by Shchukarev and Semenov (transpiration method) and Benezech and Foëx (mass spectrometry) are very different from those obtained by Ackermann and Rauh[220] and by

TABLE 31. The molecular parameters for CeO_2(g)

Parameter	Value
Ground electronic state	$^1A_1$
Symmetry group	C_{2v}
Symmetry number, σ	2
$I_A I_B I_C$ (g^3 cm^6)[a]	6.984×10^{-115}
Vibrational frequencies (cm^{-1})	757.0, 264, 736.8
Electronic states (cm^{-1})[b]	0(1), 18000(2), 19000(2), 22000(2), 24000(2), 25000(2)

[a]Product of moments of inertia.
[b]Numbers in parentheses represent the statistical weights.

TABLE 32. The enthalpy of formation of CeO_2(g) at 298.15 K

Authors	Method[a]	T/K	reaction	$\Delta_f H°$(298.15 K)/kJ mol^{-1}
Ackermann and Rauh[220]	ME	1846–2318	Ce_2O_{3+x}(cr) = (1−x)CeO(g)+(1+x) CeO_2(g)[b]	−542.8 ± 8.2
Piacente *et al.*[219]	K/M	1736–2067	CeO_2(cr) = CeO_2(g)	−532.4 ± 2.0
	K/M	1933–2134	Ce(g)+CeO_2(g) = 2CeO(g)	−573.8 ± 16.3
Staley and Norman[222]	K/M	1845–1975	CeO_2(g) = CeO(g)+0.5O_2(g)	−415.7 ± 8.0[c]
	K/M	1845–1975	CeO(g)+CaO(g) = CeO_2(g)+Ca(g)	−511.5 ± 22.5[c]
Younés *et al.*[221]	K/M	1720–2040	Ce(g)+CeO_2(g) = 2CeO(g)	−599.3 ± 9.6[c]
	K/M	1720–2040	La(g)+CeO_2(g) = LaO(g)+CeO(g)	−593.8 ± 12.3[c]
	K/M	1720–2040	CeO(g)+UO_3(g) = CeO_2(g)+ UO_2(g)	−489.4 ± 17.9[c]
	K/M	1720–2040	CeO_2(g)+UO(g) = CeO(g)+UO_2(g)	−565.7 ± 17.7[c]
Selected value:				−538 ± 20

[a]ME = mass effusion; K/M = Knudsen-cell mass spectrometry.
[b]Partial vapor pressures of CeO(g) and CeO_2(g) measured over the congruently vaporizing composition (cvc).
[c]Derived from second-law values given by the authors.

Piacente *et al.*[219] Moreover, the results have been presented in graphical form only.

Ackermann and Rauh[220] measured the vapor pressure of the congruently vaporizing composition and of $Ce_2O_{3.03}$(cr), corresponding to the reaction:

$$Ce_2O_{3+x}(cr) = (1 - x)CeO(g) + (1 + x)CeO_2(g).$$

The enthalpy of formation derived from this study are summarized in Table 32. Piacente *et al.*[219] studied the equilibrium between solid and gaseous CeO_2 by means of Knudsen effusion mass spectrometry, and have been interpreted as congruent vaporisation. In addition, these authors have studied the isomolecular exchange reaction:

$$Ce(g) + CeO_2(g) = 2CeO(g).$$

This reaction has also been studied by Younés *et al.*,[221] who reported, however, only second-law enthalpies of reaction. Younés *et al.*[221] also reported results for isomolecular reactions with La, UO, and UO_2, again giving only the second-law enthalpies of reaction (see Table 32). Staley and Norman[222] studied the isomolecular exchange reaction involving CeO(g) and CeO_2(g), as well as the isomolecular exchange reaction with CaO(g), but also in this work only second-law enthalpies of reaction have been given (Table 32).

The variation in the values obtained is large, particularly among those derived from the second-law analysis, and the selected value for $\Delta_f H°$ of CeO_2(g) is the average of the (third-law) values derived from the work of Ackermann and Rauh[220] and Piacente *et al.*,[219] which we considered the most reliable

$$\Delta_f H°(298.15\ K) = -(538 \pm 20)\ kJ\,mol^{-1}.$$

4.3. CeO(g)

4.3.1. Heat capacity and entropy

The thermal functions of CeO(g) in the standard state have been calculated using the molecular constants presented in Table 33.

The analyses of 34 electronic transitions of CeO was performed by Barrow *et al.*,[223] Linton *et al.*,[224] Linton *et al.*,[225] Linton and Dulick,[226] Linton *et al.*,[227] Kaledin *et al.*[199] and Todorova *et al.*[216] As a result, all 16 lower electronic states belonging to the lowest 4*f*6*s* electron configuration of CeO were identified (see Table 33). The configuration assignment for the lower states of these transitions was shown to be doubtless.[197,199,228–232] On the other hand, the configuration assignments for the upper states of these transitions were shown to be contradictory.[197,199,232–234] Certainly these upper states should belong to the 4*f*6*p*, 4*f*5*d*, and 4f^2 superconfigurations or to the mixed configurations. The estimated statistical weights are presented at fixed energies in Table 33, which are calculated assuming the energy intervals for 4*f*6*p*, 4*f*5*d*, and 4f^2 states to be 7000–36 000 cm^{-1}, 12 000–25 000 cm^{-1}, and 17 000–45 000 cm^{-1}, respectively. The 6s^2, 5*d*6*s*, 6*s*6*p*, 6p^2, 5d^2, and 4*f*6*s* states are taken into account in the interval 30 000–45 000 cm^{-1}.

The derived standard entropy at room temperature is

$$S°(298.15\ K) = (246.099 \pm 0.10)\ J\,K^{-1}\,mol^{-1}$$

and the coefficients of the equations for the heat capacity are

$$C_p°/(J\,K^{-1}\,mol^{-1}) = 22.01944 + 55.5050 \times 10^{-3}(T/K) - 43.14095 \times 10^{-6}(T/K)^2 + 10.89494 \times 10^{-9}(T/K)^3 - 4.23189 \times 10^{4}(T/K)^{-2}$$

for the 298.15–1300 K range, and

$$C_p°/(J\,K^{-1}\,mol^{-1}) = 62.79967 - 17.53953 \times 10^{-3}(T/K) + 5.431417 \times 10^{-6}(T/K)^2 - 0.487485 \times 10^{-9}(T/K)^3 - 4.947446 \times 10^{6}(T/K)^{-2}$$

for the 1300–4000 K range.

4.3.2. Enthalpy of formation

The results of the determination of the enthalpy of formation of CeO(g) are presented in Table 34. Several mass spectrometric measurements of isomolecular oxygen exchange

TABLE 33. Molecular constants of CeO(g)

No.	State	T_e	ω_e	$\omega_e x_e$	B_e	$\alpha_e 10^3$	$D_e 10^7$	r_e	p_i
		cm^{-1}						pm	
0[a]	$X(1)2$	0	829.5	2.6[b]	0.3553	1.6[c]	2.46[d]	181.198	2
1[a]	(1)3	82							2
2[a]	(1)1	812.7							2
3[a]	(2)2	911.8							2
4[a]	(1)0	1678.6							1
5[a]	(2)1	1875.3							2
6[a]	(2)0	1925.3							1
7[a]	(1)4	2042.6							2
8[a]	(2)3	2142.6							2
9[a]	(2)4	2618.4							2
10[a]	(3)3	2771.3							2
11[a]	(3)4	3462.2							2
12[a]	(3)1	3435.0							2
13[a]	(3)0	3818.8							1
14[a]	(4)1	4134.1							2
15[a]	(4)0	4458.0							1
16[e]		7000							7
17[e]		10 000							22
18[e]		15 000							58
19[e]		20 000							72
20[e]		25 000							56
21[e]		30 000							45
22[e]		35 000							92
23[e]		40 000							112

[a]Experimental ($4f6s$) state.
[b]Calculated using $\Delta G_{1/2} = 824.3$ cm^{-1} from Linton *et al.*[224] and the dissociation energy adopted in this work.
[c]Calculated using $B_0 = 0.35454$ cm^{-1} from Barrow *et al.*[223] and the Pekeris relation.
[d]D_0.
[e]Estimated state.

reactions have been carried out.[207,220,221,235] Results of all measurements are in remarkable agreement. The selected value for the enthalpy of formation of CeO(g)

$$\Delta_f H^\circ(\mathrm{CeO,\ g,\ 298.15\ K}) = -(132 \pm 8)\ \mathrm{kJ\,mol^{-1}}$$

is taken as a rounded average of the third-law values calculated from all mentioned works. To the selected enthalpy of formation corresponds the value of dissociation energy of CeO molecule $D_0(\mathrm{CeO}) = (794.3 \pm 8)$ kJ mol^{-1}.

4.4. PrO(g)

4.4.1. Heat capacity and entropy

The thermal functions of PrO(g) in the standard state have been calculated using the molecular constants presented in Table 35.

The analysis of 34 electronic transitions of PrO in emission, absorption, and laser fluorescence spectra was carried out by Shenyavskaya *et al.*,[236] Delaval *et al.*,[237] Beaufils *et al.*,[238] Dulick *et al.*,[239] Dulick *et al.*,[240] Dulick *et al.*,[241] Shenyavskaya and Kaledin,[242] Dulick and Field,[243] and Childs *et al.*[244] As a result, information about 12 low-lying electronic states belonging to the lowest electron configuration $4f^2 6s$ was obtained (see Table 35). The infrared spectrum of PrO was observed in solid Ar and Kr matrices at 4 K by Weltner and De Kock[245] and Willson *et al.*[246] The values of the fundamental frequency of PrO obtained in matrices are in agreement with the electronic spectra results. The $4f^2 6s$ electron configuration of PrO contains 91 Hund case "c" molecular states, and each of them is doubly degenerate. Dulick[234] calculated all these states using the crystal field theory and adjusting parameters to reproduce experimental data. The low-lying states of PrO belonging to the $4f^2 6s$ configuration were calculated also by

TABLE 34. The enthalpy of formation of CeO(g), in kJ mol^{-1}

Authors	Method[a]	T/K	Reaction	$\Delta_r H^\circ$(298.15 K)	$\Delta_f H^\circ$(298.15 K)
Walsh *et al.*[235b]	M	1700–2040	Ce(g) + LaO(g) = CeO(g) + La(g)	2.26	−131.6
Coppens *et al.*[207]	M	2146–2270	CeO(g) + La(g) = Ce(g) + LaO(g)		
Ackermann and Rauh[203]	M	1580–1920	Ce(g) + LaO(g) = CeO(g) + La(g)	3.34	−130.5
	M	1760–2160	Ce(g) + YO(g) = CeO(g) + Y(g)	−81.05	−133.5
Younés *et al.*[221]	M	1490–2030	Ce(g) + LaO(g) = CeO(g) + La(g)	2.05	−131.8
Selected value:			$D_0(\mathrm{CeO}) = 794.8 \pm 8$		-132.0 ± 8

[a]M = mass spectrometry.
[b]Recalculated by Ames *et al.*[206]

TABLE 35. Molecular constants of $^{141}Pr^{16}O(g)$

No.	State	T_e	ω_e	$\omega_e x_e$	B_e	$\alpha_e 10^3$	$D_e 10^7$	r_e	p_i
		cm^{-1}						pm	
0[a]	$X(1)3.5$	0	835.8[b]	2.22[b]	0.36175[b]	1.5[b]	2.6[b]	180.115	2
1[a]	(1)4.5	217							2
2[a]	(2)3.5	2064							2
3[a]	(1)5.5	2099							2
4[a]	(2)4.5	2154							2
5[a]	(3)4.5	3718							2
6[a]	(3)3.5	3887							2
7[a]	(1)6.5	3953							2
8[a]	(2)5.5	4225							2
9[a]	(3)5.5	5541							2
10[a]	(4)5.5	5938							2
11[c]		1870							2
12[c]		2880							2
13[c]		3170							8
14[c]		4950							10
15[c]		5247							4
16[c]		7000							5
17c		10 000							90
18[c]		15 000							150
19[c]		20 000							175
20[c]		25 000							185
21[c]		30 000							195
22[c]		35 000							200
23[c]		40 000							205

[a]Experimental ($4f^2 6s$) state.
[b]From Shenyavskaya *et al.*[236]
[c]Estimated state.

Dulick *et al.*[247] and Carrete and Hocquet[230] in Ligand field approximation and by Kotzian and Roesch[248] applying the theoretical Intermediate Neglect of Differential Overlap (INDO) MO procedure augmented with a double-group CI technique which includes spin-orbit interactions. Kotzian and Roesch[232] predicted also the lowest states below 40 000 cm^{-1} belonging to the $4f^2 5d$ and $4f^3$ configurations. The upper states of the transitions observed in the visible apparently are the $p-s$ transitions, so the $4f^2 6p$ states were taken into account in the interval 130 00–63 000 cm^{-1}.

The derived standard entropy at room temperature is

$$S^\circ(298.15\ K) = (244.367 \pm 0.05)\ J\,K^{-1}\,mol^{-1}$$

and the coefficients of the equations for the heat capacity are

$$C_p^\circ/(J\,K^{-1}\,mol^{-1}) = 22.98903 + 20.3103 \times 10^{-3}(T/K) + 20.2961 \times 10^{-6}(T/K)^2 - 14.6500 \times 10^{-9}(T/K)^3 + 2.72239 \times 10^{5}(T/K)^{-2}$$

for the 298.15–1200 K range, and

$$C_p^\circ/(J\,K^{-1}\,mol^{-1}) = 84.67666 - 28.5857 \times 10^{-3}(T/K) + 8.73036 \times 10^{-6}(T/K)^2 - 0.84566 \times 10^{-9}(T/K)^3 - 1.44324 \times 10^{7}(T/K)^{-2}$$

for the 1200–4000 K range.

4.4.2. Enthalpy of formation

The results for the enthalpy of formation of PrO(g) are presented in Table 36. Experimental data used in calculations consist of Knudsen effusion and mass spectrometric measurements. Several mass spectrometric measurements of isomolecular oxygen exchange reactions have been carried out.[235,249,250] The selected value

$$\Delta_f H^\circ(PrO,\ g,\ 298.15\ K) = -(145.5 \pm 8)\ kJ\,mol^{-1}$$

is taken as a rounded average of the third-law values calculated from all mentioned works. To the selected enthalpy of formation corresponds the value of dissociation energy of PrO molecule $D_0(PrO) = (747.1 \pm 8)$ kJ mol^{-1}.

4.5. NdO(g)

4.5.1. Heat capacity and entropy

The thermal functions of NdO(g) in the standard state have been calculated using the molecular constants presented in Table 37.

The analysis of NdO spectra in emission, absorption, and laser fluorescence was carried out by Linton *et al.*,[251] Shenyavskaya *et al.*,[252] Kulikov,[253] Kaledin and Shenyavskaya,[254] and Kaledin.[255] As a result, nine low-lying electronic states with close values of molecular constants were revealed including the ground X4 state, and numerous more or less perturbed excited states with energies 10 000–23 000 cm^{-1}. The IR spectrum of

TABLE 36. The enthalpy of formation of PrO(g), in kJ mol^{-1}

Authors	Method[a]	T/K	Reaction	$\Delta_r H°(298.15\ K)$	$\Delta_f H°(298.15\ K)$
Walsh *et al.*[235b]	M	1750–2070	Pr(g) + LaO(g) = PrO(g) + La(g)	46.45	−148.7
Fries and Cater[249]	M	2053–2191	PrO(g) + Y(g) = Pr(g) + YO(g)	31.4	−145.1
Murad[250]	M		Pr(g) + TiO(g) = PrO(g) + Ti(g)	−71.4	−142.6
Selected value:			D_0(PrO) = 747.1 ± 8		−145.5 ± 8

[a]M = mass spectrometry.
[b]Recalcualted by Ames *et al.*[206]

NdO was observed in solid Ar and Kr matrices at 4 K by Weltner and De Kock[245] and Willson *et al.*[246] The values of the fundamental frequency of NdO obtained in electronic and matrix IR spectra are in agreement.

The theoretical calculations by Dolg and Stoll[193] dealt with the molecular constants of lanthanide monoxides in their ground states. Boudreaux and Baxter[256] calculated and compared electronic structures of NdO and UO.

The low-lying electronic states of NdO were assigned to the $4f^3 6s$ electron configuration which gives rise to the electronic states with the total statistical weight 728. The states belonging to the subconfiguration $4f^3$(4I)6*s* were calculated using the crystal field theory by Kulikov[253] and Carrete and Hocquet[230] (56 states with $\Sigma p = 104$), and by Dulick *et al.*[247] (up to 1000 cm^{-1}, $\Sigma p = 98$). The best agreement with experimental data was shown by Kulikov[253] who used adjusted parameters to reproduce experimental data known at that time (4 low-lying states). Krauss and Stevens[257] confirmed above mentioned crystal field results by *ab initio* calculations and predicted also the low-lying $4f^3 5d$ and $4f^2 s^2$ states (the lower limits are 3390 cm^{-1} and 4267 cm^{-1}, respectively). Shenyavskaya *et al.*[252] tentatively assigned the [12.171]4 state to the lowest state of the $4f^2 s^2$ configuration. The strong bands observed in visible spectral region apparently are the *p*−*s* or *d*−*s* transitions. This implies that the $4f^3 5d$ and $4f^3 6p$ states should be taken into account when calculating the thermal functions. In Table 37 estimates are presented of the unobserved states belonging to the $4f^3 6s$, $4f^3 5d$, $4f^3 5p$, and $4f^3 6s^2$ configurations. The states of the $4f^3$(4I)6*s* subconfiguration are taken from the work by Kulikov.[253] The lower limits for the $4f^3$(4I)5*d* and $4f^3$(4I)5*p* states are assumed to be equal to 6000 and 13 500 cm^{-1}, respectively. The lower limits for the states belonging to the subconfigurations $4f^3$(4F)nl are estimated based on the spectrum NdIV: lower state 4I($4f^3$) is separated from the others by ∼12 000 cm^{-1}, and addition of one electron does not change considerably the interval between centers of

TABLE 37. Molecular constants of $^{142}Nd^{16}O$(g)

No.	State	T_e	ω_e	$\omega_e x_e$	B_e	$\alpha_e 10^3$	$D_e 10^7$	r_e	p_i
		cm^{-1}						pm	
0[a]	*X*(1)4	0	834.083[b]	2.2855[b]	0.362346[b]	1.4291[b]	2.7296[b]	179.91	2
1[a]	(1)5	474							2
2[a]	(1)3	1156							2
3[a]	(1)2	1351							2
4[a]	(2)4	1587							2
5[a]	(2)3	1793							2
6[a]	(2)2	1914							2
7[a]	(1)6	2124							2
8[a]	(2)5	2153							2
9[c]		1470							3
10[c]		1914							3
11[c]		3180							22
12[c]		3987							2
13[c]		5600							28
14[c]		7200							17
15[c]		7920							20
16[c]		10 000							30
17[c]		15 000							80
18[c]		20 000							250
19[c]		25 000							320
20[c]		30 000							400
21[c]		35 000							450
22[c]		40 000							520

[a]Experimental ($4f^3 6s$) state.
[b]From Shenyavskaya *et al.*[252]
[c]Estimated state.

gravity of $4f^3$(4F)nl and $4f^3$(4I)nl configurations, and these limits are assumed to be lower for all remaining states of corresponding configurations.

Our estimates of the positions of the excited configurations are based on the experimental data by Shenyavskaya *et al.*[252] for f^2s^2 configuration and on comparison with the positions of the analogous states of CeO and PrO (for f^3d, f^3p, and f^4 configurations). The energy ranges for the states included in the configurations were taken equal to those for UO (see Kaledin *et al.*[258])

The derived standard entropy at room temperature is

$$S^\circ(298.15\ \mathrm{K}) = (242.817 \pm 0.05)\ \mathrm{J\,K^{-1}\,mol^{-1}}$$

and the coefficients of the equations for the heat capacity are

$$C_p^\circ/(\mathrm{J\,K^{-1}\,mol^{-1}}) = -9.80368 + 188.146 \times 10^{-3}(\mathrm{T/K}) - 190.285 \times 10^{-6}(\mathrm{T/K})^2 + 62.3079 \times 10^{-9}(\mathrm{T/K})^3 + 5.70945 \times 10^{5}(\mathrm{T/K})^{-2}$$

for the 298.15–1100 K range, and

$$C_p^\circ/(\mathrm{J\,K^{-1}\,mol^{-1}}) = 57.65812 - 9.78465 \times 10^{-3}(\mathrm{T/K}) + 2.76479 \times 10^{-6}(\mathrm{T/K})^2 - 0.218778 \times 10^{-9}(\mathrm{T/K})^3 + 4.4284910^{5}(\mathrm{T/K})^{-2}$$

for the 1100–4000 K range.

4.5.2. Enthalpy of formation

The results of the determination of the enthalpy of formation of NdO(g) are presented in Table 38. Experimental data have been obtained by Knudsen effusion, transpiration, and mass-spectrometric measurements. Ames *et al.*[206] carried out Knudsen effusion measurement of the weight loss for Nd_2O_3(cr). Results of these measurements were treated in this work under assumption of congruent vaporization of Nd_2O_3(cr) according to reaction

$$Nd_2O_3(cr) = 2NdO(g) + O(g),$$

neglecting the possibility of formation of Nd(g) atoms in the vapor [see text on LaO(g)]. The enthalpy of formation of NdO(g) thus calculated can be more negative than the correct value, the degree of deviation being dependent on the amount of Nd atoms in vapors. Comparison with the results of Tetenbaum[259] and Murad and Hildenbrand[260] confirms this conclusion. Results of transpiration measurements[259] have significant advantage in comparison to the Knudsen effusion measurements, due to well-defined oxygen pressure, making interpretation of results more certain. The measurements of Murad[250] for two oxygen exchange reactions result in practically coinciding values of the enthalpy of formation of NdO(g). The selected value

$$\Delta_f H^\circ(\mathrm{NdO,\ g}, 298.15\mathrm{K}) = -(120 \pm 8)\ \mathrm{kJ\,mol^{-1}}$$

is taken as the rounded average of the third-law values calculated from the works of Tetenbaum[259] and Murad.[250] The selected enthalpy of formation corresponds to D_0(NdO) = (692.8 ± 8) kJ mol^{-1}.

4.6. PmO(g)

4.6.1. Heat capacity and entropy

The thermal functions of PmO(g) in the standard state have been calculated using the molecular constants given in Table 39.

Experimental data on the PmO molecular spectra are absent. The constants presented in Table 39 are estimated. Dolg and Stoll[193] showed that the molecular constants of the lanthanide monoxides in the electronic states of the same electron configuration change regularly. Thus the constants can be estimated by interpolation. Field[233] predicted the ground state X3.5 belonging to the $4f^4$(5I)6*s* subconfiguration. Dulick *et al.*[247] carried out a Ligand field calculation of this subconfiguration and obtained for the ground state $\Omega = 0.5$. For the calculation of the thermal functions this difference in Ω is of little importance because all the states of PmO belonging to this subconfiguration have statistical weight 2.

In the present work, the molecular constants of PmO are adopted (see Table 39) from the results of calculations by Dulick and Field[243] up to 10 000 cm^{-1} and on the basis of rough estimates of statistical weights for the $4f^4$6*s*, $4f^4$6*p*, and $4f^4$5*d* states at T ≥ 10 000 cm^{-1}.

The derived standard entropy at room temperature is

$$S^\circ(298.15\ \mathrm{K}) = (246.519 \pm 2.0)\ \mathrm{J\,K^{-1}\,mol^{-1}}$$

and the coefficients of the equations for the heat capacity are

$$C_p^\circ/(\mathrm{J\,K^{-1}\,mol^{-1}}) = 31.64170 + 38.6653 \times 10^{-3}(\mathrm{T/K}) - 30.3021 \times 10^{-6}(\mathrm{T/K})^2 + 8.45852 \times 10^{-9}(\mathrm{T/K})^3 - 2.08747 \times 10^{5}(\mathrm{T/K})^{-2}$$

for the 298.15–1100 K range, and

TABLE 38. The enthalpy of formation of NdO(g), in kJ mol^{-1}

Authors	Method[a]	T/K	Reaction	$\Delta_r H^\circ$(298.15 K)	$\Delta_f H^\circ$(298.15 K)
Goldstein *et al.*[202]	K	2255–2408	$Nd_2O_3 = 2NdO(g) + O(g)$	1790.3	−133.6
Tetenbaum[259]	T	2155–2485	$Nd_2O_3 = 2NdO(g) + O(g)$	1576.6	−115.8
Murad[250]	M	1933	Nd(g) + ScO(g) = PrO(g) + Sc(g)	−16.4	−122.1
	M	1999	Nd(g) + TiO(g) = PrO(g) + Ti(g)	−26.5	−122.9
Selected value:			D_0(NdO) = 692.8 ± 8		−120.0 ± 8

[a]K = Knudsen effusion; M = mass spectrometry; T = transpiration.

TABLE 39. Molecular constants of $^{145}Pm^{16}O(g)$

No.	State	T_e	ω_e	$\omega_e x_e$	B_e	$\alpha_e 10^3$	$D_e 10^7$	r_e	p_i
		cm^{-1}						pm	
0[a]	X0.5	0	832	2.9[b]	0.358[c]	1.7[c]	2.65[d]	180.7	2
1[a]		225							2
2[a]		660							2
3[a]		820							2
4[a]		1240							6
5[a]		2280							14
6[a]		2890							4
7[a]		3565							12
8[a]		4340							12
9[a]		5065							10
10[a]		5470							6
11[a]		6155							12
12[a]		6950							20
13[a]		8130							16
14[a]		9070							6
15[a]		10 000							35
16[a]		15 000							60
17[a]		20 000							180
18[a]		25 000							400
19[a]		30 000							800
20[a]		35 000							1000
21[a]		40 000							1300

[a]Experimental ($4f^4 6s$) state.
[b]Estimated state.
[c]From Shenyavskaya *et al.*[252]
[d].....

$$C_p^\circ/(J\,K^{-1}\,mol^{-1}) = 50.95780 + 1.31663 \times 10^{-3}(T/K) - 1.57622 \times 10^{-6}(T/K)^2 + 0.282026 \times 10^{-9}(T/K)^3 - 2.75930 \times 10^{6}(T/K)^{-2}$$

for the 1100–4000 K range.

4.6.2. Enthalpy of formation

No experimental data are available for the enthalpy of formation of promethium monoxide PmO(g). The quantum-mechanical calculations for the lanthanide monoxides performed till now do not have a thermochemical quality necessary for inclusion in the thermodynamic evaluations. Instead, a model based on the conception of promotion of a free atom into a "valence state" was used for evaluation of the PmO molecule stability. For the lanthanide monoxide molecules, the idea was for the first time expressed by Ames *et al.*[206] It was shown that variations in the dissociation energies of the lanthanide monoxide series correspond to the magnitude of the $4f^n \rightarrow 4f^{n-1}5d$ transitions of the Ln^{2+} ions. Murad and Hildenbrand,[260] using more reliable and more broad experimental basis, came to analogous conclusion that the $4f^n \rightarrow 4f^{n-1}5d$ excitation energy plays a major role in determining the energetics of most of the lanthanide monoxide bonds.

The model was further developed by Gibson,[261] who came to conclusion that the Ln–O and Ln–O^+ bonds "are evidently formed using two $5d$ electrons, rather than one $5d$ and one $6s$ electron". Using estimated excitation energies for the formation of atomic Pm in the $5d6s$ and $5d^2 6s$ configurations, 115 and 129 kJ mol^{-1}, Gibson obtained two values for the dissociation energy of PmO(g): 712 kJ mol^{-1} and 698 kJ mol^{-1}. Taking into account the monotonous decrease of D_0(LnO) values going from LaO to EuO, those values seem to be too high. A lower value D_0(PmO) ~ 630 kJ mol^{-1} can be obtained as a mean value between D_0(NdO) and D_0(SmO). In the present assessment a compromise between the two ways of estimation is selected: D_0(PmO) = (650 ± 50) kJ mol^{-1}. This value corresponds to

$$\Delta_f H^\circ(PmO,\ g,\ 298.15\ K) = -(145 \pm 50)\ kJ\,mol^{-1}.$$

4.7. SmO(g)

4.7.1. Heat capacity and entropy

The thermal functions of SmO(g) in the standard state have been calculated using the molecular constants given in Table 40.

Analysis of electronic transitions of SmO by Linton *et al.*,[262] Bujin and Linton,[263] Bujin and Linton,[264] Linton *et al.*,[265] Linton *et al.*,[266] and Hannigan[267] revealed 15 low-lying states including the ground $X0^-$ state. The vibrational structure of the observed transitions was not developed. The $\Delta G_{1/2}$ values were detected by Linton *et al.*[265] only for four low-lying states, but not for the ground state. The infrared spectrum of SmO was observed in solid Ar and Kr matrices by Weltner and De Kock,[245] Willson and Andrews,[213] and Willson *et al.*[246] Taking into account the matrix shift, the obtained values of the fundamental frequency are in agreement with the $\Delta G_{1/2}$ value for the first excited state of SmO in gas phase. That permits us to estimate the vibrational constant ω_e with an accuracy of 2 cm^{-1}. *Ab initio* calculations by Dolg and Stoll[193] dealt with the ground state of the molecule and resulted in theoretical spectroscopic constants.

The electron configuration assignments for the lower states of the transitions to the ground state configuration $4f^5 6s$ are doubtless. The $4f^5$(6H)$6s$ states were calculated using Ligand field theory by Carrete and Hocquet[230] and Dulick *et al.*[247] The configuration assignments for the upper states of the transitions were not considered. Table 40 gives the experimental $4f^5$(6H)$6s$ states according to Bujin and Linton[263] and the estimated statistical weights of the $4f^5 6s$, $4f^5 6p$, and $4f^5 5d$ superconfigurations at fixed energies up to 40 000 cm^{-1}.

The derived standard entropy at room temperature is

$$S^\circ(298.15\ K) = (246.592 \pm 0.10)\ J\,K^{-1}\,mol^{-1}.$$

and the coefficients of the equations for the heat capacity are

$$C_p^\circ/(J\,K^{-1}\,mol^{-1}) = 28.65158 + 45.8171 \times 10^{-3}(T/K) - 34.4081 \times 10^{-6}(T/K)^2 + 7.99213 \times 10^{-9}(T/K)^3 - 4.99673 \times 10^{4}(T/K)^{-2}$$

for the 298.15–1400 K range, and

TABLE 40. Molecular constants of $^{152}Sm^{16}O(g)$

No.	State	T_e	ω_e	$\omega_e x_e$	B_e	$\alpha_e 10^3$	$D_e 10^7$	r_e	p_i
		cm^{-1}						pm	
0[a]	$X(1)0^-$	0	829.5[b]	3.58	0.353952[c]	2.0	2.58[d]	181.415	1
1[a]	(1)1	147							2
2[a]	(1)2	567							2
3[a]	$(2)0^+$	582							1
4[a]	(2)1	879							2
5[a]	(1)3	1280							2
6[a]	$(3)0^+$	1546							1
7[a]	(2)2	1604							2
8[a]	$(4)0^+$	1661							1
9[a]	(3)1	1661							2
10[a]	(4)1	2014							2
11[a]	(3)2	2240							2
12[a]	(1)4	2287							2
13[a]	$(5)0^+$	2520							2
14[a]	(5)1	2867							2
15[e]		2710							2
16[e]		3040							4
17[e]		3450							4
18[e]		3860							12
19[e]		4490							8
20[e]		5000							4
21[e]		10 000							25
22[e]		15 000							60
23[e]		20 000							290
24[e]		25 000							380
25[e]		30 000							400
26[e]		35 000							1200
27[e]		40 000							2350

[a]Experimental ($4f^5 6s$) state.
[b]Estimated, see text.
[c]Calculated from $B_0 = 0.352952\ cm^{-1}$ according to Bujin and Linton[264] and the α_e value calculated from the Pekeris relation.
[d]Calculated from the Kratzer relation.
[e]Estimated state.

$$C_p^\circ/(\mathrm{J\,K^{-1}\,mol^{-1}}) = 70.58620 - 20.2158 \times 10^{-3}(\mathrm{T/K}) + 4.68050 \times 10^{-6}(\mathrm{T/K})^2 - 0.243006 \times 10^{-9}(\mathrm{T/K})^3 - 6.91999 \times 10^{6}(\mathrm{T/K})^{-2}$$

for the 1400–4000 K range.

4.7.2. Enthalpy of formation

The results for the enthalpy of formation of SmO(g) are presented in Table 41. Ames *et al.*[206] carried out Knudsen effusion measurement of the weight loss for Sm_2O_3(cr). The results of these measurements were treated in this work under assumption of congruent vaporization of Sm_2O_3(cr) according to reaction

$$Sm_2O_3(cr) = 2SmO(g) + O(g),$$

neglecting the possibility of formation of Sm(g) atoms in the vapor (see Sec. 4.1). The enthalpy of formation of SmO(g) thus calculated is slightly more negative in comparison with results of mass-spectrometric measurements for Al(g) + SmO(g) oxygen exchange reaction.[268] Results of the latter work can be regarded as highly reliable, due to large number of measurements carried out using both vibrating-reed electrometer and pulse counting detection. It needs to be mentioned, however, that our treatment of data from that paper resulted in a considerable difference between second- and third-law values for the enthalpy of formation of SmO(g).

TABLE 41. The enthalpy of formation of SmO(g), in kJ mol^{-1}

Authors	Method[a]	T/K	Reaction	$\Delta_r H°(298.15\ K)$	$\Delta_f H°(298.15\ K)$
Ames *et al.*[206]	K	2333–2499	$Sm_2O_3 = 2SmO(g) + O(g)$	1839.1	−113.6
	M	2360–2500	Sm(g) + YO(g) = SmO(g) + Y(g)	135.2	−170.9
Dickson and Zare[269]	B	2155–2485	$Sm(g) + NO_2 = SmO(g) + NO(g)$		≤−116.6
Hildenbrand[268]	M	2087–2298	Al(g) + SmO(g) = AlO(g) + Sm(g)	3.5	−109.0
	M	2110–2295	Al(g) + SmO(g) = AlO(g) + Sm(g)	2.6	−101.6
Selected value:			$D_0(SmO) = 555.6 \pm 8$		-105.3 ± 8

[a]K = Knudsen effusion; M = mass spectrometry; B = beam-gas chemiluminescence.
[b]Recalculated by Ames *et al.*[206]

From the short wavelength cutoff of the Sm molecular beam and NO_2(g) chemiluminescent spectra, the following lower boundary value to the ground state dissociation energy was obtained in the work of Dickson and Zare[269]: $D_0(SmO) \geq (566.9 \pm 2.9)$ kJ mol^{-1}. Comparison with both Knuden effusion[206] and mass spectrometry[268] results reveals that this lower bound value is overestimated. The mass-spectrometric results of Ames *et al.*[206] seem to be erroneous.

The selected value

$$\Delta_f H^\circ(SmO,\ g,\ 298.15K) = -(105.3 \pm 8)\ kJ\,mol^{-1}$$

is taken as a rounded average of two third-law values calculated from the data of Hildenbrand.[268] The selected enthalpy of formation corresponds to $D_0(SmO) = (555.6 \pm 8)$ kJ mol^{-1}.

4.8. EuO(g)

4.8.1. Heat capacity and entropy

The thermal functions of EuO(g) in the standard state have been calculated using the molecular constants presented in Table 42.

The electronic spectrum of EuO (single electronic transition) was investigated by McDonald,[270] but the data were not published. Some of the results for the ground state ($\omega_e \approx 688$ cm^{-1} and $B_0 = 0.32624$ cm^{-1} for ^{153}EuO) were cited by Dolg *et al.*[271] The values of the fundamental frequency of EuO were measured also in solid Ar and Kr matrices by Gabelnick *et al.*[212] (668 cm^{-1}), Willson and Andrews[213] (667.8 cm^{-1} and 633.5 cm^{-1} for $Eu^{16}O$ and $Eu^{18}O$, respectively), and Willson *et al.*[246] (668 cm^{-1}). Taking into account the matrix shift, the obtained values are in agreement with the ω_e value for EuO from gas phase. That permits to estimate the uncertainty of selected value of ω_e to be within 2 cm^{-1}.

The electronic structure of EuO was investigated by Carrete and Hocquet[230] and Dulick *et al.*[247] using Ligand field calculation and by Dolg *et al.*[271] by *ab initio* calculation. All calculations revealed the $X^8\Sigma$ ($4f^7$) ground state and the first excited state $A^8\Sigma$ ($4f^6 6s$). However the energy of the $A^8\Sigma$ state is not well defined (from 3300 up to 7937 cm^{-1}). The theoretical calculations resulted also in relative energies for the other low-lying states of the $4f^6 6s$ configuration. In the present work we select the data obtained by Carrete and Hocquet[230] (all states of the $4f^6$(7F)$6s$ subconfiguration with correction of the $A^8\Sigma$ energy (assumed 6000 cm^{-1}). In Table 42 are also presented roughly estimated statistical weights (for $4f^6 6s$, $4f^6 6d$, and $4f^6 6p$ states) at fixed energies in the 15 000–40 000 cm^{-1} interval.

TABLE 42. Molecular constants of $^{153}Eu^{16}O$(g)

No.	State	T_e	ω_e	$\omega_e x_e$	B_e	$\alpha_e 10^3$	$D_e 10^7$	r_e	p_i
		cm^{-1}						pm	
0[a]	$X^8\Sigma$	0	688	3	0.3272[b]	1.9	2.96[c]	188.63	2
1[d]	$A^8\Sigma$	6000							8
2[d]		7000							16
3[d]		8000							18
4[d]		9000							28
5[d]		13 200							28
6[d]		15 000							10
7[d]		20 000							35
8[d]		25 000							340
9[d]		30 000							670
10[d]		35 000							3300
11[d]		40 000							3600

[a]Experimental ($4f^6 6s$) state.
[b]Calculated from $B_0 = 0.32624$ cm^{-1} and the α_e value calculated from the Pekeris relation.
[c]Calculated from the Kratzer relation.
[d]Estimated state.

The derived standard entropy at room temperature is

$$S^\circ(298.15\ K) = (253.419 \pm 0.10)\ J\,K^{-1}\,mol^{-1}$$

and the coefficients of the equations for the heat capacity are:

$$C_p^\circ/(J\,K^{-1}\,mol^{-1}) = 33.8838 + 7.70507 \times 10^{-3}(T/K) - 7.38219 \times 10^{-6}(T/K)^2 + 3.41476 \times 10^{-9}(T/K)^3 - 2.52934 \times 10^{5}(T/K)^{-2}$$

for the 298.15–1700 K range, and

$$C_p^\circ/(J\,K^{-1}\,mol^{-1}) = -79.4911 + 93.4647 \times 10^{-3}(T/K) - 22.3194 \times 10^{-6}(T/K)^2 + 1.86990 \times 10^{-9}(T/K)^3 + 5.27560 \times 10^{7}(T/K)^{-2}$$

for the 1700–4000 K range.

4.8.2. Enthalpy of formation

The results for enthalpy of formation of EuO(g) are presented in Table 43. Ames *et al.*[206] carried out Knudsen effusion weight-loss measurements for Eu_2O_3(cr). Formal treatment of their data under the assumption of congruent evaporation with formation of EuO(g) and O(g) demonstrates the inadequacy of this approach due to high degree of EuO dissociation and the predominance of Eu(g) in the vapor phase. In this case, the results of the calculations of the enthalpy of formation are to be regarded as a lower boundary of the enthalpy of formation.

Dickson and Zare[269] studied the chemiluminescence resulting from the reaction of an europium molecular beam with NO_2, N_2O, and O_3 under single-collision conditions. From the short wavelength cutoff of the chemiluminescent spectra, the following lower boundary to the ground state dissociation energy was obtained from the Eu(g) + NO_2 study: $D_0(EuO) = (549.8 \pm 2.9)$ kJ mol^{-1}. This value was discarded in the paper by Murad and Hildenbrand,[272] in which a detailed discussion of the stability of EuO(g) was presented. The following values were calculated by Murad and Hildenbrand from the graph in the Dickson and Zare[269]: Eu +N_2O, $D_0(EuO) > 423$ kJ mol^{-1}; Eu + O_3, $D_0(EuO) > 457$ kJ mol^{-1} (not shown in Table 43). Both values are in agreement with mass-spectrometric data. Mass spectrometric measurements of isomolecular oxygen exchange reactions have been carried out by Murad and Hildenbrand,[272] and Balducci *et al.*[273] All results of these works are in reasonable agreement.

TABLE 43. The enthalpy of formation of EuO(g), in kJ mol^{-1}

Authors	Method[a]	T/K	Reaction	$\Delta_r H°(298.15\ K)$	$\Delta_f H°(298.15\ K)$
Ames *et al.*[206]	K	1984–2188	$Eu_2O_3 = 2EuO(g) + O(g)$	1621.7	−142.7
Dickson and Zare[269]	B		$Eu(g) + NO_2 = EuO(g) + NO(g)$		<128.4
Murad and Hildenbrand[272]	M	2026–2255	$Eu(g) + AlO(g) = EuO(g) + Al(g)$	39.1	−47.4
	M	2009–2237	$Eu(g) + BaO(g) = EuO(g) + Ba(g)$	66.3	−60.5
	M	2044–2237	$Eu(g) + TiO(g) = EuO(g) + Ti(g)$	184.5	−62.9
Balducci *et al.*[273]	M	1920–2220	$Eu(g) + WO_3(g) = EuO(g) + WO_2(g)$	118.2	−54.4
Selected value:			$D_0(EuO) = 477.9 \pm 8$		−56.5 ± 8

[a]K = Knudsen effusion; M = mass spectrometry; B = beam-gas chemiluminescence.

The selected value

$$\Delta_f H°(\mathrm{EuO,\ g,\ 298.15\,K}) = -(56.5 \pm 8)\ \mathrm{kJ\,mol^{-1}}$$

is taken as weighted average of the third-law values calculated from all mass-spectrometric works, with the weight of $WO_3 + Eu$ result of 0.5, due to less accurate reference values. The selected enthalpy of formation corresponds to $D_0(EuO) = 477.9$ kJ mol^{-1}.

4.9. GdO(g)

4.9.1. Heat capacity and entropy

The thermal functions of GdO(g) in the standard state have been calculated using the molecular constants presented in Table 44.

The first studies of the electronic spectrum of GdO were carried out at the low and moderate resolution and dealt with the vibrational structure of the spectrum (see Huber and Herzberg[179]), Yadav *et al.*,[274,275] Suarez and Grinfeld,[276] and the literature cited therein). The investigations revealed the highly complex structure of the spectrum, and the proposed vibrational analysis was doubtful. The values of the fundamental frequency of GdO were observed in solid inert gas matrices by Weltner and De Kock[245] in Ne and Ar (824 and 813 cm^{-1}, respectively), by Willson and Andrews[213] in Ar (812.7 and 770.9 cm^{-1} for $Gd^{16}O$ and $Gd^{18}O$, respectively), and by Willson *et al.*[246] in Ar (812.8 cm^{-1}).

Van Zee *et al.*[277] found by means of ESR spectroscopy in an Ar matrix at 4 K that the GdO ground state is $^9\Sigma^-$, and its vibrational quantum $\Delta G_{1/2} = 824$ cm^{-1}. Taking into account the matrix shift, the values of the fundamental frequency observed in matrices are in agreement with the value $\Delta G_{1/2} = 828.19$ cm^{-1} measured by Yadav *et al.*[274] for the lower state of the A system with multiple heads. Dmitriev *et al.*[278] analyzed the rotational spectrum of the transition connected with the ground state ($^9\Pi_1$-$X^9\Sigma^-$). Later Dmitriev *et al.*[279] and Dmitriev[280] investigated the fluorescence spectra excited by the Ar^+ laser lines in the region of the $^9\Sigma^-$-$X^9\Sigma^-$ and $^7\Sigma^-$-$a^7\Sigma^-$ systems, obtained the data on the $v = 0$-8 levels of the ground state and for the $v = 0$-3 levels of the $a^7\Sigma^-$ state, and found the excitation energy of the $a^7\Sigma^-$ state from the intercombination transitions $^9\Sigma^-$-$a^7\Sigma^-$ and $^7\Sigma^-$- $X^9\Sigma^-$. Till now the vibrational and rotational constants for these low-lying states and the energy of $a^7\Sigma^-$ state are the most precise. The molecular constants for the $X^9\Sigma^-$ and $a^7\Sigma^-$ states (see Table 44) were reported by Gurvich *et al.*[7,281]. The studies of the laser induced fluorescence spectra by Carette *et al.*[282] and by Kaledin *et al.*[258] revealed new components [18.4]4 and [19.0]0$^-$ of the $^{9,7}\Pi$ states. Kaledin *et al.*[258] showed that Ω-assignment for the components of the $^9\Pi$ state made by Dmitriev *et al.*[278] was not correct. At the same time the interpretation of the $f^7(8S)p$ states proposed by Kaledin *et al.*[258] was not convincing. In any case it shows that the $^9\Pi_5$ ([17.6]5) and $^9\Pi_4$ ([18.4]4) components known experimentally belong to the states of different multiplicity.

TABLE 44. Molecular constants of $^{158}Gd^{16}O$(g)

		T_e	ω_e	$\omega_e x_e$	B_e	$\alpha_e 10^3$	$D_e 10^7$	r_e	
No	State	cm^{-1}						pm	p_i
0[a]	$X^9\Sigma^{-}$[c]	0	831.19	2.619	0.35561	1.48	2.56	180.66	9
1[a]	$a^7\Sigma^{-}$[c]	1834.64	837.11	2.62	0.35678	1.47	2.59	180.37	7
2[a]	$A^9\Delta$?	11 300							18
3[a]		17 500							50
4[a]		20 000							28
5[a]	$^9\Sigma^-$	21 693[b]							9
6[a]	$^7\Sigma^-$	22 307[b]							7
7[c]		25 000							16
8[c]		30 000							200
9[c]		35 000							440
10[c]		40 000							1050

[a]Experimental state.
[b]All the constants for these state from Dmitriev *et al.*[279] and Dmitriev.[280]
[c]Estimated state.

Ab initio calculations of GdO by Dolg *et al.*,[271,283] dealt with well-known electronic states $X^9\Sigma^-$ and $a^7\Sigma^-$ and resulted in theoretical constants in good agreement with the experiment. Ligand field calculation by Carrete and Hocquet,[230] Dulick *et al.*[247] and *ab initio* calculations by Kotzian *et al.*[197] and Sakai *et al.*[284] considered the electronic structure of the molecule. All calculations gave the $X^9\Sigma^- f^7(8S)s$ ground state and the $a^7\Sigma^- f^7(8S)s$ first excited state. The half filled 4*f* shell along with the ground 8S state and the other states of the Gd atom lying much higher (>30 000 cm^{-1}) explain the simple structure of the GdO molecule: only 12 states of the $f^7(8S)s$, $f^7(8S)d$, and $f^7(8S)p$ subconfigurations are expected up to 30000 cm^{-1}. All the calculations except that by Dulick *et al.*,[247] who calculated only the $f^7(8S)s$ states, are in agreement that the first excited configuration of GdO is $f^7(8S)d$. However the energy of the $A^9\Delta$ state differs considerably (from 8500 to 16700 cm^{-1}). The study of the GdO^- photoelectron spectrum by Klingeler *et al.*[285] revealed the group of states near 11300 ± 400 cm^{-1} which positions coincide with the $A^9\Delta$ state calculated by Carrete and Hocquet.[230] The estimated energies and statistical weights of the unobserved states of the configuration mentioned above are presented in Table 44. It gives also the estimated statistical weights in the 30000–40000 cm^{-1} region (the f^7s and f^7d states).

The derived standard entropy at room temperature is:

$$S^\circ(298.15\ \mathrm{K}) = (253.495 \pm 0.03)\ \mathrm{J\,K^{-1}\,mol^{-1}}$$

and the coefficients of the equations for the heat capacity are:

$$C_p^\circ/(\mathrm{J\,K^{-1}\,mol^{-1}}) = 21.26451 + 40.9137 \times 10^{-3}(\mathrm{T/K}) - 30.1655 \times 10^{-6}(\mathrm{T/K})^2 + 7.50616 \times 10^{-9}(\mathrm{T/K})^3 + 6.83276 \times 10^{4}(\mathrm{T/K})^{-2}$$

for the 298.15–1300 K range, and

$$C_p^\circ/(\mathrm{J\,K^{-1}\,mol^{-1}}) = 51.77714 - 10.0325 \times 10^{-3}(\mathrm{T/K}) + 2.57810 \times 10^{-6}(\mathrm{T/K})^2 - 0.111668 \times 10^{-9}(\mathrm{T/K})^3 - 4.80380 \times 10^{6}(\mathrm{T/K})^{-2}$$

for the 1300–4000 K range.

4.9.2. Enthalpy of formation

The results for the enthalpy of formation of GdO(g) are presented in Table 45. Experimental data used in the analysis are based on Knudsen effusion[206] and mass spectrometric measurements,[260] the results being in satisfactory agreement. At the same time, the mass-spectrometric results deserve more weight, because interpretation of Knudsen effusion data is not unambiguous due to possible formation of free gadolinium atoms in the vapors (see text on LaO(g) enthalpy of formation).

The selected value

$$\Delta_f H^\circ(\mathrm{GdO,\ g,\ 298.15\ K}) = -(68.0 \pm 8)\ \mathrm{kJ\,mol^{-1}}$$

is taken as a rounded average of the third-law values calculated from two mentioned works, with a low weight for the Knudsen effusion results. The selected enthalpy of formation corresponds to $D_0(\mathrm{GdO}) = (710.2 \pm 8)$ kJ mol^{-1}.

4.10. TbO(g)

4.10.1. Heat capacity and entropy

The thermal functions of TbO(g) in the standard state have been calculated using the molecular constants given in Table 46.

The electronic spectrum of TbO was investigated in emission and absorption by Kaledin and Shenyavskaya[286,287] (see Huber and Herzberg[179] for earlier works) and in the fluorescence by Kulikov *et al.*[288,289], and Gurvich *et al.*[281] The fundamental frequency of TbO was observed in solid inert gas matrices by Weltner and De Kock[245] in Ne and Ar (824 cm^{-1}), by Willson and Andrews[213] in Ar at 10 K (823.9 and 781.4 cm^{-1} for $Tb^{16}O$ and $Tb^{18}O$, respectively), and by Willson *et al.*[246] in Ar (823.9 cm^{-1}). Taking into account the matrix shift the values of fundamental frequency obtained in matrices are in agreement with those from gas phase data. *Ab initio* calculations by Dolg and Stoll[193] dealt with the ground state of the TbO molecule and resulted in the theoretical spectroscopic constants.

The studies of the TbO electronic spectra revealed 14 low-lying states (including the X6.5 ground state), assigned to the $f^8(7F)s$ subconfiguration, and 11 excited states with energies 14 899–22 300 cm^{-1}, mostly ascribed to the $f^8(7F)d$ and $f^8(7F)p$ subconfigurations. Ligand field calculation by Carrete and Hocquet[230] and Dulick *et al.*[247] showed that up to 10 000 cm^{-1} all the states belonged to the $f^8(7F)s$ subconfiguration. The estimated energies and statistical weights of the unobserved states of the $f^8(7F)s$ subconfiguration, presented in Table 46, are selected from Carrete and Hocquet.[230] Table 46 gives also the estimated statistical weights of the $f^8(7F)d$ and $f^8(7F)p$ states assuming the energies of the lowest states at 12 000 and 18 000 cm^{-1}, respectively, and placing the other states of the f^8nl configurations higher than the corresponding $f^8(7F)$l states by approximately 15 000–20 000 cm^{-1}.

TABLE 45. The enthalpy of formation of GdO(g), in kJ mol^{-1}

Authors	Method[a]	T/K	Reaction	$\Delta_r H^\circ$(298.15 K)	$\Delta_f H^\circ$(298.15 K)
Ames *et al.*[206]	K	2408–2546	$Gd_2O_3 = 2GdO(g) + O(g)$	1935.6	−78.5
Murad and Hildenbrand[260]	M	1957–2024	Gd(g) + TiO(g) = GdO(g) + Ti(g)	−43.5	−68.5
	M	1908–1977	Gd(g) + YO(g) = GdO(g) + Y(g)	5.7	−65.4
Selected value:			$D_0(\mathrm{GdO}) = 710.2 \pm 8$		−68.0 ± 8

[a]K = Knudsen effusion; M = mass spectrometry.

TABLE 46. Molecular constants of $^{159}Tb^{16}O(g)$

No.	State	T_e	ω_e	$\omega_e x_e$	B_e	$\alpha_e 10^3$	$D_e 10^7$	r_e	p_i
		cm^{-1}						pm	
0[a]	$X(1)6.5$	0	843.1[b]	3.04[b]	0.35325	1.50	2.48[c]	181.213	2
1[a]	(1)5.5	355							2
2[a]	(1)4.5	750							2
3[a]	(1)3.5	1183							2
4[a]	(2)5.5	1624							2
5[a]	(1)2.5	1654							2
6[a]	(2)4.5	2101							2
7[a]	(1)1.5	2160							2
8[a]	(2)3.5	2610							2
9[a]	(3)5.5	2900							2
10[a]	(2)2.5	3119							2
11[a]	(3)4.5	3188							2
12[a]	(3)3.5	3506							2
13[a]	(3)2.5	3830							2
14[d]		4000							4
15[d]		4500							8
16[d]		5100							8
17[d]		6100							16
18[d]		7050							8
19[d]		7950							10
20[d]		9050							8
21[d]		10 100							9
22[d]		15 000							25
23[d]		20 000							80
24[d]		25 000							125
25[d]		30 000							170
26[d]		35 000							600
27[d]		40 000							900

[a]Experimental state.
[b]Calculated from $\Delta G_{1/2} = 837.1\ cm^{-1}$ given by Kulikov *et al.*[288] and the assumed dissociation limit.
[c]Calculated from the Kratzer relation.
[d]Estimated state.

The derived standard entropy at room temperature is

$$S^\circ(298.15\ K) = (245.758 \pm 0.10)\ J\,K^{-1}\,mol^{-1}$$

and the coefficients of the equations for the heat capacity are

$$C_p^\circ/(J\,K^{-1}\,mol^{-1}) = 30.97785 + 32.5225 \times 10^{-3}(T/K) - 19.6568 \times 10^{-6}(T/K)^2 + 4.14576 \times 10^{-9}(T/K)^3 - 1.18135 \times 10^{4}(T/K)^{-2}$$

for the 298.15–1400 K range, and

$$C_p^\circ/(J\,K^{-1}\,mol^{-1}) = 64.48191 - 8.31957 \times 10^{-3}(T/K) + 0.883659 \times 10^{-6}(T/K)^2 + 0.0270508 \times 10^{-9}(T/K)^3 - 10.4723 \times 10^{6}(T/K)^{-2}$$

for the 1400–4000 K range.

4.10.2. Enthalpy of formation

There is only one study of the determination of the enthalpy of formation of TbO(g). Ames *et al.*[206] have performed mass spectrometric measurements of isomolecular oxygen exchange reaction (1830–2040 K)

$$Tb + LaO(g) = TbO(g) + La(g)$$

for which we obtain $\Delta_r H^\circ(298.15\ K) = 80.2\ kJ\,mol^{-1}$ by third-law analysis. This results in the following selected enthalpy of formation:

$$\Delta_f H^\circ(TbO,\ g,\ 298.15\ K) = -(84.7 \pm 10)\ kJ\,mol^{-1}$$

This value corresponds to $D_0(TbO) = (715.5 \pm 10)\ kJ\,mol^{-1}$.

4.11. DyO(g)

4.11.1. Heat capacity and entropy

The thermal functions of DyO(g) in the standard state have been calculated using the molecular constants given in Table 47.

The electronic spectrum of DyO was investigated in emission and absorption by Kaledin and Shenyavskaya[286] and Yadav *et al.*[290] (see Huber and Herzberg[179] for earlier works) and in the fluorescence by Linton *et al.*[291] and Cheng.[292] The values of the fundamental frequency of DyO were observed in solid inert gas matrices by Weltner and De Kock[245] in Ar (829 cm^{-1}), Willson and Andrews[213] in Ar at 10 K (829.0 and

TABLE 47. Molecular constants of $^{159}Dy^{16}O(g)$

No.	State	T_e	ω_e	$\omega_e x_e$	B_e	$\alpha_e 10^3$	$D_e 10^7$	r_e	p_i
		cm^{-1}						pm	
0[a]	$X(1)8$	0	849[b]	3.5[b]	0.3593[c]	2.0	2.57[d]	179.4	2
1[a]	(1)7	770							2
2[a]	(1)6	1630							2
3[a]	(2)7	1683							2
4[a]	(2)6	2420							2
5[e]		2180							2
6[e]		3280							11
7[e]		4400							10
8[e]		5100							7
9[e]		6100							8
10[e]		7130							14
11[e]		8565							14
12[e]		9830							20
13[e]		11 775							20
14[e]		14 070							20
15[e]		15 000							40
16[e]		20 000							130
17[e]		25 000							350
18[e]		30 000							370
19[e]		35 000							1500
20[e]		40 000							1900

[a]Experimental state.
[b]Calculated from $\Delta G_{1/2} = 842$ cm^{-1} given by Linton *et al.*[291] and the assumed dissociation limit.
[c]Calculated from $B_0 = 0.358413$ cm^{-1} given by Linton *et al.*[291]) and $\alpha_e = 0.0020$ cm^{-1} found by Kaledin and Shenyavskaya.[286]
[d]Calculated from the Kratzer relation.
[e]Estimated state.

786.1 cm^{-1} for $Dy^{16}O$) and $Dy^{18}O$, respectively), and Willson *et al.*[246] in Ar (828.7 cm^{-1}). Taking into account the matrix shift, the values of the fundamental frequency obtained in matrices are in agreement with those from gas phase data. *Ab initio* calculations by Dolg and Stoll[193] dealt with the ground state of the molecule and resulted in theoretical spectroscopic constants.

The studies of the DyO electronic spectra by Kaledin and Shenyavskaya[286] and Linton *et al.*[291] revealed 5 low-lying states (including the X8 ground state,) which were assigned to the f^9(6H)s subconfiguration, and 6 excited states with energies 17 070–19 000 cm^{-1}, most of which could be assigned to the f^9(6H)d and f^9(6H)p configurations.

Carrete and Hocquet[230] and Dulick *et al.*[247] carried out Ligand field calculations of the DyO states belonging to the f^9(6H)s subconfiguration. Carrete and Hocquet[230] obtained all the f^9(6H)s states (total statistical weight 132), while Dulick *et al.*[247] obtained only states up to 10 000 cm^{-1} with $\Sigma p = 74$. The data obtained by Dulick *et al.*[247] are closer to experimental data because of using the other parameter $G_3 = 300$ cm^{-1} as compared with $G_3 = 150$ cm^{-1} used by Carrete and Hocquet.[230] The deviations between the results are the largest for lower states. For that reason the estimated energies and statistical weights of the unobserved states of the f^9(6H)s subconfiguration up to 10 000 cm^{-1} are selected from the Dulick *et al.*[247] and those in the interval 10 000–15 000 cm^{-1} are selected from Carrete and Hocquet[230] with corrections to mean deviation. In Table 47 also the estimated statistical weights for the f^9(6FP)s states (>15 000 cm^{-1}) are given, for the remaining f^9s states corresponding to the low multiplicity terms of the f^9-core (>21 000 cm^{-1}), for the f^9(6H)d and f^8(6H)p states assuming the energies of the lowest states at 12 500 and 18 500 cm^{-1}, respectively, and for the other states of the f^9nl configurations as in case of the f^9s configuration. The upper limit for all configurations is assumed to be $D_0 + IP$, so all the estimated states are considered stable.

The derived standard entropy at room temperature is

$$S^\circ(298.15\ \mathrm{K}) = (242.208 \pm 0.10)\ \mathrm{J\,K^{-1}\,mol^{-1}}$$

and the coefficients of the equations for the heat capacity are

$$C_p^\circ/(\mathrm{J\,K^{-1}\,mol^{-1}}) = 19.08366 + 61.7856 \times 10^{-3}(\mathrm{T/K}) - 37.4790 \times 10^{-6}(\mathrm{T/K})^2 + 7.29509 \times 10^{-9}(\mathrm{T/K})^3 + 2.19805 \times 10^{4}(\mathrm{T/K})^{-2}$$

for the 298.15–1300 K range, and

$$C_p^\circ/(\mathrm{J\,K^{-1}\,mol^{-1}}) = 68.49712 - 11.3191 \times 10^{-3}(\mathrm{T/K}) + 1.99999 \times 10^{-6}(\mathrm{T/K})^2 - 0.0418797 \times 10^{-9}(\mathrm{T/K})^3 - 8.39005 \times 10^{6}(\mathrm{T/K})^{-2}$$

for the 1300–4000 K range.

4.11.2. Enthalpy of formation

Ames *et al.*[206] carried out Knudsen effusion measurements of the weight loss of Dy_2O_3(cr) in the temperature range 2440–2637 K. The results of these measurements were treated in this work under the assumption of congruent vaporization of Dy_2O_3(cr) according to reaction

$$Dy_2O_3(cr) = 2DyO(g) + O(g),$$

neglecting possible formation of Dy(g) atoms in the vapor (see Sec. 4.1). The DyO(g) enthalpy of formation thus calculated must be more negative than the correct value, the degree of deviation being dependent on amount of Dy atoms in the vapor. The third-law enthalpy of reaction $\Delta_r H^\circ(298.15\ \mathrm{K}) = 1953.4$ kJ mol^{-1}, yields $\Delta_f H^\circ$(DyO, g, 298.15 K) = −79.2 kJ mol^{-1}, which corresponds to D_0(DyO) = 609.8 kJ mol^{-1}. Dulick *et al.*[247] have estimated the DyO dissociation energy using the crystal field model applied to diatomic molecules as D_0(DyO) = (602 ± 1) kJ mol^{-1}. In absence of additional information, this value is selected in this work for the enthalpy of formation of DyO(g):

$$\Delta_f H^\circ(\mathrm{DyO,\ g}, 298.15\ \mathrm{K}) = -(71 \pm 20)\ \mathrm{kJ\,mol^{-1}}.$$

4.12. HoO(g)

4.12.1. Heat capacity and entropy

The thermal functions of HoO(g) in the standard state have been calculated using the molecular constants given in Table 48.

TABLE 48. Molecular constants of $^{165}Ho^{16}O$(g)

No.	State	T_e	ω_e	$\omega_e x_e$	B_e	$\alpha_e 10^3$	$D_e 10^7$	r_e	p_i
		cm^{-1}						pm	
0[a]	X8.5	0	848[b]	3.5[b]	0.358477	1.50	2.56[c]	179.59	2
1[a]	(1)7.5	603							2
2[a]	(2)7.5	1130							2
3[a]	(1)6.5	1853							2
4[d]		1165							14
5[d]		2275							12
6[d]		6300							22
7[d]		7100							8
8[d]		10 050							26
9[d]		13 500							26
10[d]		15 000							50
11[d]		20 000							90
12[d]		25 000							200
13[d]		30 000							250
14[d]		35 000							700
15[d]		40 000							1150

[a]Experimental state.
[b]Calculated from $\Delta G_{1/2}$ = 841.252 cm^{-1} given by Linton and Liu[294] and the assumed dissociation limit.
[c]Calculated from the Kratzer relation.
[d]Estimated state.

The electronic spectrum of HoO was investigated in emission and absorption by Kaledin and Shenyavskaya[286] (see Huber and Herzberg[179] for earlier works), and in fluorescence by Liu *et al.*,[293] Linton and Liu,[294] and Cheng.[292] The values of fundamental frequency of HoO were measured in solid inert gas matrices by Weltner and De Kock[245] in Ar (829 cm^{-1}), Willson and Andrews[213] in Ar at 10 K (828.1 and 785.2 cm^{-1} for $Ho^{16}O$ and $Ho^{18}O$, respectively), and Willson *et al.*[246] in Ar (828.0 cm^{-1}). Taking into account the matrix shift, the values of fundamental frequency obtained in matrices are in agreement with those from the gas phase data. *Ab initio* calculations by Dolg and Stoll[193] dealt with the ground state of the molecule and gave its constants in good agreement with experiment.

The studies of the HoO electronic spectra revealed 4 low-lying states (including the X8.5 ground state) which were assigned to the f^{10}(5I)*s* subconfiguration and 6 excited states with energies 17 600–22 400 cm^{-1} most of which could be assigned to the f^{10}(5I)d and f^{10}(5I)*p* superconfigurations. The Ligand field calculations were carried out by Carrete and Hocquet,[230] who considered all the f^{10}(5I)*s* states with the total statistical weight 130, and by Dulick *et al.*,[247] who did only the f^{10}(5I)*s* states up to 10 000 cm^{-1} with $\Sigma p = 74$. The results obtained by Dulick *et al.*[247] were closer to experimental data because of using the parameter G_3 = 300 cm^{-1} as compared with $G_3 = 150$ cm^{-1} used by Carrete and Hocquet.[230] The deviations were the largest for lower states. That is why in Table 48 the estimated energies and statistical weights for the unobserved states of the f^{10}(5I)*s* subconfiguration up to 10 000 cm^{-1} are taken from Dulick *et al.*,[247] and the data in the interval 10 000–15 000 cm^{-1} are taken from Carrete and Hocquet,[230] with corrections for mean deviation. In Table 48 also the estimated statistical weights for the f^{10}(5SDFG)*s* states from 15 000 cm^{-1} are given, for the remaining $f^{10}s$ states higher than 21 500 cm^{-1}, and for the f^{10}](5I)*d* and f^{10}(5I)*p* states assuming the energies of the lowest states at 12 500 and 18 500 cm^{-1}, respectively, and placing the other states of the f^{10}nl configurations as in case of the $f^{10}s$ configuration. The upper limit for all configurations is assumed to be a sum of the dissociation energy and the ionization potential, so that all the estimated states are considered stable.

The derived standard entropy at room temperature is

$$S^\circ(298.15\ \mathrm{K}) = (244.590 \pm 0.10)\ \mathrm{J\,K^{-1}\,mol^{-1}}$$

and the coefficients of the equations for the heat capacity are

$$C_p^\circ/(\mathrm{J\,K^{-1}\,mol^{-1}}) = 48.31232 + 76.8332 \times 10^{-3}(\mathrm{T/K}) - 155.715 \times 10^{-6}(\mathrm{T/K})^2 + 76.9567 \times 10^{-9}(\mathrm{T/K})^3 - 1.57926 \times 10^{6}(\mathrm{T/K})^{-2}$$

for the 298.15–900 K range, and

$$C_p^\circ/(\mathrm{J\,K^{-1}\,mol^{-1}}) = 43.11154 - 5.49748 \times 10^{-3}(\mathrm{T/K}) + 3.07490 \times 10^{-6}(\mathrm{T/K})^2 - 0.350566 \times 10^{-9}(\mathrm{T/K})^3 + 4.11955 \times 10^{6}(\mathrm{T/K})^{-2}$$

for the 900–4000 K range.

4.12.2. Enthalpy of formation

The results for the enthalpy of formation of HoO(g) are presented in Table 49. Ames *et al.*[206] carried out Knudsen effusion measurements of the weight loss of Ho_2O_3(cr). The results of these measurements were treated in this work under the assumption of congruent vaporization of Ho_2O_3(cr) according to reaction

$$Ho_2O_3(cr) = 2HoO(g) + O(g),$$

TABLE 49. The enthalpy of formation of HoO(g), in kJ mol^{-1}

Authors	Method[a]	T/K	Reaction	$\Delta_r H°(298.15\ K)$	$\Delta_f H°(298.15\ K)$
Ames *et al.*[206]	K	2487–2711	$Ho_2O_3 = 2HoO(g) + O(g)$	1988.4	−71.0
Murad and Hildenbrand[260]	M	1855–2178	$Ho(g) + TiO(g) = HoO(g) + Ti(g)$	65.5	−57.8
Selected value:			$D_0(HoO) = 604.1 \pm 10$		-57.8 ± 10

[a]K = Knudsen effusion; M = mass spectrometry; T = transpiration.

neglecting the possible formation of Ho(g) atoms in the vapor (see Sec. 4.1). The enthalpy of formation of HoO(g) so calculated must be more negative than the correct value, the degree of deviation being dependent on amount of Ho atoms in vapors. Comparison with the results of Murad and Hildenbrand[260] confirms this conclusion. The selected value

$$\Delta_f H°(HoO,\ g,\ 298.15\ K) = -(57.8 \pm 10)\ kJ\ mol^{-1}$$

is taken as a rounded third-law value calculated from the latter work. The selected enthalpy of formation corresponds to $D_0(HoO) = (604.1 \pm 10)$ kJ mol^{-1}.

4.13. ErO(g)

4.13.1. Heat capacity and entropy

Thermal functions of ErO(g) in the standard state have been calculated using the molecular constants presented in Table 50.

The electronic spectrum of ErO was investigated in emission and absorption by Kaledin and Shenyavskaya[295] (see Huber and Herzberg[179] for references to earlier works). The observed spectrum was highly complex. Only one rotational band at 5066 Å, observed in emission and absorption, was analyzed. It was supposed to be connected with the X8 ground state of the $f^{11}(4I)s$ subconfiguration as predicted by Field.[233]

TABLE 50. Molecular constants of $^{166}Er^{16}O(g)$

No.	State	T_e	ω_e	$\omega_e x_e$	B_e	$\alpha_e 10^3$	$D_e 10^7$	r_e	p_i
		cm^{-1}						pm	
0[a]	$X0^-$	0	849[b]	3.54[b]	0.359	1.9[c]	2.57[d]	179.4	1
1[e]		25							2
2[e]		95							2
3[e]		205							2
4[e]		350							2
5[e]		525							7
6[e]		730							4
7[e]		1030							6
8[e]		1550							4
9[e]		2100							2
10[e]		6115							14
11[e]		6920							14
12[e]		11 500							24
13[e]		15 700							50
14[e]		20 000							70
15[e]		25 000							80
16[e]		30 000							280
17[e]		35 000							370
18[e]		40 000							450

[a]Experimental state.
[b]Calculated from $\Delta G_{1/2} = 841.5$ cm^{-1} (see text) and the assumed dissociation limit.
[c]Calculated from the Kratzer relation.
[d]Calculated from the Pekeris relation.
[e]Estimated state.

The values of the fundamental frequency of ErO were measured in solid inert gas matrices by Weltner and De Kock[245] in Ar (829 cm^{-1}), Willson and Andrews[213] in Ar at 10 K (828.5 and 785.5 cm^{-1} for $Er^{16}O$ and $Er^{18}O$, respectively), and Willson *et al.*[246] in Ar (828.5 cm^{-1}). Taking into account the matrix shift (~13 cm^{-1}), the value 841.5 cm^{-1} is obtained for $\Delta G_{1/2}$ in the gas phase.

In the present work, the vibrational constants for ErO are calculated from above mentioned value $\Delta G_{1/2} = 841.5$ cm^{-1} and the assumed value of the dissociation limit. Rotational constants are calculated using $B_0 = 0.3583$ cm^{-1} from Kaledin and Shenyavskaya[295] and the well known Pekeris and Kratzer relations.

The molecular constants for all lanthanide monoxides were calculated *ab initio* using pseudopotentials having the 4*f* orbitals in the core by Dolg and Stoll[193] and compared with experimental data. Although there was no overall agreement between calculated and experimental data in the LnO series, the calculations indicated that the vibrational constants and internuclear distances of the lanthanide monoxides in electronic states of the same type of configurations changed very regularly. The selected values for r_e (ErO) = 179.4 pm and $\omega_e = 849$ cm^{-1} can be compared with $r_e(DyO) = 179.4$ pm, $r_e(HoO) = 179.59$ pm, and $\omega_e(DyO) = 849$ cm^{-1} and $\omega_e(HoO) = 848$ cm^{-1}.

According to Field,[233] the ground state subconfiguration of ErO is $f^{11}(4I)s$ and the ground state is X8. Dulick *et al.*[247] and Carrete and Hocquet[230] carried out the Ligand field calculation of the subconfiguration $f^{11}(4I)s$ and confirmed the $X0^-$ ground state. Carrete and Hocquet[230] considered all the $f^{11}(4I)s$ states (total statistical weight 104), while Dulick *et al.*[247] gave only states up to 10 000 cm^{-1} with $\Sigma p = 60$. The results obtained by Dulick *et al.*[247] and and Carrete and Hocquet[230] were very close for three lowest states. In the present work we use the estimated energies of the $f^{11}(4I)s$ states as recommended by Carrete and Hocquet.[230] Table 50 presents also the estimated statistical weights for the other $f^{11}s$ states (higher 17 000 cm^{-1}), and for the $f^{11}d, f^{11}p$, and f^{12} states (higher 13 000 cm^{-1}, 20 000 cm^{-1}, and higher 40 000 cm^{-1}, respectively).

The derived standard entropy at room temperature is

$$S°(298.15\ K) = (256.473 \pm 0.10)\ J\,K^{-1}\,mol^{-1},$$

and the coefficients of the equations for the heat capacity are

$$C_p°/(J\,K^{-1}\,mol^{-1}) = 43.23815 - 4.71231 \times 10^{-3}(T/K) + 0.571735 \times 10^{-6}(T/K)^2 + 0.747515 \times 10^{-9}(T/K)^3 - 2.55285 \times 10^{5}(T/K)^{-2}$$

for the 298.15–1300 K range, and

TABLE 51. The enthalpy of formation of ErO(g), in kJ mol^{-1}

Authors	Method[a]	T/K	Reaction	$\Delta_r H°(298.15\ K)$	$\Delta_f H°(298.15\ K)$
Ames *et al.*[206]	K	2492–2687	$Er_2O_3 = 2ErO(g) + O(g)$	2017.1	−38.5
Murad and Hildenbrand[260]	M	1855–2165	$Er(g) + TiO(g) = ErO(g) + Ti(g)$	−76.8	−32.9
Selected value:			$D_0(ErO) = 593.7 \pm 8$		-32.9 ± 8

[a]K = Knudsen effusion; M = mass spectrometry.

$$C_p^\circ/(J\,K^{-1}\,mol^{-1}) = 33.60868 + 3.85434 \times 10^{-3}(T/K) - 0.382306 \times 10^{-6}(T/K)^2 + 0.0464068 \times 10^{-9}(T/K)^3 + 2.52559 \times 10^{6}(T/K)^{-2}$$

for the 1300–4000 K range.

4.13.2. Enthalpy of formation

The results for the enthalpy of formation of ErO(g) are presented in Table 51. Ames *et al.*[206] carried out Knudsen effusion measurement of weight loss for several Ln_2O_3(cr) oxides. As in the case of Sm_2O_3(cr) and other lanthanide oxides, results of these measurements were treated under assumption of congruent vaporization of Er_2O_3(cr) according to reaction

$$Er_2O_3(cr) = 2ErO(g) + O(g),$$

neglecting the possibility of formation of Er(g) atoms in the vapor. In case of considerable degree of ErO dissociation this treatment will result in overestimated ErO stability. Mass spectrometric measurements of isomolecular oxygen exchange reaction have been carried out by Murad and Hildenbrand.[260] Results of both papers do not differ significantly, the enthalpy of formation of ErO(g) calculated from results of Ames *et al.* being only ~5 kJ mol^{-1} more negative than that obtained from mass-spectrometric measurements of Murad and Hildenbrand. This closeness demonstrates that Er(g) does not predominate in the Er_2O_3(cr) vapor, in accordance with mass-spectrometric data on ErO^+/Er^+ ratio.[206]

The selected value

$$\Delta_f H^\circ(ErO,\ g,\ 298.15\ K) = -(32.9 \pm 8)\ kJ\,mol^{-1}$$

is taken as the rounded third-law value from the work of Murad and Hildenbrand.[260] The selected enthalpy of formation corresponds to $D_0(ErO) = (593.7 \pm 8)$ kJ mol^{-1}.

4.14. TmO(g)

4.14.1. Heat capacity and entropy

The thermal functions of TmO(g) in the standard state have been calculated using the molecular constants presented in Table 52.

The spectrum of TmO was measured only by infrared spectroscopy in solid inert gas matrices by Weltner and De Kock[245] and Willson *et al.*[246] in Ar (832 cm^{-1}) and by Willson and Andrews[213] in Ar at 10 K (832.0 cm^{-1} and 788.9 cm^{-1} for $Tm^{16}O$ and $Tm^{18}O$, respectively).

The molecular constants for all lanthanide monoxides were calculated *ab initio* by Dolg and Stoll[193] and compared with experimental data. Although there was no overall agreement between calculated and experimental data in the LnO series (see also Sec. 7.2.3), the calculations indicated that the vibrational constants and internuclear distances of the lanthanide monoxides in electronic states of the same type of configurations changed very regularly. In the present work we accept the extrapolated value of $r_e(TmO) = 179.0$ pm considering $r_e(HoO) = 179.59$ pm and $r_e(ErO) = 179.4$ pm. The accepted value $\Delta G_{1/2} = (845 \pm 5)$ cm^{-1} for TmO is estimated from the matrix value 832 cm^{-1} taking into account matrix shift about 13 cm^{-1}. From this value and the dissociation limit according to Birge-Sponer extrapolation one gets $\omega_e = 853.5$ cm^{-1} and $\omega_e x_e = 4.24$ cm^{-1} (compare $\omega_e(HoO) = 848$ cm^{-1}).

According to Field[233] the ground state superconfiguration of TmO is $f^{12}s$. Dulick *et al.*[247] and Carrete and Hocquet[230] carried out the Ligand field calculation of the subconfiguration $4f^{12}(3H)6s$. Kotzian *et al.*[197] calculated the $4f^{12}(3H)6s$ and some of the $4f^{12}(3F)6s$ states using the Intermediate Neglect of

TABLE 52. Molecular constants of $^{169}Tm^{16}O$(g)

No.	State	T_e	ω_e	$\omega_e x_e$	B_e	$\alpha_e 10^3$	$D_e 10^7$	r_e	p_i
		cm^{-1}						pm	
0[a]	$X(3.5)$	0	853.5[b]	4.24[b]	0.360	2.0[c]	2.56[d]	179.0	2
1[e]		24							2
2[e]		190							2
3[e]		320							2
4[e]		420							2
5[e]		510							2
6[e]		650							4
7[e]		860							2
8[e]		1670							2
9[e]		1910							2
10[e]		2560							4
11[e]		5230							4
12[e]		6490							14
13[e]		8100							14
14[e]		8900							4
15[e]		10 050							4
16[e]		12 050							10
17[e]		13 180							8
18[e]		15 000							50
19[e]		20 000							700
20[e]		25 000							90
21[e]		30 000							100
22[e]		35 000							110
23[e]		40 000							130

[a]Experimental state.
[b]Estimated (see text).
[c]Calculated from the Pekeris relation.
[d]Calculated from the Kratzer relation.
[e]Estimated state.

Differential Overlap model (INDO/S-CL). There is even no qualitative agreement between results of these calculations. Moreover, the ground state from the Ligand field calculations $\Omega = 0.5$ while from INDO/S-CL calculation $\Omega = 3.5$ (both states were derived from the same $4f^{12}(3H)6s$ subconfiguration). However, for the calculation of the thermal function it does not change much: both states have the same statistical weight ($pX = 2$). The most serious difference is in the arrangement of the states, mainly the first excited states. Kotzian *et al.*[197] calculated the first excited state at 24 cm^{-1} whereas the Ligand field calculation gave 128 or 97 cm^{-1}. In the present work we accept the data obtained by Kotzian *et al.*[197] and add the estimations of the states $f^{12}d$ (according to Kotzian *et al.*[197] above 13 150 cm^{-1}), $f^{12}p$ (higher 20 000 cm^{-1}), and f^{13} (higher 40 000 cm^{-1}).

The derived standard entropy at room temperature is

$$S^\circ(298.15\ K) = (255.041 \pm 0.15)\ J\,K^{-1}\,mol^{-1}$$

and the coefficients of the equations for the heat capacity are

$$C_p^\circ/(J\,K^{-1}\,mol^{-1}) = 37.63499 + 4.06981 \times 10^{-3}(T/K) - 2.78859 \times 10^{-6}(T/K)^2 + 0.967411 \times 10^{-9}(T/K)^3 - 6.69507 \times 10^{4}(T/K)^{-2}$$

for the 298.15–1700 K range, and

$$C_p^\circ/(J\,K^{-1}\,mol^{-1}) = 39.61651 - 0.540323 \times 10^{-3}(T/K) + 1.26385 \times 10^{-6}(T/K)^2 - 0.143823 \times 10^{-9}(T/K)^3 - 1.21233 \times 10^{6}(T/K)^{-2}$$

for the 1700–4000 K range.

4.14.2. Enthalpy of formation

The results for the enthalpy of formation of TmO(g) are presented in Table 53. Ames *et al.*[206] carried out Knudsen effusion measurement of weight loss for several Ln_2O_3(cr) oxides. As in the case of Sm_2O_3(cr) and other lanthanide oxides, the results of these measurements were treated under assumption of congruent vaporization of Tm_2O_3(cr) according to the reaction

$$Tm_2O_3(cr) = 2TmO(g) + O(g),$$

neglecting possibility of formation of Tm(g) atoms in the vapor. In case of considerable degree of TmO dissociation this treatment will result in overestimated TmO stability.

Mass spectrometric measurements of isomolecular oxygen exchange reaction have been carried out by Murad and Hildenbrand.[260] Results of both papers seriously differ, and the enthalpy of formation of TmO(g) calculated from results of Ames *et al.* is about 260 kJ mol^{-1} more negative than that obtained from mass-spectrometric measurements by Murad and Hildenbrand. This difference can be explained by a large concentration of Tm atoms in the Tm_2O_3(cr) vapor in accordance with mass-spectrometric data for the TmO^+/Tm^+ ratio.[206]

The selected value

$$\Delta_f H^\circ(TmO,\ g,\ 298.15\ K) = -(13.6 \pm 8)\ kJ\,mol^{-1}$$

is taken as a rounded third-law value from the work of Murad and Hildenbrand.[260] The selected enthalpy of formation corresponds to $D_0(TmO) = (492.7 \pm 8)$ kJ mol^{-1}.

4.15. YbO(g)

4.15.1. Heat capacity and entropy

The thermal functions of YbO(g) in the standard state have been calculated using the molecular constants presented in Table 54.

The electronic spectrum of YbO was investigated in emission by Melville *et al.*[296] and in laser excitation and fluorescence by McDonald *et al.*,[297] Linton *et al.*,[227] and Steimle *et al.*.[298] The values of the fundamental frequency of YbO were observed in solid inert gas matrices by Willson and Andrews[213] in Ar at 10 K (660.0 and 625.8 cm^{-1} for $Yb^{16}O$ and $Yb^{18}O$, respectively), and by Willson *et al.*[246] in Ar (659.9 cm^{-1}). Taking into account the matrix shift, the values obtained in matrices are in agreement with the gas phase data.

Ab initio calculations for YbO carried out by Dolg and Stoll,[193] Dolg *et al.*,[194] and Cao *et al.*[195] revealed a marked disagreement with each other and the experimental data. The theoretical calculations performed by Liu *et al.*[299] favored a $\Omega = 0^+$ ground state of a leading $f^{14}\sigma 0$ configuration (in agreement with the interpretation of the experimental data) and predicted the 5 low-lying $f^{13}s$ states.

The studies of the YbO electronic spectra revealed 7 low-lying states including the $X^1\Sigma^+$ (f^{14}) ground state, 5 of which were assigned to the $f^{13}s$ and one to the $f^{13}d$ configurations, and several excited states with energies 16 400–24 700 cm^{-1}, assigned to the $f^{13}d$ and $f^{13}p$ configurations of YbO and to the $f^{14}sp^5$ and $f^{14}dp^5$ superconfigurations of Yb^+O^-. Ligand field calculations by McDonald *et al.*[297] and Carrete and Hocquet[230] resulted in all the $f^{13}s$ states (the total statistical weight 28); Dulick *et al.*[247] obtained only the $f^{13}s$ states up to 10000 cm^{-1}

TABLE 53. The enthalpy of formation of TmO(g), in kJ mol^{-1}

Authors	Method[a]	T/K	Reaction	$\Delta_r H^\circ(298.15\ K)$	$\Delta_f H^\circ(298.15\ K)$
Ames *et al.*[206]	K	2450-2641	$Tm_2O_3(cr) = 2TmO(g) + O(g)$	1597.1	−270.4
Murad and Hildenbrand[260]	M	2249-2364	$TmO(g) + Al(g) = Tm(g) + AlO(g)$	−16.3	−13.6
Selected value:			$D_0(TmO) = 492.7 \pm 8$		-13.6 ± 8

[a]K = Knudsen effusion; M = mass spectrometry.

TABLE 54. Molecular constants of $^{174}Yb^{16}O(g)$

No.	State	T_e	ω_e	$\omega_e x_e$	B_e	$\alpha_e 10^3$	$D_e 10^7$	r_e	p_i
		cm^{-1}						pm	
0[a]	$X^1\Sigma^+$	0	689.9[b]	3.49[b]	0.352431	4.2	3.68[c]	180.7	1
1[a]	$(2)0^-$	839	832[d]	3.4[d]	0.355	1.9	2.6[d]	180.1	1
2[a]	(1)1	944							2
3[a]	(1)2	2337							2
4[a]	(2)2	2631							2
5[a]	(1)3	4216							2
6[a]	$(3)0^+$	4566							1
7[e]		1557							1
8[e]		5000							12
9[e]		7500							16
10[e]		10 000							24
11[e]		15 000							40
12[e]		20 000							50
13[e]		25 000							55
14[e]		30 000							44
15[e]		35 000							35
16[e]		40 000							35

[a]Experimental state.
[b]Calculated from $\Delta G_{1/2} = 683.107\ cm^{-1}$ given by Linton *et al.*[227] and the assumed dissociation limit.
[c]Calculated from the Pekeris relation.
[d]Calculated from the Kratzer relation.
[e]Estimated state.

with $\Sigma p = 17$. The data obtained by McDonald *et al.*[297] are presented in Table 54; they were closer to the experimental data because of the use of adjustable parameters. In Table 54 also the estimated statistical weights for the $f^{13}d$ states from the first observed ($4637\ cm^{-1}$) are presented, as well as for the $f^{13}p$ states (higher than $19000\ cm^{-1}$), and for the Yb^+O^- states assuming the energies of the lowest state at $15000\ cm^{-1}$. The widths of configurations are estimated from the YbIII spectrum.

The accepted molecular constants for the $X^1\Sigma^+$ state are derived from the high-resolution spectral data: the rotational constants from the data obtained by Melville *et al.*,[296] the vibrational constants ($\Delta G_{1/2}$) from the data obtained by Linton *et al.*[227] The vibrational levels of the $X^1\Sigma^+$ state were recorded in the latter work in the fluorescence spectrum up to $v = 8$, but with low accuracy ($\sim 6\ cm^{-1}$). Moreover the ground state was perturbed in the region near $v = 4$. The molecular constants for low-lying states are also estimated from the low-resolution fluorescence spectral data. They are typical for the $f^{N-1}s$ states of all lanthanide monoxides, and in the present work we use the average values. It should be noted that the ground state is the unique state of the f^{14} configuration. The constants for this state differ considerably from those for the other states. The low-lying f^{13}s states have practically identical potential curves and therefore the same molecular constants ($\Delta G_{1/2} \approx 825\ cm^{-1}$ and $r_e \approx 180.0$ pm). The $X^1\Sigma^+$ state does not correlate with the Yb and O atoms in their ground states: $^1S_g + {}^3P_g$ give only triplet states $^3\Pi$ and $^3\Sigma^-$. However, the components 0^+ of the $^3\Pi$ and $^3\Sigma^-$ states should affect the $X^1\Sigma^+$ state, and because of the noncrossing rule the ground state should converge to the $^1S_g + {}^3P_g$ limit. The numerous $f^{13}s$ states ($\Sigma p = 28$) obviously have a higher dissociation limit. In the present work we assume the $^3P_u + {}^3P_g$ limit lying at $17\ 288\ cm^{-1}$ above the dissociation limit to normal atoms.

The derived standard entropy at room temperature is

$$S^\circ(298.15\ K) = (238.521 \pm 0.10)\ J\,K^{-1}\,mol^{-1}$$

and the coefficients of the equations for the heat capacity are

$$C_p^\circ/(J\,K^{-1}\,mol^{-1}) = 37.70801 + 48.5496 \times 10^{-3}(T/K) - 68.4668 \times 10^{-6}(T/K)^2 + 30.5227 \times 10^{-9}(T/K)^3 - 7.73176 \times 10^5(T/K)^{-2}$$

for the 298.15–1000 K range, and

$$C_p^\circ/(J\,K^{-1}\,mol^{-1}) = 32.77497 + 17.3649 \times 10^{-3}(T/K) - 5.08804 \times 10^{-6}(T/K)^2 + 0.503717 \times 10^{-9}(T/K)^3 + 1.98479 \times 10^6(T/K)^{-2}$$

for the 1000–4000 K range.

4.15.2. Enthalpy of formation

There are no measurements of gas phase equilibria to derive the enthalpy of formation of YbO(g), due to very low concentration of YbO(g) in the high-temperature systems. A lower limit estimate of the YbO dissociation energy (see Table 55) was obtained by Yokozeki and Menzinger[300] from the short wavelength chemiluminescence cutoffs in the $Yb + O_3$ beam-gas experiment: $D_0(YbO) > (394.1 \pm 6.3)\ kJ\ mol^{-1}$. The value $D_0(YbO) = (413.8 \pm 4.8)\ kJ\ mol^{-1}$ was found by crossing a thermal beam of Yb atoms with a supersonic seeded beam of $He + O_2$ by Cosmovici *et al.*[301] As selected value we take the rounded result $(414.0 \pm 10)\ kJ\ mol^{-1}$ with increased uncertainty (Table 55), reflecting possible experimental errors in the work of Cosmovici *et al.*[301] The selected dissociation energy of YbO molecule corresponds to:

$$\Delta_f H^\circ(YbO,\ g,\ 298.15\ K) = -(16 \pm 10)\ kJ\,mol^{-1}$$

TABLE 55. The enthalpy of formation of YbO(g), in kJ mol^{-1}

Authors	Method[a]	T/K	Reaction	$\Delta_r H^\circ(298.15\ K)$	$\Delta_f H^\circ(298.15\ K)$
Yokozeki and Menzinger[300]	C	[b]	$Yb(g) + O_3(g) = YbO(g) + O_2(g)$	$> 394.1 \pm 6.3$	$< 3.9 \pm 6.3$
Cosmovici *et al.*[301]	MB	[b]	$Yb(g) + O_2(g) = YbO(g) + O(g)$	413.8 ± 4.8	-16.2 ± 10
Selected value:			$D_0(YbO) = 414 \pm 10$		-16 ± 10

[a]C = chemiluminiscence; MB = crossed molecular beam.
[b]Not specified.

TABLE 56. Molecular constants of $^{175}Lu^{16}O$(g)

No	State	T_e	ω_e	$\omega_e x_e$	B_e	$\alpha_e 10^3$	$D_e 10^7$	r_e	p_i
		cm^{-1}						pm	
0[a]	$X^2\Sigma^+$	0	844.5	3.1	0.35894	1.76	2.78[b]	179.0	2
1[a]	$A^2\Pi_{1/2}$	19 392							2
2[a]	$A^2\Pi_{3/2}$	21 470							2
3[a]	$^4\Pi$?[c]	19 520							8
4[a]	$B^2\Sigma^+$	24 440							2
5[d]		14 100							2
6[d]		15 300							2
7[d]		21 000							8
8[d]		23 700							8
9[d]		27 000							12
10[d]		31 000							4
11[d]		40 000							20

[a]Experimental state.
[b]D_0.
[c]Unknown upper state in of the transition band at 5120 Å.
[d]Estimated state.

4.16. LuO(g)

4.16.1. Heat capacity and entropy

The thermal functions of LuO(g) in the standard state have been calculated using the molecular constants presented in Table 56.

Three electronic transitions $A^2\Pi_{1/2}$-$X^2\Sigma^+$, $A^2\Pi_{3/2}$-$X^2\Sigma^+$, and $B^2\Sigma^+$-$X^2\Sigma^+$ were analyzed in the emission spectrum of LuO. Huber and Herzberg[179] reviewed the spectral data on LuO published till 1975. Later Bernard and Effantin[302] reanalyzed the known systems and found a new band at 5120 Å, which also was connected with the transition to the ground state. These are slightly different from values derived from the recent measurements of the pure rotational spectrum of $^{175}Lu^{16}O$ in its ground electronic state ($X^2\Sigma^+$) by Cooke *et al.*,[303] which were published after our analysis was completed. All the upper states of the transitions were perturbed that indicates many unobserved states. The values of the fundamental frequency of LuO were measured in solid inert gas matrices by Willson and Andrews[213] in Ar (829.3 cm^{-1} and 786.2 cm^{-1} for $Lu^{16}O$ and $Lu^{18}O$, respectively) and by Weltner and De Kock[245] in Ar and Ne (825 and 836 cm^{-1}, respectively). Taking into account the matrix shift, the values of the fundamental frequency of LuO obtained in matrices are in agreement with the gas phase data.

Ab initio calculations for the ground state of LuO carried out by Hong *et al.*,[192] Wang and Schwarz,[304] Küchle *et al.*,[305] Dolg and Stoll,[193] Dolg *et al.*,[194] and Cao *et al.*,[195] are in agreement with the experimental data. Kotzian *et al.*[197] calculated the excited states using the INDO model. According to this calculation, all the states below 45 000 cm^{-1} arise from superconfigurations $5d$ ($A'^2\Delta$, $A^2\Pi$, and $B^2\Sigma^+$), $6p$ ($^2\Pi$ and $^2\Sigma^+$), and $6s$ ($X^2\Sigma^+$), while the $4f^{13}$ states have energies much higher (100 000 cm^{-1}). These results could not explain either the upper state of the band 5120 Å, or numerous perturbations. The electronic structures of LaO and LuO are similar. In the present work the upper state of the band 5120 Å is interpreted as the lowest component of quartet states, found by Schampsand *et al.*[198] for LaO. The estimates of the excited states are based on the above mentioned data.

The accepted molecular constants for the $X^2\Sigma^+$ state are taken from the work by Bernard and Effantin.[302]

The derived standard entropy at room temperature is

$$S^\circ(298.15\ \mathrm{K}) = (242.089 \pm 0.03)\ \mathrm{J\,K^{-1}\,mol^{-1}}$$

and the coefficients of the equations for the heat capacity are

$$C_p^\circ/(\mathrm{J\,K^{-1}\,mol^{-1}}) = 28.20132 + 20.4184 \times 10^{-3}(\mathrm{T/K}) - 16.5159 \times 10^{-6}(\mathrm{T/K})^2 + 4.71909 \times 10^{-9}(\mathrm{T/K})^3 - 1.19650 \times 10^{5}(\mathrm{T/K})^{-2}$$

for the 298.15–1300 K range, and

$$C_p^\circ/(\mathrm{J\,K^{-1}\,mol^{-1}}) = 40.19679 - 0.758989 \times 10^{-3}(\mathrm{T/K}) - 0.623484 \times 10^{-6}(\mathrm{T/K})^2 + 0.273798 \times 10^{-9}(\mathrm{T/K})^3 - 2.75040 \times 10^{6}(\mathrm{T/K})^{-2}$$

for the 1300–4000 K range.

4.16.2. Enthalpy of formation

The results for the enthalpy of formation of LuO(g) are presented in Table 57. Experimental data used in calculations consist of Knudsen effusion[206] and mass spectrometric measurements of isomolecular oxygen exchange reactions.[206,260] The results of all measurements are in fair agreement. At the same time, mass-spectrometric results are more reliable in comparison with the KE data, because interpretation of Knudsen effusion data is not unambiguous (see Sec. 4.1). Among the mass-spectrometric data, the results of Murad and Hildenbrand[260] are preferred. Absence of primary experimental data makes it difficult to recalculate results of mass-spectrometric measurements of Ames *et al.*[206]

The selected enthalpy of formation of LuO(g) is taken as the rounded value from the paper by Murad and Hildenbrand[260]:

$$\Delta_f H^\circ(\mathrm{LuO,\ g,\ 298.15\ K}) = -(3.4 \pm 10)\ \mathrm{kJ\,mol^{-1}}.$$

TABLE 57. The enthalpy of formation of LuO(g), in kJ mol^{-1}

Authors	Method[a]	T/K	Reaction	$\Delta_r H^\circ$(298.15 K)	$\Delta_f H^\circ$(298.15 K)
Ames *et al.*[206]	K	2615–2700	Lu_2O_3(cr) = 2LuO(g) + O(g)	2150.4	11.5
	M	2080–2214	Lu(g) + LaO(g) = LuO(g) + La(g)	117.3	−5.8
Murad and Hildenbrand[260]	M	1782–1927	Lu(g) + YO(g) = LuO(g) + Y(g)	45.1	3.4
Selected value:			D_0(LuO) = 758.9 ± 10		3.4 ± 10

[a]K = Knudsen effusion; M = mass spectrometry.

The selected enthalpy of formation corresponds to $D_0(LuO) = (673.6 \pm 10)$ kJ mol^{-1}.

5. The Actinide Oxides in Solid and Liquid State

5.1. Ac_2O_3(cr,l)

5.1.1. Polymorphism and melting point

Actinium sesquioxide has an A-type hexagonal sesquioxide structure (space group $P\bar{3}m1$) at room temperature. Similar to the isostructural A-type lanthanide sesquioxides, high temperature transformations to the H- and X-type structures can be expected, but no experimental information exists. Considering the fact that Ac^{3+} has an ionic radius somewhat larger than La^{3+}, the transition temperatures are estimated to be slightly lower than those in La_2O_3, i.e., A → H at about 2300 K and H → X around 2370 K. Similarly, the melting point of Ac_2O_3 is estimated to be about 2600 K.

5.1.2. Heat capacity and entropy

The standard entropy of Ac_2O_3 has been estimated from the trends in the lanthanide and actinide compounds as

$$S^\circ(298.15\ \text{K}) = (138.3 \pm 5.0)\ \text{J K}^{-1}\ \text{mol}^{-1}$$

according to the method proposed by Konings *et al.*[127] This is slightly lower than the value suggested by Konings *et al.*[306] which did not take into account the structural discontinuity in the Ln_2O_3 series, as evidenced by the data for monoclinic Gd_2O_3.

5.1.3. Enthalpy of formation

The enthalpy of formation of Ac_2O_3 was estimated by Konings *et al.*[306] from the enthalpy of the idealised dissolution reaction:

$$An_2O_3(cr) + 6H^+(aq) = 2An^{3+}(aq) + 3H_2O(l)$$

relating the quantity $\{\Delta_f H^\circ(MO_{1.5}) - \Delta_f H^\circ(M^{3+}\}$ to the molar volume. They thus obtained

$$\Delta_f H^\circ(298.15\ \text{K}) = -(1107 \pm 15)\ \text{kJ mol}^{-1}$$

5.2. ThO_2(cr,l)

5.2.1. Melting point

ThO_2 has a fluorite crystal structure (space group $Fm\bar{3}m$), which is stable up to the melting point. The melting point of ThO_2 has been measured by several authors, as summarized in Table 58. The reported values vary from T = 3323 K to T = 3808 K, but the more recent ones agree on a melting point around T = 3600 K. We here consider the value measured by Ronchi and Hiernaut,[307] $T_{fus} = (3651 \pm 17)$ K, as the most accurate one as it was determined on a well-defined sample (O/Th ratio = 2.00) and with a well-defined technique.

TABLE 58. Temperature of melting of thorium dioxide

	T_{fus}/K	
Authors	Reported	ITS-90
Ruff *et al.*[308]	3323	
Wartenberg and Reusch[309]	3803	
Geach and Harper[310]	3323 ± 25	3328 ± 25
Lambertson *et al.*[311]	3573 ± 100	3578 ± 100
Benz[312]	3663 ± 100	3668 ± 100
Chikalla *et al.*[107]	3573	3572
Sibieude and Foex[313]	3473	3472
Ronchi and Hiernaut[307]	3651 ± 17	3651 ± 17
Manara *et al.*[52]	3620	3620
Selected value:		3651 ± 17

5.2.2. Heat capacity and entropy

The low-temperature heat capacity of ThO_2 has been measured by Osborne and Westrum Jr.[314] These measurements were used in the CODATA Key Values selection,[315] and selected here without change:

$$S^\circ(298.15\ \text{K}) = (65.23 \pm 0.20)\ \text{J K}^{-1}\ \text{mol}^{-1}.$$

Magnani *et al.*[316] reported heat capacity data that are in good agreement, but the numerical details of this measurement are not published and the analytical technique is less accurate.

The high-temperature enthalpy increment of ThO_2 has been measured by Jaeger and Veenstra,[317] Southard,[318] Hoch and Johnston,[319] Victor and Douglas,[320] Pears *et al.*,[58] Springer *et al.*,[321] Springer and Langedrost,[322] Fischer *et al.*,[323,324] and Dash *et al.*[325] The data cover the temperature range from 500 to 3400 K as shown in Fig. 15. Up to 2500 K the results are in fair agreement, except in the low-temperature region where the data of Victor and Douglas[320] and Springer *et al.*[321] deviate significantly due to small inaccuracies in temperature or enthalpy that become prominent close to 298.15 K when using the $\{H^\circ(T) - H^\circ(298.15\ \text{K})\}/(T - 298.15)$ function. The data listed by Springer *et al.* have been corrected for obvious typographical errors. The results of Pears *et al.*[58] are very scattered and are evidently not accurate enough. Direct heat

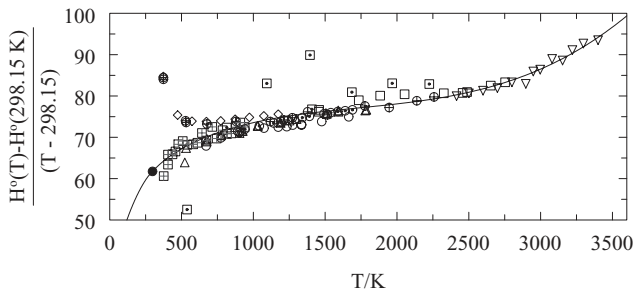

FIG. 15. The reduced enthalpy increment (in J K^{-1} mol^{-1}) of ThO_2; ◯, Jaeger and Veenstra[317]; △, Southard[318]; □, Hoch and Johnston[319]; ⊡ Pears *et al.*[58]; ◇, Victor and Douglas[320]; ⊕, Springer *et al.*[321]; ▽, Fischer *et al.*[323]; ⊞, Agarwal *et al.*[324]; ⊙ Dash *et al.*[325]; •, Osborne and Westrum Jr.[314]; the curve shows the recommended equation.

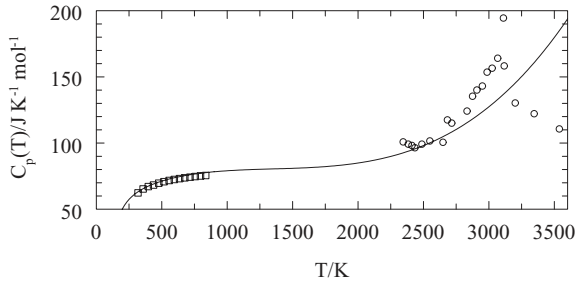

FIG. 16. The heat capacity (in J K^{-1} mol^{-1}) of ThO_2; ◯, Ronchi and Hiernaut[307]; □ Dash *et al.*[325]; the curve shows the recommended equation. Note that the data of Ronchi and Hiernaut[307] indicate a value of about 600 J K^{-1} mol^{-1} (not shown in the graph) at the maximum of the anomalie.

capacity measurements of ThO_2 have been reported by Dash *et al.*,[325] in good agreement with the enthalpy measurements (Fig. 16).

Above T = 2500 K, ThO_2 exhibits an excess enthalpy, like many high-melting refractory oxides (e.g., UO_2, PuO_2, and ZrO_2). Fischer *et al.*[323] suggested that this effect is due to a phase transformation and this possibility was studied in detail by Ronchi and Hiernaut[307] using a thermal arrest technique. From their results, Ronchi and Hiernaut concluded that a premelting transition occurs at 3090 K, which was attributed to order-disorder anion displacements in the oxygen sublattice (Frenkel defects).

For the recommended heat capacity equation the results of Southard,[318] Hoch and Johnston[319] and Fischer *et al.*[323] have been combined and fitted to the equation (298.15– 3500 K):

$$\begin{aligned} C_p^\circ/(\mathrm{J\,K^{-1}\,mol^{-1}}) = {} & 55.9620 + 51.2579 \times 10^{-3}(\mathrm{T/K}) \\ & - 36.8022 \times 10^{-6}(\mathrm{T/K})^2 \\ & + 9.2245 \times 10^{-9}(\mathrm{T/K})^3 \\ & - 5.740310 \times 10^{5}(\mathrm{T/K})^{-2} \end{aligned}$$

constrained to $C_p^\circ(298.15\ \mathrm{K}) = 61.76\ \mathrm{J\,K^{-1}\,mol^{-1}}$, as derived from the low-temperature heat capacity measurements by Osborne and Westrum Jr.[314] The C_p° derived from this function, of course, does not reproduce the heat capacity data by Ronchi and Hiernaut[307] around the order-disorder transition (see Fig. 16), with a maximum value of 600 J K^{-1} mol^{-1}(not shown in the figure).

No experimental data are available for liquid thorium dioxide. Fink *et al.*[326] estimated $C_p^\circ(\mathrm{liq}) = 61.76\ \mathrm{J\,K^{-1}\,mol^{-1}}$, which is adopted here as

$$C_p^\circ(\mathrm{ThO_2, liq, T}) = 61.8\ \mathrm{J\,K^{-1}\,mol^{-1}}.$$

The entropy of fusion is assumed to be identical to that of UO_2 (24 J K^{-1} mol^{-1}), yielding

$$\Delta_{fus}H^\circ = (88 \pm 6)\ \mathrm{kJ\,mol^{-1}}.$$

5.2.3. Enthalpy of formation

The enthalpy of formation of ThO_2 is a CODATA Key Value for Thermodynamics,[315] and is based on the enthalpy of combustion of thorium metal by Huber Jr. *et al.*:[327]

$$\Delta_f H^\circ(298.15\ \mathrm{K}) = -(1226.4 \pm 3.5)\ \mathrm{kJ\,mol^{-1}}.$$

Earlier measurements by Roth and Becker[328] gave −(1226 ± 5) kJ mol^{-1}, which is in good agreement with the selected value.

5.3. PaO_2(cr,l)

5.3.1. Melting point

PaO_2 has a fluorite crystal structure (space group $Fm\bar{3}m$). No information exists about the high temperature behavior of PaO_2, but it can be presumed that it is similar to the neighboring ThO_2 and UO_2 compounds, i.e. the fluorite structure is stable up to the melting. The melting point of PaO_2 is estimated from the trend in the actinide dioxide series, as discussed in Sec. 7.2.2, and we estimate T_{fus} = (3200 ± 60) K.

5.3.2. Heat capacity and entropy

The standard entropy of PaO_2 was estimated by Konings[329] from the trends in actinide dioxide series:

$$S^\circ(298.15\ \mathrm{K}) = (81.1 \pm 5.0)\ \mathrm{J\,K^{-1}\,mol^{-1}}.$$

The high temperature heat capacity of PaO_2 has been estimated as

$$\begin{aligned} C_p^\circ(T)/(\mathrm{J\,K^{-1}\,mol^{-1}}) = {} & 58.0078 + 50.9087 \times 10^{-3}(\mathrm{T/K}) \\ & - 35.9277 \times 10^{-6}(\mathrm{T/K})^2 + 9.5704 \\ & \times 10^{-9}(\mathrm{T/K})^3 - 0.51080 \\ & \times 10^{6}(\mathrm{T/K})^{-2} \end{aligned}$$

using the approach outlined in Konings and Beneš[330].

5.3.3. Enthalpy of formation

The enthalpy of formation of PaO_2 was estimated by Konings *et al.*[306] from the enthalpy of the idealised dissolution reaction:

$$AnO_2 + 4H^+(aq) = An^{4+}(aq) + 2H_2O(l)$$

relating this quantity to the molar volume. They thus obtained

$$\Delta_f H^\circ(298.15\ \mathrm{K}) = -(1107 \pm 15)\ \mathrm{kJ\,mol^{-1}}.$$

5.4. γ-UO_3

5.4.1. Polymorphism

γ-UO_3 is one of the many crystallographic modifications of UO_3, but probably the thermodynamic stable one above room temperature.[331,332] It has an orthorhombic cell (space group *Fddd*) at 298.15 K. It transforms at ~373 K to a closely related tetragonal structure (space group $I4_1/amd$).

5.4.2. Heat capacity and entropy

Low-temperature heat capacity measurements of UO_3 have been reported by Jones *et al.*[333] from 15 to 300 K. Based on the sample preparation and the color of the product, it is generally believed that it had the γ structure. Cordfunke and Westrum Jr.[334] measured the low-temperature heat capacity of a well-characterised γ-UO_3 sample from 5 to 350 K, yielding somewhat lower values. The selected entropy value is taken from that study

$$S^\circ(298.15\ \mathrm{K}) = (96.11 \pm 0.40)\ \mathrm{J\,K^{-1}\,mol^{-1}}.$$

The high temperature heat capacity of UO_3 of unknown crystallographic structure has been measured by Popov *et al.*[335] from 392 to 673 K. The high-temperature enthalpy increment of UO_3 has been measured by Moore and Kelley[336] from 416 to 886 K on a sample of unspecified crystallographic structure, but since it was identical to that used by Jones *et al.*[333] for the low-temperature measurements, the results most likely refer to γ-UO_3. Cordfunke and Westrum Jr.[334] measured the high-temperature enthalpy increment from 347 to 691 K on a well-defined sample having the γ structure. These measurements do not reveal the phase transition at ~373 K, which means that the entropy of transition is negligible.

The results of the two enthalpy studies agree well, and although the latter study is made on a better characterised sample, our recommended heat capacity equation is based on a fit of all results, since the study by Moore and Kelley[336] covers a wider temperature range. The enthalpy fit is constrained to $C_p^\circ(298.15\ \mathrm{K}) = 81.67\ \mathrm{J\,K^{-1}\,mol^{-1}}$ from the low-temperature measurements and yields for the heat capacity:

$$C_p^\circ/(\mathrm{J\,K^{-1}\,mol^{-1}}) = 90.2284 + 13.85332 \times 10^{-3}(\mathrm{T/K}) - 1.12795 \times 10^{6}(\mathrm{T/K})^{-2}.$$

5.4.3. Enthalpy of formation

The enthalpy of formation of γ-UO_3 is a CODATA Key Value for Thermodynamics,[315] and is based on the enthalpies of dissolution of uranium oxides in Ce(IV) solutions corrected to stoichiometric UO_3 by Fitzgibbon *et al.*,[337] and on the dissolution of γ–UO_3 and UF_6(cr) in HF solutions by Johnson and O'Hare.[338] The value is in agreement with the decomposition pressures measured by Cordfunke and Aling[332]:

$$\Delta_f H^\circ(298.15\ \mathrm{K}) = -(1223.8 \pm 2.0)\ \mathrm{kJ\,mol^{-1}}.$$

5.5. U_3O_8(cr)

5.5.1. Polymorphism and melting point

At room temperature α-U_3O_8(cr) has an orthorhombic structure (space group *C*2*mm*). It transforms to a hexagonal structure (space group $P\bar{6}2m$) at 483 K. This transition is revealed as a clear λ peak in the heat capacity studies.[339,340] They indicated two additional peaks at 568 and 850 K (see below), whose origin is not established but presumably involves further changes in ordering in the lattice.

At atmospheric pressure U_3O_8 decomposes before melting. The melting temperature of U_3O_8 was determined by Manara *et al.*[341] as (2010 ± 30) K under a pressure of 1 kbar pure helium.

5.5.2. Heat capacity and entropy

The low-temperature heat capacity of U_3O_8 has been measured by Westrum Jr. and Grønvold[342] from 5 to 350 K, which revealed a λ type transition at 25.3 K, probably of magnetic origin. The standard entropy derived from this work, also accepted as CODATA Key Value for Thermodynamics,[315] is

$$S^\circ(298.15\ \mathrm{K}) = (282.55 \pm 0.50)\ \mathrm{J\,K^{-1}\,mol^{-1}}.$$

The high-temperature heat capacity of U_3O_8 has been measured by Popov *et al.*[343] from 350 to 875 K, Girdhar and Westrum Jr.[339] from 303 to 529 K, and Inaba *et al.*[340] from 310 to 970 K. The high-temperature enthalpy increment has been measured by Maglic and Herak[344] from 312 to 927 K, Marchidan and Ciopec[345] from 273 to 1000 K, and Cordfunke whose results have not been published (cited by Cordfunke and Konings[8]). The heat capacity studies by Girdhar and Westrum Jr.[339] and Inaba *et al.*[340] reveal a λ peak at 483 K. The latter authors found two further λ peaks at 568 and 850 K. The enthalpies of the transitions of the peak at 483 K derived from these studies are, however, very different. Girdhar and Westrum Jr.[339] derive $\Delta_{trs}H^\circ = 171\ \mathrm{J\cdot mol^{-1}}$, Inaba *et al.*[340] $\Delta_{trs}H^\circ = 405\ \mathrm{J\cdot mol^{-1}}$. As can be seen in Fig. 17, the difference mainly arises from the fact that the peak is much broader in the measurements of Inaba *et al.*[340] We consider the measurement of Girdhar and Westrum Jr.[339] more precise and select the value derived from that work. For the transitions at 568 and 850 K we have taken the values from the work of Inaba *et al.*,[340] although they may be somewhat too high:

$$\Delta_{trs}H^\circ(483\mathrm{K}) = 171\ \mathrm{J\,mol^{-1}},$$
$$\Delta_{trs}H^\circ(568\mathrm{K}) = 444\ \mathrm{J\,mol^{-1}},$$
$$\Delta_{trs}H^\circ(850\mathrm{K}) = 942\ \mathrm{J\,mol^{-1}}.$$

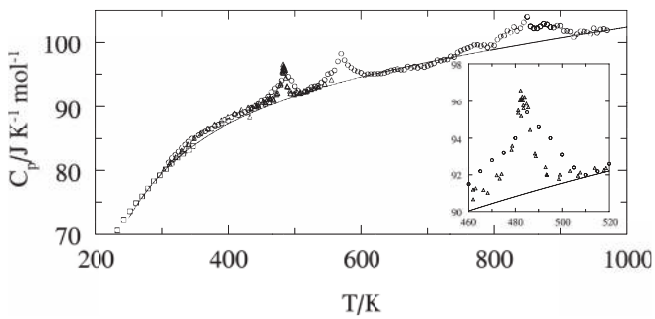

FIG. 17. The heat capacity of $UO_{2.667}$; □, Inaba *et al.*[340]; □, Westrum Jr. and Grønvold[342]; △, Girdhar and Westrum Jr.[339]

The transitions are not detected in the enthalpy drop studies since these enthalpy effects are too small.

The experimental studies indicate that the baseline heat capacity of the three phases can be represented by a single curve as a function of temperature. The selected heat capacity curve is taken from Cordfunke and Konings[8] which includes unpublished results by Cordfunke. It is subject to the constraint of $C_p^\circ(298.15\ \mathrm{K}) = 237.94\ \mathrm{J\ K^{-1}\ mol^{-1}}$, as given by Westrum Jr. and Grønvold[342]:

$$C_p^\circ/(\mathrm{J\,K^{-1}\,mol^{-1}}) = 279.267 + 27.480 \times 10^{-3}(\mathrm{T/K}) - 4.3116 \times 10^{6}(\mathrm{T/K})^{2}.$$

It is recommended to use this equation in combination with the transition enthalpies.

5.5.3. Enthalpy of formation

The enthalpy of formation of U_3O_8 is a CODATA Key Value for Thermodynamics,[315] and is based on the enthalpy of combustion of uranium measured by Huber and Holley Jr.[346]:

$$\Delta_f H^\circ(298.15\ \mathrm{K}) = -(3574.8 \pm 2.5)\ \mathrm{kJ\,mol^{-1}}.$$

This value is in close agreement with, but more precise than earlier values by Huber Jr. and Holley Jr.[98] and Popov and Ivanov.[347]

5.6. U_4O_9(cr)

5.6.1. Polymorphism

U_4O_9, which has a stability range between $2.234 < O/U < 2.245$, has three polymorphic modifications. The α form has probably a rhombohedrally distorted fluorite structure. At 348 K it transforms into the β modification which has a body-centered cubic (space group $I\bar{4}3d$). This temperature is the maximum of the λ peak in the heat capacity measured by Westrum Jr. *et al.*[348] and Grønvold *et al.*[349] Inaba and Naito[350] and Naito *et al.*[351] found that the temperature of this transition slightly increases with decreasing O/U ratio of the sample.

The β modification transforms to γ-U_4O_9 at about 893 K, as derived from electrical conductivity and X-ray diffraction measurements by Inaba and Naito.[350] The structure of this phase is not known. A disordered $UO_{2.25}$ phase is stable above 1400 K.[352] Essentially this may be regarded as an order-disorder transformation at a fixed composition, although strictly it is peritectoid decomposition from U_4O_9 (ordered) to UO_{2+x} (disordered, $x \sim 0.25$) and a small amount of U_3O_{8-y}.

5.6.2. Heat capacity and entropy

The low-temperature heat capacity of U_4O_9 has been measured by Osborne *et al.*[353] from 5 to 310 K, by Westrum Jr. *et al.*[348] from 190 to 399 K, and Flotow *et al.*[354] from 1.6 to 24 K. The results are in good agreement. The standard entropy derived from these measurements is[354]

$$S^\circ(298.15\ \mathrm{K}) = (334.1 \pm 0.7)\ \mathrm{J\,K^{-1}\,mol^{-1}}.$$

In addition to the results of Westrum Jr. *et al.*,[348] which extend to 399 K, three more high-temperature heat capacity studies have been reported. Gotoo and Naito[355] reported measurements from 297 to 515 K, Grønvold *et al.*[349] from 303 to 997 K, and Inaba and Naito[350] from 190 to 470 K. MacLeod[352] measured the enthalpy increments of U_4O_9 from 845 to 1568 K. The heat capacity studies show that the $\alpha \rightarrow \beta$ transition is associated with a strong λ-type peak. The $\beta \rightarrow \gamma$ transition is only evident from a spread in the C_p° results of Grønvold *et al.*[349] We have selected the heat capacity equation given by Cordfunke and Konings,[8] which describes the three phases with one polynomial, treating the λ transition as an enthalpy discontinuity only

$$C_p^\circ/(\mathrm{J\,K^{-1}\,mol^{-1}}) = 319.163 + 49.691 \times 10^{-3}(\mathrm{T/K}) - 3.9602 \times 10^{6}(\mathrm{T/K})^{-2}.$$

MacLeod[352] has analysed the integrated enthalpy for the $\alpha \rightarrow \beta$ transition as $\Delta_{trs}H^\circ(\alpha\text{-}\beta) = 2594\ \mathrm{J{\cdot}mol^{-1}}$. The β to γ transition has been assumed to have a negligible associated enthalpy. Although MacLeod analysed his data to suggest $\Delta_{trs}H^\circ(1395\ \mathrm{to}\ 1405\ \mathrm{K}) = 9.372\ \mathrm{kJ\ mol^{-1}}$, this calculation seems to be in error - the enthalpy difference between the disordered UO_{2+x} and the γ-phase at 1400 K, from Eqs. (5) and (6) is in fact 11.90 kJ $\mathrm{mol^{-1}}$.

5.6.3. Enthalpy of formation

The selected enthalpy of formation of U_4O_9 is

$$\Delta_f H^\circ(298.15\ \mathrm{K}) = -(4512 \pm 7)\ \mathrm{kJ\,mol^{-1}}$$

based on the enthalpies of solution of UO_2, U_4O_9 and γ-UO_3 in aqueous Ce(IV) solutions measured by Fitzgibbon *et al.*[337] This value is supported by the less precise work of Burdese and Abbatista[356] using dissolution in nitric acid.

5.7. UO_2(cr,l)

5.7.1. Melting point

UO_2 has a fluorite crystal structure (space group $Fm\bar{3}m$), which is stable up to the melting point. The reported melting temperatures are listed in Table 59, which shows considerable variation. This is due to the fact that deviations from stoichiometry and the relatively high vapor pressure have significant effects, in addition to interactions of liquid with the container material. We select the value $T_{fus} = (3130 \pm 20)$ K. The exact congruent melting composition at atmospheric pressure is still controversial. Most probably, it lies between $UO_{1.98}$ and $UO_{2.00}$.[357,358]

TABLE 59. Temperature of melting of uranium dioxide

	T_{fus}/K	
Authors	Reported	ITS-90
Ackermann[359]	2680 ± 19	
Lambertson and Handwerk[360]	3323 ± 20	
Wisnyi and Pijanowski[361]	3033 ± 30	
Ehlert and Margrave[362]	3133 ± 45	
Pijanowski and DeLuca[363]	3033 ± 30	3050 ± 30
Chikalla[364]	3003 ± 30	
Lyon and Bailey[365]	3046 ± 21	
Hausner[366]	3078 ± 15	
Lyon and Bailey[367]	3113 ± 20	
Latta and Fryxell[368]	3138 ± 15	3142 ± 15
Tachibana *et al.*[369]	3118 ± 25	3120 ± 25
Ronchi and Sheindlin[370]	3110 ± 10	3110 ± 10
Manara *et al.*[371]	3147 ± 20	3147 ± 20
Kato *et al.*[372]	3123	3123
Selected value:		3130 ± 20

5.7.2. Heat capacity and entropy

The low-temperature heat capacity of UO_2 has been measured by Jones *et al.*[333] from 15 to 300 K and Hunzicker and Westrum Jr.[373] from 5 to 330 K. These measurements reveal a transition at 30.4 K from a low-temperature antiferromagnetic state to a high-temperature paramagnetic state. The selected standard entropy is the CODATA Key Value,[315] which is solely based on the results of Hunzicker and Westrum Jr.[373] that refer to a better characterised sample:

$$S^\circ(298.15\ \mathrm{K}) = (77.03 \pm 0.20)\ \mathrm{J\,K^{-1}\,mol^{-1}}.$$

The high-temperature data for UO_2 extend into the liquid range (up to 8000 K) and have been obtained as heat capacity[335,349,379–387] and enthalpy increment values.[336,374–378,388–390] The results are shown in Figs. 18 and 19. There is in general good agreement between the different studies, with exception of the early heat capacity measurements.[335,383–385]

It is now well established that the heat capacity of UO_2 shows an anomalous increase above 1800 K. Neutron scattering measurements by Hutchings[391,392] and Clausen *et al.*[393] reveal that thermally induced disorder as a results of Frenkel pair formation on the oxygen lattice occurs at temperatures above 2000 K. These studies also showed that excitation of the electronic levels of U^{4+}

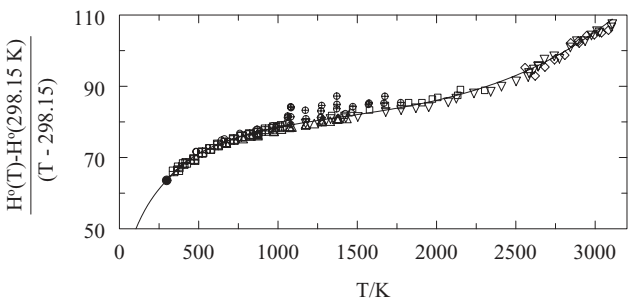

FIG. 18. The reduced enthalpy increment (in J K^{-1} mol^{-1}) of UO_2;○, Moore and Kelley[336]; □, Ogard and Leary[374]; △ Fredrickson and Chasanov[375]; ▽, Hein and Flagella[376]; ◊, Leibowitz *et al.*[377]; ⊞,[378]; ⊕, Mills *et al.*[379]; •, value derived from the low-temperature measurements by Hunzicker and Westrum Jr.[373]; the curve shows the recommended equation.

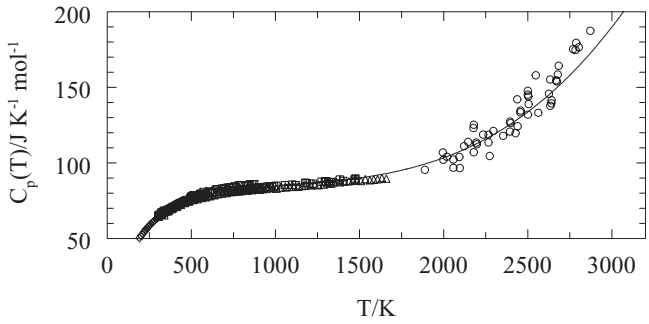

FIG. 19. The heat capacity of UO_2; ○, Ronchi *et al.*[380]; □, Grønvold *et al.*[349]; △ Amaya *et al.*[381]; ▽, Popov *et al.*[335];◊, Hunzicker and Westrum Jr.[373]; ⊞, Inaba *et al.*[382]; the curve shows the recommended equation.

contribute to the anomalous behavior. According to Ronchi and Hyland[394] the former dominate. The heat capacity measurements in the pre-melting range by Hiernaut *et al.*[386] showed a order-disorder transition with a peak at (2670 ± 30) K.[380] The heat capacity maximum of this peak reaches values above 215 J K^{-1} mol^{-1}. Above this transition also the role of Schottky effects must be taken into account.[394]

Numerous evaluations of the heat capacity of solid and liquid UO_2 have been reported. The listing for the CODATA Key values[315] is based on the evaluation in Glushko *et al.*,[395] which is also adopted for the Equation of State description of UO_2 by Ronchi *et al.*[396] That recommendation does not include the heat capacity data by Ronchi and coworkers[380,386,387] in the premelting and liquid range. For that reason we have re-fitted the experimental data in a combined treatment of enthalpy increments and heat capacity, to give

$$\begin{aligned} C_p^\circ/(\mathrm{J\,K^{-1}\,mol^{-1}}) = {} & 66.7437 + 43.1393 \times 10^{-3}(\mathrm{T/K}) \\ & - 35.640 \times 10^{-6}(\mathrm{T/K})^2 \\ & + 11.655 \times 10^{-9}(\mathrm{T/K})^3 \\ & - 1.16863 \times 10^{6}(\mathrm{T/K})^{-2}. \end{aligned}$$

This single equation describes the data below and above the λ transition, since no change in the slope of the heat capacity or enthalpy curves were observed.

The enthalpy increment of liquid UO_2 has been measured by Hein and Flagella[376] (four temperatures up to 3270 K) and by Leibowitz *et al.*[390] (six temperatures between 3173 and 3523 K). These measurements suggest a constant heat capacity value in this temperature range. The heat capacity measurements for liquid UO_2 by[387] show a decrease from about 120 J K^{-1} mol^{-1} near the melting point to about 84 J K^{-1} mol^{-1} at 4500 K, followed by an increase to the maximum temperature of the measurements, 8200 K. Since it is not possible to fit these data into a single polynomial equation of the type used in the present assessment, we have fitted the heat capacity data by Ronchi *et al.*[387] from the melting point to T = 5000 K to the following equation:

$$\begin{aligned} C_p^\circ/(\mathrm{J\,K^{-1}\,mol^{-1}}) = {} & 1365.4956 - 0.85866(\mathrm{T/K}) \\ & + 191.305 \times 10^{-6}(\mathrm{T/K})^2 \\ & - 14.1608 \times 10^{-9}(\mathrm{T/K})^3. \end{aligned}$$

The enthalpy of fusion of slightly hypostoichiometric UO_2 samples was derived from enthalpy increment measurements as 76 kJ mol^{-1} by Hein and Flagella[376] and 74 kJ mol^{-1} by Leibowitz *et al.*[377] We select

$$\Delta_{fus}H^\circ = (75 \pm 3)\ \text{kJ mol}^{-1}.$$

The selected enthalpy of fusion together with the heat capacity equations reproduce the enthalpy data for liquid UO_2 by Hein and Flagella[376] and Leibowitz *et al.*[390] within 2%.

5.7.3. Enthalpy of formation

The enthalpy of formation of UO_2 is a CODATA Key value for Thermodynamics,[315] which has been accepted here. This value is based on the combustion calorimetric experiments work by Huber and Holley Jr.[346] and Johnson and Cordfunke[397]:

$$\Delta_f H^\circ(298.15\ \text{K}) = -(1085.0 \pm 1.0)\ \text{kJ mol}^{-1}$$

5.8. Np_2O_5(cr,l)

5.8.1. Crystal structure

Np_2O_5 has a monoclinic structure (space group P2/c). It decomposes to NpO_2 and O_2 at about 700 K.[398]

5.8.2. Heat capacity and entropy

The low-temperature heat capacity of Np_2O_5 has not been measured. Merli and Fuger[399] have estimated the entropy at room temperature as $S^\circ(298.15\ \text{K}) = (186 \pm 15)\ \text{J K}^{-1}\ \text{mol}^{-1}$, and Lemire[400] as $S^\circ(298.15\ \text{K}) = (163 \pm 23)\ \text{J K}^{-1}\ \text{mol}^{-1}$. We select

$$S^\circ(298.15\ \text{K}) = (186 \pm 15)\ \text{J K}^{-1}\ \text{mol}^{-1}.$$

as this value is in agreement with the variation of the standard entropy of the uranium oxides.

The high-temperature heat capacity of Np_2O_5 has been measured by drop calorimetry from 350 to 750 K by Belyaev *et al.*,[401] who gave the following equation:

$$C_p^\circ(T)/(\text{J K}^{-1}\ \text{mol}^{-1}) = 99.2 + 98.6 \times 10^{-3}(T/\text{K}).$$

5.8.3. Enthalpy of formation

The enthalpy of formation of Np_2O_5 has been measured by Belyaev *et al.*[402] and by Merli and Fuger[399] by solution calorimetry. The results of the two studies, -2148 kJ mol^{-1} and $-(2162.7 \pm 9.3)$ kJ mol^{-1} respectively, are in poor agreement. We select the value derived by Merli and Fuger[399] as it was based on a well-defined sample and a quick and well-defined dissolution reaction. It remains unchanged when recalculated

$$\Delta_f H^\circ(298.15\ \text{K}) = -(2162.7 \pm 9.3)\ \text{kJ mol}^{-1}.$$

5.9. NpO_2(cr,l)

5.9.1. Melting point

NpO_2 has a face-centered cubic crystal structure (space group $Fm\bar{3}m$) which is stable up to the melting point. The melting point of NpO_2 was reported to be (2833 ± 50) K by Chikalla *et al.*,[403] which becomes (2836 ± 50) K on ITS-90. However, recent work by Böhler *et al.*[404] using self-crucible laser melting gave a value of (3072 ± 66) K, which is selected here. Due to the high oxygen pressure of neptunium dioxide at temperatures close to melting, it cannot be excluded that the congruent melting composition of this compound be slightly hypostoichiometric.

5.9.2. Heat capacity and entropy

The low-temperature heat capacity of NpO_2 has been measured by Westrum Jr. *et al.*[405] by adiabatic calorimetry from 5 to 300 K, yielding for the standard entropy:

$$S^\circ(298.15\ \text{K}) = (80.3 \pm 0.4)\ \text{J K}^{-1}\ \text{mol}^{-1}.$$

Magnani *et al.*[316] reported heat capacity data that are in excellent agreement, but the numerical details of this measurement have not been reported.

The high-temperature enthalpy increment of NpO_2 has been measured by Arkhipov *et al.*[406] from 350 to 1100 K, by Nishi *et al.*[407] from 334 to 1071 K and by Beneš *et al.*[408] from 376 to 1770 K. The latter two studies were made on very small samples (less than 100 mg). The results by Arkhipov *et al.*[406] are in poor agreement with the low-temperature data and are significantly higher than the other two studies (Fig. 20). The results by Nishi *et al.*[407] and Beneš *et al.*[408] are in excellent agreement and fit the low temperature data very well (Fig. 20). Several estimates of the heat capacity of NpO_2 have been also reported. Yamashita *et al.*[409] and Serizawa *et al.*[410] calculated the lattice heat capacity from the phonon and dilatation contributions using Debye temperature, thermal expansion and Grüneisen constants and the electronic contributions from crystal field energies. As shown in Fig. 20 they are in fair agreement with the experimental data.

Above 2000 K, it is likely that the heat capacity of NpO_2 exhibits an excess component due to defect formation

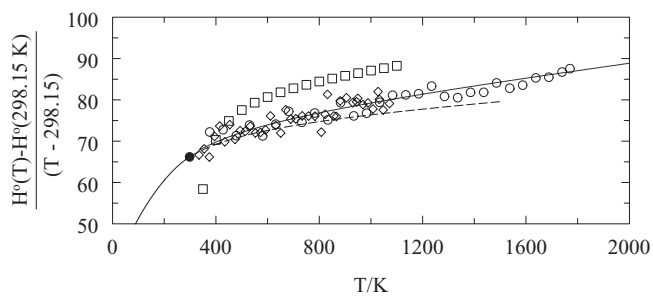

FIG. 20. The reduced enthalpy increment (in J K^{-1} mol^{-1}) of NpO_2; □, Arkhipov *et al.*[406]; ◊, Nishi *et al.*[407]; ○, Beneš *et al.*[408]; •, value derived from the low-temperature measurements by Westrum Jr. *et al.*[405]; the dashed curve shows the recommended equation based on the estimates of Serizawa *et al.*[410]

(principally oxygen Frenkel pairs). No information on this effects exists for NpO_2, but Konings and Beneš[330] estimated this contribution from the heat capacity values for ThO_2, UO_2, and PuO_2 by interpolating the enthalpy of oxygen Frenkel pair formation. By adding this contribution to the representation of the experimental results they obtained

$$C_p^\circ(T)/(\,J\,K^{-1}\,mol^{-1}) = 64.7712 + 43.8574\times10^{-3}(T/K) - 35.0695\times10^{-6}(T/K)^2 + 13.1917\times10^{-9}(T/K)^3 - 0.78932\times10^{6}(T/K)^{-2}$$

which has been constrained to 66.20 $J\,K^{-1}\,mol^{-1}$, as derived from the low-temperature heat capacity measurements by Westrum Jr. *et al.*[405]

No experimental data are available for liquid neptunium dioxide. We estimate

$$C_p^\circ(NpO_2, liq, T) = 66\ J\,K^{-1}\,mol^{-1}.$$

The entropy of fusion is assumed to be identical to that of UO_2 (24 $J\,K^{-1}\,mol^{-1}$), yielding

$$\Delta_{fus}H^\circ = (70\pm6)\ kJ\,mol^{-1}.$$

5.9.3. Enthalpy of formation

The enthalpy of formation of neptunium dioxide has been measured by Huber and Holley[411] by oxygen bomb calorimetery, the product being stoichiometric NpO_2:

$$\Delta_f H^\circ(298.15\ K) = -(1078.5\pm2.7)\ kJ\,mol^{-1}.$$

5.10. PuO_2(cr,l)

5.10.1. Melting point

PuO_2 has a face-centered fluorite structure (space group $Fm\bar{3}m$) up to its melting point. The various measurements of the melting point of PuO_2 are summarized in Table 60. Because PuO_2, similar to CeO_2, starts to lose oxygen according to the reaction:

$$PuO_2(cr) = PuO_{2-x}(cr) + \frac{x}{2}O_2(g),$$

the melting temperature determinations are difficult to interpret. For example, Chikalla[364] found that samples of stoichiometric PuO_2 had a O/Pu ratio near 1.62 after melting in inert gas atmosphere. Riley[412] realised that the melting point of stoichiometric plutonium dioxide could only be defined under a high oxygen pressure. However, his flame melting experiments were still imprecise and the samples were still affected by high temperature reduction despite the controlled atmosphere. Also the interaction of the liquid with container materials affects the results, as demonstrated by Kato *et al.*[372] They obtained a melting point for pure PuO_2 about 200 K higher than the earlier values, when using rhenium as container material instead of tungsten. This was further confirmed by De Bruycker *et al.*[413,414] who employed a containerless laser melting technique in oxygen and found an even higher melting temperature for stoichiometric PuO_2, T_{fus} = (3017 ± 28) K, which is our selected value.

TABLE 60. The melting point of PuO_2(cr)

Authors	T_{fus}/K Reported	T_{fus}/K ITS-90
Pijanowski and DeLuca[363]	2569 ± 30[a]	2586 ± 30
Russel[415]	2673[b]	
Chikalla[364]	2553 ± 30[a]	2556 ± 30
Freshley and Mattys[416]	2523	
Lyon and Bailey[365]	2511 ± 135[c]	2513 ± 135
Lyon and Bailey[367]	2663 ± 20[c]	2666 ± 20
Aitken and Evans[417]	2663[a]	
Riley[412]	2673 ± 20[b]	2682 ± 20
Kato *et al.*[372]	2843	2843
De Bruycker *et al.*[413]		3017 ± 28
Selected value:		3017 ± 28

[a]in He.
[b]in Ar.
[c]O_2.

5.10.2. Heat capacity and entropy

Low-temperature heat capacity measurements have been performed on samples of $^{239}PuO_2$ by Sandenaw[418] from 15 to 325 K and Kruger and Savage[419] from 192 to 320 K, as well as the less radioactive $^{242}PuO_2$ and $^{244}PuO_2$ from 12 to 350 K and 4 to 25 K, respectively, by Flotow *et al.*[420] In the latter samples the effects of accumulation of radiation damage are less significant and more accurate results in the very low temperature range can be obtained. For that reason our selected value for the entropy is solely based on the results by Flotow *et al.*[420]:

$$S^\circ(298.15\ K) = (66.13\pm0.30)\ J\,K^{-1}\,mol^{-1}.$$

High-temperature heat capacity of PuO_2 has been measured by Engel[384] from 300 to 1100 K, and high-temperature enthalpy increments have been measured by Kruger and Savage[419] from 298 to 1404 K, Ogard[421] from 1500 to 2715 K, and Oetting[422] from 353 to 1610 K (Fig. 21). Ogard's measurements suggest a rapid increase in C_p above 2370 K. This has been attributed to partial melting of PuO_2 through

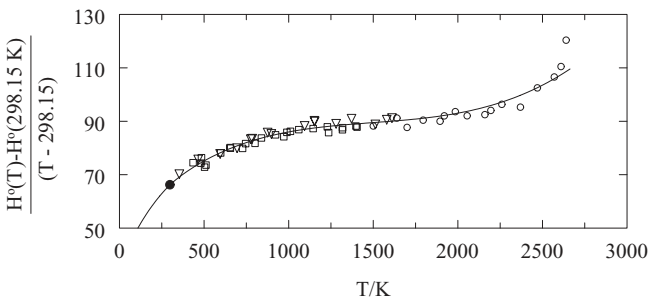

FIG. 21. The reduced enthalpy increment (in $J\ K^{-1}\,mol^{-1}$) of PuO_2; ○, Ogard[421]; □, Kruger and Savage[419]; ▽, Oetting[422]; •, value derived from the low-temperature measurements by Flotow *et al.*[420]; the curve shows the recommended equation.

interaction with the tungsten container,[422,423] although no evidence exists for this interaction. A similar rapid increase is found in the heat capacities of ThO_2, UO_2, and ZrO_2, which has been attributed to the formation of Frenkel and Schottky lattice defects at high temperatures. For that reason we have fitted all experimental data to a polynomial equation constrained to $C_p^\circ(298.15\ K) = 66.25\ J\ K^{-1}\ mol^{-1}$, as derived by Flotow *et al.*,[420] though it proved to be very difficult to fit the results to the standard form due to strong variation between room temperature and melting temperature. The following equation gives an acceptable description up to 2300 K and includes the upward trend, though the results of Ogard[421] in the 2470–2640 K range, which were given a lower weight, could not be reproduced accurately,

$$C_p^\circ/(J\,K^{-1}\,mol^{-1}) = 35.2952 + 0.15225(T/K) - 127.255 \times 10^{-6}(T/K)^2 + 36.289 \times 10^{-9}(T/K)^3 - 3.47593 \times 10^{5}(T/K)^{-2}.$$

No data for the heat capacity or enthalpy of liquid PuO_2 are known, except a single enthalpy measurement by Ogard.[421] The enthalpy of fusion is thus estimated, assuming that the entropy of fusion is identical to that of UO_2 ($22.4\ J\ K^{-1}\ mol^{-1}$), yielding

$$\Delta_{fus}H^\circ = (64 \pm 6)\ kJ\,mol^{-1}.$$

We have also estimated for the heat capacity of liquid PuO_2 from the value for UO_2 as

$$C_p^\circ = 70\ J\,K^{-1}\,mol^{-1}.$$

5.10.3. Enthalpy of formation

The enthalpy of formation of PuO_2 has been determined by Popov *et al.*,[424] Holley *et al.*[425] and Johnson *et al.*[426] by oxygen combustion calorimetry starting from pure plutonium metal. The results are in very good agreement, as shown in Table 61. We select

$$\Delta_f H^\circ(298.15\ K) = -(1055.8 \pm 1.0)\ kJ\,mol^{-1}$$

which is based to the appreciably more precise value by Johnson *et al.*,[426] who carefully analysed the metal for impurities and applied appropriate corrections.

TABLE 61. The enthalpy of formation of plutonium dioxide

Authors	Method[a]	$\Delta_f H^\circ(298.15\ K)$/kJ mol^{-1}
Popov *et al.*[424]	C	−1056.0 ± 4.6
Holley *et al.*[425]	C	−1058.0 ± 1.6
Johnson *et al.*[426]	C	−1055.8 ± 1.0
Selected value:		−1055.8 ± 1.0

[a]C = combustion calorimetry.

5.11. Pu_2O_3(cr,l)

5.11.1. Polymorphism and melting point

Pu_2O_3 has a hexagonal type-A rare-earth sesquioxide structure (space group $P\bar{3}m1$). It is likely that Pu_2O_3 may exhibit a similar high-temperature behavior as the light lanthanide sesquioxides, with the eventual appearance of H-type and the X-type structures before melting. This is however not confirmed experimentally. The melting point of stoichiometric Pu_2O_3 was measured by Chikalla *et al.*[427] and Riley[412] being in excellent agreement (Table 62), but significantly lower than the value reported by Holley *et al.*[425] for a less well-characterised sample. We select (2352 ± 10) K, based on the results of Riley,[412] corrected to ITS-90, which is, however, relatively low compared to the lanthanide sesquioxides as well as Am_2O_3 and Cm_2O_3 (see Sec. 7.2.2).

5.11.2. Heat capacity and entropy

Flotow and O'Hare[428] have measured the heat capacity of a sample of $^{244}Pu_2O_3$ from 8 K to 350 K. Their results revealed a λ-type anomaly in the heat capacity at 17.65 K, associated with an antiferromagnetic transition. The standard entropy derived from this work is:

$$S^\circ(298.15\ K) = (163.02 \pm 0.65)\ J\,K^{-1}\,mol^{-1}$$

There are no measurements of the heat capacity or enthalpy of Pu_2O_3 at high temperatures. We have here estimated the following equation, based on comparison of actinide and lanthanide oxides, which fits $C_p^\circ(298.15\ K) = 116.98\ J\ K^{-1}\ mol^{-1}$ from the low-temperature heat capacity measurements:[428]

$$C_p^\circ/(J\,K^{-1}\,mol^{-1}) = 130.6670 + 18.4357 \times 10^{-3}(T/K) - 1.70530 \times 10^{6}(T/K)^{-2}$$

Previously estimated values have been presented by various authors,[395,429] but these are about 10 kJ mol^{-1} higher at 2000 K.

We assume that Pu_2O_3 transforms to the H-type structure at $T_{trs} = (2300 \pm 50)$ K, like in the lanthanide sesquioxides and estimate for the enthalpies of transition and fusion:

$$\Delta_{trs}H^\circ(A \rightarrow H) = (32 \pm 10)\ kJ\,mol^{-1}$$
$$\Delta_{fus}H^\circ = (71 \pm 10)\ kJ\,mol^{-1}$$

TABLE 62. Temperature of melting of plutonium sesquioxide

	T_{fus}/K	
Authors	Reported	ITS-90
Holley *et al.*[425]	2513 ± 33	2516 ± 33
Chikalla *et al.*[427]	2358 ± 25	2361 ± 25
Riley[412]	2348 ± 5	2352 ± 5
Selected value:		2352 ± 10

For the heat capacity of the high temperature modifications we assume the same values as for Sm_2O_3:

$$C_p^\circ(H, T) = 165\ J\,K^{-1}\,mol^{-1}$$
$$C_p^\circ(liq, T) = 179\ J\,K^{-1}\,mol^{-1}$$

5.11.3. Enthalpy of formation

The assessment of the enthalpy of formation of Pu_2O_3 is not straightforward, as direct measurements do not exists. The value must be based on the analysis of the reaction:

$$\frac{1}{2}Pu_2O_3(cr) + \frac{1}{4}O_2(g) = PuO_2(cr)$$

This was extensively discussed in various reviews,[8,395,430] in which similar results have been derived. These studies generally refer to the assessment by Markin and Rand[431] of the oxygen potential measurements by the same authors. As discussed by Lemire *et al.*,[430] the work of Chereau *et al.*[432] suggests, however, that the partial enthalpies and entropies from the work of Markin and Rand might need some adjustment. Guéneau *et al.*,[357,433] presented a consistent analysis of the phase diagram and oxygen potential data in the Pu-O system using the CALPHAD method. The results of that analysis are in reasonable agreement with the analysis by Rand,[8,430] though a slight change in the enthalpy of formation of PuO_2 has been suggested, which is not consistent with the present review. If we take the Gibbs energy of the above reaction, and combine it with the selected values from this review, we obtain $\Delta_f H°(298.15\ K) = -1647\ kJ\ mol^{-1}$, somewhat lower than the value by Rand,[8,430] $\Delta_f H°(298.15\ K) = -(1656 \pm 10)\ kJ\ mol^{-1}$, or Glushko *et al.*,[395] $\Delta_f H°(298.15\ K) = -(1670 \pm 20)\ kJ\ mol^{-1}$. We select

$$\Delta_f H^\circ(298.15\ K) = -(1647 \pm 10)\ kJ\,mol^{-1}.$$

5.12. AmO_2(cr,l)

5.12.1. Melting point

Americium dioxide has a fcc fluorite structure (space group $Fm\overline{3}m$). The melting point of AmO_2 has been measured by McHenry.[434] His experiments were hindered by the effect of dissociation, but McHenry concluded from measurements at different heating rates that the melting point of the dioxide is about 2383 K. However, this value is probably not referring to stoichiometric AmO_2, but to AmO_{2-x} of undefined composition. Stoichiometric melting of AmO_2 is unlikely to occur at atmospheric pressure, as follows from the phase diagram.[435] Upon heating the oxide start to lose oxygen and transforms into AmO_{2-x}, which has a wide range of composition.

5.12.2. Heat capacity and entropy

No experimental study of the low-temperature heat capacity of AmO_2 has been reported. The estimate by Westrum Jr. and Grønvold[436] for the standard entropy, $S°(298.15\ K) = 83.7\ J\ K^{-1}\ mol^{-1}$, is somewhat too high, as has been demonstrated by Konings,[329,437] who analysed the systematics in the entropies of actinide(IV) compounds, deriving $S°(298.15\ K) = 75.5\ J\ K^{-1}\ mol^{-1}$, from a lattice contribution ($63.0\ J\ K^{-1}\ mol^{-1}$) and an excess contribution ($12.5\ J\ K^{-1}\ mol^{-1}$) from the $^6H_{5/2}$ electronic state of the Am^{4+} ion. This value is adopted here with an estimated uncertainty

$$S^\circ(298.15\ K) = (75.5 \pm 3.0)\ J\,K^{-1}\,mol^{-1}.$$

This value is also consistent with preliminary calculations of the vaporization data for americium oxides dissolved in plutonium oxides.[438]

The enthalpy increment of AmO_2 has been measured by Nishi *et al.*[439] on a sample of about 50 mg encapsulated in a platinum container. As a result, the scatter in the data is relatively large, and the values at the lowest temperatures are somewhat uncertain. Consequently the fit of the data by Nishi *et al.*[439] yields too low values near room temperature (Fig. 22). For that reason we have refitted the enthalpy increment data constrained to $C_p^\circ(298.15\ K) = 64.3\ J\ K^{-1}\ mol^{-1}$, as derived from the trend in the AnO_2 series by Konings.[329] We thus obtain

$$C_p^\circ/\ J\,K^{-1}\,mol^{-1} = 78.9718 + 3.8365 \times 10^{-3}(T/K) - 1.40591 \times 10^{6}(T/K)^{-2}.$$

Above about 1200 K, this equation has been fitted to the heat capacity estimated by Thiriet and Konings[440] taking ThO_2 as lattice and calculating the excess from the free ion energy levels.

5.12.3. Enthalpy of formation

The enthalpy of formation of $^{243}AmO_2$ has been measured by Morss and Fuger[441] who determined the enthalpy of solution of a well-characterized sample in a $\{H_2SO_4+KI\}$ solution using a micro-calorimeter. The thermochemical cycle used in that work, was based on the dissolution of $AmCl_3$ in the same medium. Their resulting value, which remains unchanged after recalculation, has been selected here as

$$\Delta_f H^\circ(298.15\ K) = -(932.2 \pm 3.0)\ kJ\,mol^{-1}.$$

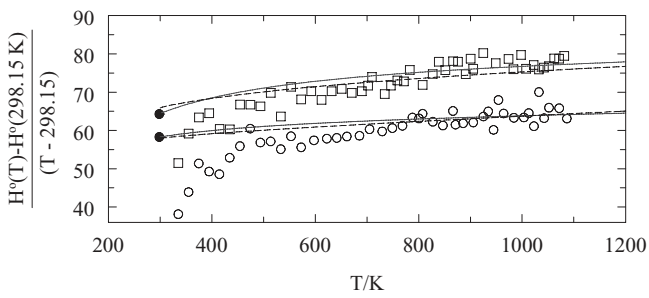

FIG. 22. The reduced enthalpy increment (in $J\ K^{-1}\ mol^{-1}$) of AmO_2 (□) and $AmO_{1.5}$ (○) by Nishi *et al.*[439]; the solid curve shows the recommended equations, the dashed curves the estimates based on comparison with other lanthanide and actinide dioxides and sesquioxides.

Eyring *et al.*[80] measured the enthalpy of solution of $^{241}AmO_2$ in a $\{HNO_3+HBF_4\}$ solution and derived for the enthalpy of formation $\Delta_f H°(298.15\ K) = -(1003.7\ kJ\ mol^{-1}$, substantially more negative. The thermochemical cycle used in that study is based on (estimated) extrapolation of the result to infinite dilution, which introduces large uncertainties.

5.13. Am_2O_3(cr,l)

5.13.1. Polymorphism and melting point

The stable crystal structure of americium sesquioxide at room temperature is not fully established. The early studies report a bcc C-type rare-earth structure (space group Ia3) at room temperatures. However, since Pu_2O_3 has a A-type hexagonal and Cm_2O_3 a B-type monoclinic structure, this is not likely. Considering the ionic radius of Am^{3+} the B-type structure is more probable (see also Sec. 7.2.2). This would be consistent with the transformation to the rare-earth type-A La_2O_3 structure at a temperature between 1073 and 1173 K as observed by Wallmann.[442] However, most experimental studies on Am_2O_3 have been made on the hexagonal form.

The melting point of Am_2O_3 was found as (2478 ± 15) K by Chikalla *et al.*,[443,444] which is $T_{fus} = (2481 \pm 15)$ K on ITS-90.

5.13.2. Heat capacity and entropy

The low-temperature heat capacity of Am_2O_3 has not been measured but several estimates have been made. Westrum Jr. and Grønvold[436] estimated the value $S°(298.15\ K) = 158.2\ J\ K^{-1}\ mol^{-1}$ (specified as cubic), by describing the entropy as the sum of the lattice entropy and an excess contribution. A similar approach, but using a more sound basis of spectroscopic and calorimetric information, was used by Konings.[127,445] The value was composed only of a lattice part, obtained by extrapolating the trend in the lanthanide sesquioxides to the actinide sesquioxides. The excess part for the Am^{3+} ion is zero as the $^7F_0$ ground state degeneracy is 1, and the first excited state $^7F_1$ does not contribute at room temperature. This value is accepted here

$$S°(298.15\ K) = (134.2 \pm 5.0)\ J\ K^{-1}\ mol^{-1}.$$

The high-temperature enthalpy increment of hexagonal (A-type) Am_2O_3 has been measured by Nishi *et al.*[439] on a sample of about 50 mg encapsulated in a platinum container. As a result, the scatter in the data is relatively large, and the values at the lowest temperatures are somewhat uncertain (Fig. 22). Consequently the fit of the data by Nishi *et al.*[439] yields too low values near room temperature (e.g., $C_p°(298.15\ K) = 88.0\ J\ K^{-1}\ mol^{-1}$) considering the results for the Ln_2O_3 compounds, for which the lattice heat capacity at 298.15 K is between 110 and 100 $J\ K^{-1}\ mol^{-1}$, and the value for Pu_2O_3 ($116.98\ J\ K^{-1}\ mol^{-1}$). For that reason we have refitted the enthalpy increment data above 700 K, constrained to $C_p° = 116.5\ J\ K^{-1}\ mol^{-1}$, as derived from comparison with the Ln_2O_3 series and the value for Pu_2O_3. We thus obtain

$$C_p°/J\,K^{-1}\,mol^{-1} = 126.0084 + 8.0097 \times 10^{-3}(T/K) - 1.05752 \times 10^{6}(T/K)^{-2}.$$

The equation has been fitted at high temperature to the heat capacity estimated on the basis of comparison to Pu_2O_3 and the lanthanide sesquioxides (Fig. 22).

The transition to the H-type structure is assumed to take place at $T_{trs} = (2350 \pm 50)$ K, and we estimate for the enthalpies of transition and fusion:

$$\Delta_{trs}H°(A \rightarrow H) = (33 \pm 10)\ kJ\,mol^{-1},$$
$$\Delta_{trs}H°(H \rightarrow X) = (10 \pm 5)\ kJ\,mol^{-1},$$
$$\Delta_{fus}H° = (74 \pm 10)\ kJ\,mol^{-1}.$$

For the heat capacity of the high temperature modifications we assume the same values as for Eu_2O_3:

$$C_p°(H,T) = 141\ J\,K^{-1}\,mol^{-1}, C_p°(liq,T) = 156\ J\,K^{-1}\,mol^{-1}.$$

5.13.3. Enthalpy of formation

Morss and Sonnenberger[446] have derived the enthalpy of formation of hexagonal Am_2O_3 from enthalpy-of-solution measurements in 6 mol dm^{-3} hydrochloric acid using a microcalorimeter. This value remains unchanged after recalculation. The thermochemical cycle used in that work, was based on the dissolution of Am(cr) in the same medium, based on the work of Fuger *et al.*[447]

$$\Delta_f H°(298.15\ K) = -(1690.4 \pm 7.9)\ kJ\,mol^{-1}.$$

5.14. Cm_2O_3(cr)

5.14.1. Polymorphism and melting point

At room temperature stoichiometric curium sequioxide has a monoclinic B-type crystal structure. Upon heating, three high-temperature transformations have been identified.[92,403] At (1888 ± 15) K the monoclinic form transforms into the A-type hexagonal structure, as was observed by high-temperature X-ray diffraction.[448] Above 2000 K transitions at (2273 ± 20) K and at (2383 ± 20) K have been observed, which are most likely transformations to the H and X structures that are known for the lanthanide sesquioxides.

There are several reports of the melting point of Cm_2O_3, as summarized in Table 63. The values are in good agreement,

TABLE 63. The melting point of Cm_2O_3(cr)

	T_{fus}/K	
Authors	Reported	ITS-90
McHenry[434]	2223	
Smith[449]	2538 ± 20	2545 ± 20
Gibby *et al.*[92a]	2548 ± 25	2551 ± 25
	2538	2541
Baybarz[450]	2533 ± 20	2532 ± 20
Selected value		2542 ± 25

[a]Also reported by Chikalla *et al.*[403]

except for the results of McHenry,[434] who used CmO_2 as starting material and assumed that it was converted to the sesquioxide during the measurements. For all values a small correction to the ITS-90 temperature scale is needed. Smith[449] used the melting points of Al_2O_3 and Tm_2O_3 as reference. For the former, a value about 7 K lower than the currently accepted value was obtained. For Tm_2O_3 no recommended value is available. We correct the value by Smith therefore with +7 K. Regarding the results of Gibby *et al.*,[92] Chikalla *et al.*[403] we think it is likely that they refer to IPTS-48. The selected value for the melting point is $T_{fus} = (2542 \pm 25)$ K.

5.14.2. Heat capacity and entropy

The low-temperature heat capacity of Cm_2O_3 has not been measured but several estimates have been made. Westrum Jr. and Grønvold[436] have estimated the value $S°(298.15\,K) = 160.7$ J K^{-1} mol^{-1} (specified as cubic), by describing the entropy as the sum of the lattice entropy and an excess contribution. A similar approach, but using a more sound basis of spectroscopic and calorimetric information, was used by Konings[127,445] who obtained (167.0 ± 5.0) J K^{-1} mol^{-1} for the monoclinic modification. The value was composed of a lattice part (133.5 J K^{-1} mol^{-1}), obtained by extrapolating the trend in the lanthanide sequioxides to the actinide sesquioxides, and an excess part (34.58 J K^{-1} mol^{-1}), calculated from the ground state degeneracy of the Cm^{3+} ion. This value is accepted here

$$S°(298.15\,K) = (168.1 \pm 5.0)\ \text{J K}^{-1}\,\text{mol}^{-1}.$$

Estimated values for the high-temperature heat capacity of monoclinic Cm_2O_3 have been presented by Gibby *et al.*,[92] who used them to convert the thermal diffusivity measurements to thermal conductivity data, which agree reasonably with direct measurements (see below). As discussed by Konings[437] Gibby's values are rather high compared to the experimental values for the lanthanide sesquioxides and Pu_2O_3. He estimated the following equation:

$$C_p°(T)/\text{J K}^{-1}\,\text{mol}^{-1} = 123.532 + 14.550 \times 10^{-3}(T/K) - 1.3489 \times 10^{6}(T/K)^{-2}.$$

Data on the heat capacity of the H, X, and liquid (L) phases and enthalpies of transition for C → H, H → X, and X → L are not available. Although rather speculative we have estimated the properties of the high temperature phases in a similar manner as for the lanthanide sesquioxides, and derive for Cm_2O_3:

$$\Delta_{trs}H°(B \rightarrow A) = (6 \pm 3)\ \text{kJ mol}^{-1},$$
$$\Delta_{trs}H°(A \rightarrow H) = (32 \pm 6)\ \text{kJ mol}^{-1},$$
$$\Delta_{trs}H°(H \rightarrow X) = (10 \pm 5)\ \text{kJ mol}^{-1},$$
$$\Delta_{fus}H° = (66 \pm 10)\ \text{kJ mol}^{-1}.$$

For the heat capacity of the high temperature H modification and liquid Cm_2O_3 we estimate

$$C_p°(A, T) = 142\ \text{J K}^{-1}\,\text{mol}^{-1},$$
$$C_p°(H, T) = C_p°(X, T) = 130\ \text{J K}^{-1}\,\text{mol}^{-1},$$
$$C_p°(liq, T) = 140\ \text{J K}^{-1}\,\text{mol}^{-1}.$$

5.14.3. Enthalpy of formation

The enthalpy of solution of curium sesquioxide in 6 mol dm^{-3} HCl(aq) has been measured by Morss *et al.*[451] by solution calorimetry using milligram samples of the monoclinic form. Combining this result with the enthalpy of solution of Cm metal in this solvent, estimated from the value for the dissolution in 1.0 mol dm^{-3} HCl(aq), the enthalpy of formation is calculated as

$$\Delta_f H°(298.15\ \text{K}) = -(1684 \pm 14)\ \text{kJ mol}^{-1}.$$

5.15. BkO_2(cr) and Bk_2O_3(cr)

5.15.1. Polymorphism and melting point

BkO_2 has a fcc fluorite structure (space group $Fm\bar{3}m$). The stable crystallographic modification of Bk_2O_3 is the bcc C-type rare-earth structure (space group Ia3).[452] Baybarz[450] studied the high temperature polymorphism and found that C-Bk_2O_3 irreversibly transforms to a monoclinic B structure at (1473 ± 50) K. The monoclinic-to-hexagonal transition was observed at about 2022 K and the melting point at (2193 ± 25) K. Correction to ITS-90 would involve a correction of −1 K if the measurements would refer to ITPS-68 and +2 K in case of ITPS-48. Since this is not clear from the paper, we choose to retain the original value.

5.15.2. Heat capacity and entropy

No experimental data exist on the heat capacity and entropy of the berkelium oxides. Konings *et al.*[306] gave the following estimates for the standard entropy based on the trends in the actinide and lanthanide series:

$$S°(BkO_2,\ \text{cr},\ 298.15\ \text{K}) = (83 \pm 5)\ \text{J K}^{-1}\,\text{mol}^{-1},$$
$$S°(Bk_2O_3,\ \text{cr},\ 298.15\ \text{K}) = (173.8 \pm 5)\ \text{J K}^{-1}\,\text{mol}^{-1}.$$

5.15.3. Enthalpy of formation

The enthalpies of formation of BkO_2 and Bk_2O_3(cr) have not been determined. Konings *et al.*[306] gave the following estimated values:

$$\Delta_f H°(BkO_2,\ \text{cr},\ 298.15\ \text{K}) = -(1023 \pm 9)\ \text{kJ mol}^{-1},$$
$$\Delta_f H°(Bk_2O_3,\ \text{cr},\ 298.15\ \text{K}) = -(1694 \pm 20)\ \text{kJ mol}^{-1}$$

based on the correlation between the difference in the enthalpy of formations of the oxides and the aqueous ions with molar volume for the AnO_2 compounds.

5.16. CfO_2(cr) and Cf_2O_3(cr)

5.16.1. Polymorphism and melting point

CfO_2 has a fcc fluorite structure (space group $Fm\bar{3}m$). The stable crystallographic modification of Bk_2O_3 is the bcc

C-type rare-earth structure (space group Ia3). It transforms to cubic or hexagonal forms due to self-irradiation.[450] The cubic (cr) to monoclinic (B) transformation has been observed at about 1673 K.[453] The melting point of Cf_2O_3 was determined to be (2023 ± 25) K by Baybarz[450] in vacuum and in helium. Correction to ITS-90 would involve a correction of −1 K it the measurements would refer to ITPS-68 and +2 K in case of ITPS-48. Since this is not clear from the paper, we choose to retain the original value.

5.16.2. Heat capacity and entropy

No experimental data exist on the heat capacity and entropy of the berkelium oxides. Konings *et al.*[306] gave the following estimated values for the standard entropy based on the trends in the actinide and lanthanide series:

$$S^\circ(CfO_2,\ cr,\ 298.15\ K) = (87 \pm 5)\ J\,K^{-1}\,mol^{-1},$$
$$S^\circ(Cf_2O_3,\ cr,\ 298.15\ K) = (173.8 \pm 5)\ J\,K^{-1}\,mol^{-1}.$$

5.16.3. Enthalpy of formation

The enthalpy of formation of CfO_2 has not been determined. Konings *et al.*[306] gave the following estimated value:

$$\Delta_f H^\circ(CfO_2,\ cr,\ 298.15\ K) = -(857 \pm 14)\ kJ\,mol^{-1}$$

based on the correlation between the difference in the enthalpy of formation of the oxides and the aqueous ions with molar volume for the AnO_2 compounds. The enthalpy of formation of cubic Cf_2O_3(cr) has been determined by Morss *et al.*[454] using solution microcalorimetry on milligram samples in 6.0 mol dm^{-3} HCl(aq), to give

$$\Delta_f H^\circ(Cf_2O_3,\ cr,\ 298.15\ K) = -(1652.6 \pm 10.3)\ kJ\,mol^{-1}$$

using a thermochemical cycle based on the solution of Cf(cr) for which the enthalpy was estimated from the experimental value in 1.0 mol dm^{-3} HCl(aq) by Fuger *et al.*[455]

6. The Gaseous Actinide Oxides

6.1. AcO(g)

6.1.1. Heat capacity and entropy

The thermal functions of AcO(g) in the standard state have been calculated using the data given in Table 64. Because no spectral data on the AcO molecule exists, the molecular constants were obtained from B3LYP calculations by Kovács[456] and estimations using the trends revealed in the spectral data of the lanthanide and actinide monoxides. The electronic structure is assumed to be analogous to that of LaO. The energies of the low-lying states taken from the LaO data are approximated to hundreds cm^{-1}. The derived standard entropy at room temperature is

$$S^\circ(298.15\ K) = (245.545 \pm 5.0)\ J\,K^{-1}\,mol^{-1}$$

TABLE 64. Molecular constants of AcO(g)

No.	State	T_e	ω_e	$\omega_e x_e$	B_e	$\alpha_e 10^3$	$D_e 10^7$	r_e	p_i
		cm^{-1}						pm	
0[a]	$X^2\Sigma^+$	0	764	2.3	0.34	1.5	2.63	194	2
1[b]	$A'\,^2\Delta_{3/2}$	7500							2
2[b]	$A'\,^2\Delta_{5/2}$	8200							2
3[b]	$A^2\Pi$	13 100							4
4[b]	$B^2\Sigma$	17 900							2
5[b]	$C^2\Pi$	22 700							4
6[b]	$D^2\Sigma$	27 000							2
7[b]	$F^2\Sigma$	28 000							4
8[b]		17 200							8
9[b]		18 500							8
10[b]		21 200							8
11[b]		24 000							20
12[b]		25 900							8
13[b]		30 200							12
14[b]		35 000							30
15[b]		40 000							36

[a]Computed state.
[b]Estimated state

and the coefficients of the equations for the heat capacity are

$$C_p^\circ/(J\,K^{-1}\,mol^{-1}) = 26.7681 + 26.00447 \times 10^{-3}(T/K) - 24.23966 \times 10^{-6}(T/K)^2 + 8.10964 \times 10^{-9}(T/K)^3 - 0.83961 \times 10^{5}(T/K)^{-2}$$

for the 298.15–1100 K range, and

$$C_p^\circ/(J\,K^{-1}\,mol^{-1}) = 47.1310 - 13.09869 \times 10^{-3}(T/K) + 6.02184 \times 10^{-6}(T/K)^2 - 0.628330 \times 10^{-9}(T/K)^3 - 2.91011 \times 10^{6}(T/K)^{-2}$$

for the 1100–4000 K range.

6.1.2. Enthalpy of formation

No experimental data exists for the derivation of the enthalpy of formation of AcO(g). We have estimated the dissociation energy as $D_0 = (860 \pm 20)$ kJ mol^{-1}. This value corresponds to:

$$\Delta_f H^\circ(AcO,\ g,\ 298.15\ K) = -(193 \pm 20)\ kJ\,mol^{-1}.$$

6.2. ThO_2(g)

6.2.1. Heat capacity and entropy

The thermodynamic functions of ThO_2(g) in the standard state have been calculated using the data given in Table 65. There are no experimental data for the structure of free gaseous ThO_2 molecules, and the ThO_2 structure is determined only from infrared spectra in the solid matrices. In an early work Kaufman *et al.*[457] found that a ThO_2 molecular beam exhibits some deflection in an inhomogeneous electric field, indicating the possibility of a bent structure for this molecule. The first quantitative information on the bent structure of ThO_2 was

TABLE 65. The molecular parameters for ThO_2(g)

Parameter	Value
Ground electronic state	$^1A_1$
Symmetry group	C_{2v}
Symmetry number, σ	2
$I_AI_BI_C$ (g^3 cm^6)[a]	1110×10^{-117}
Vibrational frequencies (cm^{-1})	808, 160, 757
Electronic states (cm^{-1})[b]	0(1), 17909(2), 18933(2), 22220(2), 23569(2), 24637(2)

[a]Product of moments of inertia.
[b]Numbers in parentheses represent the statistical weights.

obtained from infrared spectroscopy. Gabelnick *et al.*,[212] Zhou and Andrews,[458] and Andrews *et al.*[459] have studied the infrared spectra of ThO_2 isotopomers in argon and neon matrices. On the basis of ^{18}O isotope shifts a nonlinear structure has been derived for ThO_2 with the bond angle $(122.5 \pm 2)°$. Quantum-chemical calculations at DFT (Density Functional Theory),[458–460] Dirac-Hartree-Fock,[461] and SO-CASPT2 level[462] resulted in a bent structure for ThO_2 as well. The quantum chemical calculations resulted in Th–O bond lengths between 188.1–192.3 pm. The probably most accurate bond distance was suggested on the basis of the frequency–bond distance relationship derived by Kovács and Konings[460] utilizing the experimental matrix-IR data. The product of the principal moments of inertia of ThO_2 (see Table 65) was calculated using the values r_e(Th–O) = (191 ± 5) pm and O–Th–O = (122.5 ± 2)°. The r_e(Th–O) value is an average of three bond distances (190.6, 191.1, and 189.2 pm) obtained in the mentioned theoretical calculations.

The accepted vibrational frequencies ν_1 and ν_3 (see Table 65) were taken from IR spectra obtained by Gabelnick *et al.*,[212] Zhou and Andrews,[458] and Andrews *et al.*[459] for the neon matrix. ThO_2 bands detected in the Ne matrix are blue-shifted 22 cm^{-1} from the solid argon data. In comparison with Ar, the Ne matrix is less polarizable, and matrix shifts in this case are substantially less. The deformation frequency ν_2 was estimated from calculations by Zhou and Andrews,[458] Dyall,[461] Andrews *et al.*[459] and Kovács and Konings.[460]

No experimental investigations of the electronic spectra of ThO_2 were reported. Quantum chemical calculations on the molecule agree in the X^1A_1 ground state.[458–463] This state corresponds to the closed shell configuration and no low-lying electronic states may be expected for this molecule. The high electronic energy levels of ThO_2 given in Table 65 are estimated to be the same as for isoelectronic UO_2^{2+} from *ab initio* calculations by Pierloot *et al.*[464]

The derived standard entropy at room temperature is

$$S°(298.15\ K) = (285.233 \pm 2.0)\ J\,K^{-1}\,mol^{-1}.$$

and the coefficients of the equations for the heat capacity are

$$C_p°/(J\,K^{-1}\,mol^{-1}) = 36.83878 + 55.95391 \times 10^{-3}(T/K) - 56.33462 \times 10^{-6}(T/K)^2 + 20.31019 \times 10^{-9}(T/K)^3 - 1.940496 \times 10^{5}(T/K)^{-2}$$

for the 298.15–900 K range, and

$$C_p°/(J\,K^{-1}\,mol^{-1}) = 56.72155 + 2.163537 \times 10^{-3}(T/K) - 1.189606 \times 10^{-6}(T/K)^2 + 0.2274986 \times 10^{-9}(T/K)^3 - 1.407937 \times 10^{6}(T/K)^{-2}$$

for the 900–4000 K range.

6.2.2. Enthalpy of formation

The value of ThO_2(g) enthalpy of formation is based on Langmuir and Knudsen effusion measurements of ThO_2(cr) enthalpy of sublimation and mass spectrometric measurements of equilibrium constants for isomolecular oxygen exchange reactions (see Table 66). In the early Langmuir and Knudsen effusion measurements, the weight loss of thoria samples was used for calculation of the vapor pressure under assumption of ThO_2(g) as the only thorium-bearing vapor species.[465–467] Knudsen effusion studies were carried out using substantially inert tungsten effusion cells. The only exception is the work by Hoch and Johnston[466] in which a tantalum cell was used. Ackermann *et al.*[468] have performed a combined study of the thorium-oxygen system evaporation behavior in the temperature range 2000–3000 K. It was found that solid thorium dioxide evaporates congruently. Above 2800 K, a thermodynamically insignificant substoichiometry $ThO_{1.998}$ was found. A combination of mass effusion and mass-spectrometric examination of the vapor composition has led to the conclusion that ThO and ThO_2 gaseous species are of comparable importance in the thoria vapor. More detailed study of thermodynamics of thoria vaporization has been carried out by Ackermann and

TABLE 66. The enthalpy of sublimation of ThO_2(g), in kJ mol^{-1}

Authors	Method[a]	T/K	$\Delta_{sub}H°(298.15\ K)$
Shapiro[465]	L	2062–2257	791.3 ± 15.0
Hoch and Johnston[466]	K	2389–2676	(730.6)
Darnell and McCollum[467]	K	2268–2593	788.7 ± 12.0
Ackermann *et al.*[468]	K+M	2180–2871	787.9 ± 10.0
Shchukarev and Semenov[472]	K+M	2600–3000	802.9 ± 15.0
Semenov[473b]	K+M	2200–2700	779.0 ± 12.0
Ackermann and Rauh[469c]	K+M	2400–2800	797.1 ± 10.0
Hildenbrand and Murad[470d]	M	2160–2176	782.1 ± 15.0
Ackermann and Rauh[471e]	M	2320–2650	797.1 ± 15.0
Selected value:			790.8 ± 12.0

[a]K = Knudsen effusion; M = mass spectrometry; L = Langmuir effusion.
[b]Extended and reassessed data of Shchukarev and Semenov.[472]
[c]Recalculated from the Ackermann *et al.*[468] total pressure of Th-bearing species.
[d]Calculated from the enthalpy of the gaseous reaction Th + ThO_2 = 2ThO.
[e]Calculated from the enthalpy of the gaseous reaction ZrO_2 + ThO = ThO_2 + ZrO.

Rauh.[469] The congruently vaporizing composition of thoria was found $ThO_{1.994}$, instead of previous value $ThO_{1.998}$. Using the reassessed results of their previous investigation,[468] Ackermann and Rauh[469] have found equations for the temperature dependence of the ThO(g) and ThO_2(g) partial pressures over stoichiometric thoria. As follows from these equations, p(ThO)/p(ThO_2) value linearly rises from 0.20 to 0.36 in the temperature range 2000–2800 K.

The enthalpy of sublimation values presented in Table 66 were obtained using partial pressures of ThO_2(g) species calculated from the total vapor pressure over slightly substoichiometric thoria. All values of the enthalpy of sublimation are in good agreement. The only exception is the work by Hoch and Johnston.[466] Much higher values of weight loss found in this work are obviously connected with use of tantalum effusion cells for vaporization of thoria, leading to intensive formation of ThO(g). The enthalpy of sublimation values calculated from the results of mass-spectrometric measurements of gaseous equilibria[470,471] are in agreement with Knudsen effusion and Langmuir measurements.

The selected value is taken as a rounded weighted average from all works except Hoch and Johnston[466]: $\Delta_{sub}H°(298.15\ K) = (790.8 \pm 12.0)$ kJ mol^{-1}. This value corresponds to:

$$\Delta_f H°(ThO_2,\ g,\ 298.15) = -(435.6 \pm 12.6)\ \text{kJ mol}^{-1}.$$

The corresponding energy of atomization is $D_0(ThO_2) = (1531.3 \pm 13.5)$ kJ mol^{-1}.

6.3. ThO(g)

6.3.1. Heat capacity and entropy

The thermal functions of ThO(g) in the standard state have been calculated using the molecular constants presented in Table 67.

The spectroscopic properties of ThO were studied since the beginning of the last century. The data published up to 1975 were reviewed by Huber and Herzberg[179] and up to 1980 by Gurvich *et al.*[180] Later Edvinsson and Lagerqvist[474–479], Edvinsson and Jonsson,[480] published a number of papers concerning the ThO emission spectrum. The accurate Th-O

TABLE 67. Molecular constants of $^{232}Th^{16}O$(g)

No.	State	T_e	ω_e	$\omega_e x_e$	B_e	$\alpha_e 10^3$	$D_e 10^7$	r_e	p_i
		cm^{-1}						pm	
0[a]	$X^1\Sigma_0^+$	0	895.77	2.39	0.33246	1.3	1.83[b]	184.018613(24)	1
1[a]	(1)3	5335.9							2
2[a]	(1)2	6146.6							2
3[a]		9315							4
4[a]	[10.6]0	10626							2[c]
5[a]	[11.1]1	11156							2
6[a]	[14.5]1	14525							4[c]
7[a]	[15.9]1	15975							3[c]
8[a]	[16.3]0	16354							1
9[a]	[18.1]2	18053							2
10[a]	[18.4]0	18406							1
11[a]	[19.1]0	19068							1
12[a]	[19.5]1	19586							2
13[a]	[20.1]3	20112							7[c]
14[a]	[21.7]1	21756							6[c]
15[a]	[22.6]1	22685							8[c]
16[a]	[23.1]0	23155							1
17[a]	[23.2]0	23199							2
18[a]	[24.0]3	24084							4[c]
19[a]	[24.9]1	24886							6[c]
20[a]	[25.1]1	25184							3[c]
21[a]	[25.8]1	25850							8[c]
22[a]	[27.7]1	27756							6[c]
23[a]	[28.0]0	28071							2[c]
24[a]	[28.3]2	28360							2
25[a]	[28.6]1	28614							2
26[a]	[30.3]1	30346							14[c]
27[a]	[32.7]2	32770							10[c]
28[d]		35000							14
29[d]		40000							20

[a]Experimental state.
[b]D_0.
[c]Added statistical weights of near-lying predicted states.
[d]Estimated state.

TABLE 68. The enthalpy of formation of ThO(g), in kJ mol^{-1}

Authors	Method[a]	T/K	Reaction	$\Delta_r H°(298.15\ K)$	$\Delta_f H°(298.15\ K)$
Ackermann *et al.*[468]	K+M	2337–2381	$ThO_2(cr) = ThO(g) + O(g)$	1434.4	−41.2
Shchukarev and Semenov[472]	M	2573–2973	$ThO_2(cr) = ThO(g) + O(g)$	1393.2	−82.3
Ackermann and Rauh[469]	M	2400–2800	$ThO_2(cr) = ThO(g) + O(g)$	1447.6	−28.0
	K	2080–2214	$\frac{1}{2}Th(cr) + \frac{1}{2}ThO_2(cr) = ThO(g)$	599.8	−13.4
	M	1930–2280	$ThO(g) + Y(g) = Th(g) + YO(g)$	−169.5	−29.1
Hildenbrand and Murad[470]	M	1782–1927	$\frac{1}{2}Th(cr) + \frac{1}{2}ThO_2(cr) = ThO(g)$	593.1	−20.1
	M	2064–2176	$ThO(g) + Si(g) = Th(g) + SiO(g)$	77.3	−24.1
Ackermann and Rauh[469]	M	2200–2550	$ThO(g) + Hf(g) = Th(g) + HfO(g)$	73.5	−21.4
Neubert and Zmbov[496]	M	1759–1961	$ThO(g) + La(g) = Th(g) + LaO(g)$	62.8	−11.7
Murad and Hildenbrand[497]	M	2288	$ThO(g) + Zr(g) = Th(g) + ZrO(g)$	110.9	−24.4
Selected value:			$D_0(ThO) = 868.6 \pm 5.0$		-21.5 ± 5.0

[a]K = Knudsen effusion; M = mass spectrometry.

bond distance in the ground-state molecule is known from a recent microwave spectroscopic study.[481] The harmonic vibrational frequency and other rotational and vibrational constants given in Table 67 were obtained from rotationally-resolved electronic emission spectra.[474] The IR measurements of ThO isolated in low-temperature inert gas matrices[212,458,459,482,483] revealed the matrix-shift effects on the fundamental frequency.

At present, 27 states (see Table 67) classified as belonging to Hund's coupling case "c" are rotationally analyzed, and 25 of them are arranged in the term scheme by Edvinsson *et al.*[474–479,484] The analyses by Behere *et al.*[485,486] are not convincing. The ground state of the ThO molecule is $X0_0^+$ ($X^1\Sigma_0^+$), as confirmed experimentally by the studies of the electronic spectrum of ThO[179,180,474–480] and also in the numerous theoretical calculations by Paulovic *et al.*,[487,488] Watanabe and Matsuoka,[489–491] Küchle *et al.*,[492] Kaledin *et al.*,[258] Marian *et al.*,[493] Seijo *et al.*,[494] Andrews *et al.*,[459] Goncharov and Heaven,[484] Buchachenko,[495] and Infante *et al.*[462]

Kaledin *et al.*[258] carried out the Ligand field calculations and assigned all 17 states observed till that time to the electron configurations $7s^2$, $6d7s$, $7s7p$, and $5f7s$, and calculated unobserved states of these and $6d^2$ configurations. The calculations showed that the lowest unobserved states are $\Omega = 3$ (probably W-state) and $\Omega = 2$ (probably lower state of the band at 5579 Å) of the $6d7s$ configuration. In the present work the statistical weights of predicted but unobserved states are attributed to the near-lying experimental states for simplification of the input data. The $5f6d$, $6d7p$, and $5f7p$ states are taken into account in the interval 25000 - 45000 cm^{-1}.

The derived standard entropy at room temperature is

$$S°(298.15\ K) = (240.071 \pm 0.03)\ J\,K^{-1}\,mol^{-1},$$

and the coefficients of the equations for the heat capacity are

$$C_p°/(J\,K^{-1}\,mol^{-1}) = 30.10768 + 13.9388 \times 10^{-3}(T/K) - 11.5407 \times 10^{-6}(T/K)^2 + 4.92964 \times 10^{-9}(T/K)^3 - 1.86435 \times 10^{5}(T/K)^{-2}$$

for the 298.15–1500 K range, and

$$C_p°/(J\,K^{-1}\,mol^{-1}) = -13.55069 + 44.5401 \times 10^{-3}(T/K) - 8.99062 \times 10^{-6}(T/K)^2 + 0.583589 \times 10^{-9}(T/K)^3 + 1.48587 \times 10^{7}(T/K)^{-2}$$

for the 1500–4000 K range.

6.3.2. Enthalpy of formation

The results of the determination of the enthalpy of formation of ThO(g) are presented in Table 68. The value is based on Knudsen effusion and mass spectrometric studies of ThO_2(cr) and Th(cr) + ThO_2(cr) system evaporation[468–470,472] and mass spectrometric measurements of isomolecular oxygen exchange reactions.[469,470,496,497] With the exception of the results of Ackermann *et al.*[468] and Shchukarev and Semenov,[472] all values of the enthalpy of formation of ThO(g) are in good agreement. The selected value is taken as a rounded average from all sources except the two mentioned papers:

$$\Delta_f H°(ThO,\ g,\ 298.15K) = -(21.5 \pm 5.0)\ kJ\,mol^{-1}.$$

This value corresponds to $D_0(ThO) = (868.6 + 5.0)$ kJ mol^{-1}.

6.4. PaO_2(g)

6.4.1. Heat capacity and entropy

The thermodynamic functions of PaO_2(g) in the standard state have been calculated using the data given in Table 69. Experimental data on molecular structure and spectra of PaO_2 are not available. Recently, the molecular geometry, vibrational properties and low-lying electronic states have been computed by Infante *et al.*,[462] and Kovács and Konings,[460] Kovács *et al.*,[498] and Kovács.[456] The calculations agree on a linear structure of $D_{\infty h}$ symmetry in the ground electronic state, similar to all AnO_2 molecules (except ThO_2 which is bent). The moment of inertia has been evaluated using the SO-CASPT2 bond distance of 181.6 pm of the linear molecule Infante *et al.*[462] The vibrational frequencies were taken from Ref. 460.

TABLE 69. The molecular parameters for $PaO_2(g)$

Parameter	Value
Ground electronic state	$^2\Sigma_{1/2g}$
Symmetry group	$D_{\infty h}$
Symmetry number, σ	2
I (g cm^2)[a]	17.52×10^{-39}
Vibrational frequencies (cm^{-1})[b]	852, 82(2), 899
Electronic states (cm^{-1})[c]	0(2), 3961(2), 8252(2), 8924(2), 11290(2), 14430(2), 15488(2), 27933(2), 28075(2), 28617(2), 29739(2), 29914(2)

[a]Moment of inertia.
[b]Numbers in parentheses represent degeneracy.
[c]Numbers in parentheses represent the statistical weights.

The electronic ground state of PaO_2 is $^2\Sigma_{1/2g}$.[462] The vertical excitation energies to the low-lying states were calculated recently at the SO-CASPT2 level by Kovács.[456] The derived standard entropy at room temperature is

$$S^\circ(298.15\ \mathrm{K}) = (279.711 \pm 5.0)\ \mathrm{J\,K^{-1}\,mol^{-1}}$$

and the coefficients of the equations for the heat capacity are

$$C_p^\circ/(\mathrm{J\,K^{-1}\,mol^{-1}}) = 35.4855 + 69.7567 \times 10^{-3}(\mathrm{T/K}) - 71.6190 \times 10^{-6}(\mathrm{T/K})^2 + 27.8213 \times 10^{-9}(\mathrm{T/K})^3 - 0.58791 \times 10^{5}(\mathrm{T/K})^{-2}$$

for the 298.15–900 K range, and

$$C_p^\circ/(\mathrm{J\,K^{-1}\,mol^{-1}}) = 57.8335 + 4.88325 \times 10^{-3}(\mathrm{T/K}) + 6.76950 \times 10^{-8}(\mathrm{T/K})^2 - 1.07986 \times 10^{-10}(\mathrm{T/K})^3 - 1.40951 \times 10^{6}(\mathrm{T/K})^{-2}$$

for the 900–4000 K range.

6.4.2. Enthalpy of formation

Kleinschmidt and Ward[499] have measured partial pressures of Pa(g), PaO(g), and PaO_2(g) above the Pa(l) + PaO_{2-y}(cr) two-phase system and the congruently vaporizing composition PaO_{2-x} (x and y values were not specified). From the latter data Kleinschmidt and Ward calculated the enthalpy of sublimation $\Delta_{sub}H^\circ(PaO_2, \mathrm{cr}, 298.15\ \mathrm{K}) = (595 \pm 7)$ kJ mol^{-1} as an average of the second- and third-law values (thermodynamic functions of all three gaseous species were estimated; however, molecular constants and numerical values of functions were not presented in the paper). The enthalpy of formation for PaO_2(g) was derived by Kleinschmidt and Ward assuming the enthalpy of formation of solid substoichiometric protactinium dioxide equal to that for PaO_2(cr). Following this suggestion, we obtain for the enthalpy of formation $\Delta_fH^\circ(298.15\ \mathrm{K}) = -(514 \pm 17)$ kJ mol^{-1}.

To acquire some insight into reliability of the enthalpy of formation of PaO_2(g) obtained with indeterminate thermodynamic functions, we calculated the third-law enthalpy of sublimation using the thermodynamic properties for a related neighbor compound, uranium dioxide, adopted in this work: $\Delta_{sub}H^\circ(298.15\ \mathrm{K}) = 619$ kJ mol^{-1}. The 24 kJ mol^{-1} difference between two enthalpy of sublimation values can serve as an estimation of possible uncertainty in the enthalpy of formation of PaO_2(g) found by Kleinschmidt and Ward.[499] On the basis of calculations performed, we select the value derived from the paper by Kleinschmidt and Ward[499] as a provisional recommendation, with an extended uncertainty range

$$\Delta_fH^\circ(PaO_2,\ \mathrm{g},\ 298.15) = -(514.0 \pm 30)\ \mathrm{kJ\,mol^{-1}}.$$

To the selected PaO_2(g) enthalpy of formation corresponds the atomization energy value $D_0(PaO_2) = (1576.0 \pm 30)$ kJ mol^{-1}.

6.5. PaO(g)

6.5.1. Heat capacity and entropy

The thermal functions of PaO(g) in the standard state have been calculated using the data given in Table 70. The molecular constants were estimated using the trends revealed in the spectral data of the lanthanide monoxides as there is no spectral data on the PaO molecule. The electronic structure is assumed to be analogous to that of PrO. The energies of the low-lying states taken from the PrO data are approximated to hundreds cm^{-1}.

The derived standard entropy at room temperature is

$$S^\circ(298.15\ \mathrm{K}) = (250.778 \pm 10.0)\ \mathrm{J\,K^{-1}\,mol^{-1}}$$

and the coefficients of the equations for the heat capacity are

$$C_p^\circ/(\mathrm{J\,K^{-1}\,mol^{-1}}) = 22.73634 + 18.0345 \times 10^{-3}(\mathrm{T/K}) + 28.8250 \times 10^{-6}(\mathrm{T/K})^2 - 20.1289 \times 10^{-9}(\mathrm{T/K})^3 + 2.78485 \times 10^{5}(\mathrm{T/K})^{-2}$$

TABLE 70. Molecular constants of $^{231}Pa^{16}O$(g)

No.	State	T_e	ω_e	$\omega_e x_e$	B_e	$\alpha_e 10^3$	$D_e 10^7$	r_e	p_i
		cm^{-1}						pm	
0	$X^8\Sigma$	0	845	2.69	0.335	1.5	2.1	183.5	2
1		200							2
2		2000							8
3		3000							12
4		4000							8
5		5500							18
6		7000							8
7		10 000							85
8		15 000							150
9		20 000							180
10		25 000							185
11		30 000							190
12		35 000							195
13		40 000							215

for the 298.15–1100 K range, and

$$C_p^\circ/(\mathrm{J\,K^{-1}\,mol^{-1}}) = 84.42095 - 29.0423 \times 10^{-3}(\mathrm{T/K}) + 8.96146 \times 10^{-6}(\mathrm{T/K})^2 - 0.876655 \times 10^{-9}(\mathrm{T/K})^3 - 1.36244 \times 10^{7}(\mathrm{T/K})^{-2}$$

for the 1100–4000 K range.

6.5.2. Enthalpy of formation

Kleinschmidt and Ward[499] have measured the partial pressures of Pa(g), PaO(g), and PaO_2(g) above the Pa(l) + PaO_{2-y}(cr) two-phase system and the congruently vaporizing composition PaO_{2-x} (x and y values were not specified). From this data, the third-law enthalpy of formation of PaO_2(g) was found as explained above and the enthalpy of formation of Pa(g). Thermodynamic functions of all three gaseous species were estimated. However, neither molecular constants nor numerical values of functions have been presented in the paper.

The vapor pressure measurements in the two-phase region Pa(l) + PaO_{2-y}(cr) resulted in the value $\Delta_f H^\circ(298.15\ \mathrm{K}) = -(18 \pm 13)\ \mathrm{kJ\ mol^{-1}}$ for the reaction

$$PaO_2(g) + Pa(g) = 2PaO(g).$$

Combining of this enthalpy of reaction with the thermochemical values for PaO_2(g) and Pa(g), leads to the enthalpy of formation of PaO(g):

$$\Delta_f H^\circ(\mathrm{PaO,\ g,\ 298.15\ K}) = (8 \pm 30)\ \mathrm{kJ\,mol^{-1}}$$

This value corresponds to $D_0(\mathrm{PaO}) = (789 \pm 30)\ \mathrm{kJ\ mol^{-1}}$. This is in good agreement with the value $(801 \pm 59)\ \mathrm{kJ\ mol^{-1}}$ estimated by Marçalo and Gibson[500] on the basis of gas phase oxidation reactions involving the ionised species and known ionisation energies.

6.6. UO_3(g)

6.6.1. Heat capacity and entropy

The thermodynamic functions of UO_3(g) in the standard state have been calculated using the data given in Table 71. Experimental data for the structure of free gaseous UO_3 molecule does not exist in the literature. From analysis of the infrared spectra of matrix-isolated UO_3 and its oxygen-18 isotopomers, Gabelnick *et al.*[501] and Green *et al.*[502] have determined a planar T-shaped (C_{2v}) geometry for the UO_3 molecule, with a O–U–O linear fragment. Three low-frequency and two stretching modes observed in matrix-isolated UO_3 are inconsistent with a pyramidal (C_{3v}) or planar (D_{3h}) geometry. The investigation of infrared spectra of UO_3 in solid argon by Hunt and Andrews[503] is in agreement with the data of Gabelnick *et al.*[501] and Green *et al.*[502] The results of *ab initio* calculations by Pyykkö *et al.*[504] support the symmetry assignment from experiments of Gabelnick *et al.*[501] and Green *et al.*,[502] and Hunt and Andrews[503]; it has been shown that D_{3h} structure is a saddle point, 49 kJ mol^{-1} above the C_{2v} minimum. Pyykkö *et al.*[504] obtained ∠O–U–O = 161°, instead of the linear O–U–O fragment found by Gabelnick *et al.*[501] and Green *et al.*[502] Similar results have been obtained later by Privalov *et al.*[505] using a similar theoretical (SCF) level. Quantum chemical calculations at the more reliable B3LYP DFT level were performed by Zhou *et al.*[506] for the geometry and vibrational frequencies. They retain the main structural features obtained by Pyykkö *et al.*[504] and by Privalov *et al.*,[505] but with reduced difference between the shorter U–O (in the O–U–O fragment) and the longer U–O′ bonds. The product of the principal moments of inertia of UO_3 (see Table 71) is calculated with the selected molecular constants r_e(U–O) = (181 ± 5) pm, r_e(U–O′) = (185.3 ± 5) pm, and ∠O–U–O = (158.8 ± 5)° from the DFT calculations by Zhou *et al.*[506]

Experimental data on vibrational frequencies were obtained by IR spectroscopy in argon matrices,[501–503] and in neon matrix.[506] With the exception of ν_1, all vibrational modes were observed. The accepted vibrational frequencies ν_2 and ν_4 (see Table 71) were taken from the IR spectra obtained by Zhou *et al.*[506] in an neon matrix, ensuring minimal matrix shift of the frequencies. The low frequencies ν_3, ν_5, and ν_6 were accepted from infrared spectra obtained by Green *et al.*[502] The unobserved ν_1 frequency is accepted as an average of two values obtained in calculations of Green *et al.*[502] and Zhou *et al.*[506]

The experimental and theoretical investigations of electronic spectra of UO_3 are unknown. X^1A_1 ground state is accepted for UO_3 molecule from calculations of Zhou *et al.*[506] This state corresponds to the closed shell configuration and no low-lying electronic states may be expected for this molecule. Additional electronic energy levels of UO_3 given in Table 71 are accepted to be the same as for the isoelectronic UO_2^{2+} from *ab initio* calculations by Pierloot *et al.*[464]

The derived standard entropy at room temperature is

$$S^\circ(298.15\ \mathrm{K}) = (310.648 \pm 3)\ \mathrm{J\,K^{-1}\,mol^{-1}}$$

and the coefficients of the equations for the heat capacity are

$$C_p^\circ/(\mathrm{J\,K^{-1}\,mol^{-1}}) = 46.69199 + 94.69427 \times 10^{-3}(\mathrm{T/K}) - 94.91701 \times 10^{-6}(\mathrm{T/K})^2 + 34.1585 \times 10^{-9}(\mathrm{T/K})^3 - 2.793843 \times 10^{5}(\mathrm{T/K})^{-2}$$

TABLE 71. The molecular parameters for UO_3(g)

Parameter	Value
Ground electronic state	X^1A_1
Symmetry group	C_{2v}
Symmetry number, σ	2
$I_A I_B I_C$ (g^3 cm^6)[a]	4210×10^{-117}
Vibrational frequencies (cm^{-1})	860, 760, 186, 865, 212, 152
Electronic states (cm^{-1})[b]	0(1), 17909(2), 18933(2), 22220(2), 23569(2), 24637(2)

[a]Product of moments of inertia.
[b]Numbers in parentheses represent the statistical weights.

for the 298.15–900 K range, and

$$C_p^\circ/(\mathrm{J\,K^{-1}\,mol^{-1}}) = 81.70962 + 2.009478 \times 10^{-3}(\mathrm{T/K}) - 1.110505 \times 10^{-6}(\mathrm{T/K})^2 + 0.2162739 \times 10^{-9}(\mathrm{T/K})^3 - 2.580355 \times 10^{6}(\mathrm{T/K})^{-2}$$

for the 900–4000 K range.

6.6.2. Enthalpy of formation

For determination of the enthalpy of formation of $UO_3(g)$ the results of transpiration and mass-spectrometric measurements were used. Transpiration experiments with U_3O_8 with oxygen employed as a carrier gas were carried out by Ackermann *et al.*,[507] Alexander,[508] Dharwadkar *et al.*,[509] Krikorian *et al.*,[510] and Alexander.[511] In all works except of Alexander,[511] pure oxygen at 1 atm was used as carrier gas; in the latter work dry air at 1 atm total pressure was employed. It was shown by Ackermann *et al.*[507] that variation of the oxygen pressure in the carrier gas established the oxygen-uranium ratio equal to three for the volatile uranium oxide molecule. By a comparison with entropies of sublimation of molybdenum and tungsten trioxides it was inferred that gaseous monomeric uranium trioxide is the principal species produced by the reaction of U_3O_8 with oxygen. To mention is that, unlike $(MoO_3)_n$ and $(WO_3)_n$, $(UO_3)_n$ gaseous associates till now are not detected in the U-O system.

Taking into account that the U_3O_8 phase has a homogeneity range, and that at high temperatures some deviation from stoichiometry develops, the process of transpiration has to be described according to the equation

$$\frac{1}{3}U_3O_{8-z}(\mathrm{cr}) + \frac{(1+z)}{6}O_2(\mathrm{g}) = UO_3(\mathrm{g}).$$

Detailed thermodynamic characterization of the U_3O_{8-z} phase was carried out by Ackermann and Chang.[512] The U_3O_{8-z} composition equilibrated at controlled temperature and oxygen pressure values was experimentally studied in this work. The equilibrium composition of the U_3O_{8-z} phase becomes progressively substoichiometric with increasing temperature at constant oxygen pressure. At the highest temperature of experiments, 1445 K, and the oxygen pressure 1 atm, the initial composition $UO_{2.667}$ changes to $UO_{2.636}$. In air, at an oxygen pressure ≈ 0.2 atm, the composition changes to ≈ 2.627. In spite of these findings, we adopted a simplified approach in the treatment of the transpiration data, without using information on deviation from stoichiometry. This approach is justified by a weak dependence of the free energy of formation of U_3O_{8-z}(cr) on the z value at constant temperature, as was shown by Ackermann and Chang.[512] This feature becomes apparent in absence of any systematic temperature drift of the third-law enthalpy values calculated during our assessment of experimental data for the reaction

$$\frac{1}{3}U_3O_8(\mathrm{cr}) + \frac{1}{6}O_2(\mathrm{g}) = UO_3(\mathrm{g}).$$

TABLE 72. The enthalpy of formation of $UO_3(g)$, in kJ mol^{-1}

Authors	Method[a]	T/K	$\Delta_f H°(298.15\ K)$
DeMaria *et al.*[513]	M	2200–2322	−769.9 ± 20
Ackermann *et al.*[507]	T	1200–1370	−799.5 ± 6
Alexander[508]	T	1415–1760	−792.8 ± 8
Pattoret *et al.*[515b]	M	2080-2500	−805.2 ± 15
Dharwadkar *et al.*[509]	T	1525–1675	−797.2 ± 6
Younés *et al.*[221]	M	1916–2336	−785.1 ± 15
Krikorian *et al.*[510]	T	1173–1573	−789.3 ± 10
Alexander[511]	T	1410–1815	−792.9 ± 8
Selected value:			−795.0 ± 10

[a]M = mass spectrometry; T = transpiration.
[b]Results of treatment of experimental data from Drowart *et al.*[514]

Results of all investigations are summarized in Table 72. All transpiration experiments gave very close results, an average of five works being -794.3 kJ mol^{-1}. Results of mass-spectrometric measurements[221,513–515] are close to this value but show more marked scatter. The most probable reason for that is the use of different estimates for the ionization cross sections of molecules and different estimates of fragmentation degree under electron impact, the latter being especially important for UO_3 molecules. We have derived the selected value for $UO_3(g)$ enthalpy of formation as a weighted average of all results shown in Table 72 (except the results of DeMaria *et al.*[513] with the largest deviation from the mean):

$$\Delta_f H^\circ(UO_3,\ \mathrm{g},\ 298.15) = (-795.0 \pm 10)\ \mathrm{kJ\,mol^{-1}}.$$

6.7. $UO_2(g)$

6.7.1. Heat capacity and entropy

The thermodynamic functions of $UO_2(g)$ in the standard state have been calculated using the data given in Table 73.

The investigations of infrared spectra of matrix-isolated uranium oxide species by Gabelnick *et al.*,[501] Lue *et al.*,[516] and Zhou *et al.*[506] strongly indicated a linear geometry of $D_{\infty h}$ symmetry for UO_2. This is consistent with the absence in spectra of peaks attributable to ν_1 symmetric stretch for the $U^{16}O_2$ and $U^{18}O_2$ isotopomers. Consistent with the experiment results, theoretical calculations for UO_2 predict a linear symmetric ground state.[460,506,517–519] There are no experimental data on U–O bond distances in $UO_2(g)$. The principal moment of inertia of UO_2 is calculated using $r_e(\mathrm{U–O}) = (178 \pm 5)$ pm. This value is an average of five bond distances (177, 178.4, 179.5, 176.4, and 180 pm) obtained from *ab initio* and DFT calculations;[506,517–520] it is close to $r(\mathrm{U\text{-}O}) = 179$ pm estimated by Green *et al.*[502] and the value derived on the basis of the frequency-bond distance relationship by Kovács and Konings[460] utilizing an estimated "gas-phase" value for the asymmetric stretching fundamental (vide infra).

Experimental data for ν_2 bending and ν_3 asymmetric vibrations were obtained by infared spectroscopy in noble gas matrices.[501,503,506] An interesting feature of UO_2 is the large red shift (about 130 cm^{-1}) in the asymmetric stretch found when replacing a neon matrix by an argon matrix. This feature has been explained and supported by computational and

TABLE 73. The molecular parameters for UO_2(g)

Parameter	Value
Ground electronic state	$^3\Phi_{2u}$
Symmetry group	$D_{\infty h}$
Symmetry number, σ	2
I (g cm^2)[a]	17.0×10^{-39}
Vibrational frequencies (cm^{-1})[b]	860, 120(2), 915
Electronic states (cm^{-1})[c]	0(2), 360(2), 2231(2), 2588(2), 5047(2), 6148(2), 6501(2), 7081(1), 7152(2), 7431(2), 7867(2), 8268(2), 8746(2), 10089(1), 10914(2), 11221(2), 11436(1), 11510(2), 12310(1), 12564(2), 12700(1), 12958(2), 13458(2), 13919(2), 14104(2), 14654(2), 14995(2), 15196(1), 15408(2), 15455(2), 15502(2), 15860(1), 15945(1), 16625(2), 16786(2), 16949(2), 17058(2), 17127(1), 17340(2), 17516(2), 17606(1), 18355(1), 18596(2), 18913(2), 19105(2), 19317(2), 19491(2), 21300(16), 24700(22), 30100(39)

[a]Moment of inertia.
[b]Numbers in parentheses represent the degeneracies.
[c]Numbers in parentheses represent the statistical weights.

further experimental studies[506,521,522] that the more polarizable argon and krypton stabilize the low-lying ^3H_g state becoming the electronic ground state in these matrices. In neon the $^3\Phi_{2u}$ state found in the gaseous phase remains the electronic ground state.

The adopted value for ν_3 asymmetric vibrational mode of $U^{16}O_2$ is taken from the investigation of the infrared spectra in solid neon matrix[506] because neon is substantially less polarizable than argon and matrix shifts in this case are substantially less. The value of infrared inactive ν_1 mode is calculated by normal coordinate analysis using the experimental data for ν_3 of UO_2. These values are in excellent agreement with the recent assessment by Kovács and Konings,[460] who derived the gas-phase ν_3 value by correction of 5 cm^{-1} for the matrix-shift of neon and deriving the ν_1 value from the frequency-bond distance relationship.

The bending frequency $\nu_2 = 120$ cm^{-1} was observed using the resonantly enhanced multiphoton ionization (REMPI) technique in the gas phase.[523] This bending frequency is lower than the values predicted by calculations. Majumdar *et al.*[517] reported ν_2 frequency values in the range of 149–222 cm^{-1} using three different computational methods. DFT calculation by Zhou *et al.*[506] yielded 138 cm^{-1}. The gas phase bending frequency is also lower than the $\Delta G_{1/2} = 225.2$ cm^{-1} reported for UO_2 isolated in a solid Ar matrix by Green *et al.*[502] In spite of this discrepancy, the experimental value $\nu_2 = 120$ cm^{-1} derived for free UO_2 molecule by Han *et al.*[523] is selected in our work for calculations of the UO_2(g) thermodynamic functions.

Thermodynamic functions have been calculated with the inclusion of data for a wide range of excited electronic states. Experimental data on the UO_2 excited energy levels are fragmentary.[523] Several theoretical studiesof UO_2 were carried out at relativistic post-Hartree-Fock levels, reporting electronic energy levels.[503,506,516–519,524] From these diverse studies we adopted the results by[518] obtained using the Dirac-Coulomb intermediate Hamiltonian multireference coupled cluster approach (DC-IHFSCC). This method is superior to the ones applied in the other papers by (i) using the coupled cluster methods to account for electron correlation; (ii) including the 6*d* orbitals, that have so far been left out of the active space; (iii) including spin-orbit coupling effects by utilizing the 4-component Dirac-Coulomb Hamiltonian. From this study we took the excited electronic states with the energy up to 19491 cm^{-1}. The energy levels above 19491 cm^{-1} were united in combined levels with summed up statistical weights (see Table 73).

The derived standard entropy at room temperature is

$$S^\circ(298.15\ \mathrm{K}) = (277.027 \pm 3.0)\ \mathrm{J\,K^{-1}\,mol^{-1}}$$

and the coefficients of the equations for the heat capacity are

$$C_p^\circ/(\mathrm{J\,K^{-1}\,mol^{-1}}) = 44.35744 + 37.63585 \times 10^{-3}(\mathrm{T/K}) - 23.15563 \times 10^{-6}(\mathrm{T/K})^2 + 5.50268 \times 10^{-9}(\mathrm{T/K})^3 - 0.7485093 \times 10^{5}(\mathrm{T/K})^{-2}$$

for the 298.15–1500 K range, and

$$C_p^\circ/(\mathrm{J\,K^{-1}\,mol^{-1}}) = 59.57586 + 5.392403 \times 10^{-3}(\mathrm{T/K}) + 0.09463181 \times 10^{-6}(\mathrm{T/K})^2 - 0.1028723 \times 10^{-9}(\mathrm{T/K})^3 - 6.319451 \times 10^{5}(\mathrm{T/K})^{-2}$$

for the 1500–4000 K range.

6.7.2. Enthalpy of formation

The enthalpy of formation for UO_2(g) is calculated from the enthalpy of sublimation of UO_2(cr). The results of the determination of the enthalpy of sublimation of UO_2 are listed in Table 74. Mass-spectrometric investigations (see e.g., Pattoret *et al.*[515]) have shown that the vapor over congruently vaporizing uranium dioxide of slightly substoichiometric composition mainly consists of UO_2 molecules; UO and UO_3 molecules are present in the vapor with the total pressure of several % of UO_2(g). To derive the selected value of the enthalpy of sublimation, the UO(g) and UO_3(g) pressures were subtracted from the total pressure of uranium-bearing species.

TABLE 74. The enthalpy of sublimation of UO_2(g), in kJ mol^{-1}

Authors	Method[a]	T/K	$\Delta_{sub}H°$(298.15 K)
Ackermann *et al.*[531]	K	1600–2200	628.2 ± 10
Ivanov *et al.*[532]	[b]	1930–2160	623.4 ± 10
Voronov *et al.*[525]	L	1723–2573	641.9 +10/-20
Ohse[533]	K	2278–2768	622.5 ± 10
Gorban' *et al.*[534]	K	1850–2600	618.9 ± 12
Pattoret *et al.*[515]	K+M	1890–2420	621.5 ± 8
Tetenbaum and Hunt[535]	T	2080–2705	629.3 ± 12
Reedy and Chasanov[536]	T	2615–3391	614.8 ± 18
Ackermann and Tetenbaum[526]	M	1540–2315	626.2 ± 15
Selected value:			622.9 ± 12

[a]K = Knudsen effusion; L= Langmuir; M = mass spectrometry ; T = transpiration.
[b]Vaporization from a cylindrical crucible; results of weight-loss measurements are close to those of Knudsen effusion.

The values of p(UO) + p(UO_3) were calculated using thermodynamic data from Gurvich *et al.*[180]; they amounted from ≈0.01 p(total) at 1600 K to ≈0.24 p(total) at 3400 K.

The selected enthalpy of sublimation of UO_2(g) is obtained from the data presented in Table 74 as a weighted average: $\Delta_{sub}H°(UO_2, cr, 298.15) = (622.9 \pm 12)$ kJ mol^{-1}. The data of Voronov *et al.*[525] and of Ackermann and Tetenbaum[526] were not taken into account. In the former work, free evaporation of a uranium dioxide rod heated by electric current might lead to serious errors due to nonuniformity of the rod temperature and to a non unity evaporation coefficient of the substance. The result obtained by Ackermann and Tetenbaum[526] is formally close to the selected value. However, independent sensitivity calibration of the mass-spectrometric equipment was not carried out. Instead, p(UO_2) at the temperature 2050 K was taken equal to an averaged value of all published data.

Combination of the enthalpy of sublimation with the selected enthalpy of formation of UO_2(cr) gives the selected value:

$$\Delta_f H°(UO_2,\ g,\ 298.15) = -(462.1 \pm 12)\ \text{kJ mol}^{-1}.$$

This value corresponds to an atomization energy $D_0(UO_2, g) = (1486.8 \pm 15)$ kJ mol^{-1}.

In the above analysis the data of laser heating experiments on uranium dioxide and other techniques (see, e.g., Ohse *et al.*,[527] Breitung and Reil,[528] Pflieger *et al.*[529]) were not discussed. We have preferred the data which allow unambiguous application of thermodynamics of ideal gases, and to avoid difficulties in extracting the UO_2(g) partial pressure from the total pressure values at very high temperatures (up to 8000 K), complicated by the possibility of substantial deviation of the vapor from the ideal gas behavior. Nevertheless, extrapolation of our results into the region of extremely high temperatures shows satisfactory agreement with experimental data and results derived from the equation of state of uranium dioxide summarized by Fink.[530]

6.8. UO(g)

6.8.1. Heat capacity and entropy

The thermal functions of UO(g) in the standard state have been calculated using the data given in Table 75.

Electronic spectra of the uranium monoxide molecule were studied by Kaledin *et al.*[537] in absorption and emission, by Heaven *et al.*[538] at the laser excitation of jet cooled UO ($U^{16}O$ and $U^{18}O$), by Kaledin *et al.*[539] Gurvich *et al.*[540] and Kaledin *et al.*[258] ($U^{16}O$ and $U^{18}O$) in fluorescence, and by Kaledin and Heaven[541] by means of resonantly enhanced two photon ionization with mass selected ion detection ($U^{16}O$ and $U^{18}O$). The studies gave information about the ground $X\Omega = 4$ ($v \leq 6$) state, 8 low-lying and about 20 higher-lying excited electronic states. The ground state $\Delta G_{1/2}$ value was found to be 882.351 cm^{-1}. In addition, the bond distance was determined to be 183.83 pm by Kaledin *et al.*[258]

Infrared spectra of matrix-isolated uranium oxide species were investigated by Carstens *et al.*,[542] Gabelnick *et al.*,[501] Abramowitz and Acquista,[543] Hunt and Andrews,[503] and Zhou *et al.*[506] The bands observed near 820 cm^{-1} in the Ar and Kr matrices were assigned to the UO molecule. Gabelnick *et al.*[501] determined also the anharmonicity value. In the IR spectrum of uranium oxides isolated in Ne matrix the band assigned to UO was that at 882.4 cm^{-1}.[506] Most quantum chemical calculations[257,460,506,544,545] gave harmonic vibrational frequency values between 845–858 taking into account the anharmonicity and matrix-shift effects in good agreement with the Ar-matrix value. Compared to these values, however, the frequency measured in the Ne matrix is too high.

TABLE 75. Molecular constants of $^{238}U^{16}O$(g)

No.	State	T_e	ω_e	$\omega_e x_e$	B_e	$\alpha_e 10^3$	$D_e 10^7$	r_e	p_i
		cm^{-1}						pm	
0[a]	$X(1)4$	0	888.5	3.1	0.3346	3.2	1.9[c]	183.3	2
1[a]	(2)4	294							2
2[a]	(1)3	652							2
3[a]	(1)2	958							2
4[a]	(1)5	1043							2
5[b]		1200							3
6[b]		1500							2
7[a]	(3)4	1574							2
8[a]	(3)3	1941							2
9[b]		2225							7[d]
10[b]		2450							3
11[b]		4500							7[e]
12[b]		5200							9
13[b]		5700							15
14[b]		7500							38
15[b]		10 000							116
16[b]		12 500							238
17[b]		15 000							375
18[b]		20 000							615
19[b]		25 000							1060
20[b]		30 000							1125
21[b]		35 000							1215
22[b]		40 000							1610
23[b]		45 000							1615

[a]Experimental state.
[b]Estimated state.

The reason of these discrepancies is that the ground state vibrational levels of gaseous UO are irregular. Kaledin and Kulikov,[546] Kaledin *et al.*[547] found that three lowest $\Omega = 4$ states were mutually perturbed. Kaledin *et al.*[258] performed deperturbation of these levels to determine adiabatic molecular constants. The deperturbed constant $\omega_e = 846.5\ \text{cm}^{-1}$ agreed well with the bands observed in IR spectra of matrix-isolated uranium oxides (taking into account the well-known red shift in matrices) and with theoretical predictions.

The information on the excited states is not sufficient for the calculation of the thermal functions. To estimate the electronic partition function we use the results of the Ligand field theory calculations by Kaledin *et al.*[258] All but one low-lying states were assigned to f^3s and the $\Omega = 4$ state with energy 294 cm^{-1} to f^2s^2 configurations. In the present work, the detailed experimental or calculated data on low-lying electronic states up to 7500 cm^{-1} are taken into account; the calculated data on the f^3s, f^2s^2, d^2s^2, f^2ds, f^3d, f^2d^2, f^2p^2, f^2ps, f^4, fds^2, and f^2dp electronic states in the range 7500–45 000 cm^{-1} are given in Table 75 as united terms with the fixed energies and the corresponding statistical weights.

The ground state molecular constants of UO selected for the thermal functions calculations (see Table 75) are estimated from the experimental value $\Delta G_{1/2} = 882.351\ \text{cm}^{-1}$ and the adopted value of the dissociation energy; these constants describe correctly the v = 0 and 1 levels. The simple presentation of the vibrational-rotational energy levels used in our program does not permit to recalculate levels from the deperturbed values of constants. Use of the deperturbed constants ($\omega_e = 846.5\ \text{cm}^{-1}$and $\omega_e x_e = 2.3\ \text{cm}^{-1}$) would lead to large underestimation of the v = 1 level energy. Moreover the vibrational constants assumed are close to the mean of those for three lowest $\Omega = 4$ states (846, 935, and 843 cm^{-1}), and with simplification used in our program that $Q^{(i)}_{vib,rot} = (p_i/p_X)Q^{(X)}_{vib,rot}$ our choice should give better results.

The derived standard entropy at room temperature is

$$S^\circ(298.15\ \text{K}) = (252.137 \pm 1.0)\ \text{J K}^{-1}\ \text{mol}^{-1}$$

and the coefficients of the equations for the heat capacity are

$$C_p^\circ/(\text{J K}^{-1}\ \text{mol}^{-1}) = 38.48092 + 33.0187 \times 10^{-3}(\text{T/K}) - 40.4519 \times 10^{-6}(\text{T/K})^2 + 14.7496 \times 10^{-9}(\text{T/K})^3 - 5.15534 \times 10^{5}(\text{T/K})^{-2}$$

for the 298.15–1300 K range, and

$$C_p^\circ/(\text{J K}^{-1}\ \text{mol}^{-1}) = 50.04939 - 18.1106 \times 10^{-3}(\text{T/K}) + 12.3772 \times 10^{-6}(\text{T/K})^2 - 1.71438 \times 10^{-9}(\text{T/K})^3 + 2.50947 \times 10^{6}(\text{T/K})^{-2}$$

for the 1300–4000 K range.

6.8.2. Enthalpy of formation

The results of determination of the enthalpy of formation of UO(g) are listed in Table 76. From many works published, the most reliable mass spectrometric data including reference species with well established thermodynamic properties were chosen for the calculation of the enthalpy of formation. The selected enthalpy of formation value

$$\Delta_f H^\circ(\text{UO, g, 298.15K}) = (21.4 \pm 10)\ \text{kJ mol}^{-1}$$

was obtained as a weighted average of results in Table 76 with reduced weights for the most divergent values from works of Ackermann *et al.*[548] and Steiger and Cater.[549] To the selected enthalpy of formation corresponds dissociation energy of UO (g) molecule $D_0(\text{UO}) = (758.9 \pm 10)\ \text{kJ mol}^{-1}$.

6.9. NpO_2(g)

6.9.1. Heat capacity and entropy

The thermodynamic functions of NpO_2(g) in the standard state in the temperature range 298.15–4000 K have been calculated using the data given in Table 77.

Experimental data on molecular structure and spectra of NpO_2 are unknown. Neptunium dioxide was studied by relativistic DFT calculations by Liao *et al.*[550] A linear structure of $D_{\infty h}$ symmetry was found for the $X^4\Sigma_g$ ground state and the first excited state ^4H_g lies only 0.01 eV (≈80 cm^{-1}) above $X^4\Sigma_g$ state. According to Liao *et al.*[550] this small difference leaves the identity of the ground state in some doubt. The recent study of Infante *et al.*[462] at the SO-CASPT2 level clarified the electronic ground state to be $^4H_{3.5g}$. This state has a linear structure too and an equilibrium bond distance of $r_e(\text{Np–O}) =$ 176.1 pm, which was adopted for computing the principal moment of inertia of NpO_2.

TABLE 76. The enthalpy of formation of UO(g), in kJ mol^{-1}

Authors	Method[a]	T/K	Reaction	$\Delta_r H^\circ$(298.15 K)	$\Delta_f H^\circ$(298.15 K)
Drowart *et al.*[514]	M	2130–2530	UO(g)+Si(g) = U(g) + SiO(g)	−36.6	20.7
	M	1700–2150	$\frac{1}{2}$U(l) + $\frac{1}{2}$$UO_2$(cr) = UO(g)	569.9	27.4
Coppens *et al.*[208]	M	2238–2315	UO(g) + B(g) = U(g) + BO(g)	−40.2	18.1
Ackermann *et al.*[548]	M	1540–2150	$\frac{1}{2}$U(l) + $\frac{1}{2}$$UO_2$(g) = UO(g)	582.0	39.5
Steiger and Cater[549]	M	2148–2369	U(g) + YO(g) = UO(g) + Y(g)	−51.0	12.4
Younés *et al.*[221]	M	1930–2280	UO(g) + La(g) = U(g) + LaO(g)	−32.8	14.8
Selected value:			$D_0(\text{UO}) = 758.9 \pm 10$		21.4 ± 10

[a]M = mass spectrometry.

TABLE 77. The molecular parameters for NpO_2(g)

Parameter	Value
Ground electronic state	$^4H_{3.5g}$
Symmetry group	$D_{\infty h}$
Symmetry number, σ	2
I (g cm^2)[a]	16.5×10^{-39}
Vibrational frequencies (cm^{-1})[b]	939, 185(2), 880
Electronic states (cm^{-1})[c]	0(2), 470(2), 783(2), 1126(2), 1284(2), 5875(2), 5902(2), 5992(2), 6084(2), 6461(2), 6676(2), 8760(2), 9050(2), 10386(2),10386(2), 10481(2), 10846(2), 10989(2), 11264(2), 11428(2), 12000(16), 14000(20), 16000(20), 18000(12), 20000(34), 22000(22), 24000(30), 26000(24)

[a]Moment of inertia.
[b]Numbers in parentheses represent the degeneracies.
[c]Numbers in parentheses represent the statistical weights.

Liao *et al.*[550] reported two vibrational frequencies for the $X^4\Sigma_g$ state, but in Table 77 we adopted the more reliable frequencies evaluated by Kovács and Konings[460] for the ground state. Liao *et al.*[550] published also a few spin-free relativistic excitation energies to low-lying electronic states of NpO_2. In the view of the failed electronic ground state at their SO-VWN-B-P level these data have a limited reliability. Instead, we used the recent SO-CASPT2 vertical excitation energies of Kovács[456] for the evaluation of the thermodynamic functions. We have supplemented the set of NpO_2 excited electron energy levels using the experimental data on the Np^{4+} energy levels in crystals. The information on the splitting of the Np^{4+} multiplets in the crystal fields of different symmetry is available from optical spectroscopy (e.g. Lahalle *et al.*[551]), and inelastic neutron scattering experiments (e.g. Kern *et al.*[552]; Fournier *et al.*[553]). We preferred to use the energy levels derived from the low-temperature absorption spectra of low-symmetry monoclinic NpF_4(cr), interpreted and supplemented with the results of crystal-field calculations by Carnall *et al.*[554] In the crystal field of monoclinic neptunium tetrafluoride with the C_2 site symmetry the Np^{4+} multiplets split into doublets, constituting a set of levels appropriate for modeling NpO_2(g) electron energy levels (see Table 77; the energy levels above 11428 cm^{-1} represent the results of combining of several close-lying levels).

The derived standard entropy at room temperature is:

$$S^\circ(298.15\ \mathrm{K}) = (269.892 \pm 6.0)\ \mathrm{J\,K^{-1}\,mol^{-1}}$$

and the coefficients of the equations for the heat capacity are

$$\begin{aligned} C_p^\circ/(\mathrm{J\,K^{-1}\,mol^{-1}}) = {} & 56.33269 + 40.03943 \times 10^{-3}(\mathrm{T/K}) \\ & - 54.9771 \times 10^{-6}(\mathrm{T/K})^2 \\ & + 23.02883 \times 10^{-9}(\mathrm{T/K})^3 \\ & - 0.732805 \times 10^{6}(\mathrm{T/K})^{-2} \end{aligned}$$

for the 298.15–1000 K range, and

$$\begin{aligned} C_p^\circ/(\mathrm{J\,K^{-1}\,mol^{-1}}) = {} & 68.29804 - 9.034032 \times 10^{-3}(\mathrm{T/K}) \\ & + 5.459315 \times 10^{-6}(\mathrm{T/K})^2 \\ & - 0.6628476 \times 10^{-9}(\mathrm{T/K})^3 \\ & - 3.700337 \times 10^{5}(\mathrm{T/K})^{-2} \end{aligned}$$

for the 1000–4000 K range.

6.9.2. Enthalpy of formation

The evaporation behavior of neptunium dioxide has been studied by Ackermann *et al.*[438] and Gotcu-Freis *et al.*[555] by mass-spectrometric measurements, showing that the gaseous oxides NpO_2 and NpO are the only neptunium-bearing species in the vapor, NpO_2 being the major constituent. In both studies it was argued that NpO_2 becomes substoichiometric at the high temperatures in vacuum. The extent of substoichiometry, unknown in the former and about O/Np = 1.94 at 2260 K in the latter grossly affects the partial pressure of NpO(g) but has an insignificant influence on the partial pressure of NpO_2(g). This was also confirmed by Gotcu-Freis *et al.*,[555] who studied the vaporisation of NpO_2 in a slight flow of oxygen gas, showing no significant difference with the measurement in vacuum. Bartscher and Sari[556] have shown that the O/Np ratio may reach 1.97 at 1900 K. However, no thermodynamic data for the substoichiometric compositions are available in the temperature range of the vaporization experiments and, hence, the condensed phase can only be treated as stoichiometric.

Ackermann *et al.*[438] also measured the weight loss of neptunium dioxide from 1852 to 2474 K by Knudsen effusion technique. They obtained the equation for the temperature dependence of the total vapor pressure log(P/atm) = −(31 100 ± 300)/T + (8.39 ± 0.13). Considering the equilibrium to be

$$NpO_2(\mathrm{cr}) = NpO_2(\mathrm{g})$$

we obtain from this equation the values $\Delta_{sub}H^\circ(NpO_2, \mathrm{cr}, 298.15) = (619.5 \pm 10)$ kJ mol^{-1} by third-law and (623.2 ± 12) kJ mol^{-1} by second-law analysis. The mean second-law enthalpy for NpO_2 in six mass-spectrometric experiments by Ackermann *et al.* (2100-2450 K), derived from the NpO_2^+ ion currents is $\Delta_{sub}H^\circ(NpO_2, \mathrm{cr}, 298.15) = (622 \pm 5)$ kJ mol^{-1}. The second-law values derived from the measurements in oxygen and vacuum by Gotcu-Freis *et al.*[555] are (650 ± 4) and (627 ± 7) kJ mol^{-1}, in fair agreement.

We select the mean value of the work of Ackermann *et al.*,[438] which is considered more precise, $\Delta_{sub}H^\circ(NpO_2, \mathrm{cr}, 298.15) = (621 \pm 20)$ kJ mol^{-1}, which yields, when combined with the enthalpy of formation of NpO_2(cr):

$$\Delta_f H^\circ(NpO_2,\ \mathrm{g},\ 298.15) = -(457 \pm 20)\ \mathrm{kJ\,mol^{-1}}.$$

TABLE 78. Molecular constants of $^{237}Np^{16}O(g)$

No.	State	T_e	ω_e	$\omega_e x_e$	B_e	$\alpha_e 10^3$	$D_e 10^7$	r_e	p_i
		cm^{-1}						pm	
0	$X0.5$	0	840	2.92	0.334	1.6	2.1	183.5	2
1		200							2
2		700							4
3		1200							6
4		2600							18
5		4000							24
6		5300							16
7		6600							32
8		8100							20
9		10 000							40
10		15 000							100
11		20 000							200
12		25 000							600
13		30 000							900
14		35 000							1000
15		40 000							1200

6.10. NpO(g)

6.10.1. Heat capacity and entropy

The thermal functions of NpO(g) in the standard state in the temperature range 298.15–4000 K have been calculated using the data given in Table 78. As there were no spectral data on the NpO molecule at the time of writing of this review, the molecular constants were estimated using the trends revealed in the spectral data of the lanthanide monoxides. The electronic structure of the NpO molecule is assumed to be analogous to that of PmO. The energies of the ground state $4f^4 6s$ superconfiguration rounded to 2 significant digits were taken from the Ligand field calculation by Dulick *et al.*,[247] the energies of the other states were estimated as for PmO with small correction due to a little difference between relative positions the atomic states of the $5f^4$ core. These values fairly well agree with the results of recent quantum chemical studies of Infante *et al.*[462] and Kovács and Konings.[460]

The derived standard entropy at room temperature is

$$S^\circ(298.15\ \mathrm{K}) = (253.060 \pm 4.0)\ \mathrm{J\,K^{-1}\,mol^{-1}}$$

and the coefficients of the equations for the heat capacity are

$$C_p^\circ/(\mathrm{J\,K^{-1}\,mol^{-1}}) = 40.73102 + 5.06903 \times 10^{-3}(\mathrm{T/K}) + 5.58835 \times 10^{-6}(\mathrm{T/K})^2 - 3.26062 \times 10^{-9}(\mathrm{T/K})^3 - 3.95105 \times 10^{5}(\mathrm{T/K})^{-2}$$

for the 298.15–1400 K range, and

$$C_p^\circ/(\mathrm{J\,K^{-1}\,mol^{-1}}) = 53.06105 + 1.44612 \times 10^{-3}(\mathrm{T/K}) - 1.95684 \times 10^{-6}(\mathrm{T/K})^2 + 0.362588 \times 10^{-9}(\mathrm{T/K})^3 - 5.12159 \times 10^{6}(\mathrm{T/K})^{-2}$$

for the 1400–4000 K range.

6.10.2. Enthalpy of formation

In their study of the vaporisation of neptunium dioxide, Ackermann *et al.*[557] have revealed nonstoichiometric and not single-mode NpO_2 evaporation, excluding the determination of thermodynamic properties of NpO(g) directly from the effusion measurements. The thermodynamic properties of the NpO(g) molecule were determined by Ackermann and Rauh[558] from mass-spectrometric measurements of equilibrium constants for two oxygen-exchange reactions, NpO (g) + La(g) = Np(g) + LaO(g) and Np(g) + YO(g) = NpO (g) + Y(g). Results of the calculation of the enthalpy of formation from both reactions are given in Table 79. For both reactions, the results are in good agreement.

The selected value

$$\Delta_f H^\circ(\mathrm{NpO,\ g,\ 298.15\ K}) = -(16.6 \pm 10.0)\ \mathrm{kJ\,mol^{-1}}$$

is taken as a weighted mean of two values obtained, with the weight of NpO(g) + La(g) equilibrium twice as that of Np(g) + YO(g), due to the higher statistical errors of the latter. To the selected enthalpy of formation corresponds the value of dissociation energy, $D_0(\mathrm{NpO}) = (734.8 \pm 10)\ \mathrm{kJ\,mol^{-1}}$. This is in good agreement with the value $(744 \pm 21)\ \mathrm{kJ\,mol^{-1}}$ estimated by Marçalo and Gibson[500] on the basis of gas phase oxidation reactions involving the ionised species and known ionisation energies.

6.11. PuO_3(g)

6.11.1. Heat capacity and entropy

The thermodynamic functions of PuO_3(g) in the standard state in the temperature range 298.15–4000 K have been calculated using the data given in Table 80. There are no experimental data on molecular structure and spectra of PuO_3. Gao *et al.*[559] and Zaitsevskii *et al.*[560] have calculated the molecular structure for PuO_3 by Hartree-Fock and DFT methods. The results of the calculations show that the PuO_3 molecule has a planar structure of C_{2v} symmetry similar to

TABLE 79. The enthalpy of formation of NpO(g), in kJ mol^{-1}

Authors	Method[a]	T/K	Reaction	$\Delta_r H^\circ$(298.15 K)	$\Delta_f H^\circ$(298.15 K)
Ackermann *et al.*[557]	M	1665–1972	NpO(g) + La(g) = Np(g) + LaO(g)	−63.6	−15.2
	M	1173–1972	Np(g) + YO(g) = NpO(g) + Y(g)	−22.0	−19.6
Selected value:			D_0(NpO) = 734.8 ± 10		−16.6 ± 10

[a]M = mass spectrometry.

TABLE 80. The molecular parameters for PuO_3(g)

Parameter	Value
Ground electronic state	$^7B_1$
Symmetry group	C_{2v}
Symmetry number, σ	2
$I_AI_BI_C$ (g^3 cm^6)[a]	4810×10^{-117}
Vibrational frequencies (cm^{-1})	840, 700, 170, 800, 190, 145
Electronic states (cm^{-1})[b]	0(2), 2530(1), 4870(2), 6700(2), 10334(1), 10983(2), 11225(1), 11651(2), 12326(1), 16713(1), 17737(2), 18565(2), 20029(1), 22703(2), 22889(2), 23022(2), 29710(2), 32198(2), 32759(1), 34080(2), 34702(2), 34982(2)

[a]Product of moments of inertia.
[b]Numbers in parentheses represent the statistical weights.

that of UO_3. The molecular constants of PuO_3 obtained by Gao *et al.*[559] seem unreliable being significantly different from the corresponding molecular constants of UO_3. The product of the principal moments of inertia of PuO_3 (see Table 80) is calculated using r_e(Pu–O) = (185 ± 5) pm (two equal bonds), r_e(Pu–O′) = (190 ± 5) pm, and ∠O–Pu–O = (160 ± 10)°. The bond distances are estimated by comparison with molecular constants of UO, UO_2, UO_3, PuO, and PuO_2. The value of the O–Pu–O bond angle is accepted to be equal to that in UO_3 molecule (see UO_3).

The vibrational frequencies calculated by Gao *et al.*,[559] which have too low values, were not used for estimation of vibrational contribution to the PuO_3 thermodynamic functions. The values of vibrational frequencies (see Table 80) are estimated by comparison with corresponding frequencies adopted for UO, UO_2, UO_3, PuO, and PuO_2 molecules.

According to the calculations of Gao *et al.*,[559] the PuO_3 molecule has a $^7B_1$ ground state. Experimental and theoretical investigations of PuO_3 excited electron energy levels are unknown. The energy levels of PuO_3 are assumed to be approximately the same as for the isoelectronic ion PuO_2^{2+} (configuration [Rn]$5f^2$). These energy levels have been obtained by Infante *et al.*[561] using the novel relativistic intermediate Hamiltonian Fock-space coupled-cluster method.

The derived standard entropy at room temperature is

$$S^\circ(298.15\ \mathrm{K}) = (319.450 \pm 4)\ \mathrm{J\,K^{-1}\,mol^{-1}}$$

and the coefficients of the equations for the heat capacity are

$$\begin{aligned} C_p^\circ/(\mathrm{J\,K^{-1}\,mol^{-1}}) = {} & 52.89593 + 75.46988 \times 10^{-3}(\mathrm{T/K}) \\ & - 71.42497 \times 10^{-6}(\mathrm{T/K})^2 \\ & + 25.87474 \times 10^{-9}(\mathrm{T/K})^3 \\ & - 3.753825 \times 10^{5}(\mathrm{T/K})^{-2} \end{aligned}$$

for the 298.15–900 K range, and

$$\begin{aligned} C_p^\circ/(\mathrm{J\,K^{-1}\,mol^{-1}}) = {} & 76.50587 + 8.903191 \times 10^{-3}(\mathrm{T/K}) \\ & - 1.504422 \times 10^{-6}(\mathrm{T/K})^2 \\ & + 0.07709618 \times 10^{-9}(\mathrm{T/K})^3 \\ & - 16.13944 \times 10^{5}(\mathrm{T/K})^{-2} \end{aligned}$$

for the 900 K–4000 K range.

6.11.2. Enthalpy of formation

Krikorian *et al.*[562] have carried out transpiration experiments to study the volatility of PuO_2(cr) in the presence of oxygen and steam. In experiments in presence of oxygen, it was expected, in analogy to uranium vaporisation behavior, that volatilization can occur to PuO_3(g) species, with insignificant amounts of the known plutonium oxide species, PuO(g) and PuO_2(g), according to known thermodynamic data. The existence of the PuO_3 vapor species was later confirmed by Ronchi *et al.*[563] who detected the molecule in mass-spectrometric study of vapors over plutonium dioxide. Krikorian *et al.*[562] used their data for 1 atm oxygen gas present (3 points, 1482 and 1483 K) to obtain the pressures of PuO_3(g) and to calculate equilibrium constants $K_p = p(PuO_3)/a(PuO_2)p(O_2)^{1/2}$), for the reaction

$$PuO_2(s) + \frac{1}{2}O_2(g) = PuO_3(g).$$

Taking the activity of PuO_2(cr) as unity, Krikorian *et al.*[562] obtained an average third-law value $\Delta_rH^\circ(298.15\ \mathrm{K}) = (493.0 \pm 4.9)\ \mathrm{kJ\ mol^{-1}}$ (uncertainty is standard deviation). We have recalculated the equilibium constants of the above reaction with the thermodynamic functions for PuO_2(cr) and PuO_3(g) adopted in this assessment: $\Delta_rH^\circ(298.15\ \mathrm{K}) = (488.2 \pm 15)\ \mathrm{kJ\ mol^{-1}}$, with an estimate of total uncertainty. Combining this value with the enthalpy of formation of PuO_2(cr) gives the adopted value

$$\Delta_fH^\circ(PuO_3,\ g\ ,298.15) = -(567.6 \pm 15)\ \mathrm{kJ\,mol^{-1}}.$$

6.12. PuO_2(g)

6.12.1. Heat capacity and entropy

The thermodynamic functions of PuO_2(g) in the standard state have been calculated using the data given in Table 81.

The only experimental study on the molecular properties of PuO_2 is the infrared spectroscopic measurement of PuO_2 isotopomers in Ar and Kr matrices by Green and Reedy.[564] The O-Pu-O bond angle of 180° was calculated from the measured isotope shift. This is consistent with the absence of peaks attributable to ν_1 for the case of $Pu^{16}O_2$ and $Pu^{18}O_2$. There are no experimental data on Pu–O bond distance in

TABLE 81. The molecular parameters for PuO_2(g)

Parameter	Value
Ground electronic state	$^5\Sigma_g$
Symmetry group	$D_{\infty h}$
Symmetry number, σ	2
I (g cm^2)[a]	18.0×10^{-39}
Vibrational frequencies (cm^{-1})[b]	792, 109(2), 828
Electronic states (cm^{-1})[c]	0(1), 420(1), 513(1), 516(1), 525(1), 1077(1), 1079(1), 1358(1), 1383(1), 4955(1), 5094(1), 5149(1), 5149(1), 5208(1), 5277(1), 5390(1), 5571(1), 5571(1), 5698(1),5698(1), 8700(3), 9400(12), 10400(3), 11700(5), 12500(11)

[a]Moment of inertia.
[b]Numbers in parentheses represent the degeneracies.
[c]Numbers in parentheses represent the statistical weights.

PuO_2. The principal moment of inertia of PuO_2 (see Table 81) is calculated using r_e(Pu–O) = (184 ± 5) pm. This value is an average of two bond distances (181.2 and 187.0 pm) obtained in *ab initio* calculations of Liao *et al.*[550] and Archibong and Ray.[565] The recent computational study by Zaitsevskii *et al.*[560] is in fair agreement.

The adopted values of PuO_2 vibrational frequencies (see Table 81) are taken from the *ab initio* calculation of Archibong and Ray[565] at the CCSD(T) level. The adopted values ν_1 and ν_3 correlate with the results of density-functional method including spin-orbit effects.

There are no experimental data on electronic spectra of PuO_2. Only results obtained in theoretical calculations are available. According to the calculations made by Liao *et al.*[550] and Archibong and Ray[565] the ground state of PuO_2 is $X^5\Sigma_g$. Both calculations do not take into consideration the effects of spin-orbit interactions and present limited numbers of energy levels. Therefore, these data were not used for the evaluation of electronic contribution to the PuO_2 thermodynamic functions. We preferred to use the energy levels derived from the low-temperature absorption spectra of low-symmetry monoclinic PuF_4(cr), interpreted and supplemented with the results of crystal-field calculations by Carnall *et al.*[554] In the crystal field of monoclinic plutonium tetrafluoride with the C_2 site symmetry the Pu^{4+} multiplets split into singlets. These singlet levels were used for modeling PuO_2(g) levels (see Table 81; the energy levels above 5698 cm^{-1} represent the results of combining of several close-lying levels).

The derived standard entropy at room temperature is

$$S^\circ(298.15\ \mathrm{K}) = (278.741 \pm 5)\ \mathrm{J\,K^{-1}\,mol^{-1}}$$

and the coefficients of the equations for the heat capacity are

$$\begin{aligned} C_p^\circ/(\mathrm{J\,K^{-1}\,mol^{-1}}) = {} & 70.29021 - 13.46001 \times 10^{-3}(\mathrm{T/K}) \\ & + 9.065878 \times 10^{-6}(\mathrm{T/K})^2 \\ & - 1.403447 \times 10^{-9}(\mathrm{T/K})^3 \\ & - 4.810746 \times 10^{5}(\mathrm{T/K})^{-2} \end{aligned}$$

for the 298.15–1500 K range, and

$$\begin{aligned} C_p^\circ/(\mathrm{J\,K^{-1}\,mol^{-1}}) = {} & 49.85911 + 11.46596 \times 10^{-3}(\mathrm{T/K}) \\ & - 1.472281 \times 10^{-6}(\mathrm{T/K})^2 \\ & - 8.555747 \times 10^{-12}(\mathrm{T/K})^3 \\ & + 41.20745 \times 10^{5}(\mathrm{T/K})^{-2} \end{aligned}$$

for the 1500–4000 K range.

6.12.2. Enthalpy of formation

Total pressure over substoichiometric plutonium dioxide was measured in several investigations. Phipps *et al.*[566] employed the Knudsen effusion method to measure total vapor pressures between 1593 and 2063 K; evaporation was performed from a tantalum effusion cell. The authors came to conclusion that "reduction of plutonium dioxide occurs when it is heated in vacuum in a tantalum oven." Mulford and Lamar[567] reported the vapor pressure data of plutonium dioxide measured at temperatures between 2000 and 2400 K using tungsten Knudsen effusion cells. The effusion rates were considerably less than those observed by Phipps. Pardue and Keller[568] measured the vapor pressure of plutonium dioxide in air, argon, and oxygen at temperatures between 1723 and 2048 K, using the transpiration technique. Total vapor pressures of PuO_{2-x} compositions were measured by Messier[569] gravimetrically with tungsten Knudsen cells from 2070 to 2380 K, and the vapor pressure equation for the composition approximating the congruent one, $PuO_{1.82}$, was obtained. According to mass-spectrometric measurements of Battles *et al.*,[570] PuO(g) is the major species in the vapor phase of the Pu_2O_3 + $PuO_{1.61}$ system. In nonreducing atmosphere PuO pressure significantly diminishes. Nevertheless, its part in the total vapor pressure must be taken into account in deriving PuO_2 pressure over PuO_{2-x} phase.

Extensive experimental study and detailed thermodynamic analysis of the vaporization of the substoichiometric plutonium dioxide has been carried out by Ackermann *et al.*[438] The rates of evaporation of plutonium-bearing species from the plutonium dioxide phase in the range 1646–2104 K were measured by the effusion method. The effusion cells were made from tungsten, rhenium, and tantalum. The results obtained with tungsten and rhenium cells were found to be in good agreement. The total pressure calculated under assumption of PuO_2(g) as the only vapor species was

approximated by the equation

$$\log(p/atm) = -(29620 \pm 280)/(T/K) + (7.50 \pm 0.15).$$

The above equation corresponds to evaporation of the $PuO_{1.92}$ composition, which did not significantly change during the time of measurements. Results obtained with the tantalum effusion cell, i.e. under reducing conditions, correspond to the univariant evaporation of the Pu_2O_3 + $PuO_{1.61}$ system. Using data on evaporation in reducing conditions, free energy of formation of PuO(g) was derived and the PuO(g) pressure over $PuO_{1.92}$ phase was calculated. Values of PuO_2(g) pressure evaluated in the 1600–2150 K range were fitted to the equation:

$$\log(p/atm) = -29640/(T/K) + 7.67.$$

In combination with auxiliary data from literature, this equation was used by Ackermann *et al.*[438] for deriving the linear equation for the standard free energy of formation of PuO_2(g), in cal/mol:

$$\Delta_f G^\circ(PuO_2,\ g) = -113100 + 4.35(T/K).$$

This equation is combined with Gibs energy of formation of PuO_2(cr) for calculation of the PuO_2(g) pressures over stoichiometric PuO_2(cr) in the 1650–2150 K temperature range. With the pressure values so obtained we find the third-law value for the enthalpy of sublimation: $\Delta_{sub}H^\circ$ (PuO_2, s, 298.15) = (643.9 ± 15) kJ mol^{-1}, yielding $\Delta_f H^\circ$ = −(411.9 ± 15) kJ mol^{-1}.

Gotcu-Freis *et al.*[571] studied the evaporation of PuO_2 by mass spectrometry in vacuum and in a flow of low pressure oxygen. Their results in vacuum are in excellent agreement with most of the earlier studies, including Ackermann *et al.*[438] They observed, however, a significant difference between the measurement in vacuum and oxygen, suggesting that the change in O/Pu ratio has an influence on the vaporisation equilibria. From the analysis of the measurements in oxygen considering the reaction PuO_2(cr) = PuO_2(g) they obtained $\Delta_{sub}H^\circ$(298.15 K) = (627 ± 7) kJ mol^{-1} by second law analysis and $\Delta_{sub}H^\circ$(298.15 K) = (616 ± 6) kJ mol^{-1} by third law analysis, corresponding to $\Delta_f H^\circ$ = −(428 ± 7) kJ mol^{-1} and $\Delta_f H^\circ$ = −(440 ± 6) kJ mol^{-1}, respectively.

The selected value of PuO_2(g) enthalpy of formation is

$$\Delta_f H^\circ(PuO_2,\ g,\ 298.15) = -(428 \pm 20)\ kJ\,mol^{-1}.$$

6.13. PuO(g)

6.13.1. Heat capacity and entropy

The thermal functions of PuO(g) in the standard state have been calculated using the data given in Table 82.

The electronic spectrum of PuO is unknown. The $Pu^{16}O$ and $Pu^{18}O$ molecules were identified in Ar and Kr matrices by Green and Reedy.[564] The ω_e and $\omega_e x_e$ values given in Table 82 were calculated using these data taking into account the matrix shift (~15 cm^{-1}) from the condition of converging the vibrational levels to the adopted dissociation limit. The internuclear distance r_e = (184 ± 2) pm is estimated from the comparison of the r_e values in the grounds states for the CeO and NdO with the same values for the ThO and UO molecules.

TABLE 82. Molecular constants of $^{239}Pu^{16}O$(g)

No.	State	T_e	ω_e	$\omega_e x_e$	B_e	$\alpha_e 10^3$	$D_e 10^7$	r_e	p_i
		cm^{-1}						pm	
0[a]	$X0^{-c}$	0	830	3.1	0.33	1.6	2.13	184.0	1
1[b]		150							2
2[b]		600							3
3[b]		900							2
4[b]		1300							2
5[b]		1600							6
6[b]		2000							2
7[b]		2400							8
8[b]		3100							22
9[b]		4200							20
10[b]		5000							4
11[b]		10 000							20
12[b]		15 700							120
13[b]		20 000							320
14[b]		25 000							340
15[b]		30 000							470
16[b]		35 000							1640
17[b]		40 000							2400

[a]Assumed to be analogous to SmO(g).
[b]Estimated state.

Ab initio studies by Gao *et al.*[572] and by Li and Xu[573] gave the ground state $X^5\Sigma^-$, r_e = 183 pm, ω_e = 781.15 cm^{-1}; the latter value disagreed with the matrix data. The electronic structure of PuO should be analogous to that of SmO, which has the $X0^-$ ground state and near lying Ω = 1 and Ω = 2 states. The ground state configuration of SmO is $4f^5 6s$, which does not generate a $^5\Sigma^-$ state. Details of the *Ab initio* studies by Gao *et al.*[572] and by Li and Xu[573] are not available. The information was taken from abstracts in Chemical Abstract, where the symmetry of the $X^5\Sigma^-$ may be indicated erroneously. The ω_e = (830 ± 10) cm^{-1} value, derived from the matrix spectra, is characteristic for the $5f^{N-1}7s$ configuration: see ω_e(UO) ~ 846 (deperturbed value). In the present work for PuO we assume the electronic structure analogous to that of SmO. The more dense structure (total statistical weight of excited states is equal to 5382) is due to the more close arrangement of the atomic states of the $5f^5$ core PuIV.

The derived standard entropy at room temperature is

$$S^\circ(298.15\ K) = (252.254 \pm 3.0)\ J\,K^{-1}\,mol^{-1}$$

and the coefficients of the equations for the heat capacity are

$$C_p^\circ/(J\,K^{-1}\,mol^{-1}) = 25.39529 + 54.2560 \times 10^{-3}(T/K) - 36.2549 \times 10^{-6}(T/K)^2 + 6.47005 \times 10^{-9}(T/K)^3 + 3.72127 \times 10^{4}(T/K)^{-2}$$

for the 298.15–1200 K range, and

$$C_p^\circ/(J\,K^{-1}\,mol^{-1}) = 78.23663 - 27.3687 \times 10^{-3}(T/K) + 6.77906 \times 10^{-6}(T/K)^2 - 0.440726 \times 10^{-9}(T/K)^3 - 7.04572 \times 10^{6}(T/K)^{-2}$$

for the 1200–4000 K range.

6.13.2. Enthalpy of formation

The total pressure of plutonium-bearing species in the process of evaporation of plutonium oxides in tantalum crucibles is well established and is interpreted to correspond to the equilibrium state in the $Pu_2O_3 + PuO_{1.61}$ two-phase system (see Cordfunke and Konings[8]). According to mass-spectrometric measurements by Battles *et al.*,[570] PuO(g) is the major species in the vapor phase of the $Pu_2O_3 + PuO_{1.61}$ system. For calculation of the enthalpy of formation of PuO(g) the data obtained by Ackermann *et al.*[438] were used. The data of this paper are in good agreement with the work of Phipps *et al.*,[566] as well as with data of Ohse,[574] Messier[569] and Gotcu-Freis *et al.*[571] The pressure of PuO_2(g) in the system is small and can be neglected. A small amount of Pu(g) was calculated from the equilibrium constant for the reaction

$$2.584PuO_{1.161}(cr) = 0.584Pu(g) + Pu_2O_3(cr)$$

After correcting the total pressure for Pu(g), the enthalpy of formation for PuO(g) was calculated from the enthalpy of reaction

$$2.773Pu_2O_3(cr) = PuO(g) + 4.545PuO_{1.161}(cr) + 1.522O_2(g).$$

The third-law value obtained, $\Delta_r H°(298.15\ K)$ = 560.4 kJ mol^{-1} leads to the enthalpy of formation PuO(g), which is selected:

$$\Delta_f^\circ(PuO,\ g,\ 298.15\ K) = -(51.7 \pm 15)\ kJ\,mol^{-1}$$

This value corresponds to the dissociation energy D_0(PuO) = (648.7 ± 30) kJ mol^{-1}. This is in good agreement with the value (658 ± 10) kJ mol^{-1} estimated by Marçalo and Gibson[500] on the basis of gas phase oxidation reactions involving the ionised species and known ionisation energies.

6.14. AmO_2(g)

6.14.1. Heat capacity and entropy

The thermodynamic functions of AmO_2(g) in the standard state have been calculated using the data given in Table 83. Experimental data on the molecular structure and spectra of AmO_2 are not available. Theoretical calculations of the structure of the AmO_2 molecule have been made by Kovács *et al.*,[575] which showed that the molecule has a linear $D_{\infty h}$ structure with r (Am-O) = 180.7 pm. The principal moment of inertia of AmO_2 is calculated from this value. Subsequent calculations by Infante *et al.*[462] provided details on the ground-state electronic structure of the molecule. The harmonic and anharmonic vibrational frequencies were calculated by Kovács and Konings[460] using DFT methods, while the most important low-lying electronic states were reported in Ref. 575.

TABLE 83. The molecular parameters for AmO_2(g)

Parameter	Value
Ground electronic state	$X^6\Pi_{2.5u}$
Symmetry group	$D_{\infty h}$
Symmetry number, σ	2
I (g cm^2)[a]	17.35×10^{-39}
Vibrational frequencies (cm^{-1})[b]	815, 105(2), 757
Electronic states (cm^{-1})[c]	0(2), 447(2), 5515(2), 6565(2), 12622(2), 15418(2), 15668(2), 16664(2), 18676(2), 21580(2), 21925(2), 22230(2), 22469(2), 23882(2), 25844(2), 28909(2)

[a]Moment of inertia.
[b]Numbers in parentheses represent degeneracy.
[c]Numbers in parentheses represent the statistical weights.

The derived standard entropy at room temperature is

$$S°(298.15\ K) = (279.464 \pm 6)\ J\,K^{-1}\,mol^{-1}$$

and the coefficients of the equations for the heat capacity are

$$\begin{aligned} C_p^\circ/(J\,K^{-1}\,mol^{-1}) = {} & 52.7906 + 26.0768 \times 10^{-3}(T/K) \\ & - 27.1648 \times 10^{-6}(T/K)^2 \\ & + 10.2293 \times 10^{-9}(T/K)^3 \\ & - 3.3759 \times 10^{5}(T/K)^{-2} \end{aligned}$$

for the 298.15–1000 K range, and

$$\begin{aligned} C_p^\circ/(J\,K^{-1}\,mol^{-1}) = {} & 54.4906 + 7.17462 \times 10^{-3}(T/K) \\ & - 1.46280 \times 10^{-6}(T/K)^2 \\ & + 0.13147 \times 10^{-9}(T/K)^3 \\ & + 1.2604 \times 10^{6}(T/K)^{-2} \end{aligned}$$

for the 1000–4000 K range.

6.14.2. Enthalpy of formation

Gotcu-Freis *et al.*[576] measured the vapor pressure over AmO_{2-x} identifying AmO(g), AmO_2(g) and Am(g) as vapor species. However, due to the strong change in the O/Am ratio of the samples during the measurements, it is not possible to derive the enthalpy of formation of AmO_2(g) from these results. Kovács *et al.*[575] calculated the dissociation energy of the reaction $AmO_2(g) = AmO(g) + O(g)$ as 6.03 eV (581.8 kJ mol^{-1}) using multiconfigurational relativistic quantum chemical methods. From these date we obtain

$$\Delta_f H°(AmO_2,\ g,\ 298.15) = -(514.0 \pm 30)\ kJ\,mol^{-1}.$$

6.15. AmO(g)

6.15.1. Heat capacity and entropy

Thermal functions of AmO(g) in the standard state have been calculated using the data given in Table 84.

As there is no spectral data on the AmO molecule, the estimates of the molecular constants given in that table are based on the trends revealed in the spectral data of the lanthanide monoxides. After the completion of this assessment, a few quantum chemical calculations on the molecular geometry, ro-vibrational properties and low-lying electronic states were published.[460,462,575] Infante *et al.*[462] confirmed the electronic ground state of AmO to be $X^8\Sigma_{1/2}$. But significant

TABLE 84. Molecular constants of $^{243}Am^{16}O(g)$

No.	State	T_e	ω_e	$\omega_e x_e$	B_e	$\alpha_e 10^3$	$D_e 10^7$	r_e	p_i
		cm^{-1}						pm	
0	$X^8\Sigma$	0	700	2.95	0.311	1.7	2.461	190	8
1		5000							8
2		6000							16
3		7000							18
4		8000							28
5		12 000							50
6		15 000							30
7		20 000							30
8		25 000							430
9		30 000							2200
10		35 000							2800
11		40 000							3000

differences were found for the other properties ($\omega_e = 872$ cm^{-1}, $r_e = 180.1$ pm).

The electronic structure of AmO is assumed to be analogous to that of EuO. Small difference in the recommended statistical weights of the united terms is due mainly to a little smaller accepted energy of $A^8\Sigma(f^6s)$ state.

Uncertainties of the calculated thermal functions are due mainly to the unknown energy of the first excited state $A^8\Sigma(f^6s)$. The minimum on the curve presented the variation of the actinide oxides dissociation energy with the charge on the actinide atoms implies that the ground state of the AmO molecule is $X^8\Sigma(f^7)$. However, as in case of EuO, the position of $A^8\Sigma(f^6s)$ is quite unclear.

The derived standard entropy at room temperature is

$$S^\circ(298.15\ \mathrm{K}) = (259.105 \pm 5.0)\ \mathrm{J\,K^{-1}\,mol^{-1}}$$

and the coefficients of the equations for the heat capacity are

$$\begin{aligned} C_p^\circ/(\mathrm{J\,K^{-1}\,mol^{-1}}) = {} & 34.31966 + 6.13074 \times 10^{-3}(\mathrm{T/K}) \\ & - 6.40603 \times 10^{-6}(\mathrm{T/K})^2 \\ & + 4.00456 \times 10^{-9}(\mathrm{T/K})^3 \\ & - 2.68922 \times 10^{5}(\mathrm{T/K})^{-2} \end{aligned}$$

for the 298.15–1500 K range, and

$$\begin{aligned} C_p^\circ/(\mathrm{J\,K^{-1}\,mol^{-1}}) = {} & -85.66885 + 111.574 \times 10^{-3}(\mathrm{T/K}) \\ & - 30.2584 \times 10^{-6}(\mathrm{T/K})^2 \\ & + 2.82855 \times 10^{-9}(\mathrm{T/K})^3 \\ & + 4.35180 \times 10^{7}(\mathrm{T/K})^{-2} \end{aligned}$$

for the 1500–4000 K range.

6.15.2. Enthalpy of formation

No experimental measurement of the enthalpy of formation AmO(g) is known. Estimates of this value can be made using estimates of the AmO dissociation energy. The dissociation energy of AmO(g) was estimated by Haire[577] as 550 kJ mol^{-1} using correlation between dissociation energy and promotion energy, needed for excitation of the free actinide atom in the ds^2 configuration. The estimation was confirmed by ICR mass spectrometric study of reactivity of americium oxide ions by Santos *et al.*[578] From the results of experiments, Santos *et al.* estimated $D_0(Am^+\text{-}O) = (580 \pm 50)$ kJ mol^{-1} and found the ionization energy IE(AmO) = (5.9 ± 0.2) eV, or (569 ± 20) kJ mol^{-1}. Later, Marçalo and Gibson[500] revised the former value to (560 ± 28) kJ mol^{-1}. The thermochemical relation

$$\mathrm{IE(AmO) + D_0(Am^+ - O) - IE(Am) = D_0(AmO)}$$

resulted in the value $D_0(AmO) = 553$ kJ mol^{-1}, in agreement with an previous estimate.[577] The rounded value $D_0(AmO) = (550 \pm 50)$ kJ mol^{-1} is selected in this work. It corresponds to

$$\Delta_f H^\circ(\mathrm{AmO,\ g,\ 298.15\ K}) = -(15 \pm 50)\ \mathrm{kJ\,mol^{-1}}.$$

6.16. CmO(g)

6.16.1. Heat capacity and entropy

Thermal functions of CmO(g) in the standard state have been calculated using the data given in Table 85. Since there is no molecular data on the CmO molecule, the molecular constants given in this table were estimated using the trends revealed in the spectral data of the lanthanide monoxides. The electronic structure is assumed to be analogous to that of GdO. The more dense structure (total statistical weight of excited states is estimated to be equal to 3209, that of GdO to 1834) is due to the more dense arrangement of the atomic states of the $5f^5$ core CmIV. After the completion of this assessment, a few quantum chemical calculations on the molecular geometry, ro-vibrational properties and low-lying electronic states were published.[460,462,575] Infante *et al.*[462] confirmed the electronic ground state of CmO to be $X^9\Sigma_4$. The other properties agree well with the estimated values.

The derived standard entropy at room temperature is

$$S^\circ(298.15\ \mathrm{K}) = (259.071 \pm 5.0)\ \mathrm{J\,K^{-1}\,mol^{-1}}$$

and the coefficients of the equations for the heat capacity are

$$\begin{aligned} C_p^\circ/(\mathrm{J\,K^{-1}\,mol^{-1}}) = {} & 26.15923 + 23.0665 \times 10^{-3}(\mathrm{T/K}) \\ & - 11.8949 \times 10^{-6}(\mathrm{T/K})^2 \\ & + 1.83564 \times 10^{-9}(\mathrm{T/K})^3 \\ & - 3.50044 \times 10^{4}(\mathrm{T/K})^{-2} \end{aligned}$$

TABLE 85. Molecular constants of $^{247}Cm^{16}O(g)$

No.	State	T_e	ω_e	$\omega_e x_e$	B_e	$\alpha_e 10^3$	$D_e 10^7$	r_e	p_i
		cm^{-1}						pm	
0	$X^9\Sigma_4$	0	840	2.88	0.333	1.5	2.1	183.5	9
1		2300							7
2		10 000							18
3		17 000							50
4		20 000							65
5		25 000							120
6		30 000							400
7		35 000							1040
8		40 000							1500

TABLE 86. Molecular constants and enthalpies of formation for AnO(g) (An = Bk–Lr)

	ω_e	$\omega_e x_e$[a]	B_e	$\alpha_e 10^3$[a]	r_e	$\Delta_r H(0\ K)$[b] Calculated	$\Delta_r H(0\ K)$[b] Estimated[c]	$\Delta_f H(298.15\ K)$
An	cm^{-1}				pm	kJ mol^{-1}		kJ mol^{-1}
BkO	833	3	0.333	1	183.5	537	598	543
CfO	833	3	0.338	1	182.2	479	498	485
EsO	825	3	0.338	1	182.2	403	460	409
FmO	735	3	0.327	1	185.0	369	443	373
MdO	673	3	0.311	1	189.8	341	418	349
NoO	650	3	0.303	1	192.3	290	268	295
LrO	756	3	0.319	1	187.1	583	665	588

[a]Estimated on the basis of the data of light actinide monoxides.
[b]Bond dissociation AnO → An + O.
[c]Haire.

for the 298.15–1200 K range, and

$$C_p^\circ/(J\,K^{-1}\,mol^{-1}) = 46.16751 - 3.81910 \times 10^{-3}(T/K) + 0.473867 \times 10^{-6}(T/K)^2 + 0.160603 \times 10^{-9}(T/K)^3 - 3.86840 \times 10^{6}(T/K)^{-2}$$

for the 1200–4000 K range.

6.16.2. Enthalpy of formation

Smith and Peterson[579] have performed Knudsen-effusion measurements of Cm_2O_3 evaporation in the temperature range 1800–2600 K. Curium oxide has been shown to vaporize congruently. Thermodynamic analysis has led to conclusion that the predominant vaporization process is the formation of CmO(g) and O(g). From the enthalpy of reaction

$$Cm_2O_3(cr) = 2CmO(g) + O(g),$$

an approximate value $D_0(CmO) = 728\ kJ\ mol^{-1}$ was obtained, using for the curium oxide the enthalpy of formation equal to that of Pu_2O_3. The mechanism of curium oxide vaporization proposed by Smith and Peterson obtained unambiguous confirmation in the mass spectrometric work on curium vaporization from a mixed curium-plutonium oxide by Hiernaut and Ronchi.[580] It was shown that CmO is the only effective vapor species.

With the thermodynamic functions of Cm_2O_3(cr) from this assessment, the enthalpy of the above reaction was calculated from the equilibrium constant for the temperature 1843 K: $\Delta_r H°(298.15\ K) = 1782.4\ kJ\ mol^{-1}$. This value yields

$$\Delta_f H°(CmO,\ g,\ 298.15\ K) = -(75.4 \pm 20)\ kJ\,mol^{-1}$$

which is selected. The corresponding dissociation energy is $D_0(CmO) = 708.3\ kJ\ mol^{-1}$. It should be mentioned that Gibson[261] estimated the value $D_0(CmO) = 709\ kJ\ mol^{-1}$ using the concept of a Ln or An atom into a d^2s configuration thought to be needed for formation of the Ln-O or An-O bond.

6.17. Computed data for AnO(g) and AnO_2(g) (An = Bk–Lr)

Presently, there is no experimental information available in the literature on the molecular parameters on the monoxides and dioxides of the late actinides. The bond distance and harmonic vibrational frequency of LrO has been computed by Cao and Dolg.[581] The DFT study by Kovács *et al.*[498] using relativistic effective core potentials on the actinides provided the first data on the molecular geometries and harmonic vibrational frequencies of the other mono- and dioxides. That study reported also the computed dissociation enthalpies and Gibbs free energies. The reliability of the latter data can be assumed to be comparable to that for the monoxides and dioxides of early actinides, where average deviations of ca. 20 kJ mol^{-1} for the dioxides and ca. 50 kJ mol^{-1} for the monoxides were obtained as compared with available experimental dissociation enthalpies at 298 K. The computed dissociation enthalpies are in good agreement with estimated data of Haire and Eyring[582] using the promotion model. The molecular constants and thermochemical properties are summarized in Tables 86 and 87.

TABLE 87. Molecular constants and enthalpies of formation for AnO_2(g) (An = Bk–Lr)

An	ν_i cm^{-1}	Symmetry	r_e pm	∠(O–An–O)	I_A kg m^2	$\Delta_r H(0\ K)$[a] kJ mol^{-1}	$\Delta_f H°(298.15\ K)$[b] kJ mol^{-1}
BkO_2	791, 152(2), 725	2	182.0	180.0	1.75952×10^{-45}	420	425
CfO_2	795, 183(2), 716	2	181.7	180.0	1.75303×10^{-45}	434	440
EsO_2	816, 213(2), 738	2	179.5	180.0	1.71066×10^{-45}	427	433
FmO_2	816, 221(2), 730	2	179.1	180.0	1.70399×10^{-45}	413	419
MdO_2	789, 182(2), 703	2	181.2	180.0	1.74408×10^{-45}	354	360
NoO_2	753, 170(2), 668	2	184.3	180.0	1.80437×10^{-45}	291	296
LrO_2	686, 114, 271	2	194.0	101.5	1.6373×10^{-135}[c]	330	334

[a]Bond dissociation AnO_2 → AnO + O.
[b]Neglecting electronic contributions.
[c]$I_A I_B I_C$ for LrO_2 in kg^3 m^6.

7. Discussion and Conclusions

7.1. Comparison to existing reviews

The current review has resulted in a consistent set of thermodynamic data for the lanthanide and actinide oxides as summarized in Tables 88 and 89. As mentioned in the Introduction, a number of critical reviews are existing but they are generally restricted to the condensed state and do not include the gaseous oxides, which were treated in detail in the present work. In 1968 Holley Jr. *et al.*[583] published a rather complete review of the crystalline lanthanide oxides based on the emerging literature on these intriguing compounds. The current work has extended that review by providing data in a wider temperature range, and including many more recent literature sources. Although the selected values are generally in good agreement with the recommendations of Holley Jr. *et al.*,[583] differences may exist, particularly for the high temperature properties. During the course of our work Zinkevich[584] published a comprehensive review of the thermodynamics of the rare earth sesquioxides. He also gave rather complete overview of the existing literature, and complemented the known values with estimated data. A major difference between that work and the current results is obvious for the (estimated) properties of the phase transitions. Whereas we have based the estimation of the entropies of transition and fusion on the high pressure work by Hoekstra,[116] the experimental study of Gd_2O_3 by Barkhatov *et al.*,[148] the recent DTA work on La_2O_3 by Ushakov and Navrotsky,[14] and the observation for the lanthanide trihalides that the sum of the transition and melting entropies is fairly constant throughout those series,[160] Zinkevich[584] based his estimations on the measured entropies of fusion for Y_2O_3 and Sc_2O_3 and a comparison to the relation between volume change upon melting and entropy of fusion for the lanthanide metals. These are two different approaches, resulting in somewhat different values, but in absence of experimental data it is difficult to validate them. We think that our approach based on comparison to the (ionic) halides is physically more justified than the comparison to metals.

A comprehensive review for the actinide oxides that treats the condensed and the gaseous phases in a consistent manner does not exist. In the frame of the thermodynamic database project OECD/NEA[430,585–587] the solid oxides of Th, U, Np, Pu and U were reviewed, but with emphasis on the room temperature values. No significant differences exist between our and that work, since the same sources of information have been used, with the exception of the high temperature heat capacity of the oxides of Np and Am for which new measurements were reported recently. The molecular species of some of the major actinides (Th, U, Pu) have been dealt with in general thermochemical assessments[395,588] but the information was very limited at the time those works were completed. Currently quantum chemical computational methods are a main source of molecular data for most actinide oxide species, and are considered to be more reliable than the assumed analogy with the better known lanthanide compounds. There are four comprehensive quantum chemical studies[460,518,575,589] used in this assessment which covered the mono- and dioxides of early actinides (Th, Pa, U, Np, Pu, Am, Cm), although in some cases the information appeared too late to be included. Quantum chemical studies are also used to calculate dissociation energies of early actinide oxides species and their cations (e.g., Averkiev *et al.*[589]). Although the errors of several experimental values are quite large, the comparison indicates that the quantum chemical computations are sufficiently reliable to predict trends among various actinides but also that the reliability of the computed values still does not reach that of the advanced gas-phase experimental methods.

7.2. Trends

The thermodynamic data from the present review allow evaluating the trends in the lanthanide and actinide series, as we have also done for the elements.[590] As is obvious from the sections for the individual compounds, these trends have been used extensively for checking consistency and estimating unknown properties. However, unlike the metals the comparison of the trends in the lanthanide and actinide oxides is less obvious because the electronic configurations are different. Whereas in the lanthanide series the compounds are predominantly trivalent due to the fact that the 4*f* electrons do not participate in the bonding (localised), this is not the general case for the actinide series. In the light actinides (Th-Am) the 5*f* electron are delocalised (itinerant) and as a result these elements show a wide range of valence states in compounds. The crystalline sesquioxides are formed in both series for a large number of elements and can be compared very well. The crystalline dioxides are typical for the actinides, and are stable only for a few lanthanides. In the gas phase the LnO and AnO molecules are stable for all elements, the AnO_2 and AnO_3 molecules are again typical for the light actinides (Th-Am). We will shortly discuss the trends in the crystalline sesquioxides, the crystalline dioxides and the gaseous monoxides.

7.2.1. The crystalline sesquioxides

A comparison of the polymorphism of the actinide with the lanthanide sesquioxides is made in Fig. 23, which is a remake of Fig. 4 showing the stability domain of the crystallographic modification not as a function of the position in the lanthanide series, but as a function of the ionic radius. It is evident that the actinide sesquioxides fall in the mid range where the polymorphism is most complex. It can be seen that the polymorphism of Cm_2O_3 fits reasonably well in the Ln_2O_3 series, but the other An_2O_3 compounds show discrepancies: the transition temperatures, particularly the melting points, are significantly lower.

Figure 24 shows the trend in the standard entropy of the sesquioxides, which can be well described as the sum of a lattice component, arising mainly from the vibrations of the

TABLE 88. Selected thermodynamic data of the solid and liquid phases of the lanthanide and actinide oxides

Phase	$\Delta_f H°(298.15)$ kJ mol^{-1}	$S°(298.15)$ J K^{-1} mol^{-1}	C_p/J K^{-1} mol^{-1} = A + B·T + C·T^2 + D·T^3 + E·T^{-2} A	B	C	D	E	Temperature range (K)	T_{trs}/K	$\Delta_{trs}H$ kJ mol^{-1}
La_2O_3(A)	−1791.6 ± 2.0	127.32 ± 0.84	120.6805	13.42414×10^{-3}			-14.13668×10^5	298–1800	2313 ± 30 (A → H)	23 ± 5
La_2O_3(H)	–	–	150	–	–	–	–	2313–2386	2386 ± 30 (H → X)	17 ± 5
La_2O_3(X)	–	–	150	–	–	–	–	2386–2577	2577 ± 15 (X → liq)	78 ± 10
La_2O_3(liq)	–	–	162	–	–	–	–	>2577		
CeO_2(cr)	−1090.4 ± 1.0	62.29 ± 0.07	74.4814	5.83682×10^{-3}	–	–	-1.29710×10^6	298–3083	3083 ± 50 (cr → liq)	69 ± 5
CeO_2(liq)	–	–	120	–	–	–	–	>3083		
Ce_2O_3(A)	−1799.8 ± 1.8	148.1 ± 0.4	113.736	28.4344×10^{-3}	–	–	-6.41205×10^5	298–2392	2392 ± 30 (A → H)	28 ± 8
Ce_2O_3(H)	–	–	145	–	–	–	–	2392–2406	2406 ± 30 (H → X)	19 ± 5
Ce_2O_3(X)	–	–	145	–	–	–	–	2406–2512	2512 ± 50 (X → liq)	85 ± 10
Ce_2O_3(liq)	–	–	157	–	–	–	–	>2512		
PrO_2(cr)	−959.1 ± 2.3	80.8 ± 2.0	72.9881	16.628×10^{-3}	—	–	-0.9990×10^5	298–663		
$PrO_{1.833}$(cr)	−944.6 ± 2.5	79.2 ± 2.0	68.4932	15.9207×10^{-3}	–	–	-8.0968×10^5	298–750		
Pr_2O_3(A)	−1809.9 ± 3.0	152.7 ± 0.3	121.6594	25.5611×10^{-3}	–	–	-9.8942×10^5	298–2310	2310 ± 30 (A → H)	28 ± 8
Pr_2O_3(H)	–	–	145	–	–	–	–	2310–2397	2397 ± 30 (H → X)	19 ± 5
Pr_2O_3(X)	–	–	145	–	–	–	–	2397–2583	2583 ± 25 (X → liq)	88 ± 10
Pr_2O_3(liq)	–	–	157	–	–	–	–	>2583		
Nd_2O_3(A)	−1806.9 ± 3.0	158.7 ± 1.0	117.1079	28.13655×10^{-3}	–	–	-1.25845×10^6	298–2379	2379 ± 30 (A → H)	29 ± 8
Nd_2O_3(H)	–	–	145	–	–	–	–	2379–2477	2477 ± 30 (H → X)	20 ± 5
Nd_2O_3(X)	–	–	145	–	–	–	–	2477–2577	2577 ± 15 (X → liq)	88 ± 10
Nd_2O_3(liq)	–	–	160	–	–	–	–	>2577		
Pm_2O_3(B)	−1811 ± 21	158 ± 5.0	122.9493	30.0141×10^{-3}	–	–	-1.85217×10^6	298–2013	2013 ± 20 (B → A)	6 ± 3
Pm_2O_3(A)	–	–	129.454	19.960×10^{-3}	–	–	–	2013–2407	2407 ± 20 (A → H)	31 ± 8
Pm_2O_3(H)	–	–	165	–	–	–	–	2407–2497	2497 ± 20 (H → X)	20 ± 5
Pm_2O_3(X)	–	–	165	–	–	–	–	2497–2592	2592 ± 30 (X → liq)	88 ± 10
Pm_2O_3(liq)	–	–	179	–	–	–	–	>2597		
Sm_2O_3(C)	−1826.8 ± 4.8		132.4358	18.7799×10^{-3}	–	–	-2.40860×10^6	298–900	~ 900 (C → B)	6 ± 3
Sm_2O_3(B)	−1823.0 ± 4.0	150.6 ± 0.3	129.7953	19.03114×10^{-3}	–	–	-1.86227×10^6	298–2190	2190 ± 20 (B → A)	7 ± 3
Sm_2O_3(A)	–	–	140	–	–	–	–	2190–2395	2395 ± 20 (A → H)	32 ± 8
Sm_2O_3(H)	–	–	165	–	–	–	–	2395–2533	2533 ± 30 (H → X)	20 ± 5
Sm_2O_3(X)	–	–	165	–	–	–	–	2533–2613	2613 ± 15 (X → liq)	89 ± 10
Sm_2O_3(liq)	–	–	179	–	–	–	–	>2613		
Eu_2O_3(C)	−1662.5 ± 6.0	135.4 ± 2.0	136.2978	14.9877×10^{-3}	–	–	-1.4993×10^6	298–1350	1350 ± 15 (C → B)	9 ± 3
Eu_2O_3(B)			133.3906	16.6443×10^{-3}	–	–	-1.42435×10^6	298–2327	2327 ± 30 (B → A)	7 ± 2
Eu_2O_3(A)	–	–	141	–	–	–	–	2327–2427	2427 ± 30 (A → H)	33 ± 8
Eu_2O_3(H)	–	–	144	–	–	–	–	2427–2557	2557 ± 30 (H → X)	21 ± 5
Eu_2O_3(X)	–	–	144	–	–	–	–	2557–2622	2622 ± 20 (X → liq)	89 ± 10
Eu_2O_3(liq)	–	–	156	–	–	–	–	>2622		
Eu_3O_4(cr)	−2276 ± 10	315 ± 4	182.464	26.108×10^{-3}	–	–		298–2000		
EuO(cr)	−593.2 ± 5.0	83.6 ± 0.8	46.5453	7.360×10^{-3}	–	–	1.42047×10^4	419–1724		
Gd_2O_3(C)	−1819.7 ± 3.6	150.6 ± 0.2	114.8086	17.2911×10^{-3}	–	–	-1.28397×10^6	298–2000	1473 (C → B)	9 ± 2
Gd_2O_3(B)			114.6104	15.2344×10^{-3}	–	–	-1.24917×10^6	298–2430	2430 ± 30 (B → A)	6.3 ± 3.3
Gd_2O_3(A)	–	–	142	–	–	–	–	2430–2470	2470 ± 30 (A → H)	34.7 ± 3.3
Gd_2O_3(H)	–	–	130	–	–	–	–	2470–2538	2538 ± 20 (H → X)	20 ± 5
Gd_2O_3(X)	–	–	130	–	–	–	–	2538–2693	2693 ± 15 (X → liq)	92 ± 10
Gd_2O_3(liq)	–	–	140	–	–	–	–	>2693		
TbO_2(cr)	−972.2 ± 5.0	86.9 ± 3.0	73.259	$13.2023 \cdot 10^{-3}$	–	–	1.0424×10^6	298–1400	Decomposition	
Tb_2O_3(C)	−1865.2 ± 6.0	159.2 ± 3.0	120.6682	22.17194×10^{-3}	–	–	-1.00261×10^6	298–1823	1823 ± 30 (C → B)	12 ± 4
Tb_2O_3(B)	–	–	152	–	–	–	–	1823–2488	2488 ± 30 (B → H)	55 ± 8
Tb_2O_3(H)	–	–	170	–	–	–	–	2488–2682	2682 ± 15 (H → liq)	83 ± 8
Tb_2O_3(liq)	–	–	182	–	–	–	–	>2682		
Dy_2O_3(C)	−1863.4 ± 5.0	149.8 ± 0.15	121.2302	15.27609×10^{-3}	–	–	-8.4580×10^5	298–2223	2223 ± 30 (C → B)	14 ± 5
Dy_2O_3(B)	–	–	155	–	–	–	–	2223–2488	2488 ± 30 (B → H)	55 ± 8
Dy_2O_3(H)	–	–	173	–	–	–	–	2488–2680	2680 ± 15 (H → liq)	83 ± 8
Dy_2O_3(liq)	–	–	188	–	–	–	–	>2680		
Ho_2O_3(C)	−1883.3 ± 8.2	156.38 ± 0.15	121.9340	10.11623×10^{-3}	–	–	-8.8628×10^5	298–2538	2538 ± 30 (C → B)	16 ± 5
Ho_2O_3(B)	–	–	135	–	–	–	–	2538–2588	2588 ± 30 (B → H)	57 ± 8
Ho_2O_3(H)	–	–	149	–	–	–	–	2588–2686	2686 ± 15 (H → liq)	83 ± 8
Ho_2O_3(liq)	–	–	162	–	–	–	–	>2686		
Er_2O_3(C)	−1900.1 ± 6.5	153.13 ± 0.15	123.2921	8.62245×10^{-3}	–	–	-1.54433×10^6	298–2538	2538 ± 30 (C → H)	25 ± 5
Er_2O_3(H)	–	–	162	–	–	–	–	2538–2690	2690 ± 15 (H → liq)	83 ± 5
Er_2O_3(liq)	–	–	176	–	–	–	–	>2690		
Tm_2O_3(C)	−1889.3 ± 5.7	139.7 ± 0.4	128.4322	5.23209×10^{-3}	–	–	-1.17891×10^6	298–2588	2588 ± 30 (C → H)	26 ± 5
Tm_2O_3(H)	–	–	155	–	–	–	–	2588–2682	2682 ± 30 (H → liq)	83 ± 8
Tm_2O_3(liq)	–	–	168	–	–	–	–	>2682		
Yb_2O_3(C)	−1814.5 ± 6.0	133.1 ± 0.3	130.6438	3.34628×10^{-3}	–	–	-1.44820×10^6	298–2687	2687 ± 20 (C → H)	27 ± 5
Yb_2O_3(H)	–	–	134	–	–	–	–	2687–2707	2707 ± 15 (H → liq)	84 ± 8
Yb_2O_3(liq)	–	–	146	–	–	–	–	>2707		
Lu_2O_3(cr)	−1877.0 ± 7.7	109.96 ± 0.13	122.4593	7.29001×10^{-3}	–	–	-2.03414×10^6	298–2762	2762 ± 15 (C → liq)	113 ± 10
Lu_2O_3(liq)	–	–	152	–	–	–	–	>2762		
ThO_2(cr)	−1226.4 ± 3.5	65.23 ± 0.20	55.9620	5.12579×10^{-2}	-3.68022×10^{-5}	9.2245×10^{-9}	-5.740310×10^5	298–3500	3651 ± 17 (cr → liq)	88 ± 6
ThO_2(liq)	–	–	61.8	–	–	–	–	>3651		
γ-UO_3(cr)	–1223.8 ± 2.0	96.11 ± 0.40	90.2284	1.385332×10^{-2}	–	–	-1.12795×10^6	416–886	–	–

TABLE 88. Selected thermodynamic data of the solid and liquid phases of the lanthanide and actinide oxides—Continued

Phase	$\Delta_f H°(298.15)$ kJ mol^{-1}	$S°(298.15)$ J K^{-1} mol^{-1}	C_p/J K^{-1} mol^{-1} = A + B·T + C·T^2 + D·T^3 + E·T^{-2} A	B	C	D	E	Temperature range (K)	T_{trs}/K	$\Delta_{trs}H$ kJ mol^{-1}
α-U_3O_8(cr)	−3574.8 ± 2.5	282.55 ± 0.50	279.267	2.7480×10^{-2}	–	–	-4.3116×10^6	298–483	483	0.171
			279.267	2.7480×10^{-2}	–	–	-4.3116×10^6	483–658	658	0.444
			279.267	2.7480×10^{-2}	–	–	-4.3116×10^6	658–850	850	0.942
			279.267	2.7480×10^{-2}	–	–	-4.3116×10^6	>850		
U_4O_9(cr)	−4512 ± 7	334.1 ± 0.7	319.163	4.9691×10^{-2}	–	–	-3.9602×10^6	298–1600	–	–
UO_2(cr)	−1085.0 ± 1.0	77.03 ± 0.20	66.7437	4.31393×10^{-2}	-3.5640×10^{-5}	1.1655×10^{-8}	-1.16863×10^6	298–3000	3120 ± 20 (cr → liq)	75 ± 3
UO_2(liq)	–	–	1365.4956	−0.85866	1.91305×10^{-4}	-1.41608×10^{-8}	–	3120–5000		
Np_2O_5(cr)	−2162.7 ± 9.3	186 ± 15	99.2	9.86×10^{-2}	–	–	–	298–750	~ 700 (decomposition)	–
NpO_2(cr)	−1078.5 ± 2.7	80.3 ± 0.4	64.7712	43.8574×10^{-3}	-35.0695×10^{-6}	13.1917×10^{-9}	-0.78932×10^6	298–3072	3072 ± 66 ± 50 (cr → liq)	70 ± 6
NpO_2(liq)	–	–	66	–	–	–	–	>3072		
PuO_2(cr)	−1055.8 ± 1.0	66.13 ± 0.30	35.2952	1.5225×10^{-1}	-1.27255×10^{-4}	3.6289×10^{-8}	-3.47593×10^5	298–3017	3017 ± 28 (cr → liq)	64 ± 6
PuO_2(liq)	–	–	70	–	–	–	–	>3017		
Pu_2O_3(A)	−1647 ± 10 ±	163.02 ± 0.65	130.6670	1.84357×10^{-2}	–	–	-1.70530×10^6	298–2300	2300 ± 50 (A → H)	32 ± 10
Pu_2O_3(H)	–	–	165	–	–	–	–	2300–2352	2352 ± 10 (H → liq)	71 ± 10
Pu_2O_3(liq)	–	–	179	–	–	–	–	>2352		
AmO_2(cr)	−932.2 ± 3.0	75.5 ± 3.0	78.9718	3.8365×10^{-3}	–	–	-1.40591×10^6	298–1200		-
Am_2O_3(A)	−1690.4 ± 7.9	134.2 ± 5.0	126.0084	8.0097×10^{-3}	–	–	-1.05752×10^6	298–2350	2350 ± 50 (A → H)	33 ± 10
Am_2O_3(H)	–	–	141	–	–	–	–	2350–2410	2410 ± 50 (H → X)	10 ± 10
Am_2O_3(X)	–	–	141	–	–	–	–	2410–2481	2481 ± 15 (X → liq)	74 ± 10
Am_2O_3(liq)	–	–	156	–	–	–	–	>2481		
Cm_2O_3(B)	−1684 ± 14	167 ± 5	123.532	1.4550×10^{-2}	–	–	-1.3489×10^6	298–1888	1888 ± 15 (B → A)	6 ± 3
Cm_2O_3(A)	–	–	142	–	–	–	–	1888–2273	2273 ± 20 (A → H)	32 ± 6
Cm_2O_3(H)	–	–	130	–	–	–	–	2273–2383	2383 ± 20 (H → X)	10 ± 5
Cm_2O_3(X)	–	–	130	–	–	–	–	2283–2543	2543 ± 15 (H → liq)	66 ± 10
Cm_2O_3(liq)	–	–	140	–	–	–	–	>2543		

ions in the crystal, and an excess component, which is of electronic origin:[127,445]

$$S° = S_{lat} + S_{exs}. \quad (9)$$

S_{exs} is zero for the lanthanide ions with empty (La, $4f^0$), half-filled (Gd, $4f^7$) and completely filled (Lu, $4f^{14}$) f subshell and thus the lattice contribution can be derived from the experimental data for the sesquioxides of those elements. From the results it is clear that the lattice entropy for the lanthanide sesquioxides falls in two groups, the hexagonal and monoclinic compounds in which the Ln coordination is sixfold, and the cubic compounds in which it is eightfold. This trend has been used in this work to estimate the values for those compounds for which experimental data are missing. Figure 25 shows how the trend for the lanthanides has been extrapolated to the actinides, based on the single experimental value for Pu_2O_3. A similar relation hold for the heat capacity.

The trends in the enthalpies of formation are shown in Fig. 26. We have plotted the hypothetical solution enthalpy of the reaction ($\Delta_{sln}H°(298.15\ K)$),

$$M_2O_3(cr) + 6H^+(aq) = 2M^{3+}(aq) + 3H_2O(l),$$

which represents in part the difference between the lattice enthalpy of the crystalline dioxide and the enthalpy of hydration of its ionic components. As it can be seen, the results for the lanthanide sesquioxides fall into three groups of isostructural compounds. The few results for the actinides parallel the trend for the lanthanide sesquioxides very well, irrespectively of the crystal structure, suggesting that the reaction enthalpy is about 20–30 kJ mol^{-1} less negative than the corresponding lanthanide sesquioxides. Morss *et al.*[454] suggested a relationship between the solution enthalpy of the above reaction and the molar volume (Fig. 27). That correlation captured well the three crystallographic groups of the lanthanide sesquioxides, but it did not show a correlation between the lanthanides and actinides, except for the B-type structure.

7.2.2. The crystalline dioxides

The melting point of the actinide dioxides have been revisited by Manara *et al.*[371,404,413] recently. These authors have shown that, due to the high oxygen potential of these compounds at temperatures close to melting, their observed melting/freezing behavior is not independent of the atmosphere in which fusion and solidification occur. Taking into account this important aspect, the trend established with these new data is shown in Fig. 28. It shows a strong decrease from ThO_2 to UO_2, after which the melting temperature decreases further in a moderate way. The absence of data for the melting of PaO_2 make it difficult the establish the trend in a more reliable way. A similar trend is observed

TABLE 89. Selected thermodynamic data of the gaseous lanthanide and actinide oxides

Phase	$\Delta_f H°(298.15)$ kJ mol^{-1}	$S°(298.15)$ J K^{-1} mol^{-1}	C_p/J K^{-1} mol^{-1} = A + B·T + C·T^2 + D·T^3 + E·T^{-2}					Temperature range (K)
			A	B	C	D	E	
LaO(g)	−119 ± 8	239.594 ± 0.03	28.0550	21.9688×10^{-3}	-1.925691×10^{-5}	6.083418×10^{-9}	-1.145313×10^{5}	298–1200
			41.7593	-6.82858×10^{-3}	3.529957×10^{-6}	-2.81197×10^{-10}	-1.500459×10^{6}	1200–4000
CeO(g)	−132 ± 8	246.099 ± 0.10	22.01944	55.5050×10^{-3}	-4.314095×10^{-5}	1.089494×10^{-8}	-4.23189×10^{4}	298–1300
			62.79967	-1.753953×10^{-2}	5.431417×10^{-6}	-4.87485×10^{-10}	-4.947446×10^{6}	1300–4000
CeO_2(g)	−538 ± 20	274.417 ± 3.0	37.7646	55.1209×10^{-3}	-57.1816×10^{-6}	21.2692×10^{-9}	-2.6077×10^{5}	298–900
			55.9864	2.90431×10^{-3}	-1.4361×10^{-6}	0.25254×10^{-9}	-1.11908×10^{6}	900–4000
PrO(g)	−145.5 ± 8	244.367 ± 0.05	22.98903	20.3103×10^{-3}	2.02961×10^{-5}	-1.46500×10^{-8}	2.72239×10^{5}	298–1200
			84.67666	-2.85857×10^{-2}	8.73036×10^{-6}	-8.4566×10^{-10}	-1.44324×10^{7}	1200–4000
NdO(g)	−120 ± 8	242.817 ± 0.05	−9.80368	1.88146×10^{-1}	-1.90285×10^{-4}	6.23079×10^{-8}	5.70945×10^{5}	298–1100
			57.65812	-9.784651×10^{-3}	2.76479×10^{-6}	-2.18778×10^{-10}	4.42849×10^{5}	1100–4000
PmO(g)	−145 ± 50	246.519 ± 2.0	31.6417	3.86653×10^{-2}	-3.03021×10^{-5}	8.45852×10^{-9}	-2.08747×10^{5}	298–1100
			50.9578	1.31663×10^{-3}	-1.57622×10^{-6}	2.82026×10^{-10}	-2.75930×10^{6}	1100–4000
SmO(g)	−105.3 ± 8	246.592 ± 0.10	28.65158	4.58171×10^{-2}	-3.44081×10^{-5}	7.99213×10^{-9}	-4.99673×10^{4}	298–1400
			70.5862	-2.02158×10^{-2}	4.6805×10^{-6}	-2.43006×10^{-10}	-6.91999×10^{6}	1400–4000
EuO(g)	−56.5 ± 8	253.419 ± 0.10	33.8838	7.70507×10^{-3}	-7.38219×10^{-6}	3.41476×10^{-9}	-2.52934×10^{5}	298–1700
			−79.4911	9.34647×10^{-2}	-2.23194×10^{-5}	1.8699×10^{-9}	5.2756×10^{7}	1700–4000
GdO(g)	−68.0 ± 8	253.495 ± 0.03	21.26451	4.09137×10^{-2}	-3.01655×10^{-5}	7.50616×10^{-9}	6.83276×10^{4}	298–1300
			51.77714	-1.00325×10^{-2}	2.57810×10^{-6}	-1.11668×10^{-10}	-4.8038×10^{6}	1300–4000
TbO(g)	−84.7 ± 10	245.758 ± 0.10	30.97785	3.25225×10^{-2}	-1.96568×10^{-5}	4.14576×10^{-9}	-1.18135×10^{4}	298–1400
			64.48191	-8.31957×10^{-3}	8.83659×10^{-7}	2.70508×10^{-11}	-1.04723×10^{7}	1400–4000
DyO(g)	−71 ± 20	242.208 ± 0.10	19.08366	6.17856×10^{-2}	-3.7479×10^{-5}	7.29509×10^{-9}	2.19805×10^{4}	298–1300
			68.49712	-1.13191×10^{-2}	1.99999×10^{-6}	-4.18797×10^{-11}	-8.39005×10^{6}	1300–4000
HoO(g)	−57.8 ± 10	244.590 ± 0.10	48.31232	7.68332×10^{-2}	-1.55715×10^{-4}	7.69567×10^{-8}	-1.57926×10^{6}	298–900
			43.11154	-5.49748×10^{-3}	3.07490×10^{-6}	-3.50566×10^{-10}	4.11955×10^{6}	900–4000
ErO(g)	−32.9 ± 8	256.473 ± 0.10	43.23815	-4.71231×10^{-3}	5.71735×10^{-7}	7.47515×10^{-10}	-2.55285×10^{5}	298–1300
			33.60868	3.85434×10^{-3}	-3.82306×10^{-7}	4.64068×10^{-11}	2.52559×10^{6}	1300–4000
TmO(g)	−13.6 ± 8	255.041 ± 0.15	37.63499	4.06981×10^{-3}	-2.78859×10^{-6}	9.67411×10^{-10}	-6.69507×10^{4}	298–1700
			39.61651	-5.40323×10^{-4}	1.26385×10^{-6}	-1.43823×10^{-10}	-1.21233×10^{6}	1700–4000
YbO(g)	−16 ± 10	238.521 ± 0.10	37.70801	4.85496×10^{-2}	-6.84668×10^{-5}	3.05227×10^{-8}	-7.73176×10^{5}	298–1000
			32.77497	1.73649×10^{-2}	-5.08804×10^{-6}	5.03717×10^{-10}	1.98479×10^{6}	1000–4000
LuO(g)	−3.4 ± 10	242.089 ± 0.03	28.20132	2.04184×10^{-2}	-1.65159×10^{-5}	4.71909×10^{-9}	-1.1965×10^{5}	298–1300
			40.19679	-7.58989×10^{-4}	-6.23484×10^{-7}	2.73798×10^{-10}	-2.75040×10^{6}	1300–4000
AcO(g)	−193 ± 20	245.545 ± 5.0	26.7681	26.00447×10^{-3}	-24.23966×10^{-6}	8.10964×10^{-9}	-0.83961×10^{5}	298–1100
			47.1310	-13.09869×10^{-3}	6.02184×10^{-6}	-0.628330×10^{-9}	-2.91011×10^{6}	1100–4000
ThO_2(g)	−435.6 ± 12.6	285.233 ± 2.0	36.83878	55.95391×10^{-3}	-56.33462×10^{-6}	20.31019×10^{-9}	-1.94049×10^{5}	298–900
			56.72155	2.163537×10^{-3}	-1.189606×10^{-6}	0.227498×10^{-9}	-1.407937×10^{6}	900–4000
ThO(g)	−21.5 ± 5.0	240.071 ± 0.03	30.10768	1.39388×10^{-2}	-1.15407×10^{-5}	4.92964×10^{-9}	-1.86435×10^{5}	298–1500
			−13.55069	4.45401×10^{-2}	-8.99062×10^{-6}	5.83589×10^{-10}	1.48587×10^{7}	1500–4000
PaO_2(g)	−514.0 ± 30	279.711 ± 5	35.4855	69.7567×10^{-3}	-71.6190×10^{-6}	27.8213×10^{-9}	-0.58791×10^{5}	298–900
			57.8335	4.88325×10^{-3}	6.76950×10^{-8}	-1.07986×10^{-10}	-1.40951×10^{6}	900–4000
PaO(g)	8 ± 30	250.778 ± 10	22.73634	1.80345×10^{-2}	2.8825×10^{-5}	-2.01289×10^{-8}	2.78485×10^{5}	298–1100
			84.42095	-2.90423×10^{-2}	8.96146×10^{-6}	-8.76655×10^{-10}	-1.36244×10^{7}	1100–4000
UO_3(g)	−795.0 ± 10	310.648 ± 3	46.69199	94.6942×10^{-3}	-94.91701×10^{-6}	34.1585×10^{-9}	-2.793843×10^{5}	298–900
			81.70962	2.009478×10^{-3}	-1.110505×10^{-6}	0.2162739×10^{-9}	-2.580355×10^{6}	900–4000
UO_2(g)	−462.1 ± 12	277.027 ± 3	44.35744	37.6358×10^{-3}	-23.15563×10^{-6}	5.50268×10^{-9}	-0.7485093×10^{5}	298–900
			59.57586	5.392403×10^{-3}	$0.09463181 \times 10^{-6}$	$-0.1028723 \times 10^{-9}$	-6.319451×10^{5}	900–4000
UO(g)	21.4 ± 10	252.137 ± 1.0	38.48092	3.30187×10^{-2}	-4.04519×10^{-5}	1.47496×10^{-8}	-5.15534×10^{5}	298–1300
			50.04939	-1.81106×10^{-2}	1.23772×10^{-5}	-1.71438×10^{-9}	2.50947×10^{6}	1300–4000
NpO_2(g)	−457 ± 20	269.892 ± 6	56.33269	40.03943×10^{-3}	-54.97771×10^{-6}	23.02883×10^{-9}	-7.32805×10^{5}	298–1000
			68.29804	-9.034032×10^{-3}	5.459315×10^{-6}	$-0.6628476 \times 10^{-9}$	-3.700337×10^{5}	1000–4000
NpO(g)	−16.6 ± 10	253.060 ± 4	40.73102	5.06903×10^{-3}	5.58835×10^{-6}	-3.26062×10^{-9}	-3.95105×10^{5}	298–1400
			53.06105	1.44612×10^{-3}	-1.95684×10^{-6}	3.62588×10^{-10}	-5.12159×10^{6}	1400–4000
PuO_3(g)	−567.6 ± 15	319.450 ± 4	52.89593	75.46988×10^{-3}	-71.42497×10^{-6}	25.87474×10^{-9}	-3.753825×10^{5}	298–900
			76.50587	8.903191×10^{-3}	-1.504422×10^{-6}	$0.07709618 \times 10^{-9}$	-16.13944×10^{5}	900–4000
PuO_2(g)	−428 ± 20	278.741 ± 5	70.29021	-13.46001×10^{-3}	9.065878×10^{-6}	-1.403447×10^{-9}	-4.810746×10^{5}	298–1500
			49.85911	11.46596×10^{-3}	-1.472281×10^{-6}	-8.55574×10^{-9}	41.20745×10^{5}	1500–4000
PuO(g)	−51.7 ± 15	252.254 ± 3	25.39529	5.42560×10^{-2}	-3.62549×10^{-5}	6.47005×10^{-12}	3.72127×10^{4}	298–1200
			78.23663	-2.73687×10^{-2}	6.77906×10^{-6}	-4.40726×10^{-10}	-7.04572×10^{6}	1200–4000
AmO_2(g)	−514.0 ± 30	279.464 ± 6	52.7906	26.0768×10^{-3}	-27.1648×10^{-6}	10.2293×10^{-9}	-3.3759×10^{5}	298–1000
			54.4906	7.17462×10^{-3}	-1.46280×10^{-6}	$+0.13147 \times 10^{-9}$	1.2604×10^{6}	1000–4000
AmO(g)	−15 ± 50	259.105 ± 5	34.31966	6.13074×10^{-3}	-6.40603×10^{-6}	4.00456×10^{-9}	-2.68922×10^{5}	298–1500
			−85.66885	1.11574×10^{-1}	-3.02584×10^{-5}	2.82855×10^{-9}	4.35180×10^{7}	1500–4000
CmO(g)	−75.4 ± 20	259.071 ± 5	26.15923	2.30665×10^{-2}	-1.18949×10^{-5}	1.83564×10^{-9}	-3.50044×10^{4}	298–1200
			46.16751	-3.81910×10^{-3}	4.73867×10^{-7}	1.60603×10^{-10}	-3.86840×10^{6}	1200–4000

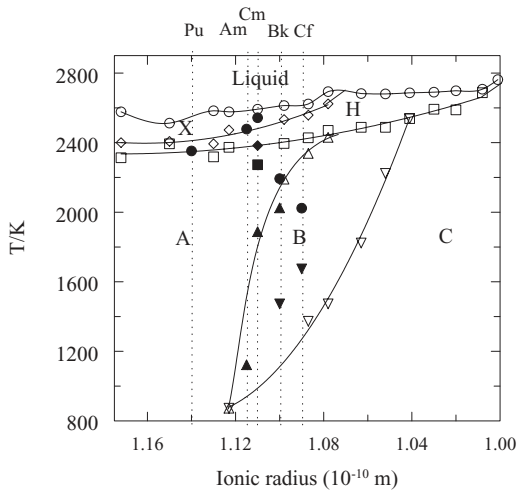

FIG. 23. The polymorphism of Ln_2O_3 (open symbols) and An_2O_3 (closed symbols) compounds expressed as ionic radius versus temperature. The lines are based on the transition temperatures in the lanthanide series (see Fig. 4).

in other properties of the actinide dioxides, for example the enthalpy of sublimation, which is a good measure for the cohesion energy in the crystalline lattice, shown also in the figure. It suggests a notable influence of the 5*f* electrons on the bonding. In the lanthanide series, only the melting point of CeO_2 is known, which is substantially lower than the value of ThO_2. Although it is somewhat speculative, this is consistent with the much lower enthalpy of sublimation compared to the actinide dioxides.

The trend in the standard entropies of the actinide dioxides is shown in Fig. 29, which has served as a basis for estimating the values for actinide and lanthanide dioxides for which no experimental data are existing. As is the case for the sesquioxides, the trend in the dioxides can be well described by Eq. (9), estimating the lattice from the measured compounds, in absence of experimental data for the $5f^7$ compound (CmO_2). Again, in the lanthanide series only the entropy of CeO_2 has been measured.

The trend in the enthalpy of formation of the solid dioxides has been evaluated from the hypothetical solution enthalpy of the reaction

$$MO_2(cr) + 4H^+(aq) = M^{4+}(aq) + 2H_2O(l).$$

As shown in Fig. 30, the trend for this quantity in the actinide series is quite regular, showing a slightly deviating value for NpO_2. The values for the three lanthanide dioxides indicate also a negative slope, but less than the actinides. Morss and Fuger[441] used a different approach by correlating the hypothetical solution enthalpy to the molar volume, as shown in Fig. 31. In this case the lanthanide and actinide dioxides plot almost on a straight line, with the exception of TbO_2 that deviates significantly. Morss and Fuger[441] suggested this may be due to an erroneous value of the enthalpy of formation of Tb^{4+}(aq), but this remains speculative.

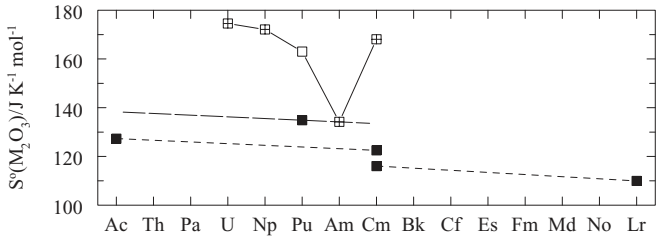

FIG. 25. The standard entropy S°(298.15 K) of the actinide sesquioxides; ■ the lattice entropies derived from experimental studies; □ experimental value for Pu_2O_3; ⊞ estimated values from the lattice and excess entropy as explained in the text.

7.2.3. The gaseous monoxides

The bond distances of LnO and AnO molecules are compared in Fig. 32. Those of the LnO molecules are mostly experimental data derived from rotationally resolved electronic spectra. In the AnO series only the bond distances of ThO and UO have been determined experimentally (derived similarly from electronic spectra), while the others were taken from the theoretical study of Kovács *et al.*,[498] except AcO, which was calculated at the same level of theory in the present study. The theoretical level used in the latter study (B3LYP/small-core relativistic pseudopotentials for the

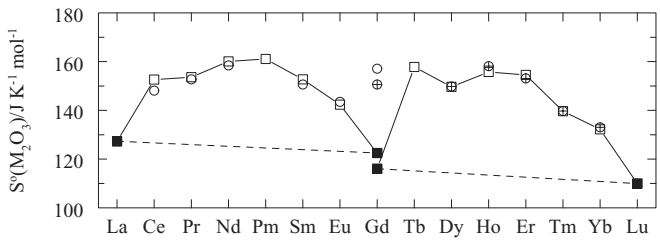

FIG. 24. The standard entropy S°(298.15 K) of the lanthanide sesquioxides; ■ the lattice entropies derived from experimental studies; □ values calculated from the lattice, represented by the dashed lines, and excess entropy as explained in the text; ○ and ⊕ the experimental values from the hexagonal/monoclinic and cubic compounds, respectively.

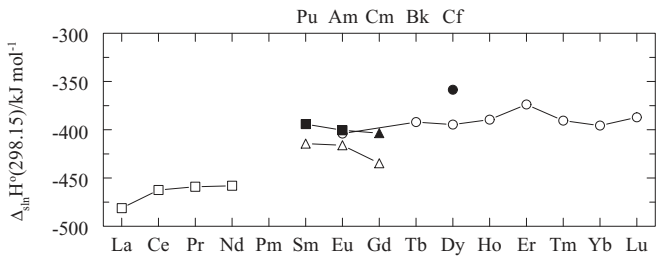

FIG. 26. The enthalpy of the hypothetical solution reaction for the lanthanide (open symbols) and actinide (closed symbols) sesquioxides, indicating the different structures (A-type, □; B-type, △; C-type, ○).

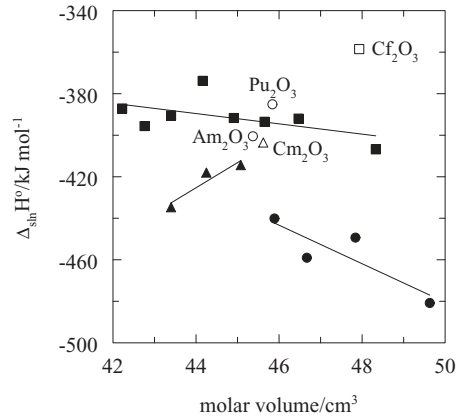

FIG. 27. The enthalpy of the hypothetical solution reaction for the lanthanide (open symbols) and actinide (closed symbols) sesquioxides as a function of the molar volume, indicating the different structures (A-type, □; B-type, △; C-type, ○).

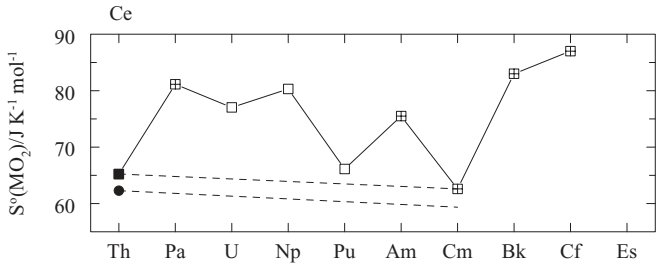

FIG. 29. The standard entropy S°(298.15 K) of the actinide dioxides; ■ the lattice entropies derived from experimental studies. The experimental value of CeO_2 is also shown (●).

actinides) gave bond distances in excellent agreement (within 0.7 pm) with the experimental data of ThO and UO. A similar reliability may be expected for the other actinide monoxides.

Both the LnO and AnO curves show a double-well shape with some distinct differences. These differences can be attributed to some special features in the electronic structures of the concerned molecules. The very long bond distance in AcO is in agreement with the covalent radii of Ac larger by about 1 pm with respect to that of Th.[591] According to our present population analysis the explanation of the longer bond of AcO may mainly be related to the unpaired 7*s* electron requiring larger space than the closed $7s^2$ subshell in ThO and PaO. On the other hand, in test computations of LaO, CeO, and PrO we observed an open $7s^1$ subshell.

The considerably longer bonds toward the end of the actinide row in FmO, MdO, and NoO have been ascribed to substantial population of antibonding orbitals in these molecules.[498] These antibonding orbitals consist of 5*f* An and 2*p* O atomic orbitals. Such low-energy antibonding orbitals are not present in the LnO molecules due to the core-like nature of 4*f* electrons. Therefore the partly filled 4*f* orbitals have no substantial influence on the bond distance of LnO molecules.

Population analysis shows that the bonding in EuO is significantly different from the other LnO molecules. While in those other LnO molecules the 4*f* orbitals have a core-like character (being lower-energy, not mixing with O orbitals and with each other), in EuO the 4*f* orbitals participate in the bonding orbitals with 2*p* orbitals of O, and even the non-bonding 4*f* orbitals are also high-energy (higher than the bonding orbitals). Hence they do not have a core-character in Eu.

The dissociation energy of the lanthanide and actinide monoxides are plotted in Fig. 33. The trends for the two series are very similar. It is generally accepted that this trend can be described by a base energy D_0 and an excess energy ΔE,[260,261,582] arising from the promotion energy from the ground state of the metal to the bonding state in the molecule.

7.3. Recommendations for further research

Our review has shown that the thermodynamic properties of the lanthanide sesquioxides are well established in the low to medium temperature range (up to about 2000 K). At high temperature, still large uncertainty exists about the properties of the H, X, and liquid phases. This is still *terra incognita* and is a challenging topic for further research. Additionally, the thermodynamic properties of the intermediate oxides of general formula Ln_nO_m that occur in several of the Ln-O systems, are still poorly known.

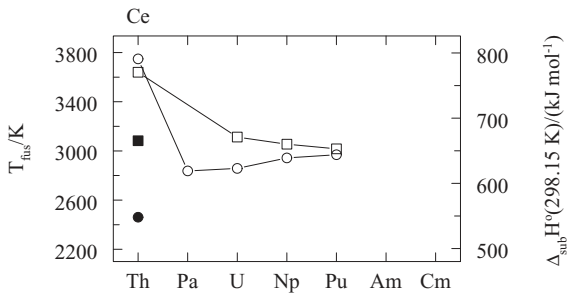

FIG. 28. The melting temperature (□, ■) and the enthalpies of sublimation (○,●) of the actinide (open symbols) and lanthanide (closed symbols) dioxides.

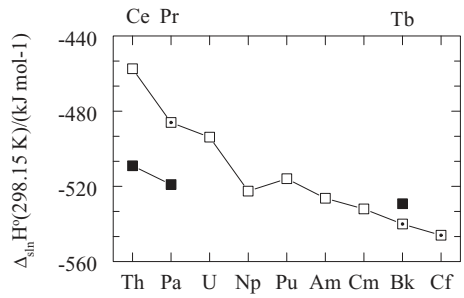

FIG. 30. The enthalpy of formation of the lanthanide(■) and actinide (□) dioxides.

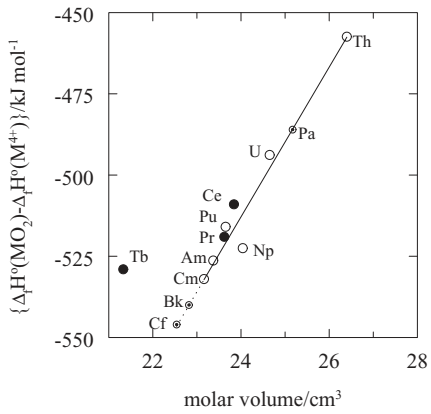

FIG. 31. The enthalpy of formation of the actinide dioxides as a function of molar volume.

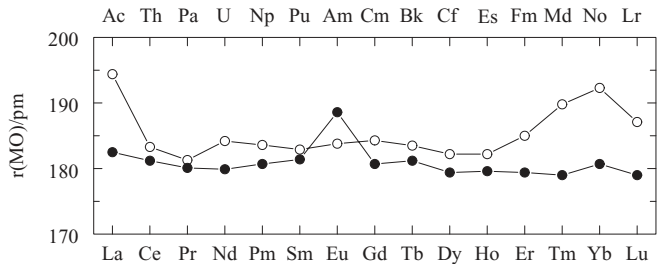

FIG. 32. The interatomic bond distance of the lanthanide (●) and actinide (○) gaseous monoxides.

For the actinide oxides the situation is somewhat different, also because the issue of radioactivity comes into play. The thermodynamic properties of the crystalline dioxides of the major actinides (ThO_2, UO_2, and PuO_2) are also well established, even at very high temperatures, though further studies of the liquid phase would be welcomed. The properties of the crystalline oxides of the minor actinides (Np, Am, Cm) are still poorly known, which is in part due to their highly radioactive nature. Some progress has been made in recent years, making use of measuring techniques suitable for small quantities, but also for these compounds high temperature studies are highly needed. Their properties are mainly based on estimation methods that need further validation. The other actinide oxides are hardly studied, and this will probably not change. Improvement for these compounds must be the result of better understanding of the trends in the actinide series.

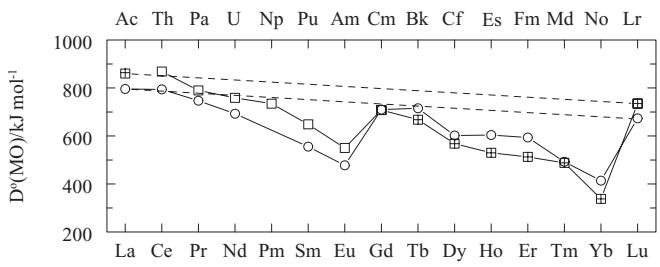

FIG. 33. The dissociation enthalpy of the lanthanide (○) and actinide (□) gaseous monoxides.

Acknowledgments

This article is the final result of a series of studies on the properties of the lanthanide and actinide oxides, and the authors would like acknowledge Eric Cordfunke, Lester Morss, Gerry Lander, and Christine Guéneau, who have helped and stimulated us in various ways with its realisation. Part of the work has been financed in the frame of the MetroFission project in the European Metrology Research Programme of EURAMET.

8. References

[1]F. H. Spedding and A. H. Daane, J. Metals **6**, 504 (1954).
[2]K. A. Gschneidner, Jr. and J. Capellen, J. Less-Common Met. **126**, xvii (1986).
[3]E. H. P. Cordfunke and R. J. M. Konings, Thermochim. Acta **375**, 65 (2001).
[4]J. D. Cox, D. D. Wagman, and V. A. Medvedev, *CODATA Key Values for Thermodynamics* (Hemisphere, New York, 1989).
[5]V. B. Parker, D. D. Wagman, and D. Garvin, Technical Report NBSIR 75, 1976.
[6]O. Söhnel and P. Novotný, *Densities of Aqueous Solutions of Inorganic Substances* (Elsevier, Amsterdam, 1985).
[7]L. V. Gurvich, I. V. Veyts, and C. B. Alcock, *Thermodynamic Properties of Individual Substances*, 4th ed. (Hemisphere Publishing Corp., New York, 1989), Vol. 1.
[8]E. H. P. Cordfunke and R. J. M. Konings, *Thermochemical Data for Reactor Materials and Fission Products* (North-Holland, Amsterdam, 1990).
[9]M. W. Chase Jr., *NIST-JANAF THERMOCHEMICAL TABLES*, Fourth Edition, Monograph 9 (Part I and Part II) (1998), 1963 pp. (1998).
[10]M. Foex and J. P. Traverse, Rev. Int. Hautes Temper. Refract. **3**, 429 (1966).
[11]L. M. Lopato, A. Shevchenko, A. E. Kushchevskii, and S. G. Tresvyatskii, Inorg. Mater. **10**, 1276 (1974).
[12]F. Wehner, E. T. Henig, and H. L. Lukas, Thermochim. Acta **20**, 17 (1977).
[13]A. V. Shevthenko and L. M. Lopato, Thermochim. Acta **93**, 537 (1985).
[14]S. V. Ushakov and A. Navrotsky, J. Mater. Res. **26**(7), 845 (2011).
[15]J. P. Coutures and M. H. Rand, Pure Appl. Chem. **61**, 1461 (1989).
[16]H. V. Wartenberg and H. J. Reusch, Z. Anorg. Allg. Chem. **207**, 1 (1932).
[17]W. A. Lambertson and F. H. Gunzel, Technical Report AECD-3465 (U.S. Atomic Energy Commission, 1952).
[18]T. Sata and R. Kiyoura, Bull. Tokyo Inst. Technol. **53**, 39 (1963).
[19]M. Foex, Rev. Int. Hautes Temp. Refract. **3**, 309 (1966).
[20]O. A. Mordovin, N. I. Timofeeva, and L. N. Drozdova, Izv. Akad. Nauk SSSR, Neorg. Mater. **3**, 187 (1967).
[21]T. Noguchi and M. Mizuno, Sol. Energy **11**, 90 (1967).
[22]S. G. Treswjatskii, L. M. Lopato, A. V. Schevtschenko, and A. E. Kutschevskii, Colloq. Int. C. N. R. S. **N205**, 247 (1972).
[23]J. P. Coutures, F. Verges, and M. Foex, Rev. Int. Hautes Temp. Refract. **12**, 181 (1975).
[24]M. Mizuno, T. Yamada, and T. Noguchi, Yogyo Kyokaishi **89**, 488 (1981).
[25]M. Yoshimura, S. Somiya, and T. Yamada, *Rare Earths* (The Rare Earth Society Japan, 1985), Vol. 6, p. 88.
[26]H. W. Goldstein, E. F. Neilson, and P. N. Walsh, J. Phys. Chem. **63**, 1445 (1959).
[27]E. G. King, W. W. Weller, and L. B. Pankratz, Technical Report RI-5857 (U.S. Bureau of Mines, 1961).
[28]B. H. Justice and E. F. Westrum, Jr., J. Phys. Chem. **67**, 339 (1963).
[29]J. O. Blomeke and W. T. Ziegler, J. Am. Chem. Soc. **73**, 5099 (1951).
[30]T. S. Yashvili, D. S. Tsagareishvili, and G. G. Gvelesiani, High Temp. **6**, 781 (1968).
[31]D. Sedmidubský, O. Beneš, and R. J. M. Konings, J. Chem. Thermodyn. **37**, 1098 (2005).
[32]R. Basili, A. El-Sharkawy, and S. Atalla, Rev. Int. Hautes Temp. Refract. **16**, 331 (1979).

[33]P. Wu and A. D. Pelton, J. Alloys Compd. **179**, 259 (1992).
[34]E. H. P. Cordfunke and R. J. M. Konings, Thermochim. Acta **375**, 51 (2001).
[35]E. J. Huber, Jr. and C. E. Holley, Jr., J. Am. Chem. Soc. **75**, 5645 (1953).
[36]R. L. Montgomery and T. D. Hubert, Technical Report USBM-RI-5525 (U.S. Bureau of Mines, 1959).
[37]G. C. Fitzgibbon, C. E. Holley, Jr., and I. Wadsö, J. Phys. Chem. **69**, 2464 (1965).
[38]G. G. Gvelesiani and T. S. Yashvili, Zh. Neorg. Khim. **12**, 3233 (1967).
[39]L. Merli, F. Rorif, and J. Fuger, Radiochim. Acta **82**, 3 (1998).
[40]W. Muthmann and L. Weis, Ann. **331**, 1 (1904).
[41]C. Matignon, Ann. Chim. Phys. **10**, 101 (1906).
[42]H. C. Kremers and R. G. Stevens, J. Am. Chem. Soc. **45**, 614 (1923).
[43]J. E. Moose and S. W. Parr, J. Am. Chem. Soc. **46**, 2656 (1924).
[44]G. Beck, Z. Anorg. Allg. Chem. **174**, 31 (1928).
[45]W. A. Roth, U. Wolf, and O. Fritz, Z. Electrochem. **46**, 42 (1940).
[46]H. von Wartenberg, Z. Anorg. Allg. Chem. **299**, 227 (1959).
[47]H. Oppermann, A. Morgenstern, and S. Ehrlich, Z. Naturforsch. B **52**, 1062 (1997).
[48]M. Zinkevich, D. Djurovic, and F. Aldinger, Solid State Ionics **177**, 989 (2006).
[49]A. M. Tshieryepanov and S. G. Trjesvyatsky, Mettallgyzdat M. 358 (1964).
[50]F. Trombe, cited by Noguchi and Mizino (1967).
[51]M. D. Watson, Ph.D. thesis (Georgia Institute of Technology, 1977).
[52]D. Manara, R. Böhler, K. Boboridis, L. Capriotti, A. Quaini, L. Luzzi, F. D. Bruycker, C. Guéneau, N. Dupin, and R. Konings, Procedia Chem. **7**, 505 (2012).
[53]Y. Du, M. Yashima, T. Koura, M. Kakihana, and M. Yoshimura, Scr. Metall. Mater. **31**, 327 (1994).
[54]O. Ruff, Z. Anorg. Allg. Chem. **82**, 373 (1913).
[55]H. von Wartenberg and W. Gurr, Z. Anorg. Chem. **196**, 374 (1930).
[56]E. F. Westrum, Jr. and A. F. Beale, Jr., J. Chem. Phys. **65**, 353 (1961).
[57]F. A. Kuznetsov, T. N. Rezukhina, and A. N. Golubenko, Russ. J. Phys. Chem. **34**, 1010 (1960).
[58]C. D. Pears, S. Oglesby, J. G. Allen, D. S. Neel, W. H. Mann, P. H. Rhodes, D. Osment, W. J. Barrett, S. G. Holder, and J. O. Honeycutt, Jr. *et al.*, Technical Report AASD-TDR-62-765 (Southern Research Institute, Birmingham, Alabama, 1963).
[59]R. Mezaki, E. W. Tilleux, T. F. Jambois, and J. L. Margrave, in *Proceedings of 3rd ASME Symposium on Advanced Thermophysical Property of Extreme Temperature, Lafayette, Indiana* (New York, 1965).
[60]T. S. Yashvili, D. S. Tsagareishvili, and G. G. Gvelesiani, Soobshch. Akad. Nauk Gruz. SSR **46**, 409 (1967).
[61]I. Riess, M. Ricken, and J. Nölting, J. Solid State Chem. **57**, 314 (1985).
[62]S. A. Gallagher and W. R. Dworzak, J. Am. Ceram. Soc. **68**, C206 (1985).
[63]F. B. Baker, E. J. Huber, Jr., C. E. Holley, Jr., and N. H. Krikorian, J. Chem. Thermodyn. **3**, 77 (1971).
[64]H. Hirsch, Trans. Electrochem. Soc. **20**, 57 (1911).
[65]L. B. Pankratz and K. K. Kelly, Technical Report RI-6248 (U.S. Bureau of Mines, 1963).
[66]W. W. Weller and E. G. King, Technical Report RI-6245 (U.S. Bureau of Mines, 1963).
[67]B. H. Justice and E. F. Westrum, Jr., J. Phys. Chem. **73**, 1959 (1969).
[68]M. E. Huntelaar, A. S. Booij, E. H. P. Cordfunke, R. R. van der Laan, A. C. G. van Genderen, and J. C. van Miltenburg, J. Chem. Thermodyn. **32**, 465 (2000).
[69]J. B. Gruber, B. H. Justice, E. F. Westrum, Jr., and B. Zandi, J. Chem. Thermodyn. **34**, 457 (2002).
[70]F. A. Kuznetsov, V. I. Belyi, T. N. Rezukhina, and Y. I. Gerasimov, Dokl. Acad. Nauk SSSR **139**, 1405 (1961).
[71]R. Venkata Krishnan and K. Nagarajan, Thermochim. Acta **440**, 141 (2006).
[72]A. D. Mah, Technical Report USBM-RI-5676 (U.S. Bureau of Mines, 1961).
[73]F. B. Baker and C. E. Holley, Jr., J. Chem. Eng. Data **13**, 405 (1968).
[74]R. L. Putnam, A. Navrotsky, E. H. P. Cordfunke, and M. E. Huntelaar, J. Chem. Thermodyn. **32**, 911 (2000).
[75]F. H. Spedding and C. F. Miller, J. Am. Chem. Soc. **74**, 4195 (1952).
[76]L. R. Morss and R. J. M. Konings, *Binary Rare Earth Oxides* (Springer-Verlag, 2004), Chap. 7, pp. 163–188.
[77]B. G. Hyde, E. E. Garver, U. E. Kuntz, and L. Eyring, J. Phys. Chem. **69**, 1667 (1965).
[78]S. V. Ushakov and A. Navtrosky, in *Proceedings of the 23rd Rare Earth Research Conference, Davis, USA* (Academic Press, San Diego, California, 2002).
[79]C. H. Gardiner, A. T. Boothroyd, P. Pattison, M. J. McKelvy, G. J. McIntyre, and S. J. S. Lister, Phys. Rev. B **70**, 024415 (2004).
[80]H. Eyring, R. Lohr, and B. B. Cunningham, J. Am. Chem. Soc. **74**, 1186 (1952).
[81]S. A. Gramsch and L. R. Morss, J. Chem. Thermodyn. **27**, 551 (1995).
[82]L. B. Pankratz, Techical Report RI-6781 (U.S. Bureau of Mines, 1966).
[83]R. P. Turcotte, J. M. Warmkessel, R. J. D. Tilley, and L. Eyring, J. Solid State Chem. **3**, 265 (1971).
[84]C. T. Stubblefield, H. Eick, and L. Eyring, J. Am. Chem. Soc. **78**, 3877 (1956).
[85]G. C. Fitzgibbon, E. J. Huber, Jr., and C. E. Holley, Jr., Rev. Chim. Miner. **10**, 29 (1973).
[86]C. T. Stubblefield, Rev. Sci. Instrum. **40**, 456 (1969).
[87]M. V. Kravchonskaya, A. K. Kuznetsov, P. A. Tckhonov, and E. K. Koehler, Ceram. Int. **4**, 14 (1978).
[88]F. A. Kuznetsov and T. N. Rezukhina, Russ. J. Phys. Chem. **36**, 729 (1962).
[89]I. Warshaw and R. Roy, J. Phys. Chem. **65**, 2048 (1961).
[90]L. B. Pankratz, E. G. King, and K. K. Kelly, Technical Report RI-6033 (U.S. Bureau of Mines, 1962).
[91]P. Aldebert and J. P. Traverse, Mater. Res. Bull. **14**, 303 (1979).
[92]R. L. Gibby, C. E. McNeilly, and T. D. Chikalla, J. Nucl. Mater. **34**, 299 (1970).
[93]M. Bober, H. U. Karow, and K. Muller, High Temp.-High Press. **12**, 161 (1980).
[94]J. P. Coutures, J. Am. Ceram. Soc. **68**, 105 (1985).
[95]T. P. Salikhov and V. V. Kan, Int. J. Thermophys. **20**, 1801 (1999).
[96]S. Stecura and W. J. Campbell, Technical Report RI-5847 (U.S. Bureau of Mines, 1961).
[97]C. Matignon, Ann. Chim. Phys. **10**, 101 (1907).
[98]E. J. Huber, Jr. and C. E. Holley, Jr., J. Am. Chem. Soc. **74**, 5530 (1952).
[99]F. H. Spedding, K. Gschneidner, Jr., and A. H. Daane, Trans. Metall. Soc. AIME **215**, 192 (1959).
[100]G. C. Fitzgibbon, D. Pavone, and C. E. Holley, Jr., J. Chem. Eng. Data **13**, 547 (1968).
[101]T. S. Yashvili and G. G. Gvelesiani, Russ. J. Phys. Chem. **45**, 551 (1971).
[102]L. R. Morss, C. M. Haar, and S. Mroczkowski, J. Chem. Thermodyn. **21**, 1079 (1989).
[103]A. A. Popova and A. S. Monaenkova, Zh. Fiz. Khim. **63**, 2340 (1989).
[104]C. Hennig and H. Oppermann, Z. Naturforsch. B **53**, 175 (1998).
[105]J. M. Stuve, Technical Report USBM-RI-6697 (U.S. Bureau of Mines, 1965).
[106]L. A. Tiflova, Ph.D. thesis, Moscow State University, 1990.
[107]T. D. Chikalla, C. E. McNeilly, J. L. Bates, and J. J. Rasmussen, (1972), Vol. **N205**, p. 351.
[108]R. L. Gibby, T. D. Chikalla, R. P. Nelson, and C. E. McNeilly, Technical Report BNWL-SA-1796-A (Battelle Memorial Institute, 1968).
[109]R. J. M. Konings, J. Nucl. Mater. **301**, 223 (2002).
[110]T. D. Chikalla, C. E. McNeilly, and F. P. Roberts, J. Am. Ceram. Soc. **55**, 428 (1972).
[111]L. G. Wisnyi and S. Pijanowski, Technical Report TID 7530 (U.S. Atomic Energy Commission, 1957).
[112]C. E. Curtis and J. R. Johnson, J. Am. Ceram. Soc. **40**, 15 (1957).
[113]B. H. Justice and E. F. Westrum, Jr., J. Phys. Chem. **67**, 345 (1963).
[114]L. B. Pankratz, E. G. King, and K. K. Kelley, Technical Report RI 6033 (U.S. Bureau of Mines, 1961).
[115]G. G. Gvelesiani, D. S. Tsagareishvili, and T. S. Yashvili, Izv. Akad. Nauk SSSR, Neorg. Mater. **4**, 553 (1968).
[116]H. R. Hoekstra, Inorg. Chem. **5**, 754 (1966).
[117]E. J. Huber, Jr., C. O. Matthews, and C. E. Holley, Jr., J. Am. Chem. Soc. **77**, 6493 (1955).
[118]F. B. Baker, G. C. Fitzgibbon, D. Pavone, C. E. Holley, Jr., L. D. Hansen, and E. A. Lewis, J. Chem. Thermodyn. **4**, 621 (1972).
[119]C. Hennig and H. Oppermann, Z. Naturforsch. B **52**, 1517 (1997).
[120]S. Stecura, Technical Report USBM-RI-6616 (U. S. Bureau of Mines, 1965).
[121]R. S. Roth and S. J. Schneider, J. Res. Natl. Bur. Stand. **64A**, 309 (1960).
[122]J. B. Ainscough, D. A. Moore, and S. C. Osborn, J. Nucl. Mater. **55**, 229 (1975).
[123]H. Suzuki, T. Iseki, and T. Maruyama, J. Am. Ceram. Soc. **59**, 451 (1976).

[124]I. S. Sukhushina, I. A. Vasil'eva, and S. B. Dashkov, Russ. J. Phys. Chem. **67**, 1776 (1993).
[125]S. J. Schneider, J. Res. Natl. Bur. Stand., Sect. A **65**, 429 (1961).
[126]N. S. Lyutsareva, G. A. Berezovskii, and I. E. Paukov, Zh. Fiz. Khim. **68**, 1179 (1994).
[127]R. J. M. Konings, J. C. van Miltenburg, and A. G. G. van Genderen, J. Chem. Thermodyn. **37**, 1219 (2005).
[128]L. B. Pankratz and E. G. King, Techical Report RI-6175 (U.S. Bureau of Mines, 1962).
[129]D. S. Tsagareishvili and G. G. Gvelesiani, Russ. J. Inorg. Chem. **10**, 171 (1965).
[130]E. C. Curtis and A. G. Tharp, J. Am. Ceram. Soc. **42**, 151 (1959).
[131]R. L. Wilfong, L. P. Domingues, L. R. Furlong, and J. A. Finlayson, Technical Report RI-6180 (U. S. Bureau of Mines, 1962).
[132]E. J. Huber, Jr., G. C. Fitzgibbon, and C. E. Holley, Jr., J. Phys. Chem. **68**, 2720 (1964).
[133]G. C. Fitzgibbon, E. J. Huber, Jr., and C. E. Holley, Jr., J. Chem. Thermodyn. **4**, 349 (1972).
[134]C. Hennig, H. Oppermann, and A. Blonska, Z. Naturforsch. B **53**, 1169 (1998).
[135]J. M. Stuve, Technical Report USBM-RI-6640 (U.S. Bureau of Mines, 1965).
[136]R. G. Bedford and E. Catalano, J. Solid State Chem. **3**, 112 (1971).
[137]J. M. Haschke and H. A. Eick, J. Phys. Chem. **72**, 4235 (1968).
[138]H. A. Eick, N. C. Baenziger, and L. Eyring, J. Am. Chem. Soc. **78**, 5147 (1956).
[139]O. D. McMasters, K. A. Gschneider, Jr., E. Kaldis, and G. Sampietro, J. Chem. Thermodyn. **6**, 845 (1974).
[140]G. J. McCarthy and W. B. White, J. Less-Common Met. **22**, 409 (1970).
[141]M. W. Shafer, J. B. Torrance, and T. Penney, J. Phys. Chem. Solids **33**, 2251 (1972).
[142]T. B. Reed and R. E. Fahey, J. Cryst. Growth **8**, 337 (1971).
[143]D. T. Teany and V. L. Moruzzi, *Les Eléments des Terres Rares, Tome II* (Centre National de la Recherche Scientifique, Paris, 1970), p. 131.
[144]J. L. Burnett, Technical Report UCRL-11850, 1964.
[145]E. J. Huber and C. E. Holley, Jr., J. Chem. Thermodyn. **1**, 301 (1969).
[146]E. J. Huber and C. E. Holley, Jr., J. Chem. Thermodyn. **2**, 896 (1970).
[147]M. W. Shafer and R. Roy, J. Am. Ceram. Soc. **42**, 563 (1959).
[148]L. S. Barkhatov, L. I. Zhmakin, D. N. Kagan, V. V. Koroleva, and E. E. Shpil'rain, High Temp.-High Press. **13**, 39 (1981).
[149]F. M. Spiridonov, V. A. Stephanov, L. N. Komissarova, and V. I. Spitsyn, J. Less-Common Met. **14**, 435 (1968).
[150]M. Mizuno, T. Yamada, and T. Noguchi (personal communication, 1989).
[151]K. W. Kang, J. H. Yang, J. H. Kim, Y. W. Rhee, D. J. Kim, K. S. Kim, and K. W. Song, Thermochim. Acta **455**, 134 (2007).
[152]G. R. Stewart, J. L. Smith, J. C. Spirlet, and W. Müller, in *Proceedings of 3rd Conference on Superconductivity in 5f and 6d Metals, La Jolla, California*, edited by H. Subl and M. B. Maple (Academic, New York, 1979), pp. 65–70.
[153]A. E. Miller, F. J. Jelinek, K. A. Gschneidner, Jr., and B. C. Gerstein, J. Chem. Phys. **55**, 2647 (1971).
[154]S. S. Rosenblum, H. Sheinberg, and W. A. Steyert, IEEE Trans. Magn. **MAG-13**, 834 (1977).
[155]D. S. Tsagareishvili, G. G. Gvelesiani, and T. S. Yashvili, Russ. J. Phys. Chem. **43**, 487 (1969).
[156]E. J. Huber, Jr. and C. E. Holley, Jr., J. Am. Chem. Soc. **77**, 1444 (1955).
[157]A. T. Lowe and L. Eyring, J. Solid State Chem. **14**, 383 (1975).
[158]G. C. Fitzgibbon and C. E. Holley, Jr., J. Chem. Eng. Data **13**, 63 (1968).
[159]R. W. Hill, J. Phys. C **19**, 673 (1986).
[160]R. J. M. Konings and A. Kovács, *Handbook on the Physics and Chemistry of Rare Earths* (North-Holland, Amsterdam, 2003), Vol. 33, Chap. 213, pp. 147–247.
[161]B. H. Justice and E. F. Westrum, Jr., J. Phys. Chem. **67**, 659 (1963).
[162]E. J. Huber, Jr., G. C. Fitzgibbon, and C. E. Holley, Jr., J. Chem. Thermodyn. **3**, 643 (1971).
[163]E. J. Huber, Jr., E. L. Head, and C. E. Holley, Jr., J. Phys. Chem. **60**, 1457 (1956).
[164]D. S. Tsagareishvili and G. G. Gvelesiani, Inorg. Mater. **7**, 1679 (1971).
[165]E. J. Huber, Jr., E. L. Head, and C. E. Holley, Jr., J. Phys. Chem. **61**, 1021 (1957).
[166]L. R. Morss, P. P. Day, C. Felinto, and H. Brito, J. Chem. Thermodyn. **25**, 415 (1993).
[167]J. M. Stuve, Technical Report USBM-RI-7046 (U. S. Bureau of Mines, 1967).
[168]Y. J. Tang, X. W. Cao, J. C. Ho, and H. C. Ku, Phys. Rev. B **46**, 1213 (1992).
[169]D. S. Tsagareishvili and G. G. Gvelesiani, High Temp. **9**, 588 (1971).
[170]E. E. Shpil'rain, D. N. Kagan, L. S. Barkhatov, and V. V. Koroleva, High Temp.-High Press. **8**, 183 (1976).
[171]E. J. Huber, Jr., E. L. Head, and C. E. Holley, Jr., J. Phys. Chem. **60**, 1582 (1956).
[172]R. L. Montgomery and J. M. Stuve, Technical Report USBM-RI-5892 (U.S. Bureau of Mines, 1961).
[173]J. Fuger, L. R. Morss, and D. Brown, J. Chem. Soc. Dalton Trans. **1980**, 1076.
[174]B. H. Justice, E. F. Westrum, Jr., E. Chang, and R. Radebaugh, J. Phys. Chem. **73**, 333 (1969).
[175]E. J. Huber, Jr., E. L. Head, and C. E. Holley, Jr., J. Chem. Phys. **33**, 1849 (1960).
[176]H. Li, C. Y. Wu, and J. C. Ho, Phys. Rev. B **49**, 1447 (1994).
[177]A. K. Shirvinskaya and V. F. Popova, Dokl. Akad. NAuk SSSR **233**, 1110 (1977).
[178]E. J. Huber, Jr., E. L. Head, and C. E. Holley, Jr., J. Phys. Chem. **64**, 1768 (1960).
[179]K. P. Huber and G. Herzberg, *Molecular Spectra and Molecular Structure. IV. Constants of Diatomic Molecules* (Van Nostrand Reinhold, New York, 1979).
[180]L. V. Gurvich, I. V. Veyts *et al.*, *Termodinamicheskiye Svoistva Individual'nykh Veschestv*, 3rd ed. (Nauka, Moscow, 1978), Vols. 1–4.
[181]A. Bernard and A. M. Sibai, Z. Naturforsch. **35a**, 1313 (1980).
[182]C. B. Suarez, Spectrosc. Lett. **18**, 507 (1985).
[183]P. Carette, J. Mol. Spectrosc. **140**, 269 (1990).
[184]A. Bernard and J. Vergès, J. Mol. Spectrosc. **201**, 172 (2000).
[185]T. C. Steimle and W. Virgo, J. Chem. Phys. **116**, 6012 (2002).
[186]A. Bernard, F. Taher, A. Topouzkhanian, and G. Wannous, Astron. Astrophys. Suppl. Ser. **139**, 163 (1999).
[187]W. J. Childs, G. L. Goodman, L. S. Goodman, and L. Young, J. Mol. Spectrosc. **119**, 166 (1986).
[188]R. D. Suenram, F. J. Lovas, G. T. Fraser, and K. Matsumura, J. Chem. Phys. **92**, 4724 (1990).
[189]T. Törring, K. Zimmermann, and J. Hoeft, Chem. Phys. Lett. **151**, 520 (1988).
[190]L. Andrews, M. Zhou, G. V. Chertihin, and C. W. Bauschlicher, Jr., Phys. Chem. A **103**, 6525 (1999).
[191]L. Zhang, L. Shao, and M. Zhou, Chem. Phys. **272**, 27 (2001).
[192]G. Hong, M. Dolg, and L. Li, Chem. Phys. Lett **334**, 396 (2001).
[193]M. Dolg and H. Stoll, Theor. Chim. Acta **75**, 369 (1989).
[194]M. Dolg, H. Stoll, H. J. Flad, and H. Preuss, J. Chem. Phys. **97**, 1162 (1992).
[195]X. Cao, W. Liu, and M. Dolg, Sci. China, Ser. B: Chem. **45**, 91 (2002).
[196]A. Marquez, M. J. Capitan, A. Odriozola, and J. F. Sanz, Int. J. Quantum Chem. **52**, 1329 (1994).
[197]M. Kotzian, N. Roesch, and M. C. Zerner, Theor. Chim. Acta **81**, 201 (1992).
[198]J. Schamps, M. Bencheikh, J.-C. Barthelat, and R. W. Field, J. Chem. Phys. **103**, 8004 (1995).
[199]L. A. Kaledin, J. E. McCord, and M. Heaven, J. Mol. Spectrosc. **158**, 40 (1993).
[200]R. Klingeler, G. Luttgens, N. Pontius, R. Rochow, P. S. Bechthold, M. Neeb, and W. Eberhardt, Eur. Phys. J. D **9**, 263 (1999).
[201]L. Schoonveld and S. Sundaram, Astrophys. J., Suppl. **27**, 307 (1974).
[202]H. W. Goldstein, P. N. Walsh, and D. White, J. Phys. Chem. **65**, 1400 (1961).
[203]R. J. Ackermann and E. Rauh, J. Chem. Thermodyn. **3**, 445 (1971).
[204]W. A. Chupka, M. G. Inghram, and R. F. Porter, J. Chem. Phys. **24**, 792 (1956).
[205]S. Smoes, J. Drowart, and G. Verhaegen, J. Chem. Phys. **43**, 732 (1965).
[206]L. L. Ames, P. N. Walsh, and D. White, J. Phys. Chem. **71**, 2707 (1967).
[207]P. Coppens, S. Smoes, and J. Drowart, Trans. Faraday Soc. **63**, 2140 (1967).
[208]P. Coppens, S. Smoes, and J. Drowart, Trans. Faraday Soc. **64**, 630 (1968).
[209]J. L. Gole and C. L. Chalek, J. Chem. Phys. **65**, 4384 (1976).
[210]A. C. Parr (private communication, 1974); cited in L. M. Biann and P. G. Wahlbeck, High Temp. Sci. **6**, 179 (1974).
[211]R. L. DeKock and W. Weltner, Jr., J. Phys. Chem. **75**, 514 (1971).

[212]S. D. Gabelnick, G. T. Reedy, and M. G. Chasanov, J. Chem. Phys. **60**, 1167 (1974).
[213]S. P. Willson and L. Andrews, J. Phys. Chem. A **103**, 3171 (1999).
[214]C. Heinemaan, H. H. Cornehl, D. Schröder, M. Dolg, and H. Schwarz, Inorg. Chem. **35**, 2463 (1996).
[215]M. Hülsen, A. Weigand, and M. Dolg, Theor. Chem. Acc. **122**, 23 (2009).
[216]T. K. Todorova, I. Infante, L. Gagliardi, and J. M. Dyke, Int. J. Quantum Chem. **109**, 2068 (2009).
[217]S. A. Shukarev and G. A. Semenov, Dokl. Akad. Nauk SSSR **141**, 652 (1961).
[218]G. Benezech and M. Foex, Compt. Rend. (Paris) **268C**, 2315 (1969).
[219]V. Piacente, G. Bardi, L. Malaspina, and A. Desideri, J. Chem. Phys. **59**, 31 (1973).
[220]R. J. Ackermann and E. Rauh, J. Chem. Thermodyn. **3**, 609 (1971).
[221]C. Younés, L. D. Nguyen, and A. Pattoret, High Temp.-High Press. **13**, 105 (1981).
[222]H. G. Staley and J. H. Norman, J. Mass. Spectrom. Ion. Phys. **2**, 35 (1969).
[223]R. F. Barrow, R. Clements, S. M. Harris, and P. P. Jenson, Astrophys. J. **229**, 439 (1979).
[224]C. Linton, M. Dulick, and R. W. Field, J. Mol. Spectrosc. **78**, 428–436 (1979).
[225]C. Linton, M. Dulick, R. W. Field, P. Carrete, and R. Barrow, J. Chem. Phys. **74**, 189 (1981).
[226]C. Linton and M. Dulick, J. Mol. Spectrosc. **89**, 569 (1981).
[227]C. Linton, M. Dulick, R. W. Field, P. Carette, P. C. Leyland, and R. F. Barrow, J. Mol. Spectrosc. **102**, 441 (1983).
[228]R. B. Dushin and L. D. Shcherba, Khim. Fiz. **4**, 321 (1985).
[229]L. A. Kaledin, J. E. McCord, and M. C. Heaven, J. Mol. Spectrosc. **170**, 166 (1995).
[230]P. Carrete and A. Hocquet, J. Mol. Spectrosc. **131**, 301 (1988).
[231]M. Dolg, H. Stoll, and H. Preuss, J. Mol. Struct. (THEOCHEM) **231**, 243 (1991).
[232]M. Kotzian and N. Roesch, Eur. J. Solid State Inorg. Chem. **28**(Suppl.), 127 (1991).
[233]R. W. Field, Ber. Bunsenges. Phys. Chem. **86**, 771 (1982).
[234]M. Dulick, Ph.D. thesis, Massachusetts Institute of Technology, Cambridge, Mass., 1982.
[235]P. N. Walsh, D. F. Dever, and D. White, J. Phys. Chem. **65**, 1410 (1961).
[236]E. A. Shenyavskaya, I. V. Egorova, and V. N. Lupanov, J. Mol. Spectrosc. **47**, 355 (1973).
[237]J. M. Delaval, J. Van Heems, and J. C. Beaufils, Can. J. Spectrosc. **22**, 117 (1977).
[238]J. C. Beaufils, P. Carette, and J. Blondeau, J. Mol. Spectrosc. **77**, 1 (1979).
[239]M. Dulick, R. W. Field, and J. C. Beaufils, J. Mol. Spectrosc. **78**, 333 (1979).
[240]M. Dulick, R. W. Field, and J. C. Beaufils, J. Mol. Spectrosc. **87**, 268 (1981).
[241]M. Dulick, R. W. Field, J. C. Beaufils, and J. Schamps, J. Mol. Spectrosc. **87**, 278 (1981).
[242]E. A. Shenyavskaya and L. A. Kaledin, J. Mol. Spectrosc. **91**, 22 (1982).
[243]M. Dulick and R. W. Field, J. Mol. Spectrosc. **113**, 105–141 (1985).
[244]W. J. Childs, Y. Azuma, and G. L. Goodman, J. Mol. Spectrosc. **144**, 70 (1990).
[245]W. Weltner and R. L. De Kock, J. Chem. Phys. **75**, 514 (1971).
[246]S. P. Willson, L. Andrews, and M. Neurock, J. Phys. Chem. A **104**, 3446 (2000).
[247]M. Dulick, E. Murad, and R. F. Barrow, J. Chem. Phys. **85**, 385 (1986).
[248]M. Kotzian and N. Roesch, J. Mol. Spectrosc. **147**, 346 (1991).
[249]J. A. Fries and E. D. Cater, Technical Report COO-1182-27 (U.S. Atomic Energy Commission/University of Iowa, Iowa City, 1969).
[250]E. Murad, Chem. Phys. Lett. **59**, 359 (1978).
[251]C. Linton, C. Effantin, P. Crozet, A. J. Ross, E. A. Shenyavskaya, and J. d'Incan, J. Mol. Spectrosc. **225**, 132 (2004).
[252]E. A. Shenyavskaya, A. Bernard, and J. Vèrges, J. Mol. Spectrosc. **222**, 240 (2003).
[253]A. N. Kulikov, Ph.D. thesis, Moscow State University, Moscow, 1985).
[254]L. A. Kaledin and E. A. Shenyavskaya, Opt. Spectrosc. (USSR) **47**, 564 (1979).
[255]L. A. Kaledin, E. A. Shenyavskaya, and I. Kovacs, Acta Phys. Hung. **54**, 189 (1983).
[256]E. A. Boudreaux and E. Baxter, Int. J. Quantum Chem. **90**, 629 (2002).
[257]M. Krauss and W. J. Stevens, Mol. Phys. **101**, 125 (2003).
[258]L. A. Kaledin, J. E. McCord, and M. Heaven, J. Mol. Spectrosc. **164**, 27 (1994).
[259]M. Tetenbaum, High Temp. Sci. **7**, 37 (1975).
[260]E. Murad and D. L. Hildenbrand, J. Chem. Phys. **73**, 4005 (1980).
[261]J. K. Gibson, J. Phys. Chem. A **107**, 7891 (2003).
[262]C. Linton, A. M. James, and B. Simard, J. Chem. Phys. **99**, 9420 (1993).
[263]G. Bujin and C. Linton, J. Mol. Spectrosc. **147**, 120 (1991).
[264]G. Bujin and C. Linton, J. Mol. Spectrosc. **137**, 114 (1989).
[265]C. Linton, G. Bujin, R. Rana, and J. A. Gray, J. Mol. Spectrosc. **126**, 370 (1987).
[266]C. Linton, G. Bujin, R. Rana, and J. A. Gray, J. Phys. Colloq. **48**, 663 (1987).
[267]M. C. Hannigan, J. Mol. Spectrosc. **99**, 235 (1983).
[268]H. L. Hildenbrand, Chem. Phys. Lett. **48**, 340 (1977).
[269]C. R. Dickson and R. N. Zare, Chem. Phys. **7**, 361 (1975).
[270]S. A. McDonald, Ph.D. thesis, Massachusetts Institute of Technology, 1985).
[271]M. Dolg, H. Stoll, and H. Preuss, Chem. Phys. Lett. **174**, 208 (1990).
[272]E. Murad and D. L. Hildenbrand, J. Chem. Phys. **65**, 3250 (1976).
[273]G. Balducci, G. Gigli, and M. Guido, J. Chem. Phys. **67**, 147 (1977).
[274]B. R. Yadav, S. B. Rai, and D. K. Rai, Can. J. Phys. **54**, 2429 (1976).
[275]B. R. Yadav, S. B. Rai, and D. K. Rai, J. Mol. Spectrosc. **89**, 1 (1981).
[276]C. B. Suárez and R. Grinfeld, J. Chem. Phys. **53**, 1110 (1970).
[277]R. J. Van Zee, R. F. Ferrante, K. J. Zeringue, and W. Weltner, J. Chem. Phys. **75**, 5297 (1981).
[278]Y. N. Dmitriev, L. A. Kaledin, E. A. Shenyavskaya, and L. V. Gurvich, Acta Phys. Hung. **55**, 467 (1984).
[279]Y. N. Dmitriev, L. A. Kaledin, A. Kobylyanskii, A. N. Kulikov, E. A. Shenyavskaya, and L. V. Gurvich, Acta Phys. Hung. **61**, 51 (1987).
[280]Y. N. Dmitriev, Ph.D. thesis, Moscow State University, 1988.
[281]L. V. Gurvich, Y. N. Dmitriev, L. A. Kaledin, A. Kobylyanskii, A. N. Kulikov, and E. A. Shenyavskaya, Izv. Akad. Nauk SSSR, Ser. Geogr. Geofiz. **48**, 721 (1984).
[282]P. Carette, A. Hocquet, M. Douay, and B. Pinchemel, J. Mol. Spectrosc. **124**, 243 (1987).
[283]M. Dolg, W. Liu, and S. Kalvoda, Int. J. Quantum Chem. **76**, 359 (2000).
[284]Y. Sakai, T. Nakai, K. Mogi, and E. Miyoshi, Mol. Phys. **101**, 117 (2003).
[285]R. Klingeler, N. Pontius, G. Luttgens, P. S. Bechthold, M. Neeb, and W. Eberhardt, Phys. Rev. A **65**, 032502 (2002).
[286]L. A. Kaledin and E. A. Shenyavskaya, Optika i Spektroskopiya **51**, 934 (1981).
[287]L. A. Kaledin and E. A. Shenyavskaya, J. Mol. Spectrosc. **90**, 590 (1981).
[288]A. N. Kulikov, L. A. Kaledin, A. I. Kobylyanskii, and L. V. Gurvich, Zh. Fiz. Khim. **58**, 2854 (1984).
[289]A. N. Kulikov, L. A. Kaledin, A. I. Kobylyanskii, and L. V. Gurvich, Can. J. Phys. **62**, 1855 (1984).
[290]B. R. Yadav, S. B. Rai, and D. K. Rai, Pramana **14**, 379 (1980).
[291]C. Linton, D. M. Gaudet, and H. Shall, J. Mol. Spectrosc. **115**, 58 (1986).
[292]C. H. Cheng, Diss. Abstr. Int. B **54**, 4212 (1994).
[293]Y. C. Liu, C. Linton, H. Shall, and R. W. Field, J. Mol. Spectrosc. **104**, 72 (1984).
[294]C. Linton and Y. C. Liu, J. Mol. Spectrosc. **131**, 367 (1988).
[295]L. A. Kaledin and E. A. Shenyavskaya, J. Mol. Spectrosc. **133**, 469 (1989).
[296]T. C. Melville, I. Gordon, K. Tereszchuk, J. A. Coxon, and P. F. Bernath, J. Mol. Spectrosc. **218**, 235 (2003).
[297]S. A. McDonald, S. R. Rice, R. W. Field, and C. Linton, J. Chem. Phys. **93**, 7676 (1990).
[298]T. C. Steimle, D. M. Goodridge, and C. Linton, J. Chem. Phys. **107**, 3723 (1997).
[299]W. Liu, M. Dolg, and L. Li, J. Chem. Phys. **108**, 2886 (1998).
[300]A. Yokozeki and M. Menzinger, Chem. Phys. **14**, 427 (1976).
[301]C. B. Cosmovici, E. D'Anna, A. D'Innocenzo, G. Leggieri, A. Perrone, and R. Dirscherl, Chem. Phys. Lett. **47**, 241 (1977).
[302]A. Bernard and C. Effantin, Can. J. Phys. **64**, 246–251 (1986).
[303]S. A. Cooke, C. Krumrey, and M. C. L. Gerry, J. Mol. Spectrosc. **267**, 108 (2011).
[304]S. G. Wang and W. H. E. Schwarz, J. Phys. Chem. A **99**, 11687 (1995).
[305]W. Küchle, M. Dolg, and H. Stoll, J. Phys. Chem. A **101**, 7128 (1997).
[306]R. J. M. Konings, L. R. Morss, and J. Fuger, *The Chemistry of the Actinide and Transactinide Elements* (Springer-Verlag, Berlin, 2006), Chap. 19, pp. 2113–2224.
[307]C. Ronchi and J. Hiernaut, J. Alloys Compd. **240**, 179 (1996).
[308]O. Ruff, F. Ebert, and H. Woitinek, Z. Anorg. Allg. Chem. **180**, 252 (1929).

[309]H. V. Wartenberg and H. J. Reusch, Z. Anorg. Allg. Chem. **208**, 369 (1932).
[310]G. A. Geach and M. E. Harper, Metallurgia **47**, 269 (1953).
[311]W. A. Lambertson, M. H. Mueller, and F. H. Gunzel, J. Am. Ceram. Soc. **36**, 397 (1953).
[312]R. Benz, J. Nucl. Mater. **29**, 43 (1969).
[313]F. Sibieude and M. Foex, J. Nucl. Mater. **56**, 229 (1975).
[314]D. W. Osborne and E. F. Westrum, Jr., J. Chem. Phys. **21**, 1884 (1953).
[315]J. D. Cox, D. D. Wagman, and V. A. Medvedev, *CODATA Key Values for Thermodynamics* (Hemisphere, New York, 1989).
[316]N. Magnani, P. Santini, G. Amoretti, R. Caciuffo, P. Javorský, F. Wastin, J. Rebizant, and G. H. Lander, Physica B **359–361**, 1087 (2005).
[317]F. M. Jaeger and W. A. Veenstra, Proc. R. Acad. Sci. Amsterdam **37**, 327 (1934).
[318]J. C. Southard, J. Am. Chem. Soc. **63**, 3142 (1941).
[319]M. Hoch and H. L. Johnston, J. Phys. Chem. **65**, 1184 (1961).
[320]A. C. Victor and T. B. Douglas, J. Res. Natl. Bur. Stand., Ser. A **65**, 105 (1961).
[321]J. Springer, E. A. Eldridge, M. U. Goodyear, T. R. Wright, and J. F. Langedrost, Technical Report BMI-X-10210 (Battelle Memorial Institute, 1967).
[322]J. Springer and J. F. Langedrost, Technical Report BMI-X-10231 (Battelle Memorial Institute, 1968).
[323]D. F. Fischer, J. K. Fink, and L. Leibowitz, J. Nucl. Mater. **102**, 220 (1981).
[324]R. Agarwal, R. Prasad, and V. Venugopal, J. Nucl. Mater. **322**, 98 (2003).
[325]S. Dash, S. C. Parida, Z. Singh, B. K. Sen, and V. Venugopal, J. Nucl. Mater. **393**, 267 (2009).
[326]J. K. Fink, M. G. Chasanov, and L. Leibowitz, Technical Report ANL-CEN-RSD–77-1 (Argonne National Laboratory, 1977).
[327]E. J. Huber, Jr., C. E. Holley, Jr., and E. H. Meierkord, J. Am. Chem. Soc. **74**, 3406 (1952).
[328]W. A. Roth and G. Becker, Z. Phys. Chem. **A159**, I (1932).
[329]R. J. M. Konings, J. Chem. Thermodyn. **36**, 121 (2004).
[330]R. J. M. Konings and O. Beneš, J. Phys. Chem. Solids **74**(5), 653 (2013).
[331]A. R. Beketov and G. W. Vlasov, Zh. Prikl. Khim. **38**, 2103 (1965).
[332]E. H. P. Cordfunke and P. Aling, Trans. Faraday Soc. **61**, 50 (1965).
[333]W. M. Jones, J. Gordon, and E. A. Long, J. Chem. Phys. **20**, 695 (1952).
[334]E. H. P. Cordfunke and E. F. Westrum, Jr., Thermochim. Acta **124**, 285 (1988).
[335]M. M. Popov, G. L. Galchenko, and M. D. Senin, Zh. Neorg. Khim. **3**, 1734 (1958).
[336]G. E. Moore and K. K. Kelley, J. Am. Chem. Soc. **69**, 2105 (1947).
[337]G. C. Fitzgibbon, D. Pavone, and C. E. Holley, Jr., J. Chem. Eng. Data **12**, 122 (1968).
[338]G. K. Johnson and P. A. G. O'Hare, J. Chem. Thermodyn. **10**, 577 (1978).
[339]H. L. Girdhar and E. F. Westrum, Jr., J. Chem. Eng. Data **13**, 531 (1968).
[340]H. Inaba, H. Shimizu, and K. Naito, J. Nucl. Mater. **64**, 66 (1977).
[341]D. Manara, R. Pflieger-Cuveiller, and M. Sheindlin, Int. J. Thermophys. **26**, 1193 (2005).
[342]E. F. Westrum, Jr. and F. Grønvold, J. Am. Chem. Soc. **81**, 1777 (1959).
[343]M. M. Popov, F. A. Kostylev, and N. V. Zubova, Russ. J. Inorg. Chem. **4**, 770 (1959).
[344]K. Maglic and R. Herak, Rev. Int. Hautes Temp. Refract. **7**, 247 (1970).
[345]D. I. Marchidan and M. Ciopec, Rev. Roum. Chim. **20**, 143 (1975).
[346]E. J. Huber and C. E. Holley, Jr., J. Chem. Thermodyn. **1**, 267 (1969).
[347]M. M. Popov and M. I. Ivanov, Sov. At. Energy **2**, 360 (1957).
[348]E. F. Westrum, Jr., Y. Takahashi, and F. Grønvold, J. Phys. Chem. **69**, 3192 (1965).
[349]F. Grønvold, N. J. Kveseth, A. Sveen, and J. Tichy, J. Chem. Thermodyn. **2**, 665 (1970).
[350]H. Inaba and K. Naito, J. Nucl. Mater. **49**, 181 (1973).
[351]K. Naito, T. Tsuji, and T. Matsui, J. Nucl. Mater. **48**, 58 (1973).
[352]A. C. MacLeod, J. Chem. Thermodyn. **4**, 699 (1972).
[353]D. W. Osborne, E. F. Westrum, Jr., and H. R. Lohr, J. Am. Chem. Soc. **79**, 529 (1957).
[354]H. E. Flotow, D. W. Osborne, and E. F. Westrum, Jr., J. Chem. Phys. **49**, 2438 (1968).
[355]K. Gotoo and K. Naito, J. Phys. Chem. Solids **26**, 1673 (1965).
[356]A. Burdese and F. Abbatista, Ric. Sci. **328**, 1634 (1958).
[357]C. Guéneau, N. Dupin, C. Martial, J. C. Dumas, S. Gossé, S. Chatain, B. Sundman, F. D. Bruycker, D. Manara, and R. Konings, J. Nucl. Mater. **419**, 145 (2011).
[358]F. D. Bruycker, K. Boboridis, R. Konings, M. Rini, R. Eloirdi, C. Guéneau, N. Dupin, and D. Manara, J. Nucl. Mater. **419**, 186 (2011).
[359]R. J. Ackermann, Techical Report ANL-5482, Argonne National Laboratory (1955).
[360]W. A. Lambertson and J. H. Handwerk, Technical Report (ANL-5053, Argonne National Laboratory, 1956).
[361]L. G. Wisnyi and S. Pijanowski, Technical Report KAPL-1702, 1957.
[362]T. C. Ehlert and J. L. Margrave, J. Am. Ceram. Soc. **41**, 330 (1958).
[363]S. W. Pijanowski and L. S. DeLuca, Technical Report KAPL-1957, 1960.
[364]T. D. Chikalla, Technical Report HW-69832, 1961.
[365]W. L. Lyon and W. E. Bailey, Technical Report GEAP-64640, 1964.
[366]H. Hausner, J. Nucl. Mater. **15**, 179 (1965).
[367]W. L. Lyon and W. E. Bailey, J. Nucl. Mater. **22**, 332 (1967).
[368]R. E. Latta and R. E. Fryxell, J. Nucl. Mater. **35**, 195 (1970).
[369]T. Tachibana, T. O. S. Yamanouchi, and T. Itaki, J. Nucl. Sci. Technol. **22**, 155 (1985).
[370]C. Ronchi and M. Sheindlin, Int. J. Thermophys. **23**, 293 (2002).
[371]D. Manara, C. Ronchi, and M. Sheindlin, High Temp.-High Press. **35/36**, 25 (2003).
[372]M. Kato, K. Morimoto, H. Sugata, K. Konashi, M. Kashimura, and T. Abe, J. Nucl. Mater. **373**, 237 (2008).
[373]J. J. Hunzicker and E. F. Westrum, Jr., J. Chem. Thermodyn. **3**, 61 (1971).
[374]A. E. Ogard and J. A. Leary, in *Proceedings of Thermodynamics of Nuclear Materials, International Atomic Energy Agency, Vienna* (IAEA, Vienna, 1967), p. 651.
[375]D. R. Fredrickson and M. G. Chasanov, J. Chem. Thermodyn. **2**, 623 (1970).
[376]R. A. Hein and P. N. Flagella, Technical Report GEMP-578, 1968.
[377]L. Leibowitz, L. W. Mishler, and M. G. Chasanov, J. Nucl. Mater. **29**, 356 (1969).
[378]Y. Takahashi and M. Asou, J. Nucl. Mater. **201**, 108 (1993).
[379]K. C. Mills, F. H. Ponsford, M. J. Richardson, N. Zaghini, and P. Fassina, Thermochim. Acta **139**, 107 (1989).
[380]C. Ronchi, M. Shiendlin, M. Musella, and G. J. Hyland, J. Appl. Phys. **85**, 776 (1999).
[381]M. Amaya, K. Une, and K. Minato, J. Nucl. Mater. **294**, 1 (2001).
[382]H. Inaba, K. Naito, and M. Oguma, J. Nucl. Mater. **149**, 341 (1987).
[383]C. Afforit, High Temp.-High Press. **1**, 27 (1969).
[384]T. K. Engel, J. Nucl. Mater. **31**, 211 (1969).
[385]C. Afforit and J. Marcon, Rev. Int. Hautes Temp. Refract **7**, 236 (1970).
[386]J. P. Hiernaut, G. J. Hyland, and C. Ronchi, Int. J. Thermophys. **14**, 259 (1993).
[387]C. Ronchi, J. P. Hiernaut, R. Selfslag, and G. J. Hyland, Nucl. Sci. Eng. **113**, 1 (1993).
[388]J. B. Conway and R. A. Hein, J. Nucl. Mater. **15**, 149 (1965).
[389]R. A. Hein, L. A. Sjodahl, and R. Szwarc, J. Nucl. Mater. **25**, 99 (1968).
[390]L. Leibowitz, M. G. Chasanov, and L. W. Mishler, J. Nucl. Mater. **39**, 115 (1971).
[391]M. T. Hutchings, K. Clausen, M. H. Dicken, W. Hayes, J. K. Kjems, P. G. Schnabel, and C. Smith, J. Phys. C **17**, 3903 (1984).
[392]M. T. Hutchings, J. Chem. Soc., Faraday Trans. 2 **83**, 1083 (1987).
[393]K. Clausen, W. Hayes, J. E. Macdonald, and R. Osborn, Phys. Rev. Lett. **52**, 1238 (1984).
[394]C. Ronchi and H. Hyland, J. Alloys Compd. **213/214**, 159 (1994).
[395]V. P. Glushko, L. V. Gurvich, G. A. Bergman, I. V. Veyts, V. A. Medvedev, G. A. Khachkuruzov, and V. S. Yungman *Termodinamicheskie Svoitsva Individual'nykh Veshchestv. Tom IV* (Nauka, Moscow, 1982).
[396]C. Ronchi, I. L. Iosilevski, and E. Yakub, *Equation of State of Uranium Dioxide* (Springer-Verlag, Berlin, 2004).
[397]G. K. Johnson and E. H. P. Cordfunke, J. Chem. Thermodyn. **13**, 273 (1981).
[398]K. Richter and C. Sari, J. Nucl. Mater. **148**, 266 (1987).
[399]L. Merli and J. Fuger, Radiochim. Acta **66/67**, 109 (1994).
[400]R. J. Lemire, Technical Report AECL-7817, 1984.
[401]Y. I. Belyaev, V. N. Dobretsov, and V. A. Ustinov, Sov. Radiochem. **21**, 386 (1979).
[402]Y. I. Belyaev, N. L. Smirnov, and A. P. Taranov, Sov. Radiochem. **21**, 590 (1979).

[403]T. D. Chikalla, C. E. McNeilly, J. L. Bates, and J. J. Rasmussen, Technical Report BNWL-SA-3818, 1971.
[404]R. Böhler, M. J. Welland, K. Boboridis, A. Janssen, R. Eloirdi, R. J. M. Konings, and D. Manara, J. Appl. Phys. **111**, 113501 (2012).
[405]E. F. Westrum, Jr., J. B. Hatcher, and D. W. Osborne, J. Chem. Phys. **21**, 419 (1953).
[406]V. A. Arkhipov, E. A. Gutina, V. N. Dobretsov, and V. A. Ustinov, Sov. Radiochem. **16**, 123 (1974).
[407]T. Nishi, A. Itoh, M. Takano, M. Numata, M. Akabori, Y. Arai, and K. Minato, J. Nucl. Mater. **376**, 78 (2008).
[408]O. Beneš, P. Gotcu, F. Schwörer, R. J. M. Konings, and T. Fanghänel, J. Chem. Thermodyn. **43**, 651 (2011).
[409]T. Yamashita, N. Nitani, T. Tsuji, and T. Kato, J. Nucl. Mater. **247**, 90 (1997).
[410]H. Serizawa, Y. Arai, and K. Nakajima, J. Chem. Thermodyn. **33**, 615 (2001).
[411]E. J. Huber, Jr. and C. Holley, Jr., J. Chem. Eng. Data **13**, 545 (1968).
[412]B. Riley, Sci. Ceram. **5**, 83 (1970).
[413]F. De Bruycker, K. Boboridis, D. Manara, P. Pöml, M. Rini, and R. J. M. Konings, Mater. Today **13**(11), 52 (2010).
[414]F. D. Bruycker, K. Boboridis, P. Pöml, R. Eloirdi, R. Konings, and D. Manara, J. Nucl. Mater. **416**, 166 (2011).
[415]L. E. Russel, in *Proceedings of the 2nd International Conference on Plutonium Metallurgy, Grenoble, France* (Cleaver-Hume Press, London, 1961), p. 492.
[416]M. D. Freshley and H. M. Mattys, Technical Report HW-76559, 1962.
[417]E. A. Aitken and S. K. Evans, Technical Report USAEC GEAP-5672, 1968.
[418]T. A. Sandenaw, J. Nucl. Mater. **10**, 165 (1963).
[419]O. L. Kruger and H. Savage, J. Chem. Phys. **49**, 4540 (1968).
[420]H. E. Flotow, D. W. Osborne, S. M. Fried, and J. G. Malm, J. Chem. Phys. **65**, 1124 (1976).
[421]A. E. Ogard, *Plutonium 1970 and Other Actinides* (Metallurgical Society of the American Institute of Mining, New York, 1970), p. 78.
[422]F. L. Oetting, J. Nucl. Mater. **105**, 257 (1982).
[423]J. K. Fink, Int. J. Thermophys. **3**, 165 (1982).
[424]M. M. Popov, F. A. Kostylev, and T. F. Karpova, Russ. J. Inorg. Chem. **2**, 9 (1957).
[425]C. E. Holley, R. N. R. Mulford, E. J. Huber, E. L. Head, and C. W. Bjorklund, in *Proceedings Second International Conference on Peaceful Uses of Atomic Energy, Geneva* (United Nations, Geneva, 1958), p. 215.
[426]G. K. Johnson, E. H. V. Deventer, O. L. Kruger, and W. N. Hubbard, J. Chem. Thermodyn. **1**, 89 (1969).
[427]T. D. Chikalla, C. E. McNeilly, and R. E. Skavdahl, J. Nucl. Mater. **12**, 131 (1964).
[428]H. E. Flotow and P. A. G. O'Hare, J. Chem. Phys. **74**, 3046 (1981).
[429]T. M. Besmann and T. E. Lindemer, J. Am. Ceram. Soc. **166**, 782 (1983).
[430]R. J. Lemire, J. Fuger, H. Nitsche, P. Potter, M. H. Rand, J. Rydberg, K. Spahiu, J. C. Sullivan, W. Ullman, P. Vitorge *et al.*, *Chemical Thermodynamics of Neptunium and Plutonium* (Elsevier, Amsterdam, 2001).
[431]T. L. Markin and M. H. Rand, *Thermodynamics : proceedings of the symposium on thermodynamics with emphasis on nuclear materials and atomic transport in solids* (International Atomic Energy Agency, Vienna, 1966), pp. 145–156.
[432]P. Chereau, G. Dean, M. de Franco, and M. Gerdanian, J. Chem. Thermodyn. **9**, 211 (1977).
[433]C. Guéneau, C. Chatillon, and B. Sundman, J. Nucl. Mater. **378**, 257 (2008).
[434]R. E. McHenry, Trans. Am. Nucl. Soc. **8**, 75 (1965).
[435]P. Gotcu-Freis, J. Y. Colle, C. Guéneau, N. Dupin, B. Sundman, and R. J. M. Konings, J. Nucl. Mater. **414**, 408 (2011).
[436]E. F. Westrum, Jr. and F. Grønvold, in *Proceedings of a Symposium on Thermodynamics of Nuclear Materials. International Atomic Energy Agency, Vienna* (IAEA, Vienna, 1962), p. 3.
[437]R. J. M. Konings, J. Nucl. Mater. **298**, 255 (2001).
[438]R. J. Ackermann, R. L. Faircloth, and M. H. Rand, J. Phys. Chem. **70**, 3698 (1966).
[439]T. Nishi, A. Itoh, K. Ichise, and Y. Arai, J. Nucl. Mater. **414**, 109 (2011).
[440]C. Thiriet and R. J. M. Konings, J. Nucl. Mater. **320**, 292 (2003).
[441]L. R. Morss and J. Fuger, J. Inorg. Nucl. Chem. **43**, 2059 (1981).
[442]J. C. Wallmann, J. Inorg. Nucl. Chem. **26**, 2053 (1964).
[443]T. D. Chikalla, C. E. McNeilly, J. L. Bates, and J. J. Rasmussen, Technical Report BNWL-SA-3818, 1973.
[444]T. D. Chikalla, C. E. McNeilly, J. L. Bates, and J. J. Rasmussen, in *Proceedings of International on Colloquium on High Temperature Phase Transformations, CNRS Publ. No. 205* (CNRS, Paris, 1973), p. 351.
[445]R. J. M. Konings, J. Nucl. Mater. **295**, 57 (2001).
[446]L. R. Morss and D. C. Sonnenberger, J. Nucl. Mater. **130**, 266 (1985).
[447]J. Fuger, J. C. Spirlet, and W. Müller, Inorg. Nucl. Chem. Lett. **8**, 709 (1972).
[448]W. C. Mosley, J. Inorg. Nucl. Chem. **34**, 539 (1972).
[449]P. K. Smith, J. Inorg. Nucl. Chem. **31**, 241 (1969).
[450]R. D. Baybarz, J. Inorg. Nucl. Chem. **35**, 4149 (1973).
[451]L. R. Morss, J. Fuger, J. Goffart, and R. G. Haire, Inorg. Chem. **22**, 1993 (1983).
[452]J. R. Peterson and B. B. Cunningham, Inorg. Nucl. Chem. Lett. **3**, 327 (1967).
[453]R. D. Baybarz and M. L. Adair, J. Inorg. Nucl. Chem. **34**, 3127 (1972).
[454]L. R. Morss, J. Fuger, J. Goffart, N. Edelstein, and G. V. Shalimoff, J. Less-Common Met. **127**, 251 (1987).
[455]J. Fuger, R. G. Haire, and J. R. Peterson, J. Less-Common Met. **98**, 315 (1984).
[456]A. Kovács (2012) (unpublished).
[457]M. Kaufman, J. Muenter, and W. Klemperer, J. Chem. Phys. **47**, 3365 (1967).
[458]M. Zhou and L. Andrews, J. Chem. Phys. **111**, 11044 (1999).
[459]L. Andrews, M. Zhou, B. Liang, J. Li, and B. E. Bursten, J. Am. Chem. Soc. **122**, 11440 (2000).
[460]A. Kovács and R. J. M. Konings, J. Phys. Chem. A **115**, 6646 (2011).
[461]K. G. Dyall, Mol. Phys. **96**, 511 (1999).
[462]I. Infante, A. Kovács, G. La Macchia, A. R. M. Shahi, J. K. Gibson, and L. Gagliardi, J. Phys. Chem. A **114**, 6007 (2010).
[463]W. R. Wadt, J. Am. Chem. Soc. **103**, 6053 (1981).
[464]K. Pierloot, E. van Besien, E. van Lenthe, and E. J. Baerends, J. Chem. Phys. **126**, 194311 (2007).
[465]E. Shapiro, J. Am. Chem. Soc. **74**, 5233 (1952).
[466]M. Hoch and H. L. Johnston, J. Amer. Chem. Soc. **76**, 4833 (1954).
[467]A. J. Darnell and W. A. McCollum, Atomics International, Technical Report NAA-SR-6498, 1961.
[468]R. J. Ackermann, E. G. Rauh, R. J. Thorn, and M. C. Cannon, J. Phys. Chem. **67**, 762 (1963).
[469]R. J. Ackermann and E. G. Rauh, High Temp. Sci. **5**, 463 (1973).
[470]D. L. Hildenbrand and E. Murad, J. Chem. Phys. **61**, 1232 (1974).
[471]R. J. Ackermann and E. G. Rauh, High Temp. Sci. **7**, 304 (1975).
[472]S. A. Shchukarev and G. A. Semenov, *Issledovanya v Oblasti Khimii Silikatov I Okislov* (Nauka, Moscow, 1965), p. 208.
[473]G. A. Semenov, Technical Report, Chemical Department of Leningrad State University (1969).
[474]G. Edvinsson and A. Lagerqvist, Phys. Scr. **30**, 309 (1984).
[475]G. Edvinsson and A. Lagerqvist, Phys. Scr. **32**, 602 (1985).
[476]G. Edvinsson and A. Lagerqvist, J. Mol. Spectrosc. **113**, 93 (1985).
[477]G. Edvinsson and A. Lagerqvist, J. Mol. Spectrosc. **122**, 428 (1987).
[478]G. Edvinsson and A. Lagerqvist, J. Mol. Spectrosc. **128**, 117 (1988).
[479]G. Edvinsson and A. Lagerqvist, Phys. Scr. **41**, 316 (1990).
[480]G. Edvinsson and J. Jonsson, Technical Report USIP-91-01, 1991; ETN-91-99499, 1991.
[481]C. T. Dewberry, K. C. Etchison, and S. A. Cooke, Phys. Chem. Chem. Phys. **9**, 4895 (2007).
[482]M. J. Linevsky, U.S. Govt. Res. Develop. Rep. **40**(3), 58 (1964).
[483]G. P. Kushto and L. Andrews, J. Phys. Chem. A **103**, 4836 (1999).
[484]V. Goncharov and M. C. Heaven, J. Chem. Phys. **124**, 064312 (2006).
[485]S. H. Behere, T. Wentink, Jr., and B. B. Laud, Indiana J. Phys., B **58B**(1), 15 (1984).
[486]S. H. Behere, T. Wentink, Jr., and B. B. Laud, Indiana J. Phys., B **58B**(1), 52 (1984).
[487]J. Paulovic, T. Nakajima, K. Hirao, and L. Seijo, J. Chem. Phys. **117**, 3597 (2002).
[488]J. Paulovic, T. Nakajima, K. Hirao, R. Lindh, and P. Malmqvist, J. Chem. Phys. **119**, 798 (2003).
[489]Y. Watanabe and O. Matsuoka, J. Chem. Phys. **107**, 3738 (1997).
[490]Y. Watanabe and O. Matsuoka, J. Chem. Phys. **109**, 8182 (1998).
[491]Y. Watanabe and O. Matsuoka, J. Chem. Phys. **116**, 9585 (2002).
[492]W. Küchle, M. Dolg, H. Stoll, and H. Preuss, J. Chem. Phys. **100**, 7535 (1994).
[493]C. M. Marian, U. Wahlgren, O. Gropen, and P. Pyykkö, THEOCHEM **169**, 339 (1988).

[494]L. Seijo, Z. Barandiarán, and E. Harguindey, J. Chem. Phys. **114**, 118 (2001).
[495]A. A. Buchachenko, J. Chem. Phys. **133**, 041102 (2010).
[496]A. Neubert and K. F. Zmbov, High Temp. Sci. **6**, 303 (1974).
[497]E. Murad and D. L. Hildenbrand, J. Chem. Phys. **63**, 1133 (1975).
[498]A. Kovács, P. Pogány, and R. J. M. Konings, Inorg. Chem. **51**, 4841 (2012).
[499]P. D. Kleinschmidt and J. W. Ward, J. Less-Common Met. **121**, 61 (1986).
[500]J. Marçalo and J. K. Gibson, J. Phys. Chem. A **113**, 12599 (2009).
[501]S. D. Gabelnick, G. T. Reedy, and M. G. Chasanov, J. Chem. Phys. **58**, 4468 (1973).
[502]D. W. Green, G. R. Reedy, and S. D. Gabelnick, J. Chem. Phys. **73**, 4207 (1980).
[503]R. D. Hunt and L. Andrews, J. Chem. Phys. **98**, 3690 (1993).
[504]P. Pyykkö, J. Li, and N. Runeberg, J. Phys. Chem. **98**, 4809 (1994).
[505]T. Privalov, B. Schimmelpfennig, U. Wahlgren, and I. Grenthe, J. Phys. Chem. A **106**, 11277 (2002).
[506]M. Zhou, L. Andrews, N. Ismail, and C. Marsden, J. Phys. Chem. A **104**, 5495 (2000).
[507]R. J. Ackermann, R. J. Thorn, C. Alexander, and M. Tetenbaum, J. Phys. Chem. **64**, 350 (1960).
[508]C. A. Alexander, Ph.D. thesis, Ohio State University, 1961.
[509]S. R. Dharwadkar, S. N. Tripathi, M. D. Karkhanavala, and M. S. Chandrasekharaiah, *Thermodynamics of Nuclear Materials* (International Atomic Energy Agency, Vienna, 1975), Vol. II, pp. 455–465.
[510]O. H. Krikorian, B. B. Ebbinghaus, M. G. Adamson, A. S. Fontes, Jr., and D. L. Fleming, Technical Report UCRL-ID-114774, 1993.
[511]C. A. Alexander, J. Nucl. Mater. **346**, 312 (2005).
[512]R. J. Ackermann and A. T. Chang, J. Chem. Thermodyn. **5**, 873 (1973).
[513]G. DeMaria, R. P. Burns, J. Drowart, and M. B. Inghram, J. Chem. Phys. **32**, 1373 (1960).
[514]J. Drowart, A. Pattoret, and S. Smoes, Proc. Br. Ceram. Soc. **8**, 67 (1967).
[515]A. Pattoret, J. Drowart, and S. Smoes, in *Proceedings of a Symposium on Thermodynamics of Nuclear Materials, Vienna, 1967* (International Atomic Energy Agency, Vienna, 1968), pp. 635–636.
[516]C. J. Lue, J. Jin, M. J. Ortiz, J. C. Rienstra-Kiracofe, and M. C. Heaven, J. Am. Chem. Soc. **126**, 1812 (2004).
[517]D. Majumdar, K. Balasubramanian, and H. Nitsche, Chem. Phys. Lett. **361**, 143 (2002).
[518]I. Infante, Ph.D. thesis, Vrije Universiteit, Amsterdam, 2006.
[519]T. Fleig, H. J. A. Jensen, J. Olsen, and L. Visscher, J. Chem. Phys. **124**, 104106 (2006).
[520]I. Infante, E. Eliav, M. J. Vilkas, Y. Ishikawa, U. Kaldor, and L. Visscher, J. Chem. Phys. **127**, 124308 (2007).
[521]J. Li, B. E. Bursten, L. Andrews, and C. J. Marsden, J. Am. Chem. Soc. **126**, 3424 (2004).
[522]I. Infante, L. Andrews, X. Wang, and L. Gagliardi, Chem.-Eur. J. **16**, 12804 (2010).
[523]J. D. Han, V. Goncharov, L. A. Kaledin, A. Komissarov, and M. C. Heaven, J. Chem. Phys. **120**, 5155 (2004).
[524]L. Gagliardi, M. C. Heaven, J. W. Krogh, and B. O. Roos, J. Am. Chem. Soc. **127**, 86 (2005).
[525]N. M. Voronov, A. S. Danilin, and I. T. Kovalev, in *Proceedings of the International Symposium on Thermodynamics of Nuclear Materials, Vienna, Austria, 21–25 May 1962* (International Atomic Energy Agency, Vienna, Austria, 1963), pp. 789–800.
[526]R. J. Ackermann and M. Tetenbaum, High Temp. Sci. **13**, 91 (1980).
[527]R. Ohse, J. Babelot, C. Cercignani, J. Hiernaut, M. Hoch, G. J. Hyland, and J. Magill, J. Nucl. Mater. **130**, 165 (1985).
[528]W. Breitung and O. Reil, Nucl. Sci. Eng. **101**, 26 (1989).
[529]R. Pflieger, J. Y. Colle, I. Iosilevskiy, and M. Sheindlin, J. Appl. Phys. **109**, 033501 (2011).
[530]J. K. Fink, J. Nucl. Mater. **279**, 1 (2000).
[531]R. J. Ackermann, P. W. Gilles, and R. J. Thorn, J. Chem. Phys. **25**, 1089 (1956).
[532]V. E. Ivanov, A. A. Kruglykh, V. S. Pavlov, G. P. Kovtun, and V. M. Amonenko, in *Proceedings of the International Symposium on Thermodynamics of Nuclear Materials, Austria, 21–25 May 1962* (International Atomic Energy Agency, Vienna, Austria, 1963), pp. 735–746.
[533]R. W. Ohse, J. Chem. Phys. **44**, 1375 (1966).
[534]Y. A. Gorban', L. V. Pavlinov, and V. N. Bykov, Atomnaya Energiya **22**, 465 (1967).
[535]M. Tetenbaum and P. D. Hunt, J. Nucl. Mater. **34**, 86 (1970).
[536]G. T. Reedy and M. G. Chasanov, J. Nucl. Mater. **42**, 341 (1972).
[537]L. A. Kaledin, E. A. Shenyavskaya, and L. V. Gurvich, Zh. Fiz. Khim. **60**, 1049 (1986).
[538]M. C. Heaven, J. P. Nicolai, S. J. Riley, and E. K. Parks, Chem. Phys. Lett. **119**, 229 (1985).
[539]L. A. Kaledin, A. N. Kulikov, A. I. Kobyliansky, E. A. Shenyavskaya, and L. V. Gurvich, Zh. Fiz. Khim. **61**, 1374 (1987).
[540]L. V. Gurvich, Y. N. Dmitriev, L. A. Kaledin, A. Kobylyanskii, A. N. Kulikov, and E. A. Shenyavskaya, Izv. Akad. Nauk SSSR, Ser. Fiz. **53**, 1731 (1989).
[541]L. A. Kaledin and M. C. Heaven, J. Mol. Spectrosc. **185**, 1 (1997).
[542]D. H. W. Carstens, D. M. Gruen, and J. P. Kozlowski, High Temp. Sci. **4**, 436 (1972).
[543]S. Abramowitz and N. J. Acquista, J. Res. Natl. Bur. Stand. **78A**, 421 (1974).
[544]M. J. Krauss and W. J. Stevens, Chem. Phys. Lett. **99**, 417 (1983).
[545]J. Paulovič, L. Gagliardi, J. M. Dyke, and K. Hirao, J. Chem. Phys. **122**, 144317 (2005).
[546]L. A. Kaledin and A. N. Kulikov, Zh. Fiz. Khim. **63**, 1697 (1989).
[547]L. A. Kaledin, A. N. Kulikov, and L. V. Gurvich, Zh. Fiz. Khim. **63**, 801 (1989).
[548]R. J. Ackermann, M. Kojima, E. G. Rauh, and R. R. Walters, J. Chem. Thermodyn. **1**, 527 (1969).
[549]R. P. Steiger and D. E. Cater, High Temp. Sci **7**, 288 (1975).
[550]M. S. Liao, T. Kar, and S. Scheiner, J. Phys. Chem. A **108**, 3056 (2004).
[551]M. P. Lahalle, J. C. Krupa, R. Guillaumont, and C. Rizzoli, J. Less-Common Met. **122**, 65 (1986).
[552]S. Kern, J. Morris, C. K. Loong, G. L. Goodman, G. H. Lange, and B. Cort, J. Appl. Phys. **63**, 3598 (1988).
[553]J. M. Fournier, A. Blaise, G. Amoretti, R. Caciuffo, J. Larroque, M. T. Hutchings, R. Osborn, and A. D. Taylor, Phys. Rev. B **43**, 1142 (1991).
[554]W. T. Carnall, G. K. Liu, C. W. Williams, and M. F. Reid, J. Chem. Phys. **95**, 7194 (1991).
[555]P. Gotcu-Freis, J. P. Hiernaut, J. Y. Colle, and R. J. M. Konings, J. Chem. Thermodyn. **43**, 492 (2011).
[556]W. Bartscher and C. Sari, J. Nucl. Mater. **140**, 91 (1986).
[557]R. J. Ackermann, R. L. Faircloth, E. G. Rauh, and R. J. Thorn, J. Inorg. Nucl. Chem. **28**, 111 (1966).
[558]R. J. Ackermann and E. G. Rauh, J. Chem. Phys. **62**, 108 (1975).
[559]T. Gao, Z.-H. Zhu, X.-L. Wang, Y. Sun, and D.-Q. Meng, Acta Chim. Sin. **62**, 454 (2004).
[560]A. V. Zaitsevskii, A. V. Titovb, S. S. Malkovc, I. G. Tananaev, and Y. M. Kiseleve, Dokl. Chem. **448**, 1 (2013).
[561]I. Infante, A. S. P. Gomes, and L. Visscher, J. Chem. Phys. **125**, 073401 (2006).
[562]O. H. Krikorian, A. S. Fontes, Jr., B. B. Ebbinghaus, and M. G. Adamson, J. Nucl. Mater. **247**, 161 (1997).
[563]C. Ronchi, F. Capone, J. Y. Colle, and J. P. Hiernaut, J. Nucl. Mater. **280**, 111 (2000).
[564]D. W. Green and G. T. Reedy, J. Chem. Phys. **69**, 544 (1978).
[565]E. F. Archibong and A. K. Ray, J. Mol. Struct. (THEOCHEM) **530**, 165 (2000).
[566]T. E. Phipps, G. W. Sears, and O. C. Simpson, J. Chem. Phys. **18**, 724 (1950).
[567]R. N. R. Mulford and L. E. Lamar, in *Plutonium*, edited by E. Grisoti, W. B. H. Lord, and R. D. Fowlereds (Cleaver-Hume Press, Ltd., London, 1961), pp. 411–421.
[568]W. M. Pardue and D. L. Keller, J. Am. Ceram. Soc. **47**, 610 (1964).
[569]D. R. Messier, J. Am. Ceram. Soc. **751**, 710 (1968).
[570]J. E. Battles, W. A. Shinn, and J. W. Reihus, Technical Report ANL 7575, 1969.
[571]P. Gotcu-Freis, J. Y. Colle, J. P. Hiernaut, F. Naisse, C. Guéneau, and R. J. M. Konings, J. Chem. Thermodyn. **43**, 1164 (2011).
[572]T. Gao, H.-Y. Wang, Y.-G. Yi, M.-L. Tan, Z.-H. Zhu, Y. Sun, X.-L. Wang, and Y.-B. Fu, Acta Phys. Sin. **48**, 2222 (1999).
[573]Q. Li and C. Xu, J. Sichuan Normal Univ. (Nat. Sci) **23**, 386 (2000).
[574]R. W. Ohse, Tech. Rep. Progress Report No. 5 (Institute for Transuranium Elements, 1968).
[575]A. Kovács, R. J. M. Konings, J. Raab, and L. Gagliardi, Phys. Chem. Chem. Phys. **10**, 1114 (2008).

[576]P. Gotcu-Freis, J. P. Hiernaut, J. Y. Colle, and R. J. M. Konings, J. Nucl. Mater. **409**, 194 (2011).
[577]R. G. Haire, J. Alloys Compd. **213/214**, 185 (1994).
[578]M. Santos, J. Marcalo, J. P. Leal, A. P. de Matos, J. Gibson, and R. G. Haire, Int. J. Mass Spectrom. **228**, 457 (2003).
[579]P. K. Smith and D. E. Peterson, J. Chem. Phys. **52**, 4963 (1970).
[580]J. P. Hiernaut and C. Ronchi, J. Nucl. Mater. **334**, 133 (2004).
[581]X. Y. Cao and M. Dolg, THEOCHEM **673**, 203 (2004).
[582]R. G. Haire and L. Eyring, *Handbook on the Physics and Chemistry of Rare Earths* (North-Holland, Amsterdam, 1994), Vol. 18, Chap. 125, pp. 413–505.
[583]C. E. Holley, Jr., E. J. Huber, Jr., and F. B. Baker, *Progress in the Science and Technology of the Rare Earths* (Pergamon, Oxford, 1968), Vol. 3, pp. 343–433.
[584]M. Zinkevich, Prog. Mater. Sci. **52**, 597 (2007).
[585]I. Grenthe, J. Fuger, R. J. M. Konings, R. J. Lemire, A. B. Muller, C. Nguyen-Trung, and H. Wanner, *Chemical Thermodynamics of Uranium* (Elsevier, Amsterdam, 1992).
[586]R. J. Silva, G. Bidoglio, M. H. Rand, P. B. Robouch, H. Wanner, and I. Puigdomenech, *Chemical Thermodynamics of Americium* (Elsevier, Amsterdam, 1995).
[587]M. Rand, J. Fuger, I. Grenthe, V. Neck, and D. Rai, *Chemical Thermodynamics of Thorium* (OECD Publishing, Paris, 2009).
[588]E. H. P. Cordfunke, R. J. M. Konings, and E. F. Westrum, Jr., J. Nucl. Mater. **167**, 205 (1989).
[589]B. Averkiev, M. Mantina, R. Valero, I. Infante, A. Kovács, D. G. Truhlar, and L. Gagliardi, Theor. Chem. Acc. **129**, 657 (2011).
[590]R. J. M. Konings and O. Beneš, J. Phys. Chem. Ref. Data **39**, 043102 (2010).
[591]P. Pyykkö, S. Riedel, and M. Patzschke, Chem.-Eur. J. **11**, 3511 (2005).